Anne Elizabeth Margaret Robins

St Catherine's College

'Senescence and the Innate Immune System'

July 2021

This dissertation is submitted for the degree of Doctor of Medicine

This dissertation is the result of my own work and includes nothing which is the outcome of work done in collaboration except as declared in the Preface and specified in the text.

It is not substantially the same as any that I have submitted or is being concurrently submitted for a degree or diploma or other qualification at the University of Cambridge or any other University or similar institution except as declared in the Preface and specified in the text. I further state that no substantial part of my dissertation has already been submitted, or is being concurrently submitted for any such degree, diploma or other qualification at the University of Cambridge or any other University of similar institution except as declared in the Preface and specified in the text.

It does not exceed the prescribed word limit of 60,000 words.

Senescence and the Innate Immune System – Dr Anne Robins

Abstract

Cellular senescence prevents deoxyribonucleic acid (DNA) damaged cells undergoing proliferation, protecting against malignancy but at the expense of senescent cell accumulation. Since the proportion of senescent hepatocytes in man correlates closely with liver injury, fibrosis stage and mortality, prevention of malignancy occurs at the expense of impaired organ function. Senescent cells are removed by the innate immune system, including natural killer (NK) cells, during normal embryonic development and healthy wound healing. Since eradication of senescent cells in mice leads to resistance against age-related disorders and functional restoration, one approach to liver injury might be enhanced removal of senescent cells. The non-classical human leukocyte antigen class I molecules E, F and G (HLA-E, -F and -G), are ligands for NK cells and considered tolerogenic. For example, HLA-E binds with the NK inhibitory receptors, killer cell lectin like receptor D1 (CD94) and c-type lectin family receptors (NKG2), preventing NK mediated killing. Less is known of HLA-F, which is present in placental trophoblasts, possibly promoting foetal tolerance. HLA-G is expressed on trophoblast cells and is considered a key component mediating foetal tolerance. Little is known of HLA-E or -F in liver injury, while a few immunohistochemical studies have suggested increased hepatocyte expression of HLA-G in cirrhosis of all aetiologies.

My hypothesis was that senescent hepatocytes are removed from healthy liver by the innate immune system, as in healthy wound healing, but that in chronic liver disease there is a failure of this response, leading to an accumulation of senescent cells, fibrosis and cirrhosis. I examined hepatic expression of HLA class I, HLA-E, -F and -G in health and disease. Secondly, I assessed the major histocompatibility complex (MHC) class I ligands, the NK cell receptors. Finally, the various components of the antigen presentation pathway in health and disease were studied.

My study shows that HLA class I is present in liver tissue and is upregulated in cirrhosis. HLA-E and -F are expressed in liver tissue and are also upregulated in cirrhosis. The expression of HLA-E and -F was largely intracellular and consistent with retention within the golgi, however, some less marked surface expression was also seen. The data on expression of HLA-G was clear, but inconsistent with the literature. While immunohistochemistry work was indeed congruent with published data showing widespread expression in cirrhosis, all other biochemical techniques, undertaken herein for the first time, failed to detect HLA-G protein in healthy liver tissue or cirrhosis; HLA-G RNA was only identified in hepatitis B infected liver tissue. These data suggest that previous reports linking HLA-G and liver injury may be artefactual.

The NK cell receptors, killer cell immunoglobulin like receptors 2DL2 and 2DS2, were significantly upregulated in cirrhosis although the numbers studied were low suggesting that NK cell activation is altered in cirrhosis.

Tapasin and tapasin related protein (TAPBPR), both parts of the antigen presentation pathway are expressed in liver tissue and show a slight upregulation in liver disease. This suggests that aberrant expression via this pathway may be part of the liver pathology.

In summary there is altered expression of HLA molecules in cirrhosis, specifically HLA-E and -F. Secondly, altered expression of inhibitory molecules is seen on circulating NK cells. These findings are consistent with reduced clearance of damaged hepatocytes in cirrhosis. It proved impossible, despite numerous approaches, to link increased hepatocyte HLA expression with senescence.

My study concludes that HLA class I is present in liver tissue and is upregulated in cirrhosis. The expression of HLA-E and -F is identified in liver tissue for the first time and is shown to be upregulated in cirrhosis. This altered expression of HLA-E and -F may have a role in the pathogenesis of cirrhosis and could be a target for future therapies.

Contents

Figures

Tables

Abbreviations

α	Alpha
α1AT	Alpha-1-Anti-Tripsin Deficiency
β	Beta
β2m	β2-microglobulin
β-galactosidase	Beta Galactosidase
γ	Gamma
γH2AX	Phosphorylated H2A histone family member X
µg	Microgram
µl	Microlitre
µM	Micromolar
~	Approximately
^0C	Degrees Centigrade
%	Percent
20X	20 Times Magnification
40X	40 Times Magnification
63X	63 Times Magnification
AIH	Autoimmune Hepatitis
AMPS	2-Acrylamido-2-Methylpropane Sulfonic Acid
Anti-HBe	Hepatitis B e-Antibody
ARLD	Alcohol Related Liver Disease
ASGPR	Asialoglycoprotein Receptor
B-Cells	B-Lymphocytes
BFA	Brefeldin A
BSA	Bovine Serum Albumin
C2	Complement Component 2
C4	Complement Component 4
$CaCl_2$	Calcium Chloride
CD3	Cluster of Differentiation 3
CD4	Cluster of Differentiation 4
CD4+	Cluster of Differentiation 4 Positive

CD8+	Cluster of Differentiation 8 Positive
CD14	Cluster of Differentiation 14
CD16	Cluster of Differentiation 16
CD19	B-Lymphocyte Surface Antigen B4
CD45	Protein Tyrosine Phosphatase Receptor Type C
CD49a	Cluster of Differentiation 49
CD56	Neural Cell Adhesion Molecule
$CD56^{bright}$	Neural Cell Adhesion Molecule Bright
$CD56^{dim}$	Neural Cell Adhesion Molecule Dim
CD57	Cluster of Differentiation 57
CD69	Cluster of Differentiation 69
CD94	Killer Cell Lectin-like Receptor subfamily D1
CD94:NKG2	C-Type Lectin Receptors
cDNA	Complementary DNA
c-Fos	Proto-Oncogene c-Fos
CK18	Cytokeratin 18
CMV	Cytomegalovirus
Cyc A	Cyclin Family Protein A
Cyc B	Cyclin Family Protein B
DAB	3,3'-Diaminobenzidine
ddH_20	Double Distilled Water
DMSO	Dimethylsulphoxide
DNA	Deoxyribonucleic Acid
DCM	Dead Cell Marker
DPX	Dibutylphthalate Polystyrene Xylene
dT(18)	Deoxythymine 18
DTT	DL-dithiothreitol
EASL	European Association for the Study of the Liver
EDTA	Ethylene Diamine Tetra Acetic Acid
EGTA	Ethylene Glycol-Bis (β-Aminoethyl Ether)-N, N, N', N'-Tetraacetic Acid
Endo H	Endoglycosidase H

ER	Endoplasmic Reticulum
ERp57	Endoplasmic Reticulum Protein 57
ERAP	Endoplasmic Reticulum Aminopeptidase
Facs	Fluorescence Activated Cell Sorting
FCS	Fetal Calf Serum
FSC-A	Forward Scatter
g	Gram
G_0	Quiescent or Senescent Phase
G_1	Gap 1 Phase
G_2	Gap 2 Phase
GAPDH	Glyceraldehyde 3-Phosphate Dehydrogenase
H_20	Water
H_20_2	Hydrogen Peroxide
HBV	Hepatitis B Virus
HBeAg	Hepatitis B e-Antigen
HBsAg	Hepatitis B Surface Antigen
HCL	Hydrochloric Acid
HCV	Hepatitis C Virus
HFE	Haemochromatosis
HIV	Human Immunodeficiency Virus
HLA	Human Leukocyte Antigen
HLA-A, -B, -C	Classical Human Leukocyte Class I Antigens A, B and C
HLA-DM, -DO	Non-Classical Human Leukocyte Class II Antigens DM and DO
HLA-DP, -DQ, -DR	Classical Human Leukocyte Class II Antigens DP, DQ and DR
HLA-E, -F, -G	Non-Classical Human Leukocyte Class I Antigens E, F and G
HPRT	Hypoxanthine-Guanine Phosphoribosyltransferase
HRP	Horseradish peroxidase
HSP	Heat Shock Protein
HSP60	Heat Shock Protein 60
HSV	Herpes Simplex Virus
IAA	Idoactamide
IFNγ	Interferon Gamma

IgG	Immunoglobulin G
IgG2a	Immunoglobulin G subclass 2a
IL-1β	Interleukin 1 β
IL-6	Interleukin 6
IL-8	Interleukin 8
ILT2	Immunoglobulin like Transcript 2
ILT4	Immunoglobulin like Transcript 4
INK4	Inhibitors of CDK4 proteins
IP	Immunoprecipitation
IQR	Interquartile Range
kDa	Kilodalton
Ki67	Marker of Proliferation Ki67
KIR2D	Killer Cell Immunoglobulin like Receptor with Two Immunoglobulin Domains
KIR2DL1	Killer Cell Immunoglobulin like Receptor with Two Immunoglobulin Domains and Long Cytoplasmic Tail 1
KIR2DL2	Killer Cell Immunoglobulin like Receptor with Two Immunoglobulin Domains and Long Cytoplasmic Tail 2
KIR2DL3	Killer Cell Immunoglobulin like Receptor with Two Immunoglobulin Domains and Long Cytoplasmic Tail 3
KIR2DL4	Killer Cell Immunoglobulin like Receptor with Two Immunoglobulin Domains and Long Cytoplasmic Tail 4
KIR2DS1	Killer Cell Immunoglobulin like Receptor with Two Immunoglobulin Domains and Short Cytoplasmic Tail 1
KIR2DS2	Killer Cell Immunoglobulin like Receptor with Two Immunoglobulin Domains and Short Cytoplasmic Tail 2
KIR3DL1	Killer Cell Immunoglobulin like Receptor with Three Immunoglobulin Domains and Long Cytoplasmic Tail 1
KIR3DS1	Killer Cell Immunoglobulin like Receptor with Three Immunoglobulin Domains and Short Cytoplasmic Tail 1
KIR(s)	Killer Inhibitory Receptors
LILRB1	Leukocyte Immunoglobulin like Receptor B1
LILRB2	Leukocyte Immunoglobulin like Receptor B2
LILR(s)	Leukocyte Immunoglobulin like Receptors
LMP2	Low Molecular Weight Polypeptide 2

LMP7	Low Molecular Weight Polypeptide 7
LSEC	Liver Sinusoidal Endothelial Cells
LTA	Lymphotoxin Alpha
LTB	Lymphotoxin Beta
M	Molar
mAb	Monoclonal Antibody
MAIT	Mucosal Associated T-Cells
Mcm-2	Mini-Chromosome Maintenance Protein 2
MECL-1	Multi-Catalytic Endopeptidase Complex-like 1
MFI	Mean Fluorescence Intensity
mg	Milligram
MHC	Major Histocompatibility Complex
MICA	MHC Class I Polypeptide-Related Sequence A
MICB	MHC Class I Polypeptide-Related Sequence B
ml	Millilitre
mM	Millimolar
Na_2EDTA	Ethylenediaminetetraacetic Acid Disodium Salt Dihydrate
Na_3VO_4	Sodium Vanadate
NaCl	Sodium Chloride
NAFLD	Non-Alcohol Related Fatty Liver Disease
NEM	N-Ethylmaleimide
ng	Nanograms
NK	Natural Killer Cells
NKG2	Killer Cell Lectin-like Receptors
NKG2A	Killer Cell Lectin-like Receptor C1
NKG2B	Killer Cell Lectin-like Receptor C1
NKG2C	Killer Cell Lectin-like Receptor C2
NKG2D	Killer Cell Lectin-like Receptor K1
nM	Nanomolar
NP-40	Nonyl Phenoxypolyethoxylethanol
p16	Cyclin Dependent Kinase Inhibitor 2A
p21	Cyclin Dependent Kinase Inhibitor 1A

p53	Cellular Tumour Antigen p53
PBC	Primary Biliary Cholangitis
PBS	Phosphate Buffered Saline
PBSA	Phosphate-Buffered Saline with Albumin
PBMC	Peripheral Blood Mononuclear Cells
PCNA	Proliferating Cell Nuclear Antigen
PCR	Polymerase Chain Reaction
PFA	Paraformaldyhyde
pH	Power of Hydrogen
PLC	Peptide Loading Complex
PMSF	Phenylmethylsulfonyl Fluoride
pRB	Retinoblastoma Protein
PSC	Primary Sclerosing Cholangitis
PTC	Percutaneous Transhepatic Cholangiogram
qRT-PCR	Quantitative Real-Time PCR
R^2	R-Squared
REC	Research Ethics Committee
RNA	Ribonucleic Acid
ROS	Reactive Oxygen Species
RPMI	Roswell Park Memorial Institute Media
S	Synthesis Phase
SAHF	Senescence Associated Heterochromatin Foci
SASP	Senescence Associated Secretory Phenotype
SDF	Senescence Associated DNA Damage Foci
SDS	Sodium Dodecyl Sulfate
SLS	Sodium Lauryl Sulfate
SSC-A	Side Scatter
T-Cell	T-Lymphocyte
TAP	Transporter Associated with Antigen Presentation
TAP1	Transporter Associated with Antigen Presentation 1
TAPBPR	Tapasin Related Protein
TBE	1,1,2,2-Tetrabromoethane

TBS	Tris-Buffered Saline
TEMED	N, N, N', N'- Tetramethylethylenediamine
TIPSS	Transjugular Intrahepatic Portosystemic Shunt
TNFα	Tumour Necrosis Factor Alpha
Tris	Tris(hydroxymethyl)aminomethane
Triton X-100	2-(4-(2,4,4-Trimethylpentan-2-yl) Phenoxy) Ethanol
Tween20	Polyethylene Glycol Sorbitan Monolaurate
UGT1	UDP-Glucose Glycoprotein Glucosyltransferase 1
UK	United Kingdom
ULBP1	UL 16 Binding Protein 1
ULBP2	UL 16 Binding Protein 2
UV	Ultraviolet
V	Volts
VEGF	Vascular Endothelial Growth Factor
xg	Times Gravity

Acknowledgements

This thesis would not have been completed without the help and guidance of many people. Firstly, my supervisors Dr Louise Boyle and Professor Graeme Alexander, their support, encouragement, and motivation has been paramount to the completion of this work. I am so grateful for their patience and inspiration. I must also thank all members of the Boyle laboratory, especially Andreas Neerincx, for their assistance and training with the biochemical techniques.

Integral to this research was the collection of liver tissue which was often late at night or at weekends. Dr Nicola Owen and I shared this task collecting tissue for each other and I am indebted to her for this arrangement. I also thank the hepatobiliary and transplant surgeons for assisting in this tissue collection and to the transplant co-ordinators for the logistical arrangements.

For the immunohistochemistry work I must thank Professor Nicholas Coleman and the members of his laboratory including Dr Cinzia Scarpini and Dawn Ward. Also, to Dr Heather Griffin for the use of the MIRAX scanner.

For my flow cytometry work I must thank Dr Martin Ivarsson and Dr Oishin Huhn for their guidance. Finally for the use of the category two plus facilities and the provision of placental tissue I am grateful to Professor Ashley Moffett and her laboratory members including Dr Lucy Gardner.

Other people who I also owe thanks include Addenbrookes Hospital Tissue Bank for the provision of human tissue and paraffin slides, Dr Judith Heaney for instruction in biochemical techniques at the start of the research project and to Professor Arthur Kaiser and his laboratory at the Department of Medicine.

I am grateful for the financial support from the Hepatology Endowment Fund and most importantly to all patients donating liver tissue or blood to enable this research.

Finally special thanks to my family for their support during this work especially my husband Martin and my sons Daniel and Samuel who were both born during this project.

Chapter 1 Introduction

1.1 Human Immune System

The immune system protects the body from damage and can destroy diseased or infected cells. It also protects the body against pathogens which are daily challenges. The immune system is split into two broad subsections: the innate and adaptive immune systems.

1.1.1 Innate Immune System

The innate immune system is a non-specific defence mechanism that takes effect within hours of antigen identification in the body (Gasteiger et al., 2017). It includes the physical barrier of the skin, as well as cytokines inducing an inflammatory response (Lotze and Tracey, 2005) and non-specific immune cells that can attack foreign cells or cells containing exogenous deoxyribonucleic acid (DNA) or ribonucleic acid (RNA) in the body. Once a pathogen is identified, cytokines are released attracting further cells of the innate immune system and activation of the adaptive immune system (Griffith et al., 2014). The effector cells are discussed below:

Neutrophils are found in the greatest number in the bloodstream and are the first cells to arrive at the site of infection (Rosales, 2018). Chemotaxis attracts the cells due to the release of cytokines which then phagocytose the infected or damaged cells (Gasteiger et al., 2017).

Macrophages have many roles including detection, phagocytosis and destruction of bacteria and other harmful organisms. They also act as antigen presenting cells to T-lymphocytes (T-cells). Finally, they can initiate inflammation by releasing cytokines (Elhelu, 1983).

Natural Killer (NK) cells are a subset of lymphocytes which can kill cells without prior activation (Rosenberg et al., 1972) killing virally infected cells and detecting and controlling early signs of cancer. They express a variety of different receptors which can be either activating or inhibitory. Activating receptors, which include the C-type lectin family receptors (CD94:NKG2) and the activating killer immunoglobulin receptors (KIRs) (Yawata et al., 2002), can recognise molecular changes on stressed or infected cells (Apps et al., 2008c). The inhibitory receptors, which include Killer Cell Lectin-like Receptors C1 (NKG2A and NKG2B), the inhibitory KIRs and members of the leukocyte immunoglobulin-like receptors (LILRs), mainly monitor expression of classical and non-classical major histocompatibility complex (MHC) class I molecules, the absence of which causes NK cell activation (Iannello et al., 2008). NK cells can kill their target cell and also release cytokines such as interferon gamma (IFNγ) and tumour necrosis factor alpha (TNFα) to enhance the immune response (Eissmann, 2020).

Other cells of the innate immune system include monocytes, eosinophils, and basophils.

1.1.2 Adaptive Immune System

The innate immune system activates the adaptive immune system. In this process the response is specific to the pathogen identified. The main effector cells are listed below.

T-cells are lymphocytes which are divided into two groups. Cluster of differentiation eight positive (CD8+) cytotoxic T-cells kill cancer cells or viral infected cells directly. Cluster of differentiation four positive (CD4+) helper T-cells identify damaged or infected cells and release cytokines to attract other immunes cells to attack (Luckheeram et al., 2012). This is known as cell-mediated immunity.

B-lymphocytes (B-cells) main function is to secrete antibodies. However they can also present antigens and release cytokines (Cooper, 2015). This leads to humoral immunity.

The adaptive immune system can create a memory so antibodies can be recalled if needed at a later stage (Bonilla and Oettgen, 2010).

1.2 Major Histocompatibility Complex

The major histocompatibility complex (MHC) is a collection of genes found on chromosome six in humans that encode molecules expressed on the cell surface, which have a major role in regulating the immune system. In humans, these are known as human leukocyte antigens (HLA) (Dausset, 1981). These polymorphic molecules were first identified in graft rejection (Gorer, 1936), are unique to each individual and enable the immune system to identify 'self' cells and distinguish foreign proteins. There are three different subgroups of the HLA family, HLA class I, class II and class III.

1.2.1 HLA Class I

HLA class I antigens are split into the classical human leukocyte antigens A, B and C (HLA-A, -B and -C) and the non-classical human leukocyte antigens E, F and G (HLA-E, -F and -G). An individual inherits six class I HLA alleles: one HLA-A, -B and -C from each parent and so expresses up to six different classical HLA molecules on their cells. These classical MHC class I molecules, HLA-A, -B and -C, play a key role in antigen presentation to CD8+ T-cells and are also monitored by NK cells (Carrillo-Bustamante et al., 2016). In basic terms, the MHC class I molecules deliver fragments of proteins produced within the cell to the cell surface. This is a quality control mechanism; if an abnormal

protein is presented in conjunction with an HLA molecule, the peptides bind to CD8+ T-cells inducing the death of the cell. Similarly, if the MHC class I is downregulated or absent, cell death is activated (Karre et al., 1986). HLA class I antigens are found on most cell types; however, the level of expression depends on the cell type. They are present at high density in lymphoid and myeloid tissue, at a lower level in health in the kidney, liver and lung and have only very low expression in brain and muscle (Boegel et al., 2018).

MHC class I molecules are a heterodimer of a heavy alpha polypeptide chain, encoded in the MHC and a smaller polypeptide beta (β)-2-microglobulin (β2m) which is encoded by a gene on human chromosome 15. The alpha (α) chain is composed of three extracellular domains numbered (α1, 2 and 3) as well as a transmembrane region and a cytoplasmic tail (Klein and Sato, 2000). The α1 and α2 domain form the peptide binding groove for antigenic peptides and is the major point of contact between MHC and the T-cell receptor **(Figure 1.1)**. The α3 and β2m chains form the membrane proximal region (Bjorkman et al., 1987). The binding groove of the MHC class I molecule is closed as the ends of the two alpha chain domains come together, therefore, the peptides presented are generally restricted to eight-eleven amino acids in length. Only ten percent of the peptides generated in a cell are the correct size to be able to bind to the MHC class I antigen (Dausset, 1981). Specific amino acids within the groove form binding pockets called anchor residues, which bind to corresponding side chains on the peptide (Garrett et al., 1989).

Figure 1.1 - The structure of the HLA class I antigen*. The α1 and α2 chains form the peptide binding groove. The differing structure of HLA class II is also shown. Sourced from (Winchester, 2008).*

1.2.2 HLA Class II

HLA class II molecules are again split into three classical human leukocyte antigens DP, DQ and DR (HLA-DP, -DQ and -DR) and two non-classical human leukocyte antigens DM and DO (HLA-DM and -DO). The 'D' stands for a class II antigen and the second letter describes the family: P, Q or R. These

are only found on specific cells, which are part of the immune system, including dendritic cells, macrophages and B-cells, although they can be induced on other cells types by IFNγ (Mangalam et al., 2013). The classical MHC class II molecules (HLA-DP, -DQ and -DR) are expressed on the cell surface and present antigens to T-cell receptors for inspection. HLA class II molecules interact with CD4+ T-cells, to recruit and drive B-cells to produce antibodies to the pathogen or antigen. The peptides presented are often derived from extracellular self-proteins or proteins being made by extracellular organisms which have been phagocytosed by the cell, although some intracellular protein presentation is also performed. The peptides presented by MHC class II molecules are generated in the endosomal system. MHC class II molecules are also heterodimers but formed of one alpha and one beta chain each with two domains (α1, α2, β1 and β2), which are of a more equal size (Jones et al., 2006). These chains also form a groove, which can bind the antigenic peptides **(Figure 1.1)**.

1.2.3 MHC Class I Presentation Pathway

HLA class I molecules process and present antigenic peptides via the antigen presentation pathway shown in **Figure 1.2**; the peptides may include fragments of viral proteins, self-proteins and tumour antigens (Rock and Goldberg, 1999). Intracellular proteins targeted for degradation are bound to a molecule called ubiquitin and can then be identified by proteasomes. In the cytosol, proteasomes breakdown proteins bound to ubiquitin into smaller peptides. Peptides which are the correct size can enter the endoplasmic reticulum (ER) via the transporters associated with antigen presentation (TAP) (Spies et al., 1990), which carry the peptide into the ER lumen, the site of MHC class I folding. Multi-catalytic endopeptidase complex-like 1 (MECL-1) and two MHC linking low molecular weight proteins, low molecular weight polypeptides 2 and 7 (LMP2 and LMP7) generate peptides that are more suitable to be transported by TAP and bind to MHC class I (Gaczynska et al., 1994). Inside the ER, aminopeptidases called endoplasmic reticulum aminopeptidases (ERAP) can further trim the peptides to optimise binding length (Serwold et al., 2002).

The HLA class I heavy chains are also translocated into the ER where they are glycosylated and then folded by the chaperone calnexin. Calnexin also uses endoplasmic reticulum protein 57 (ERp57) to assist with correct folding (Zhang et al., 2006). Once folded, the MHC class I heavy chain can now associate with β2m to form the MHC class I heterodimer (Vassilakos et al., 1996). The peptide receptive MHC class I heterodimer gets incorporated into the peptide loading complex (PLC), a multi-protein complex composed of the TAP molecule, tapasin, calreticulin and ERp57 (Van-Hateren et al., 2010). Tapasin which is linked to the TAP transporter binds to the MHC class I molecule while

calreticulin replaces the calnexin bound to the MHC class I heavy chain. The ERp57 acts as a bridge between calreticulin and MHC class I heavy chain stabilising the complex (Frickel et al., 2002) **(Figure 1.2)**. The PLC is the major site of peptide loading onto MHC class I molecules. Once the peptide is loaded and MHC class I heterotrimer is formed it is subsequently released from the PLC. The peptide loaded MHC class I complex then undergoes a quality control check by UDP-glucose glycoprotein glucosyltransferase 1 (UGT1) (Zhang et al., 2011). If a sub-optimal peptide is loaded it is removed and the MHC class I sent back for re-processing. Successfully loaded MHC-peptide complexes travel to the cell surface for presentation. `

Tapasin performs multiple functions including bridging MHC class I to the TAP transporters (Sadasivan et al., 1996), increasing levels of TAP (Lehner et al., 1998) and optimising peptide loading by performing peptide editing (Williams et al., 2002). In tapasin deficient mice, a reduction in MHC class I expression has been identified (Garbi et al., 2000). It has been suggested that tapasin widens the groove in the MHC class I allowing the release of a low affinity peptide and its replacement by one of higher affinity (Fisette et al., 2016). In the context of the liver, a study using mice hepatocytes showed that TAP and tapasin were upregulated in response to stress (Chen et al., 2005).

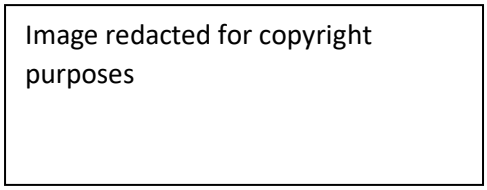

Figure 1.2 - The MHC class I antigen presentation pathway*. Peptides are initially broken down by proteasomes in the cytosol before being transported into the ER via TAP transporters. Once inside the ER, ERAP (ERAAP on this diagram) trim the peptides to the correct size. Calnexin and ERp57 assist in folding the MHC class I heavy chain to bind with β2m and into the correct form to be incorporated into the peptide loading complex. The peptide loading complex made up of TAP, tapasin, calreticulin, ERp57 and the MHC class I molecule binds to a suitable peptide. Quality control checks are undertaken by UGT1. Successfully loaded MHC class I molecules are transported to the cell surface. Sourced from British Society of Immunology (Nesmiyanov, 2020).*

1.2.4 Tapasin Related Protein

A tapasin related protein (TAPBPR) has more recently been identified as an additional component of the MHC class I antigen processing and presentation pathway (Boyle et al., 2013). It shares 22 percent (%) similarity with the tapasin molecule (Teng et al., 2002) and binds to MHC class I molecules associated with β2m (Boyle et al., 2013). TAPBPR was found to be orientated on MHC class I in a similar manner to tapasin (Hermann et al., 2013). Subsequently, TAPBPR was shown to function as a MHC class I peptide editor (Hermann et al., 2015). However, human TAPBPR is not a component of the PLC, but performs peptide editing in a distinct environment to tapasin. Furthermore, unlike tapasin TAPBPR does not contain an ER retention motif in its cytoplamic tail and therefore it can pass through the golgi. In addition to directly editing peptide on MHC class I, TAPBPR can further influence peptide selection by binding with UGT1 (Neerincx et al., 2017). Through re-glucosylating MHC class I, UGT1 can promote the re-association of MHC class I with calrecticulin, recycling MHC class I back to the PLC for a further attempt at peptide loading (Zhang et al., 2011). Like other components of the antigen processing and presentation pathway, including TAP, LMP2, LMP7, tapasin and ERAP, TAPBPR expression is IFNγ inducible (Tanaka and Kasahara, 1998, Boyle et al., 2013).

1.3 Non-Classical HLA Class I

1.3.1 HLA-E

HLA-E has a specialised antigen presentation role in that it presents the lead peptides (nine amino acid peptides) of HLA-A, -B and -C and is recognised by CD94:NKG2 receptors expressed on NK cells (Braud et al., 1998a). Therefore, HLA-E molecules are expressed when HLA-A, -B and -C are presented and prevent killing of cells. This is through engagement with inhibitory receptors expressed on NK cells and cytotoxic T-cells known as KIRs. NK cells normally recognise these KIR receptors present on a healthy cell membrane preventing lysis of normal cells (Colonna and Samaridis, 1995, Lanier, 1997).

MHC class I expression can be modified or downregulated by viruses to avoid the immune attack allowing a virus to persist (Hewitt, 2003). However, this results in decreased expression of HLA-E, resulting in the lack of inhibitory receptor engagement causing NK cells to attack. Ultimately, if HLA-E is not expressed on a cell then the NK cells can attack and destroy the cell.

HLA-E is also involved when cell stress or DNA damage occurs. In the event of cell stress, heat shock protein 60 (HSP60) is produced and can displace or replace absent MHC class I derived peptides from

the HLA-E binding cleft (Michaelsson et al., 2002). This complex is still presented on the cell surface but in the absence of the HLA class I molecule NK killing is induced.

HLA-E has been identified to be associated with a poor outcome in patients with hepatitis C (Araujo et al., 2018). It has been proposed that the hepatitis C virus forms a peptide that binds to HLA-E which stabilizes its surface expression and impairs NK cell killing (Nattermann et al., 2005). Conversely, a study showed reduced expression of MHC class I including HLA-E in hepatitis B infected hepatic cell lines and mice hepatocytes (Chen et al., 2006). A further study showed higher expression of soluble HLA-E in hepatitis B associated chronic liver disease compared to healthy controls (Zidi et al., 2016). Increased expression of HLA-E may help the virus to evade immune attack and lead to a more progressive infection, however, further work is needed to understand the pathophysiology behind this correlation.

1.3.2 HLA-F

The role of HLA-F is unknown; however, over the last few years a greater understanding of its potential function is starting to evolve (Geraghty et al., 1990). Initially it was identified that HLA-F may have a role in antigen cross-presentation (Goodridge et al., 2013). Recently, it has also been recognised that HLA-F is the ligand for the NK activating receptor, killer cell immunoglobulin like receptor with three immunoglobulin domains and short cytoplasmic tail 1 (KIR3DS1) (Garcia-Beltran et al., 2016). Also, it has now been shown that HLA-F does present peptides and activates the immune system via NK cell receptors (Dulberger et al., 2017). Finally, it is now being suggested that HLA-F could also have a role during pregnancy and viral infection (Persson et al., 2020).

1.3.3 HLA-G

The non-classical class I molecule HLA-G has seven different variants (HLA-G1-7). Variants HLA-G1-4 are membrane bound while variants HLA-G5-7 produce soluble proteins (Apps et al., 2008b). HLA-G is unique, in that it is only known to be expressed on the placenta by the extravillous trophoblast (Apps et al., 2008b) and is expressed throughout pregnancy (Djurisic and Hviid, 2014). The presence of the HLA-G molecule helps to protect the foetus from attack by the maternal immune system as 'non self'(McMaster et al., 1998). The placenta lacks expression of classical MHC class I to prevent attack by CD8+ cells; however, the downregulation should stimulate NK cells and activate the innate immune system. HLA-G prevents NK mediated killing by carrying a binding site for inhibitory NK cell receptors (Lash et al., 2010) including immunoglobulin like transcript 2 and 4 (ILT2 and ILT4) or killer

cell immunoglobulin like receptor with two immunoglobulin domains and long cytoplasmic tail 4 (KIR2DL4).

During pregnancy NK cells are present in much greater quantities; 70% of immune cells seen at the maternal foetal interface, (Moffett-King, 2002) compared to 5-15% in peripheral blood. Trophoblast cells express HLA-C, -E and -G, but do not express HLA-A or -B. Downregulation of HLA-A and -B should initiate NK cell attack, but this does not occur in pregnancy. HLA-C inhibits NK cells via KIR receptors including killer cell immunoglobulin like receptor with two immunoglobulin domains and long cytoplasmic tail 1 (KIR2DL1), killer cell immunoglobulin like receptor with two immunoglobulin domains and long cytoplasmic tail 2 (KIR2DL2) and killer cell immunoglobulin like receptor with two immunoglobulin domains and long cytoplasmic tail 3 (KIR2DL3). It is thought increased expression of HLA-G prevents NK cell attack (Trowsdale and Moffett, 2008). HLA-G interacts with ILT2 on the NK cell to inhibit its function (Borges et al., 1997).

Traditionally it was believed that expression of HLA-G was limited only to the placenta and experts in the field still believe this is true. However, over the last few years many studies suggest the presence of HLA-G in other tissues and a role in disease. Studies have showed that viruses including human immunodeficiency virus (HIV), cytomegalovirus (CMV) and herpes simplex virus (HSV) upregulate HLA-G to protect the host cell against NK cells (Onno et al., 2000). Similar findings have also been seen in patients with hepatitis B virus (HBV) where HLA-G was identified in the hepatocytes of HBV infected patients but not in healthy controls (Souto et al., 2011). HLA-G expression was altered in HBV and hepatitis C virus (HCV) infections suggesting a role in the pathogenesis of the disease (Catamo et al., 2014). Chronic inflammatory conditions are believed to cause aberrant HLA-G expression as a mechanism to prevent chronic immune medicated damage (Carosella et al., 2001). Recent work has suggested that HLA-G is also expressed by various cancer cells (Lin and Yan, 2018).

A paper investigating the role of HLA-G in hepatitis and hepatocellular carcinoma showed that higher HLA expression was associated with a lower survival rate and a shorter disease-free survival (Cai et al., 2009). An investigation was undertaken into the expression of HLA-G in post liver transplant patients which found no association with acute rejection. However, they did show cirrhotic hepatocytes to be positive for HLA-G by immunohistochemistry. They also identified high levels of serum HLA-G in these patients (Moroso et al., 2015).

1.3.4 Other HLA Molecules

A molecule, initially named HLA-H, has subsequently been identified as the human haemochromatosis gene (HFE) coding for a gene binding to a transferrin receptor. A defect in this receptor leads to the disease haemochromatosis (Brissot et al., 2018). There are many other genes found within the MHC chromosome region. These are labelled as MHC class III antigens and have a more physiological role, unrelated to my project. They secrete proteins which are directly or indirectly related to the immune system. These proteins include components of the complement system (such as complement components 2 and 4 (C2 and C4) and complement B factor), cytokines (such as TNF-α, lymphotoxin alpha and beta (LTA, LTB)) and heat shock proteins (HSP) (Gruen and Weissman, 2001). MHC class I polypeptide-related sequence A and B molecules (MICA and MICB) are also found within this MHC locus (Bahram et al., 1994). These molecules are stress inducible and mainly present in the thymus and gastrointestinal tracts. These are recognised by killer cell lectin-like receptor K1 (NKG2D) and have a role in NK and T-cell anti-tumour response.

1.4 Liver Disease

Liver disease is a major cause of worldwide morbidity and mortality. In the United Kingdom (UK) alone, two million people are affected with liver disease (NHS24, 2020) and 40 die every day (British Liver Trust, 2020). Initial treatment involves the removal of the causative agent (Ellis and Mann, 2012). However, if this is unsuccessful the only cure for patients with decompensated liver disease is a liver transplant. Around 1000 are performed in the UK each year (British Liver Trust, 2020); however, many patients do not survive long enough, or are not fit enough for this to be undertaken. Clearly new interventions are needed to treat liver conditions at earlier stages. However, there is a vast gap in our understanding of the fundamental molecular mechanisms underlying chronic liver disease, which need to be determined before novel effective treatments can be developed.

1.4.1 Liver Anatomy

The liver is a vital organ for human function without which humans cannot survive. Its functions include detoxification of the blood from toxins, cholesterol and glycogen storage, synthesis of proteins and amino acids, absorption of vitamins and the production of bile for digestion (John Hopkins Medicine, 2020) . What is often overlooked is that the liver is an important component of host immunity and the largest organ of the immune system.

Figure 1.3 shows the blood supply to the liver and **Figure 1.4** illustrates the sinusoidal function. **Figure 1.3** shows the portal tract, which comprises of the portal vein, hepatic artery, and common bile duct. Oxygenated blood from the heart passes to the liver via the hepatic artery. Blood enriched with food from the intestines passes to the liver via the portal vein. In the sinusoids **(Figure 1.4)** nutrients are extracted from this blood and toxins removed. The sinusoids are lined with liver sinusoidal endothelial cells (LSECs) which have fenestrations allowing the blood to pass to the hepatocytes for utilisation (Zhou et al., 2016). These waste products are transported into the bile ductules and thereby eventually into the common bile duct. The deoxygenated and used blood returns to the central vein and eventually the vena cava to return to the heart and lungs.

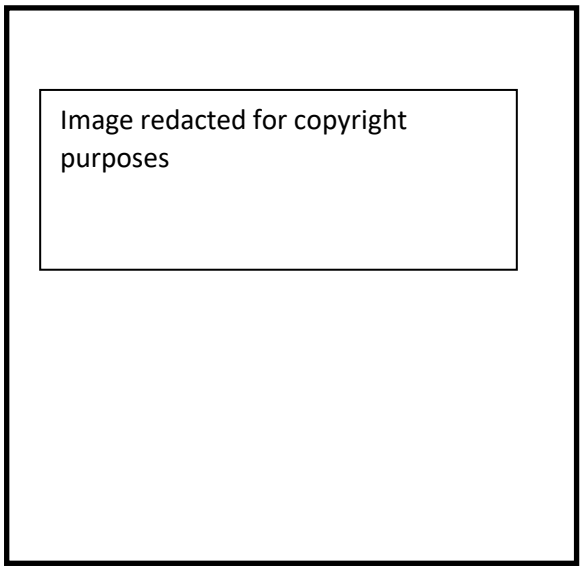

Figure 1.3 - The blood supply to the liver. *Oxygenated blood arrives to the liver via the hepatic artery. Blood rich in nutrients arrives via the portal vein from the intestinal system. Blood leaves the liver via the hepatic vein and vena cava. Sourced from (Neuroendocrine Tumor Research Foundation, 2020) .*

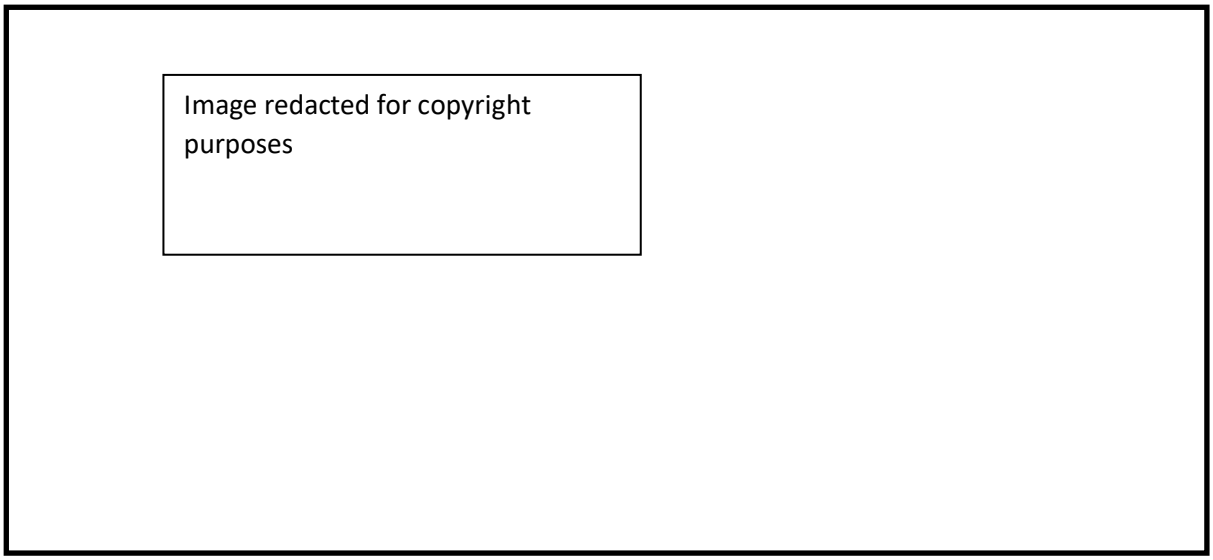

Figure 1.4 - The passage of blood through the liver sinusoid. *Blood passes from the portal field along towards the central vein. As it does so nutrients pass from the blood into the hepatocytes via osmosis. The waste products from the hepatocytes pass into the portal tract to the bile ductule within the portal field. Immune cells line the sinusoid as the bodies defence mechanism including endothelial cells and Kupffer cells. Stellate cells rest in a quiescent state in the space of Disse and when activated they lead to fibrosis. Sourced from (Frevert et al., 2005).*

1.4.2 Pathophysiology of Liver Disease

There are numerous causes of liver disease which all cause damage to the liver through inflammation, which in turn drives the development of fibrosis (Puche et al., 2013). The most common causes in the UK are non-alcohol related fatty liver disease (NAFLD) and alcohol related liver disease (ARLD) (Williams et al., 2014). The next most common group are the viral causes with HCV being most prominent in Western Europe and HBV in Asian countries. However, with the new antiviral medications the goal is to eliminate HCV over the next few years (Harris et al., 2020). There are several rarer conditions including the autoimmune diseases; autoimmune hepatitis (AIH), primary biliary cholangitis (PBC) and primary sclerosing cholangitis (PSC) and finally metabolic liver diseases including haemochromatosis, Wilsons disease and alpha-1-anti-tripsin deficiency (α1AT) (Bloom et al., 2012).

Inflammation is necessary to maintain the healthy liver environment. These inflammatory processes lead to haemodynamic changes, capillary permeability, white blood cell migration and inflammatory mediator secretion (Robinson et al., 2016). The aim is to remove the immediate danger and repair damage. Up to a point, the liver can fully regenerate and recover from injury (Malato et al., 2011).

However, ongoing inflammation becomes pathological and leads to over-activation of the normal response to injury and mechanism of repair. Stellate cells are found next to the hepatocytes and usually maintain a quiescent state (Tsuchida and Friedman, 2017). Liver damage leads to activation of stellate cells, fibrin deposition and progressive fibrosis. As inflammation continues, this fibrosis progresses leaving collagen scar tissue which leads to a loss of functioning hepatocytes and an altered structure of the liver itself (Schuppan and Afdhal, 2008). If the inflammation is arrested (e.g. the stimulus is removed with abstention from alcohol, or antiviral therapy for HCV or HBV), then fibrosis may improve with recent data even suggesting reversal of cirrhosis in many cases, an event considered impossible 20 years ago (Ellis and Mann, 2012).

Once the liver becomes cirrhotic, the architecture of the liver is lost, and it loses its regenerative and functional capacity. Initially the liver can still function known as compensated cirrhosis; however, if the damage continues this leads to decompensated cirrhosis. It is at this stage that patients develop signs of liver failure including jaundice, ascites, encephalopathy and variceal bleeding (Gines et al., 1987). If a liver transplant is not available, the patient will eventually die of liver failure, with 50% mortality at two years. Also, with cirrhosis there is an increased risk of developing hepatocellular carcinoma (European Association for the Study of the Liver (EASL), 2012). **Figure 1.5** shows this disease pathway.

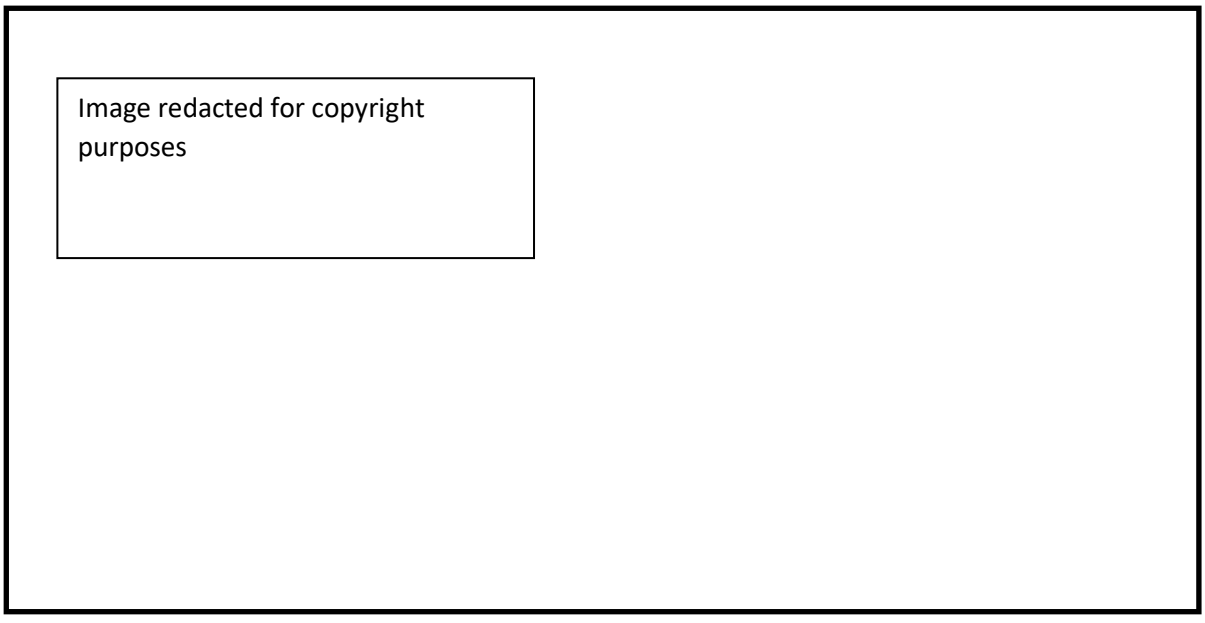

Figure 1.5 – The pathogenesis of cirrhosis *progressing from inflammation to fibrosis and finally cirrhosis. Sourced from nature reviews immunology (Pellicoro et al., 2014).*

1.4.3 Immunology of the Liver

The liver is exposed to a very large blood supply and therefore many immune cells (Wick et al., 2002). The liver is known as a tolerant organ as it needs to tolerate self-antigens from the body but also act as a defence against pathogens. The liver is exposed daily to bacterial products through dietary intake which it must tolerate but still be alert to harmful agents (Robinson et al., 2016). Therefore, close regulation of the inflammatory pathways in health is required, which could cause life-threatening inflammation in response to challenges such as viral infection, autoimmunity and malignancy if not controlled (Protzer et al., 2012). By using these tolerant mechanisms pathogens can persist within the liver leading to chronic disease.

The sinusoids are populated with liver resident immune cells including those of both the innate and adaptive immune systems and antigen presenting cells (Knolle, 2016). Kupffer cells are liver resident macrophages **(Figure 1.4)**. They account for a third of the non-hepatocyte population of the liver (Bilzer et al., 2006). They phagocytose blood pathogens and release inflammatory cytokines (Dixon et al., 2013). Dendritic cells are resident within the liver and act as antigen presenting cells, regulating responses to blood-borne pathogens while also contributing to hepatic immune tolerance and liver homeostasis (Rahman and Aloman, 2013). Neutrophils are absent from the liver in health and are present only during infection and inflammation (Gregory et al., 1996). The population of NK cells within the liver is different to that of the circulating blood volume, most liver resident NK cells are neural cell adhesion molecule bright ($CD56^{bright}$) in contrast to only 10% of blood NK cells (Hata et al., 1991). Regarding the adaptive immune system, CD4+ and CD8+ T-cells and B-cells are all found in the healthy liver (Norris et al., 1998). The adult liver also maintains a population of haemopoietic progenitor cells (Robinson et al., 2016).

Non-immune cells also have an immunological role in the liver microenvironment. LSECs regulate the immunity within the liver (Ebrahimkhani et al., 2011) and act as a barrier between the blood cells and hepatocytes **(Figure 1.4)**. They also control the stellate cells and inhibit fibrosis (Poisson et al., 2017). LSECs and hepatocytes can act as antigen presenting cells to activate T-cells (Thomson and Knolle, 2010). Consequently, an imbalance in the interaction between the immune cells and liver tissue has a role in disease leading to pathological inflammation (Robinson et al., 2016).

1.4.4 NK Cells and the Liver

NK cells have been shown to have an anti-fibrotic role on hepatic stellate cells. Activation of stellate cells leads to the overexpression of ligands which cause NK killing including NKG2D, UL 16 binding

protein 1 and 2 (ULBP 1 and 2) and MICA and MICB (Glassner et al., 2012). A study in 2008 showed that ethanol treated mice developed accelerated fibrosis in the presence of reduced NK activity (Jeong and Gao, 2008). Tregs (CD4+ cells) interact with NK cells affecting the development of fibrosis by two methods; direct cell to cell contact inhibition of NK cells and the release of soluble factors which downregulate NK activating receptor ligands (Langhans et al., 2015).

There is a specific intra-hepatic population of NK cells which are cluster of Differentiation 49 (CD49a) positive known as tissue resident NK cells (Marquardt et al., 2015). They are believed to be a more mature and terminally differentiated cohort of cells. Neural cell adhesion molecule dim ($CD56^{dim}$) liver resident NK cells are phentypically similar to peripheral NK cells and are believed to re-circulate (Mikulak et al., 2019). $CD56^{bright}$ liver resident NK cells are phenotypically different with higher levels of cluster of differentiation 69 (CD69) (Fan and Rudensky, 2016) and high levels of cytokine secretion (Tang et al., 2016).

1.5 Senescence

There are many consequences when a cell is subject to injury including DNA damage. These include DNA repair with a subsequent return to normal function, apoptosis, and cellular senescence. In the latter, progress through the cell cycle is arrested in gap 1 (G_1) phase **(Figure 1.6)** (Collado et al., 2007) and therefore cells are unable to undergo further cell division or respond to mitotic stimuli. **Figure 1.6** shows the normal cell cycle and how the cell cycle is arrested in senescence.

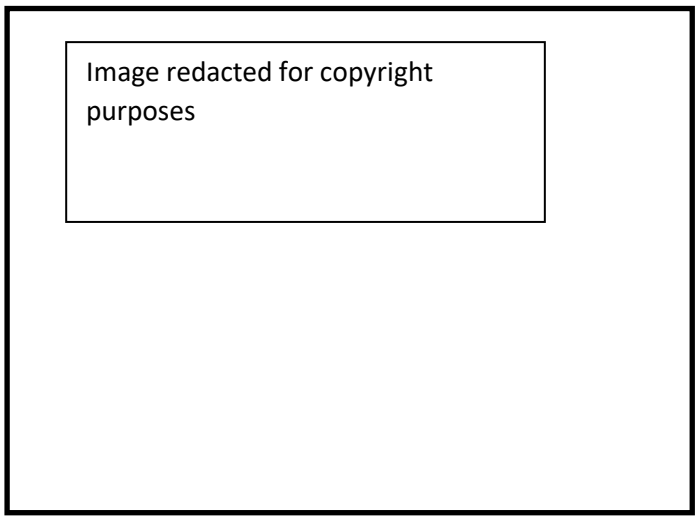

Figure 1.6 The normal cell cycle. *The quiescent or senescent phase is shown as G_0.*

Sourced from (Mind Anthology, 2012).

1.5.1 Cellular Senescence

Senescent cells are resistant to apoptosis as a consequence of altered enzyme production (Marcotte et al., 2004). The metabolic state of senescent cells is altered substantially, and the normal cell function is lost. The number of senescent cells increases with time in human organs and their function may be compromised by the accumulation of senescent cells (Campisi and Fagagna, 2007). A study of senescent cells present in skin naevi suggests they can persist in an unaltered state for many years (Michaloglou et al., 2005).

Senescent cells show altered gene expression. There is increased expression of inhibitors of cell cycle progression including cyclin dependent kinase inhibitor 1A (p21) and inhibitors of CDK4 (INK4) proteins including cyclin dependent kinase inhibitor 2A (p16) (Campisi, 2001), kinases which are controlled by the cellular tumour antigen p53 (p53) and retinoblastoma protein (pRB) pathways. In contrast, there is reduced expression of those factors that aid safe progression through the cell cycle, including the proto-oncogene c-fos (c-Fos) and cyclin family proteins A and B (Cyc A and B) which aid progression through the synthesis (S) and gap 2 phase (G_2) of the cell cycle respectively. Proliferating cell nuclear antigen (PCNA) (Stein et al., 1991), marker of proliferation Ki67 (Ki67) and mini-chromosome maintenance protein 2 (Mcm-2), which identify cells that have entered the cell cycle can be detected in senescent cells, but later cell cycle phase markers are not detected, indicative of slow cell cycle progress or cell cycle arrest.

Perhaps the only marker considered specific for senescent cells is expression of beta-galactosidase (β-galactosidase) (Trak-Smayra et al., 2004) but this can only be detected on fresh frozen sections with confidence. Senescent cells can also be identified by the presence of a group of markers including senescence associated DNA damage foci (SDF), for example phosphorylated H2A histone family member X (gamma (γ)H2AX) and p53 binding proteins (Campisi and Fagagna, 2007). They also express senescence associated heterochromatin foci (SAHF), which develop over several days and allow cells to remain stable in the senescent state as the SAHF inhibit the genes required for cell proliferation (Narita et al., 2003). Senescent cells have a specific phenotype, which can be seen readily with microscopy; cells are larger and flatter with increased nuclear size, and in the liver often show nuclear vacuolation (Aravinthan et al., 2012).

Cellular senescence needs to be distinguished from the normal ageing process, as the number of senescent cells in organs does increase with healthy ageing (Campisi and Fagagna, 2007) and studies have suggested that the functional deterioration of a particular organ may be due to the accumulation of senescent cells in that organ (Campisi, 2005).

Cell senescence has a protective role, preventing cells subjected to DNA damage from undergoing further proliferation, thereby protecting against tumorigenesis (Hanahan and Weinberg, 2000); the cause of DNA damage may be direct, related to oncogene activation or telomere shortening which occurs with healthy ageing and is accelerated in inflammatory conditions (Campisi and Fagagna, 2007, Ben-Porath and Weinberg, 2005).

1.5.2 Replicative Senescence

Replicative senescence was first described in 1961 (Hayflick and Moorhead, 1961), suggesting that cells stop dividing after a fixed number of cell divisions, which varied according to the cell type. Later work revealed that this phenomenon was related to the shortening of telomere DNA with each cell division, until there was a risk of damage to coding DNA which is followed by the induction of senescence (Harley et al., 1990).

Telomeres are repeated sequences of DNA at the end of each chromosome that prevent damage during replication (Akbar et al., 2004). DNA polymerase cannot replicate completely to the end of the DNA sequence, so that some telomere DNA is lost with each replicative cycle (Shay and Wright, 2007). Once the telomere is compromised then genomic DNA is susceptible to damage and a DNA damage signal induces senescence to prevent further replication (Schmucker and Wang, 1980). The length of the telomere can be used to assess the 'biological age' of a cell, which may be significantly older than its 'chronological age'. Lifestyle risk factors for shorter telomeres include obesity, excessive alcohol consumption, lack of exercise and smoking (Valdes et al., 2005) and shorter telomeres have been associated in a large number of studies with an earlier onset of age-related diseases and an increased mortality (Cawthon et al., 2003).

1.5.3 Senescence within the Immune System

Cellular senescence is also observed within the immune system. T-lymphocyte cells turn over constantly and in response to challenge. After a finite number of replications, T-cells eventually reach a mature stage where further replication is not possible. This is known as replicative senescence (Akbar et al., 2000); numerous longitudinal studies have shown that immune senescence is associated with an increase in age related disorders such as infections, malignancy and vascular disease and with increased mortality. Shorter lymphocyte telomeres correlate with worsening fibrosis and an adverse liver related outcome in patients with liver disease, including chronic HBV and HCV infection, ARLD and NAFLD as well as α1AT (Hoare et al., 2010a, Hoare et al., 2010b,

Tachtatzis et al., 2015, Mela et al., 2020). There is also evidence that lymphocyte telomere length correlates with clinical outcome in patients post-liver transplantation (Hoare et al., 2010b).

Cellular senescence can also be a response to oncogene activation or DNA damage by toxins or irradiation (Ben-Porath and Weinberg, 2005). Direct DNA damage occurs by oxidative stress, which subsequently leads to accelerated telomere shortening and the induction of senescence (Von-Zglinicki et al., 1995). Oncogene activation leads to senescence by inducing reactive oxygen species (ROS), which leads to oxidative damage of both DNA and protein (Lee et al., 1999). This also shortens telomeres and induces senescence.

Senescent cells induce senescence in surrounding cells in a paracrine manner (Nelson et al., 2012). This is a protective measure, which probably limits local growth signals and prevents malignant transformation in surrounding cells (Kuilman and Peeper, 2009). Unfortunately, senescent cells can also stimulate or aid tumour formation. The senescence associated secretory phenotype (SASP) may stimulate local tumour vascularisation via vascular endothelial growth factor (VEGF) (Coppé et al., 2006) or secrete other factors that promote cell proliferation.

1.5.4 Senescence in Liver Disease

An investigation into the difference between senescent hepatocytes and normal liver hepatocytes identified 354 genes that were upregulated in cellular senescence (Aravinthan et al., 2014). These were compared to published gene signatures of chronic liver disease which supported cellular senescence as the key to liver fibrosis. After analysis of these upregulated genes, a question highlighted is whether there is a role of the innate immune system in the preservation of these cells. This is due to the surprising presence of the NK cell ligands, NKG2A, killer cell lectin-like receptor C2 (NKG2C) and NKG2D within these genes.

Furthermore, increased numbers of senescent hepatocytes are associated with an increased hepatic fibrosis stage and an adverse liver related outcome (Aravinthan et al., 2013a). The hepatocyte expression of p21, a marker of senescence correlates with the severity of liver disease and fibrosis stage (Aravinthan et al., 2013b).

Senescent cells also secrete a variety of substances, known as the SASP, that act in a paracrine fashion and influence the local milieu (Shelton et al., 1999) maintaining the senescence state locally. It has been suggested that senescent hepatocytes and the SASP affect hepatic stellate cells and collagen deposition (Gonzalez-Reimers et al., 1988). It is also suggested that the SASP is pro-inflammatory (Kuilman et al., 2008), releasing factors including interleukin 6 (IL-6), that also

promote fibrogenesis. Of note, when hepatic stellate cells become senescent, they cease to produce collagen and instead, have been shown to limit further fibrosis (Krizhanovsky et al., 2008).

Senescence is therefore more beneficial to younger organisms, preventing malignant transformation but at the expense in later life of accelerated aging and an increased age-related mortality (known as antagonistic pleiotropy) (Kirkwood and Austad, 2000). A study designed to eradicate senescent cells in mice models, lead to mice that became resistant to age-related disease. They hypothesised that removing senescent cells prevented tissue dysfunction and prolonged survival (Baker et al., 2011).

Senescence can be regarded as potentially reversible. A study of liver transplant tissue was performed and immediately post implantation the level of senescent vascular cells in the donor liver was high. However, all vascular tissue was free of senescence when a second liver biopsy was performed within 30 days of liver transplantation. Since the major inflammatory event in the first 30 days post liver transplantation is acute rejection, where vascular tissue is the main target, the hypothesis is that a functioning recipient innate immune system clears donor vascular senescent cells since it is these that are the dominant infiltrating cells in acute rejection. By implication, failure of the innate immune system could allow an acute wound injury to mature to chronic inflammation with persistence of senescent hepatocytes in chronic liver injury (M Shah and G Alexander, personal communication).

Senescent cells can also be cleared by the immune system. Healthy murine hepatocytes were shown to develop senescence in vivo in response to oncogenes. The study identified that these newly senescent cells secreted chemokines and cytokines which activated the innate immune system leading to the removal or clearance of the senescent cells by macrophages (Kang et al., 2011).

Senescence has been described as an evolutionary development to remove unwanted structures and to support an embryo in development. However, the same process in later life is part of the response to damage or stress, to protect the cell against tumours or further tissue damage (Van-Deursen, 2014). The development of these senescent cells may protect against tumours, but their accumulation is at the expense of fibrosis and altered cell function.

1.5.5 Senescence in Pregnancy

While investigating the role of the innate immune system in pregnancy it was identified that NK cells become senescent in pregnancy (Moffett-King, 2002, Rajagopalan, 2014). Deciduous NK cells from first trimester abortions (Koopman et al., 2003) reveal upregulation of senescence associated genes, including IL-6, Interleukin 8 (IL-8), Interleukin 1 β (IL-1β) and p21. Paradoxically, it appears that cell

senescence favours foetal development during pregnancy. Senescent NK cells stimulated by HLA-G trophoblast cells prevent cell proliferation, NK mediated killing and promote the secretion of substances to aid the remodelling of the maternal vasculature (Rajagopalan, 2014). Recent studies have identified an association between pre-eclampsia and other adverse maternal complications with a prematurely aging placenta. Oxidative stress and vascular remodelling lead to mitochondrial dysfunction and cellular senescence (Manna et al., 2019, Sultana et al., 2017).

1.5.6 Parallel Between Senescence in Pregnancy and Liver Disease

The apparent tolerance to senescent hepatocytes in chronic liver disease intriguingly parallels the tolerance observed to the foetus during pregnancy. During pregnancy NK cells are key players in tolerance. However, these NK cells exhibit an altered functional phenotype typified by reduced cytotoxicity and an altered profile of cytokine secretion. Furthermore, these NK cells become senescent (Moffett-King, 2002, Rajagopalan, 2014). In the liver NK cells are also known to contribute to health and disease. Through release of pro-inflammatory cytokines, NK cells in the liver are involved in apoptosis of hepatocytes. In HBV infection the function of NK cells is impaired; a situation which favours HBV persistence (Peppa et al., 2010, Peppa et al., 2013). In addition, in patients with chronic liver disease NK cells can also control fibrosis (Wang and Yin, 2015, Glassner et al., 2012, Langhans et al., 2015). Furthermore, in mice reduced NK activity is associated with accelerated fibrosis (Jeong and Gao, 2008).

I hypothesise that NK cells are inhibited in chronic liver disease and that this consequently leads to an accumulation of senescent dysfunctional hepatocytes (Figure 1.7).

Of potential relevance, the array analysis of up-regulated genes following induction of senescence in vitro included the NK cell ligands NKG2 A/C/D (Aravinthan et al., 2014). The work will investigate if the engagement of inhibitory receptors and/or a failure of signalling through activating receptors in the immune system contributes to chronic liver disease.

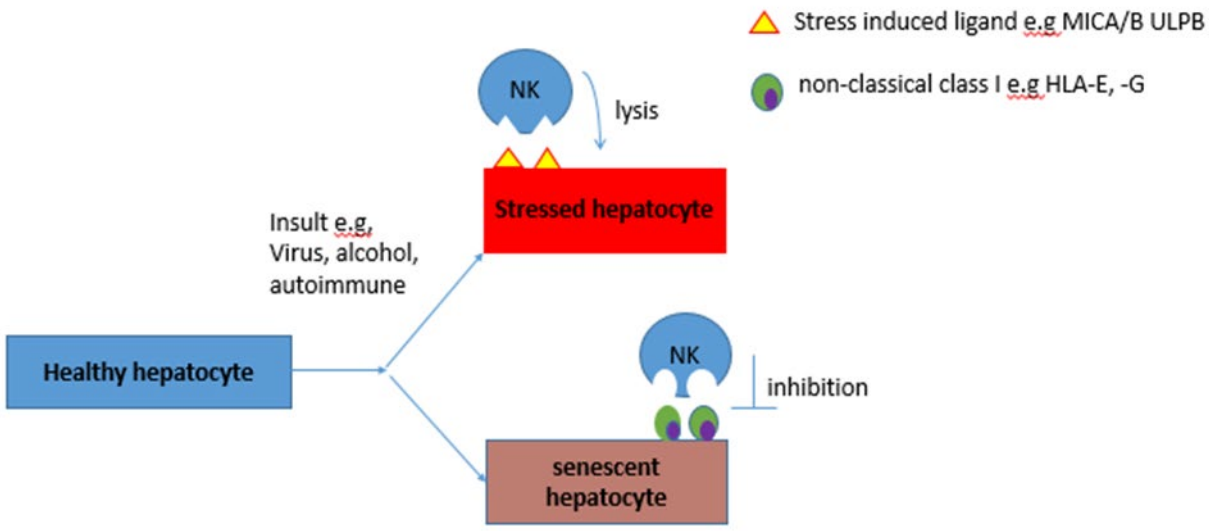

Figure 1.7 - Working model for the lack of clearance of senescent hepatocytes in chronic liver disease*. Healthy hepatocytes are injured by all causes of liver disease. I hypothesise that cell surface expression of stress induced ligands and MHC class I are altered in injured or stressed hepatocytes which can result in their clearance via NK cells. However, I propose in chronic liver disease hepatocytes become senescent, and express a different signature of ligands on their cell surface which results in resistance to NK cell clearance and consequently leads to accumulation of dysfunction hepatocytes and impaired organ function.*

1.6 Summary and Aims

Cellular senescence has real benefits for the cell, organ, and the host, but reversing senescence, if it was possible, is likely to carry an increased risk of malignancy. However, in the liver, cellular senescence in hepatocytes also drives fibrosis and is associated with a poor outcome. The quandary then is how to improve patient outcome without reversing cellular senescence in hepatocytes. The logical options are to induce apoptosis in senescent hepatocytes or to enhance removal of senescent hepatocytes, thereby allowing regeneration to replace the lost hepatocytes. NK cells become senescent during pregnancy, and I suggest they may also become senescent in chronic liver disease allowing the persistence of senescent hepatocytes.

I propose that senescent hepatocytes are removed from healthy liver but that in chronic liver disease there is a failure of homeostasis and senescent cells accumulate. Possible reasons for this inability to remove senescent hepatocytes include a failure of the immune system (Childs et al., 2014), a failure of apoptosis (Feng et al., 2007) or failure to reach the damage threshold required (Van-Deursen, 2014). The aim of my work is to investigate why senescent hepatocytes in patients

with liver disease are not recognised and removed by the immune system. Elucidating the molecular mechanisms underlying the lack of clearance of the senescent hepatocytes could potentially lead to novel targets for new interventions in liver disease.

Finally, TAPBPR a novel peptide editor in the antigen presentation pathway has not previously been studied in liver disease. I want to investigate whether it is expressed in human liver and whether it has a role in disease. As a novel protein it may have an aberrant function in the pathogenesis of cirrhosis.

1.7 Hypothesis

Hypothesis: Senescent hepatocytes accumulate in chronic liver disease due to a failure of detection and removal by the innate immune system (Figure 1.7).

In order to test this hypothesis, I will explore the following research questions:

1) Are there differences in the expression of NK cells ligands (e.g. MHC class I molecules) in healthy and diseased liver?

2) Are there differences in receptor expression on NK cells in healthy and diseased liver?

3) Is TAPBPR expressed in human liver, and does it have a role in the control of the immune system?

Chapter 2 Materials and Methods

2.1 Materials

2.1.1 Ethics

Ethical approval was granted by the Research Ethics Committee (REC) (reference 15/SC/0127) to collect human liver samples **(Appendix 2)**. Cirrhotic liver samples were collected from explant livers from patients who were undergoing liver transplantation at Addenbrooke's Hospital, Cambridge, UK. Ethical constraints and reality make it impossible to collect normal liver samples, so control liver tissue was collected from the healthy margins at liver resection for tumour metastases. These patients were all reviewed to ensure they did not have primary liver cancers. The liver sections were reviewed by an experienced liver histopathologist and considered to have normal appearances. However, while these tissues can never be considered truly normal, they are as close as is possible and controls are essential. These patients were selected to ensure they had not been exposed to chemotherapy agents prior to resection. Placenta tissue was provided by the Moffett laboratory, Department of Pathology, University of Cambridge. The health and gestation of the donated placental tissue was unknown. The Human Tissue Bank based at Addenbrooke's Hospital Cambridge, also provided what they considered to be liver and placenta samples with normal appearances. Ethical approval was also obtained to use surplus tissue obtained from liver biopsy samples.

Informed written consent **(Appendix 3)** was obtained from all donors by myself (Dr Anne Robins) or my colleague Dr Nicola Owen, a fellow Hepatology Registrar. 155 patients with cirrhosis were consented from which 33 liver samples were collected **(Table 2.1)**. 19 patients undergoing liver resection for metastatic tumours **(Table 2.2)** and 14 patients undergoing a routine liver biopsy **(Table 2.3)** were consented and tissue collected**.** The placenta tissue used is listed in **Table 2.4.**

All liver samples were collected by myself or my colleague Dr Nicola Owen directly from the theatre. Once the liver had been explanted or the resected segment removed, a small sample was isolated by the surgeon. The sample was snap frozen in liquid nitrogen before long term storage at minus 80 degrees centigrade (^{0}C). The samples were transported in batches on dry ice from Addenbrooke's Hospital to Department of Pathology, Tennis Court Road.

Paraffin embedded tissue sections of cirrhotic tissue, control liver and placenta were also provided by Addenbrooke's Hospital Tissue Bank. These were all anonymised, so that the only information I held was the underlying aetiology.

2.1.2 Human Tissue

Cirrhotic Sample	Cause of Liver Disease
L3	Alcohol Related Liver Disease
L6	Primary Biliary Cholangitis
L9	Alcohol Related Liver Disease
L11	Primary Biliary Cholangitis
L14	Hepatitis C / Hepatocellular Carcinoma
L16	Hepatitis C
L18	Alcohol Related Liver Disease / Non-Alcohol Related Fatty Liver Disease
L19	Hepatitis C
L21	Hepatitis C
L22	Hepatitis C / Alcohol Related Liver Disease
L24	Primary Biliary Cholangitis
L50	Non-Alcohol Related Fatty Liver Disease
L51	Primary Biliary Cholangitis
L52	Alpha-1-Anti-Tripsin Deficiency
L53	Alcohol Related Liver Disease
L54	Alcohol Related Liver Disease
L55	Non-Alcohol Related Fatty Liver disease
L56	Hepatitis C (RNA Negative Post Treatment)
L57	Hepatitis B (DNA Negative)
L58	Primary Sclerosing Cholangitis
L59	Primary Sclerosing Cholangitis
L60	Non-Alcohol Related Fatty Liver disease
L61	Primary Biliary Cholangitis
L62	Primary Sclerosing Cholangitis
L63	Primary Sclerosing Cholangitis
L64	Non-Alcohol Related Fatty Liver disease
L65	Hepatitis B
L66	Autoimmune Hepatitis
L67	Primary Biliary Cholangitis
L69	Alcohol Related Liver Disease
L70	Alcohol Related Liver Disease
L71	Hepatitis C
L73	Alcohol Related Liver Disease

Table 2.1 - Underlying aetiology of the cirrhotic samples

Control Sample	Tissue and Source	Background Liver Report
C2	Control Liver (Resection)	Normal
C3	Control Liver (Resection)	Normal
C4	Control Liver (Resection)	Normal
C5	Control Liver (Resection)	Normal
C6	Control Liver (Resection)	Normal
C7	Control Liver (Resection)	Normal but Mild Zone 3 Atrophy
C8	Control Liver (Resection)	Mild Steatosis
C10	Control Liver (Resection)	Normal
C11	Control Liver (resection)	Mild Steatosis
C12	Control Liver (Resection)	Normal but Surgical Handling Artefact
C13	Control Liver (Resection)	Moderate Steatosis
C14	Control Liver (Resection)	Moderate Steatosis
C15	Control Liver (Resection)	Mild Steatosis
N01	Control Liver (Tissue Bank)	Unknown
N02	Control Liver (Tissue Bank)	Unknown
N03	Control Liver (Tissue Bank)	Unknown
N04	Control Liver (Tissue Bank)	Unknown
N05	Control Liver (Tissue Bank)	Unknown

Table 2.2 – Control liver samples and source

Biopsy Samples	Cause of Liver Disease	Stage of Liver Disease
100	Autoimmune Hepatitis	Moderate Fibrosis
101	Non-Alcohol Related Fatty Liver Disease	Minimal Fibrosis
103	Non-Alcohol Related Fatty Liver Disease	Severe Fibrosis
104	Non-Alcohol Related Fatty Liver Disease	Cirrhosis
105	Non-Alcohol Related Fatty Liver Disease	Minimal Fibrosis
107	Non-Alcohol Related Fatty Liver Disease	Mild Fibrosis
108	Non-Alcohol Related Fatty Liver Disease	Moderate - Severe Fibrosis
109	Non-Alcohol Related Fatty Liver Disease	Mild - Moderate Fibrosis
110	Non-Alcohol Related Fatty Liver Disease	Mild - Moderate Fibrosis
111	Alcohol Related Liver Disease	Cirrhosis
112	Non-Alcohol Related Fatty Liver Disease	Cirrhosis
113	Hepatitis B	Mild Fibrosis
114	Hepatitis B (DNA Negative)	Mild Fibrosis

Table 2.3 - Underlying aetiology of the liver biopsy samples

Placenta Sample	Tissue and Source
P01	Placenta (Tissue Bank)
P02	Placenta (Tissue Bank)
P03	Placenta (Tissue Bank)
P4	Placenta (Moffett Lab)
P6	Placenta (Moffett Lab)
P87	Placenta (Moffett Lab)
P88	Placenta (Moffett Lab)
P90	Placenta (Moffett Lab)
P91	Placenta (Moffett Lab)

Table 2.4 – Placenta control samples and source

2.1.3 Blood Samples

Peripheral blood samples were also collected from healthy controls and patients with cirrhosis **(Table 2.5)**. Informed written consent was taken by myself (Dr Anne Robins) (REC reference 11/NE0356). The blood samples were collected by either myself or one of Addenbrookes' phlebotomists with their regular bloods. The peripheral blood mononuclear cells (PBMC) were isolated from the bloods the same day and stored at -80^{0}C. Acute rejection samples were donated for use in this study by Dr William Gelson, Consultant Hepatologist (REC reference 05/Q0104/38).

Sample	Aetiology	Age	Sex
Control 1	Control	41	Female
Control 2	Control	34	Male
Control 3	Control	21	Male
Control 4	Control	19	Female
Control 5	Control	20	Male
Cirrhotic 1	Primary Sclerosing Cholangitis	71	Male
Cirrhotic 2	Hepatitis C	65	Male
Cirrhotic 3	Hepatitis C	64	Male
Cirrhotic 4	Non-Alcohol Related Liver Disease	56	Female
Cirrhotic 5	Primary Sclerosing Cholangitis	48	Male
Cirrhotic 6	Primary Biliary Cholangitis	55	Female
Cirrhotic 7	Hepatitis C	65	Male
Cirrhotic 8	Primary Sclerosing Cholangitis	49	Male
Cirrhotic 9	Alcohol Related Liver Disease	56	Female
Acute Rejection 1	Acute Rejection	70	Female
Acute Rejection 2	Acute Rejection	51	Male
Acute Rejection 3	Acute Rejection	83	Female
Acute Rejection 4	Acute Rejection	46	Male
Acute Rejection 5	Acute Rejection	52	Female
Acute Rejection 6	Acute Rejection	25	Female

Table 2.5 - Blood samples and underlying aetiology

2.1.4 Antibodies

The details of the antibodies used with their concentrations for western blot **(Table 2.6)**, immunoprecipitation **(Table 2.7)**, immunohistochemistry **(Table 2.8-2.10)** and flow cytometry **(Table 2.11)** are described in the tables below.

Antibody Name	Target	Source	Species	Concentration	Usage	References
EMR 8-5	MHC Class I	Abcam Ab70328	Mouse	1mg/ml	1 in 5000	(Tsukahara et al., 2006)
HC10	MHC Class I	Hybridoma	Mouse	1mg/ml	1 in 5000	(Stam et al., 1986)
HCA2	MHC Class I	Hybridoma	Mouse	1mg/ml	1 in 5000	(Seitz et al., 1998)
L31	HLA-C	Media Pharma MP-AA-7	Mouse	0.5mg/ml	1 in 5000	(Beretta et al., 1987) (Setini et al., 1996)
MEME02	HLA-E	Abcam Ab2216	Mouse	1mg/ml	1 in 5000	(Menier et al., 2003)
MEME07	HLA-E	Abcam Ab11820	Mouse	1mg/ml	1 in 5000	(Palmisano et al., 2005)
3D11	HLA-F	Dan Geraghty / Jodie Goodridge	Mouse	1mg/ml	1 in 3000	(Lee and Geraghty, 2003) (Ishitani et al., 2003)
4A11	HLA-F	Dan Geraghty / Jodie Goodridge	Mouse	1mg/ml	1 in 3000	(Lee and Geraghty, 2003)
EPR6803	HLA-F	Abcam Ab126624	Rabbit	1mg/ml	1 in 5000	
4H84	HLA-G	Abcam Ab52455	Mouse	1mg/ml	1 in 2000	(Riteau et al., 2001b) (McMaster et al., 1998)
MEMG01	HLA-G	Abcam Ab7759	Mouse	1mg/ml	1 in 2000	(Menier et al., 2003) (Lozano et al., 2002) (Hurks et al., 2001)
RO21	TAPBPR	Hybridoma	Rabbit	5.2mg/ml	1 in 5000	(Hermann et al., 2013)
TAPBPR	TAPBPR	Abcam Ab57411	Mouse	0.5mg/ml	1 in 5000	
Rgp48n	Tapasin	Pete Cresswell	Mouse	1mg/ml	1 in 5000	(Sadasivan et al., 1996)

Tampe	TAP1	Robert Tampe	Mouse	3mg/ml	1 in 5000	(Fisette et al., 2016)
Calnexin	Calnexin	EnzoLife Sciences AD1-SPA-860	Rabbit	1mg/ml	1 in 5000	
UGT1	UGT1	Abcam Ab124879	Rabbit	1mg/ml	1 in 10000	
6C5	GAPDH	Abcam Ab8245	Rabbit	1mg/ml	1 in 1000	
Goat Anti-Mouse	Anti-Mouse	Dako P0447	Goat	1mg/ml	1 in 5000	
True Blot Anti-Mouse	Anti-Mouse	Rockland Antibodies 18-8817-33	Goat	1mg/ml	1 in 5000	
Goat Anti-Rabbit	Anti-Rabbit	Dako P0448	Goat	1mg/ml	1 in 5000	
True Blot Anti-Rabbit	Anti-Rabbit	Rockland Antibodies 18-8816-33	Goat	1mg/ml	1 in 5000	

Table 2.6 - The various antibodies used for western blotting experiments. *Their source and the conditions under which they were used.*

Antibody Name	Target	Source	Species	Concentration	Usage	References
W6/32	MHC Class I	Hybridoma	Mouse	1mg/ml	5µg per IP	(Parham et al., 1979) (Apps et al., 2009)
DT9	HLA-C and -E	Hybridoma	Mouse	1mg/ml	5µg per IP	(Braud et al., 1997)
3D12	HLA-E	Biosciences 342604	Mouse	0.5mg/ml	5µg per IP	(Lee et al., 1998)
3D11	HLA-F	Dan Geraghty / Jodie Goodridge	Mouse	1mg/ml	5µg per IP	(Lee and Geraghty, 2003) (Ishitani et al., 2003)
4A11	HLA-F	Dan Geraghty / Jodie Goodridge	Mouse	1mg/ml	5µg per IP	(Lee and Geraghty, 2003)
FG1	HLA-F	Eric Lepin / Christopher O'Callaghan	Mouse	3.5mg/ml	7µg per IP	(Lepin et al., 2000)
G233	HLA-G	Lucy Gardiner	Mouse	1mg/ml	5µg per IP	(Loke et al., 1997) (Apps et al., 2009)
MEMG09	HLA-G	Abcam Ab7758	Mouse	1mg/ml	5µg per IP	(Riteau et al., 2001a) (Menier et al., 2003)
PeTe4	TAPBPR	Hybridoma	Mouse	1.5mg/ml	6µg per IP	(Boyle et al., 2013)
R014	TAPBPR	Hybridoma	Rabbit	4.2mg/ml	8.4µg per IP	
Ring4C	TAP	Peter Creswell	Rabbit	1mg/ml	5µg per IP	(Ortmann et al., 1997)
Tampe	TAP	Robert Tampe	Mouse	3mg/ml	6µg per IP	(Meyer et al., 1994)
Pasta1	Tapasin	Peter Creswell	Mouse	1.2mg/ml	6µg per IP	(Dick et al., 2002)
IgG2a	IGg2a	Dako X0943	Mouse	1mg/ml	10µg per IP	

Table 2.7 - The various antibodies used for immunoprecipitation experiments. *Their source and the conditions under which they were used.*

Antibody name	Target	Source	Species	Concentration	Usage
HC10	MHC Class I	Hybridoma	Mouse	2.2mg/ml	1 in 500
L31	HLA-C	Mediapharma MP-AA-7	Mouse	0.5mg/ml	1 in 100
MEME02	HLA-E	Abcam Ab2216	Mouse	1mg/ml	1 in 100
FG1	HLA-F	Eric Lepin / Christopher O'Callaghan	Mouse	3.5mg/ml	1 in 200
MEMG01	HLA-G	Abcam Ab7759	Mouse	1mg /ml	1 in 100
P21	P21	Cell Signalling 2947	Rabbit	0.1mg/ml	1 in 50
P21	P21	Abcam Ab109520	Rabbit	1mg/ml	1 in 200
SX118	P21	Dako M7202	Mouse	1mg/ml	1 in 200
PeTe4	TAPBPR	Hybridoma	Mouse	2.2mg/ml	1 in 50
BM25	Mcm-2	Cinzia Scarpini	Mouse	1mg/ml	1 in 50

Table 2.8 - The various antibodies used for immunohistochemistry. *Their source and the conditions under which they were used.*

Target	Source	Species	Concentration	Usage
Anti-Mouse FITC	Sigma F9137	Goat	1mg/ml	1 in 100
Anti-FITC Rabbit	Invitrogen 711900	Rabbit	1mg/ml	1 in 300
Anti-Rabbit FITC	Sigma	Goat	1mg/ml	1 in 500

Table 2.9 - The various antibodies used for immunofluorescent experiments with a green fluorochrome. *Their source and the conditions under which they were used.*

Target	Source	Species	Concentration	Usage
Anti-Rabbit Biotin	Dako 0105	Goat	1mg/ml	1 in 200
Avidin Texas Red	Vector BA-2016	Rabbit	1mg/ml	1 in 400
Anti-Avidin Biotin	Vector BA 0800	Goat	1mg/ml	1 in 100
Avidin Cy3	Vector SA-1300	Rabbit	1mg/ml	1 in 400
Anti-Avidin Goat	Vector BA 0300	Goat	1mg/ml	1 in 100
m-IgGk (FL555)	Santa Cruz 516177	Mouse	Unknown	1 in 100

Table 2.10 - The various antibodies used for immunofluorescent experiments with a red fluorochrome. *Their source and the conditions under which they were used.*

Antibody Name	Target	Fluorochrome	Source	Concentration
ASGPR	ASGPR 1/2	PE	BD Pharmogen 563655	1 in 50
CD3	CD3	PE/Cy5	Biolegend 300310	1 in 200
CD4	CD4	BV510	Biolegend 317444	1 in 100
CD14	CD14	BV510	Biolegend 301842	1 in 100
CD16	CD16	AlexaFlor700	Biolegend 302026	1 in 100
CD19	CD19	BV510	Biolegend 202242	1 in 100
CD45	CD45	BV650	Biolegend 304044	1 in 100
CD49a	CD49a	Biotin	Miltenyi Biotech 130-101-404	1 in 25
CD56	CD56	PE/Dazzle	Biolegend 318348	1 in 200
CD57	CD57	Pacific Blue	Biolegend 322316	1 in 200
CD68	CD68	PE	Biolegend 333807	1 in 50
CD69	CD69	PE	Biolegend 310906	1 in 25
CK18	CK18	APC	Biolegend A657	1 in 50
NKG2A	NKG2A	FITC	Miltenyi Biotech 130-105-646	1 in 50
NKG2A	NKG2A	APC	Miltenyi Biotech 130-105-646	1 in 50
NKG2C	NKG2C	PE-Vio 770	Miltenyi Biotech 130-103637	1 in 50
LILRB1	LILRB1	PE/Cy7	Biolegend 222673	1 in 50
LILRB2	LILRB2	AF700	R and D Systems MAB2078	1 in 50
KIR2DL1	KIR2DL1	PE	Miltenyi Biotech 130-103-967	1 in 50
11PB6	KIR2DL1/ KIR2DS1	PE-Vio 770	Miltenyi Biotech 130-099-891	2ul for last 10 minutes
GL183	KIR2DL2/ KIR2DL3/ KIR2DS2	PerCP-5.5	Beckman A66900	1 in 50
KIR2DL3	KIR2DL3	FITC	Miltenyi Biotech 130-100-125	1 in 50
KIR2DL4	KIR2DL4	PE	Biolegend 347005	1 in 100
KIR3DL1/ KIR3DS1	KIR3DL1/ KIR3DS1	APC	Beckman PN-A60795	1 in 50
KIR3DL1	KIR3DL1	BV421	Biolegend 312714	1 in 100
Anti-DCM	Dead Cell	Ultra-red	Lifetech L10119	1 in 400
QD605	QD605	Streptavidin	Lifetech Q1010IMP	1 in 400

Table 2.11 - The various antibodies used in flow cytometry experiments*. Their target, source, and the conditions under which they were used.*

2.1.5 Oligonucleotides

All primers were designed against the open reading frame of the gene of interest using the Primer3 website (http://bioinfo.ut.ee/primer3-0.4.0/). To work with the previous established polymerase chain reaction (PCR) cycler conditions, the melting temperature for all primers was chosen to be 60˚C and the total length of the amplicon was chosen to be between 80 to 140 base pairs in total length. For each gene of interest, three different primer pair combinations were designed and tested for efficiency with different complementary DNA (cDNA) concentrations (R-squared (R^2) > 0.95). The primer combination with the highest R^2 value was used in this study **(Table 2.12)**. All oligonucleotides were purchased from Sigma.

Primer	Sequence
HLA-C Forward	ATCGTTGCTGGCCTGGCTGTCCT
HLA-C Reverse	TCATCAGAGCCCTGGGCACTGTT
HLA-E Forward	GAAGGGGGTCATGGTAGACA
HLA-E Reverse	GGCAGAGGAATATGCAGAGG
HLA-F Forward	GGGGACTCTGGCTTCTCTTT
HLA-F Reverse	TGTAGCGTCTCCTTCCCATT
HLA-G Forward	AGGAGACACGGAACACCAAG
HLA-G Reverse	GCATACTGTTCATACCCGCG
HPRT Forward	GTAGCCCTCTGTGTGCTCAA
HPRT Reverse	TCACTATTTCTATTCAGTGCTTTGATG
Calnexin Forward	GAGCAGGTGGCTTGTTAAGG
Calnexin Reverse	AGCTGGGGATCTGAGGAAAT
Actinin Forward	TATCTGTGTCGGCTGTCTCG
Actinin Reverse	GCATCATGAGCATTGTGGAC
18s Forward	GCAATTATTCCCCATGAACG
18s Reverse	CTCCCATTCTCCATCCATGT
GAPDH Forward	ACACCCACTCCTCCACCTTT
GAPDH Reverse	TGACAAAGTGGTCGTTGAGG

Table 2.12 - The primers used in PCR experiments and the nature of the target sequence.

2.2 Methods

2.2.1 Formation of Liver Lysate Samples

A small piece of liver tissue was cut from the sample while it was still frozen, chopped into small pieces and added to one millilitre (ml) of lysate solution. The solution was prepared as follows; tris(hydroxymethyl)aminomethane (tris)-buffered saline (TBS) (20 millimolar (mM) tris-hydrochloric acid (HCL) (power of hydrogen (pH) 7.4), 150mM sodium chloride (NaCl), 2.5mM calcium chloride ($CaCl_2$)), containing 1mM phenylmethylsulfonyl fluoride (PMSF) (Sigma), 10mM N-ethylmaleimide (NEM) (Sigma), 1 in 50 dilution of protease inhibitor cocktail tablets (Roche) and 1% 2-(4-(2,4,4-

trimthylpentan-2-yl) phenoxy) ethanol (triton X-100). Triton X-100 was excluded from the solution when samples were prepared for digitonin-based immunoprecipitation and for experiments into the antigen presentation pathway. Initial experiments were undertaken in ripa (20 mM Tris-HCl (pH 7.5) 150 mM NaCl, 1 mM ethylenediaminetetraacetic acid disodium salt dihydrate (Na_2EDTA), 1 mM ethylene glycol-bis (β-aminoethyl ether)-N, N, N', N'-tetraacetic acid (EGTA), 1% nonyl phenoxypolyethoxylethanol (NP-40), 1% sodium deoxycholate, 2.5 mM sodium pyrophosphate, 1 mM β-glycerophosphate, 1 mM Sodium vanadate (Na_3VO_4) and one microgram (µg) per ml leupeptin). The lysate was formed using a gentleMACS dissociator (Miltenyl Biotec) and then snap frozen in small aliquots. A protein assay was undertaken on all lysate samples using Pierce Thermo-scientific kit 2322715 to assess the protein concentration.

2.2.2 Gel Electrophoresis and Western Blotting

Liver lysates containing 10µg of protein were loaded into a 10% acrylamide gel (2.75ml water (H_2O), 3.75ml one molar (M) tris-HCL (pH 8.8), 100 microlitres (µl) 10% sodium dodecyl sulfate (SDS), 3.4ml 30% acrylamide, 70µl 2-Acrylamido-2-methylpropane sulfonic acid (AMPS) and 7µl N, N, N', N'-tetramethylethylenediamine (TEMED)). Separation of proteins by gel electrophoresis was then carried out at 200 volts (V) using the biorad system. The proteins were transferred onto an immobilon transfer membrane (Millipore) at 100V for 90 minutes. The membrane was blocked with 0.5% marvel blocking solution for 30 minutes (five-gram (g) marvel milk power in 100ml of 0.05% polyethylene glycol sorbitan monolaurate (tween20) in phosphate buffered saline (PBS)). The primary antibody **(Table 2.6)** was incubated for two hours at room temperature (or 4˚C overnight) on spiramix. The membrane was washed in tween20 in PBS three times for ten minutes. The secondary antibody **(Table 2.6)** was incubated for one hour on spiramix. Finally, the membrane was washed again as above and developed using enhanced chemiluminescence reagent (western lightning; Perkin Elmer) and exposed on X-ray film to visualise the protein band.

2.2.3 Immunoprecipitation

Immunoprecipitation (IP) was undertaken on samples lysed with 1% triton X-100 (HLA work) or 1% digitonin (antigen presentation pathway and mass spectrometry) in TBS, containing 1mM PMSF, 10mM NEM and 1 in 50 dilution of protease inhibitor cocktail tablets. The volume of lysate required for 100µg of protein was identified by the protein assay and additional lysis buffer added to make the final volume 1ml. Cell lysis was performed on rotation at 4˚C for 30 minutes. The samples were then centrifuged at 12000 times gravity (xg) for 20 minutes. Pre-clear was performed twice with a

mixture of protein A (or G depending on the antibody) (Generon) and immunoglobulin G (IgG) sepharose beads (Biosciences) for 30 minutes at 4˚C rotation. The samples were again centrifuged at 12000xg for two minutes. Lysate samples of 50µl were removed at this stage. Immunoprecipitation was then performed on the residual lysate for two hours at 4˚C rotation with the antibody at a concentration of 5µg per IP and protein A (or G depending on the antibody) beads (Generon). Following immunoprecipitation, the beads were washed thoroughly (seven times) in 1ml of 0.1% TBS-tween20. The bound proteins were eluted by heating the samples to 99˚C for ten minutes in reducing sample buffer (125 nanomolar (nM) tris-HCL (pH 6.8), 4% SDS, 20% Glycerol, 0.04% bromophenol blue) containing β-mercaptoethanol (80µl reducing sample buffer added to IP samples and 50µl to lysate samples). Separation was then undertaken by gel electrophoresis (20µl sample loaded per well) and analysis by western blotting.

2.2.4 Immunoprecipitation using Antibodies which Recognise Non-Conformational Epitopes

100µg protein lysate mixed with denaturing lysis buffer (1% SDS, Tris-NaCl with DL-dithiothreitol (DTT) (stock solution 1M used 1 in 100) and benzonaze (15µl in 10ml) and made up to 100µl. The samples were then boiled to 96˚C for ten minutes before cooling for a further ten minutes. 900µl quenching buffer (1% Tris-NaCl with 20mM Idoactamide (IAA)) was then added and the samples were left to react for ten minutes at room temperature. Immunoprecipitation, gel electrophoresis and western blotting were undertaken as described above.

2.2.5 Endoglycosidase H Digest

Immunoprecipitated samples were mixed with 1000units of Endoglycosidase H (Endo H) (New England Biolabs) in buffer for one hour at 37˚C. Gel electrophoresis and western blot analysis was then undertaken as described above.

2.2.6 Immunoprecipitation and Mass Spectrometry

Immunoprecipitations were performed using digitonin and samples sent for mass spectroscopy performed by Robin Antrobus (Cambridge Institute for Medical Research).

2.2.7 RNA Extraction

RNA was extracted from human liver cells using RNeasy Mini Kit (Qiagen) and eluted in RNAse free water following manufacturers' instructions. Subsequently, the concentration of the extracted RNA was measured using a NANODROP LITE photometer (Thermo Fisher Scientific). Samples were only used for cDNA synthesis if the RNA concentration was above 100 nanograms (ng) per µl. All RNA samples were stored at -80˚C.

2.2.8 Reverse Transcription of RNA

For cDNA synthesis, 1µg of extracted RNA was reverse transcribed using the RevertAid First Strand cDNA Synthesis Kit (Thermo Fisher Scientific) with the oligo deoxythymine 18 (dT(18)) primer provided according to the manufacturers' protocol.

2.2.9 Quantitative Real-Time PCR

Quantitative real-time PCR (qRT-PCR) was performed using the Quanti-Tech SYBR Green 2x Mix (Qiagen) on a 7500 fast real-time PCR system cycler (Applied Biosystems) in 96 well PCR plate format. 50ng cDNA in 10µl double distilled water (ddH_20), 0.6µl forward primer and 0.6µl reverse primer **(Table 2.12)** in a total volume of 20µl SYBR Green Mix was used for every reaction.

All reaction mixes were prepared on ice. Each sample was run in triplicates and each experiment was performed at least three times. The PCR was performed under following conditions **(Figure 2.13)**.

Temperature (Degrees Centigrade)	Time (Minutes)	Number of Cycles
95	15.00	1
94 60 72	0.15 0.30 0.33	40
95	0.15	1
60	1.00	1
95	0.15	1

Table 2.13 - The temperature, duration, and number of cycles during PCR. *The last three steps are the primer dissociation curve to ensure that the primer binding worked correctly.*

2.2.10 Agarose Gel

To ensure that the correct cDNA fragments were amplified in the qRT-PCR reactions, selected DNA fragments from each experiment were separated for analysis by agarose gel electrophoresis using 3% agarose. Agarose powder was dissolved in 1,1,2,2-Tetrabromoethane (TBE) (10xTBE 0.89M Tris, 0.89M boric acid and 20mM Na_2EDTA) by boiling. The liquid agarose was poured into a gel cast system mixed with 6µl of ethidium bromide solution (Sigma). 10µl of the DNA sample was mixed with 2µl of DNA loading buffer (Thermo Fisher Scientific) prior to loading onto the gel. GeneRuler Low Range DNA ladder (Thermo Fisher Scientific) was used as a standard. The agarose gel was run at 80V for one hour or until separation of the fragments was achieved. Bands were visualized on a Syngene G:Box using ultraviolet (UV) light.

2.2.11 Sequencing

For sequencing of selected DNA fragments, the required fragments were cut from the agarose gel and DNA was extracted from the gel piece using NucleoSpin Gel and PCR clean up kit (Macherey Nagel 740609.50) following manufacturers' instructions. Samples were sent for overnight sequencing to SourceBioscience (Cambridge) using the same forward primer that was used in the qRT-PCR reaction.

2.2.12 Immunohistochemistry Single Staining

Paraffin embedded slides were initially de-waxed and rehydrated using xylene, followed by reducing concentrations of ethanol (20 minutes in xylene followed by five minutes at 100%, 90%, 70% and 50% ethanol). Antigen retrieval was then performed with ethylene-diamine-tetra-acetic acid (EDTA) buffer for seven minutes in pressure cooker. The slides were blocked with hydrogen peroxide (H_20_2) for 30 minutes. Further blocking of the antibody was performed with 10% goat serum mixed with bovine serum albumin (BSA) (30 milligram (mg) BSA, 300µl goat serum and 2.7ml TBS) for two hours at room temperature. The primary antibody **(Table 2.8)** was incubated overnight at 4˚C mixed with 1% BSA with TBS and 0.1% Triton (30mg BSA, 0.9ml 0.3% Triton in TBS and 2.1ml TBS). Slides were washed twice for five minutes with TBS between each step. A secondary antibody kit for peroxidase was then used for one hour at room temperature (Goat Anti-Mouse Dako Envision R System HRP K4006 or Goat Anti-Rabbit ImmPRESS MP-7451). The slides were then stained using 3, 3'-diaminobenzidine (DAB) substrate (Dako) for ten minutes. Finally, the slides with stained with haematoxylin for 30 seconds. The slides underwent dehydration with increasing concentrations of ethanol and xylene before mounting in dibutylphthalate polystyrene xylene (DPX).

2.2.13 Immunohistochemistry Dual Staining

Dual staining was initially performed with Envision G/2 Double Stain System (Dako K5361); however excessive background and some cross reactivity was noted and therefore I designed a new protocol.

Slides were initially de-waxed and rehydrated with xylene and reducing concentrations of ethanol; twice for ten minutes in xylene followed by five minutes at 100%, 90%, 70% and 50% ethanol. Antigen retrieval was performed in EDTA buffer for seven minutes in a pressure cooker. Slides were blocked with H_20_2 for 30 minutes. Blocking of the antibody was performed with 10% goat serum mixed with BSA (30mg BSA, 300µl goat serum and 2.7ml TBS) for two hours at room temperature. The primary antibody **(Table 2.8)** was incubated overnight at 4°C mixed with 1% BSA with TBS and 0.1% Triton (30mg BSA, 0.9ml 0.3% Triton in TBS and 2.1ml TBS). Samples were washed with TBS between each step. A secondary antibody kit was then used for one hour at room temperature either mouse or rabbit (Dako). Samples were then stained using DAB substrate for ten minutes. The samples were then blocked with 10µl dual stain block (Dako K5361) before a further block with 10% goat serum (30mg BSA, 300µl goat serum and 2.7ml TBS) for two hours. The second primary antibody **(Table 2.8)** was added overnight at 4°C mixed with 1% BSA with TBS and 0.1% Triton (30mg BSA, 0.9ml 0.3% Triton in TBS and 2.1ml TBS) before the secondary antibody with alkaline phosphatase (Goat Anti-Rabbit ImmPRESS AP reagent kit MP-5401) for one hour at room temperature. Fast red (Sigma F4648) or fast blue (Sigma B-5655) was mixed with levamizole (1mM) block for 20 minutes at room temperature. 10µl Dapi was then added for ten minutes at room temperature. Finally, the slides were mounted in Vectashield (Vectalaboratories).

2.2.14 Immunofluorescence

Initial preparation for immunofluorescence was as above for immunohistochemistry. Following rehydration, de-waxing, antigen retrieval and blocking the primary antibody **(Table 2.8)** was incubated overnight at 4°C mixed with BSA and TBS (30mg BSA, 0.9ml 0.3% Triton in TBS and 2.1ml TBS). Slides were washed twice with TBS for five minutes between each step. The secondary antibody **(Tables 2.9 and 2.10)** was incubated for one hour at room temperature before staining with 10µl Dapi for ten minutes at room temperature. A blocking solution or method was used at this stage if required. The stained slides were mounted in Vectashield (Vectalaboratories).

2.2.15 Auto-Fluorescent Blocking

Several methods of auto-fluorescent blocking were trialled.

1. Vecta-shield 927301: avidin/biotin block as per manufacturers' instructions.
2. Copper Sulphate: 100mM copper sulphate in 500mM ammonia acetate; slides blocked for two hours.
3. Erichrome Black T (1.65%) in TBS; slides blocked for ten minutes.
4. UV radiation prior to antigen retrieval; dose for two or 12 hours.

2.2.16 Analysis of Immunohistochemistry

The slides were scanned, and four random sections taken from each sample. A likert scale was designed for each molecule and staining graded 1-5. Images were reviewed by myself and a random sample also assessed by my supervisor. The development of the techniques was supervised by Dr Cinzia Scarpini. Qualitative and quantitative analyses of the immunohistochemistry was undertaken primarily by myself, with support from Professor Alexander, Professor Coleman and Dr Cinzia Scarpini.

2.2.17 Isolation of Cells from Liver Segment or Biopsy

Samples were placed on a petri dish and covered with 100µl roswell park memorial institute media (RPMI). The cells were prised gently from the fibrous tissue of the liver. A further 10ml RPMI was added to the sample which was transferred into a universal container. The sample was centrifuged at 450xg for ten minutes before washing twice with PBS.

2.2.18 Isolation of Peripheral Blood Mononuclear Cells from Blood Samples

The isolation fluid comprised of 2.5g bovine albumin added to 500ml phosphate buffered saline with albumin (PBSA). 10mls of Lymphoprep (Sigma) were placed in falcon tube while the blood sample was poured into a labelled falcon tube with 10mls of PBSA added. The collected blood sample was slowly pipetted onto the Lymphoprep. The falcon tube was then centrifuged for 20 minutes at 450xg with low acceleration and brakes on settings.

A pasteur pipette was used to isolate the PBMC layer, which was transferred into a universal container and centrifuged for ten minutes at 450xg with the brakes on. The supernatant was discarded and 10ml PBSA was added to the cell pellet. After two repeat washes, 10µl of cell

suspension was mixed with 10µl 0.4% tryptan blue to count cells. The cell number was adjusted to 10 x 10^6 cells in 100µl.

2.2.19 Freeze and Thawing of Peripheral Blood Mononuclear Cell Samples

Freeze

Mr Frosty freezing container (Thermo-Scientific) was prepared by adding isopropyl alcohol. The cells were spun for five minutes at 360xg and the supernatant was discarded. Cells were frozen at 10 x 10^6 per ml in each cryo-vial. 1ml freezer mix (1ml dimethylsulphoxide (DMSO), 2ml RPMI and 2ml fetal calf serum (FCS)) was added to each cell pellet before re-suspension, with 1ml placed in each cryo-vial. Mr Frosty was placed in -80°C freezer for 48 hours before cells were transferred to liquid nitrogen.

Thaw

10ml RPMI with 20% FCS (8ml RPMI and 2ml FCS) was heated in a water bath. The cells were thawed in the water bath at 37°C until almost thawed before filling the cryo-vial with pre-warmed media. The sample was centrifuged at 220xg for seven minutes and the cells were re-suspended in 3ml RPMI before counting the cells.

2.2.20 Flow Cytometry

The prepared cells were washed and split into staining wells on a 96-well plate with 10 x 10^6 cells per well, then washed in fluorescence activated cell sorting (facs) wash (PBS with 2mM EDTA and 2% FCS) for five minutes followed by two minutes centrifuge at 360xg. The primary antibody **(Table 2.11)** was added for 30 minutes at 4°C followed by two washes. The secondary antibody (including dead cell marker (DCM)) **(Table 2.11)** was added for 20 minutes at 4°C followed by two washes. If no intracellular staining was required, the cells were fixed in 1% paraformaldyhyde (PFA) for ten minutes at 4°C. When intracellular staining was required fix/perm buffer was added (ebiosciences 00.512343 and 00.522356) for 45 minutes at 4°C, before washes with fix/perm wash (ebiosciences 00.83335) and then an intracellular stain for 30 minutes at 4°C. The samples were washed, 150µl of facs wash added for analysis and stored at 4°C. Samples were run on the Fortessa and analysed using Flow Jo Software.

Chapter 3 Results - Characterisation of MHC Class I Expression in Liver Tissue

3.1 Introduction

One hypothesis being tested in my thesis is that senescent hepatocytes are removed from healthy liver and acute injury with resolution, but that senescent hepatocytes accumulate in chronic liver disease because of a failure of the innate immune system. One possible hypothesis for the evolution of cirrhosis is that the failure to clear senescent hepatocytes in chronic liver injury is a form of tolerance, thus resembling the failure of the maternal immune system to detect the foetus (Ferreira et al., 2017), mediated in part by senescent NK cells. It is in the best interest of the liver not to delete DNA-damaged hepatocytes because of the risk of liver failure, but to maintain hepatocyte numbers and liver structure with induction of hepatocyte senescence. One process by which the failure to clear senescent hepatocytes from the diseased liver might be mediated could be via altered expression of MHC class I molecules.

The classical MHC class I molecules, HLA-A, -B and -C, play a key role in antigen presentation to CD8+ T-cells and NK cells (Carrillo-Bustamante et al., 2016), acting as ligands for the innate immune system. Surface expression of HLA-E is thought to be a complimentary system by which the immune system can determine if a cell has normal antigen presentation and processing pathways. HLA-E molecules are recognised and interact with NK cells expressing a CD94:NKG2 subunit.

Previous work has shown that classical HLA class I molecules are expressed in normal human liver (Boegel et al., 2018). Furthermore, immunohistochemistry has previously confirmed the presence of HLA class I on normal and cirrhotic hepatocytes from liver biopsies (Fukusato et al., 1986). Interestingly, however, altered expression of non-classical MHC class I, specifically HLA-G, has been linked with liver disease. A study in liver transplant recipients revealed that HLA-G was detected by immunohistochemistry in cirrhosis on hepatocytes, but not other hepatic cell lines (Moroso et al., 2015). Furthermore, independent studies using immunohistochemistry have reported that the presence of hepatocyte HLA-G is associated with a poor prognosis in chronic hepatitis B virus infection (Souto et al., 2011) and hepatocellular carcinoma (Catamo et al., 2014, Cai et al., 2009). Typically, HLA-G is considered in the context of inducing tolerance at the maternal-foetal interface, being uniquely expressed on extra-villous trophoblast (Kovats et al., 1990). While there have been many reports linking HLA-G expression in tumours to disease progression and poor prognosis, for example in metastatic melanoma (Ibrahim et al., 2004, Paul et al., 1999), many of these studies are somewhat controversial primarily because the antibodies initially used to detect HLA-G i.e. HCA2 and 4H84 have subsequently been shown to cross-react with HLA-A, HLA-B, and HLA-E (Seitz et al., 1998, Zhao et al., 2012b). Thus, careful attention needs to be paid to both the techniques and the

reagents used to when investigating the expression of HLA molecules in tissues. In the context of liver disease, to date, HLA-G expression has only been investigated using immunohistochemistry and the antibodies MEMG01 and MEMG02 (Moroso et al., 2015, Cai et al., 2009). Ideally, results should be verified using several molecular and biochemical methods to further validate any findings.

In this chapter I investigate the expression of both classical and non-classical MHC class I molecules in both healthy and diseased liver tissue using a variety of techniques and antibodies in order to determine if there are differences in the expression of NK cell ligands (e.g. MHC class I) between healthy and diseased liver.

3.2 HLA Class I is Expressed in Human Liver

Initially, I performed exploratory experiments using western blot analysis to examine whether the expression of both classical HLA and non-classical HLA molecules could be detected in frozen human liver tissue. In the first instance, western blot analysis was performed to detect HLA expression from four cirrhotic samples (L3, L9, L19 and L22). A sample of healthy liver (C) and placenta (P) which should express HLA-G as well as HLA-E, were included as controls provided by the human tissue bank.

Using EMR 8-5, an antibody reported to detect classical HLA class I (Tsukahara et al., 2006), a band between 40-45 kilodalton (kDa) in size, which corresponds to the expected expression of MHC class I, was detected **(Figure 3.1)**. The results suggested expression of HLA class I may be higher in the cirrhotic samples than control or placenta. Using the antibody MEME07 (Palmisano et al., 2005) for detection of HLA-E, a single band which ran at approximately (~) 43kDa was clearly detected in the placenta sample **(Figure 3.1)**. However, this antibody failed to detect any protein in the liver sample from the healthy control **(Figure 3.1)**. Surprisingly, western blotting using MEME07 detected a double band at ~43 & ~45kDa in three out of the four cirrhotic samples while in the other cirrhotic sample (L3), a single band at 45kDa was detected **(Figure 3.1)**. Upon staining with EPR6803, an antibody supposedly specific for HLA-F detected single band which ran at 41kDa in all samples, with no difference in intensity between the various conditions **(Figure 3.1)**. While blotting using MEMG01 to detect HLA-G (Menier et al., 2003), a band was detected at around 39kDa, the expected size for HLA-G, in the cirrhotic tissue and the placental control with of similar intensity, but failed to detect protein in the control liver tissue **(Figure 3.1)**. Blotting for glyceraldehyde 3-phosphate dehydrogenase (GAPDH) as a loading control suggested all control and cirrhotic liver samples were equal but suggested there was some underloading of the placenta sample **(Figure 3.1)**.

While these initial results were suggestive that both classical MHC class I and non-classical MHC class I could be identified from frozen liver lysate samples by western blotting, using antibodies highly specific to the HLA protein is vital to obtain specific results.

However, work on HLA class I is difficult as the different molecules share similar sequences but also exhibit marked polymorphism (Apps et al., 2009). This means that antibodies designed to detect specific MHC class I molecules may cross react with others (Apps et al., 2009). Another difficultly in this series of experiments is that the samples were anonymised and consequently the HLA tissue type of the liver samples was not known, emphasising the importance of determining cross reactivity. Following research into this area including a literature review and discussions with experienced colleagues, a more refined panel of antibodies was picked carefully to try to ensure optimal specificity for subsequent experiments.

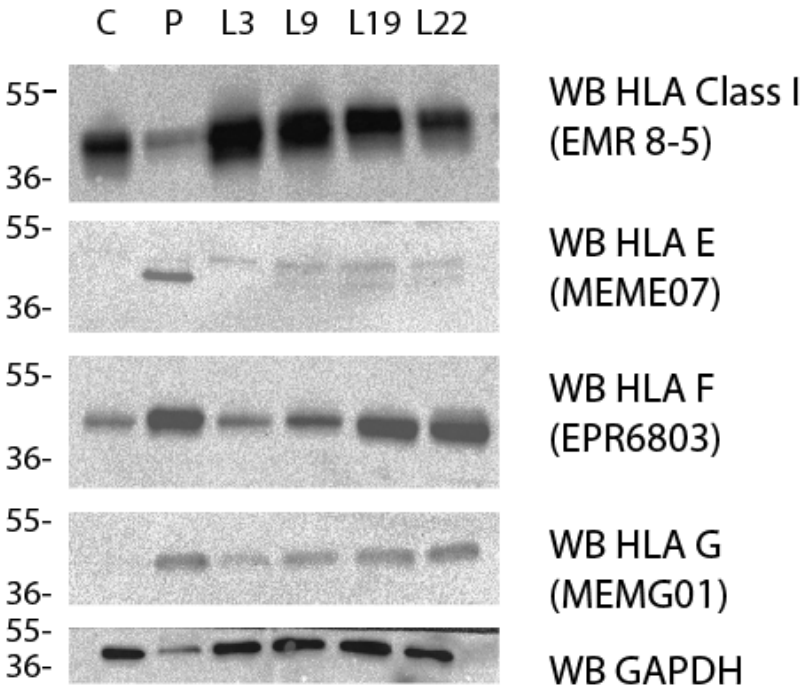

Figure 3.1 – Detection of HLA class I in human liver. *Western blot analysis was performed on whole lysate samples from cirrhosis (L3, L9, L19 & L22), a healthy liver (C) and from placenta (P) using the antibodies EMR 8-5 to detect classical HLA-A, -B, & -C, MEME07 to detect HLA-E, EPR6803 to detect HLA-F and MEMG01 to detect HLA-G. Western blotting for GAPDH was included as a loading control.*

3.3 Characterising the Expression of Classical MHC Class I in Liver

3.3.1 Western Blot Analysis using HC10 and HCA2 Suggests Increased Expression of Classical HLA Class I in Cirrhosis Compared with Healthy Liver

In the preliminary experiment in **Figure 3.1**, the antibody EMR 8-5 was used to detect classical MHC class I molecules. However, it is known that it only reacts with the following HLA class I isotypes (Tsukahara et al., 2006):

HLA-A*2402, A*0101, A*1101, A*0201, A*0207, B*0702, B*0801, B*1501, B*3501, B*4001, B*4002, B*4006, B*4403, Cw*0102, Cw*0801, Cw*1202 and Cw*1502. Therefore, it was decided to use alternative antibodies, which would cover a broader range of HLA-A, -B, and -C molecules. The antibodies selected were HC10 and HCA2.

HC10 antibody is known to react with the majority of HLA-B and -C heavy chains and a well-defined series of HLA-A heavy chains (HLA-A10, HLA-A28, HLA-A29, HLA-A30, HLA-A31, HLA-A32, HLA-A33) (Stam et al., 1986). HCA2 has been shown to react with many the HLA-A molecules. Furthermore, HCA2 has also been found to react with HLA-E and HLA-G molecules (Seitz et al., 1998). Used in combination, these two antibodies will cover the majority of HLA-A, -B and -C subtypes.

Further western blot analysis was undertaken to investigate the expression of MHC class I in a larger number of control and cirrhotic samples to confirm the early results. A panel was developed to include two placenta control samples, four control livers and eight cirrhotic livers covering a broad range of aetiologies **(Tables 2.1-2.4**, pages 24-26).

Using HC10 and HCA2 for detection, a 43kDa band was seen in all samples confirming detectable expression of HLA class I protein in the tested liver samples and placental tissue **(Figure 3.2).** The results also suggested there may be increased expression of MHC class I in cirrhotic samples compared to the placenta and the healthy liver controls. Western blotting for calnexin as a loading control suggested higher protein loading per lane for samples from the placenta and control liver samples compared with the cirrhotic samples **(Figure 3.2)**, further supporting the notion that MHC class I expression may be higher in cirrhosis than in healthy liver tissue or placenta.

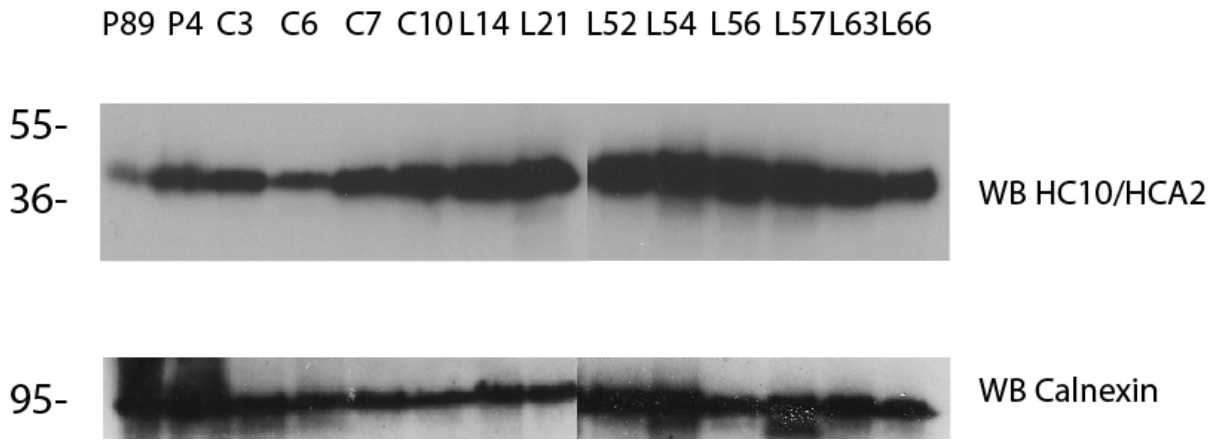

Figure 3.2 – Detection of classical MHC class I in human liver using HC10 and HCA2. *Western blot analysis was performed on whole lysate samples from cirrhotic tissue (L14-L66), healthy control liver (C3-C7) and from placental tissue (P89 & P4) using the antibodies HC10 and HCA2 to detect HLA-A, -B, & -C. Western blotting for calnexin was included as a loading control.*

3.3.2 Immunoprecipitation Experiments Confirm the Presence of HLA Class I in Liver Tissue and Suggest Higher Expression in Cirrhosis

In order to validate the expression of MHC class I in liver samples and ensure the protein bands detected were indeed MHC class I heavy chain, a second approach was employed, namely immunoprecipitation of MHC class I using W6/32, an antibody which reacts with peptide loaded MHC class I molecules associated with β2m (Parham et al., 1979), followed by western blot analysis. Previous work has confirmed the reactivity of W6/32 to a wide range of HLA molecules, including 31 subclasses of HLA-A, 49 subclasses of HLA-B and 16 subclasses of HLA-C (Apps et al., 2009). As the tissue type of the liver tissue was unknown use of this antibody would improve the specificity of the results and allow better quantification. Prior to using precious human tissue samples, I performed some initial immunoprecipitation experiments on the 721.221 cell line. While this cell line is an MHC class I deficient human lymphoblastoid cell line (Shimizu et al., 1988), variants expressing a panel of MHC class I molecule including HLA-A2, -B7 and -B27 following transduction were available. **Figure 3.3** shows I could successfully isolate various MHC class I from these cell lines using immunoprecipitation with W6/32 antibody (Apps et al., 2009), followed by western blot analysis with HC10 and HCA2.

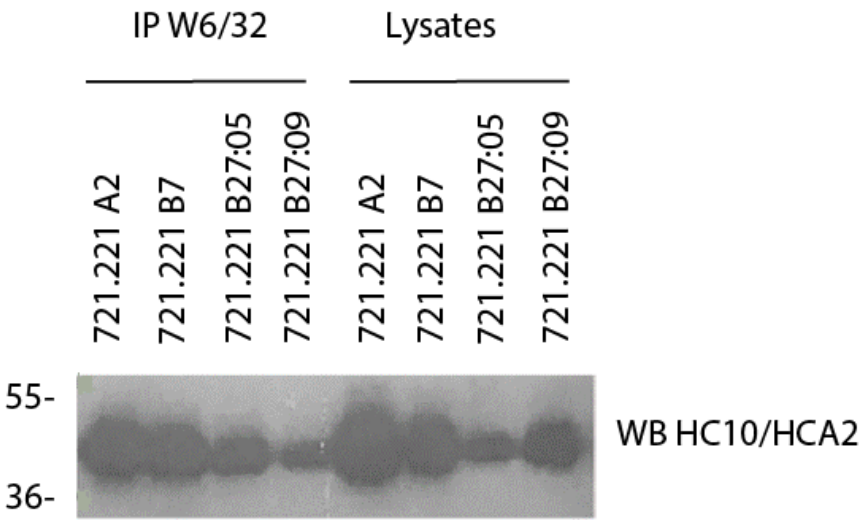

Figure 3.3 – Successful isolation of HLA class I by immunoprecipitation with W6/32. *Western blot analysis using HC10 and HCA2 to detect the MHC class I heavy chain on both W6/32 immunoprecipitates, and as a control on cell lysates, from 721.221 cells expressing HLA-A2, -B7 and -B27.*

Subsequently, immunoprecipitation using W6/32 antibodies was undertaken on a panel of whole liver and placenta lysates to validate MHC class I expression **(Figure 3.4)**. The results show that HLA class I was abundantly expressed within the liver lysate samples and was also detectable, but at lower levels in the placental tissue. Interestingly, while MHC class I appeared to be more highly expressed in some cirrhotic tissue compared to control liver, further analysis suggested there may be a disease-associated variation in MHC class I expression. For example, while patient samples from L54 and L60, which had ARLD and NAFLD respectively, have relatively low MHC class I expression, liver samples L14, L21, L56 and L57, which were derived from patients with hepatitis C or B virus infection appear to express much higher levels of MHC class I **(Figure 3.4)**. Furthermore, patient samples L66 and L63, which were derived from patients with AIH and PSC respectively, exhibit intermediate expression on MHC class I **(Figure 3.4)**. This hierarchy of MHC class I expression (placenta < control < ARLD / NAFLD < AIH / PSC < HBV / HCV) was also identified on western blot analysis on the lysates from these samples, **figure 3.2** shows an example. A total of 33 cirrhotic, 13 control liver and 9 placenta samples were tested all showing a similar pattern of expression.

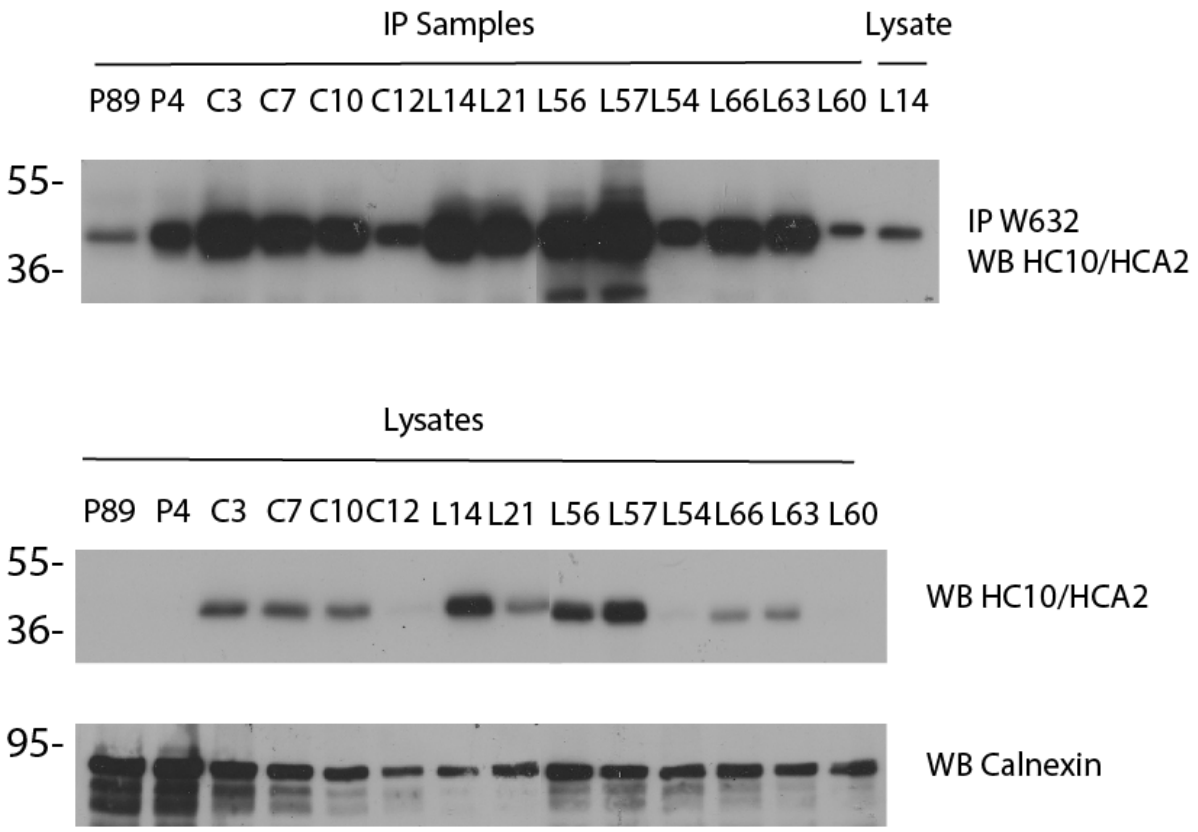

Figure 3.4 – Immunoprecipitation experiments confirm the presence of HLA class I in liver tissue. *Western blot analysis using HC10 / HCA2 to detect the MHC class I heavy chain on both W6/32 IP samples and on cell lysates from placenta (P89 & P4), control liver (C3-C12) and cirrhosis (L14-L60). The cirrhotic samples include patients with HCV (L14, L21, L56), HBV (L57), AIH (L66), PSC (L63), ARLD (L54) and NAFLD (L60). Western blotting for calnexin on lysates is included as a loading control.*

3.3.3 Western Blot Analysis Using L31 Suggests Increased Expression of HLA-C in Cirrhosis

The experiments undertaken thus far using an approach based on western blots and careful selection of antibodies for detection show that MHC class I is seen in liver tissue. However, the various MHC class I have different roles and may contribute individually to disease beneficially or adversely, necessitating further investigation into the individual types.

HLA-C has a specific role during pregnancy in helping the developing foetus evade the immune system and attack (Apps et al., 2008a). My working hypothesis is that senescent cells evade immune attack in a similar manner and therefore I next investigated whether there was altered expression of HLA-C in liver disease. As discussed above, identifying an antibody which is specific for MHC class I can be challenging because of cross-reactivity. L31 antibody was used for western blot detection of HLA-C (Beretta et al., 1987). It reacts with most HLA-C antigens in the absence of β2m. However, this

antibody has been shown to cross-react with some HLA-B antigens including HLA-B7, -B8, -B35 and -B51 (Setini et al., 1996).

Western blot analysis using L31 detected a 41kDa band in all samples, which exhibited increased intensity in cirrhotic samples compared to both the placenta and healthy control liver samples **(Figure 3.5)**. The calnexin control confirms equal loading of all samples with one exception (L52), confirming the validity of the experiment **(Figure 3.5)**.

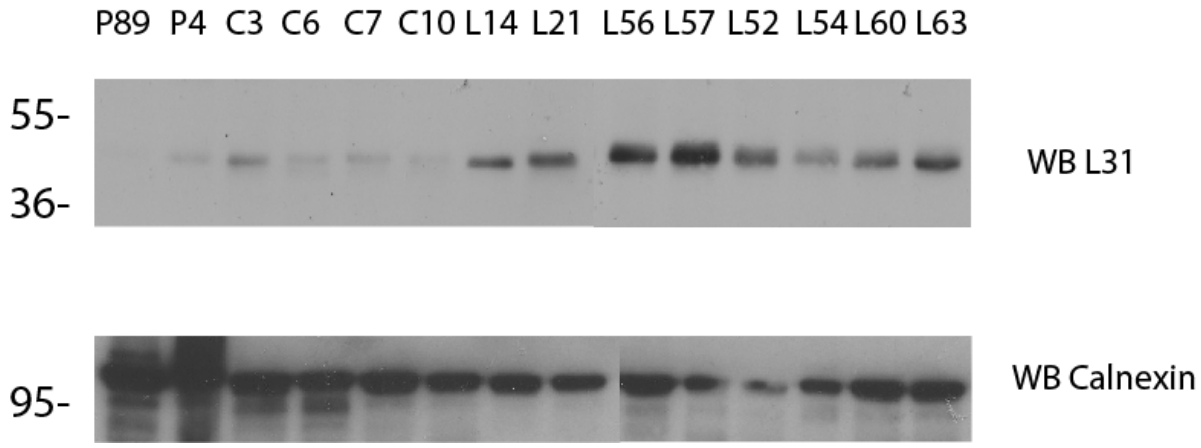

Figure 3.5 – Western blot analysis using L31 suggests increased expression of HLA-C in cirrhosis. *Western blot analysis was performed on whole lysate samples from placental tissue (P89 & P4), healthy control liver (C3-C10) and cirrhosis (L14-L63) using the antibody L31 to detect HLA-C. Western blotting for calnexin was included as a loading control.*

3.3.4 Immunoprecipitation Experiments Confirm the Presence of HLA-C in Liver Tissue and Suggest Higher Expression in Cirrhotic Samples

To improve the specificity of HLA-C detection further experiments based on immunoprecipitation were undertaken. Initially, immunoprecipitation was performed using the pan-class I antibody W6/32 to isolate MHC class I, after which a western blot was carried out using L31 to detect HLA-C. Using this method, HLA-C was detected in liver tissue with a band at 41kDa and once more, increased expression of HLA-C was seen in the cirrhotic samples compared with the control liver and placental samples **(Figure 3.6)**.

However, as mentioned above, the L31 antibody cross-reacts with certain HLA-B molecules, which would also be precipitated by the pan class I antibody W6/32. For this reason, the immunoprecipitation was repeated with the more specific antibody DT9. This monoclonal antibody

was generated to react with HLA-E but on subsequent analysis was found to react with HLA-C molecules (Braud et al., 1998b). It does not react with HLA-A or HLA-B so eliminating the possibility of cross reactivity of the L31 antibody with these loci (Braud et al., 1998b).

Using DT9 for immunoprecipitation confirmed the expression of HLA-C in human liver samples and suggested increased expression of HLA-C in cirrhotic samples compared to healthy control liver **(Figure 3.7)**.

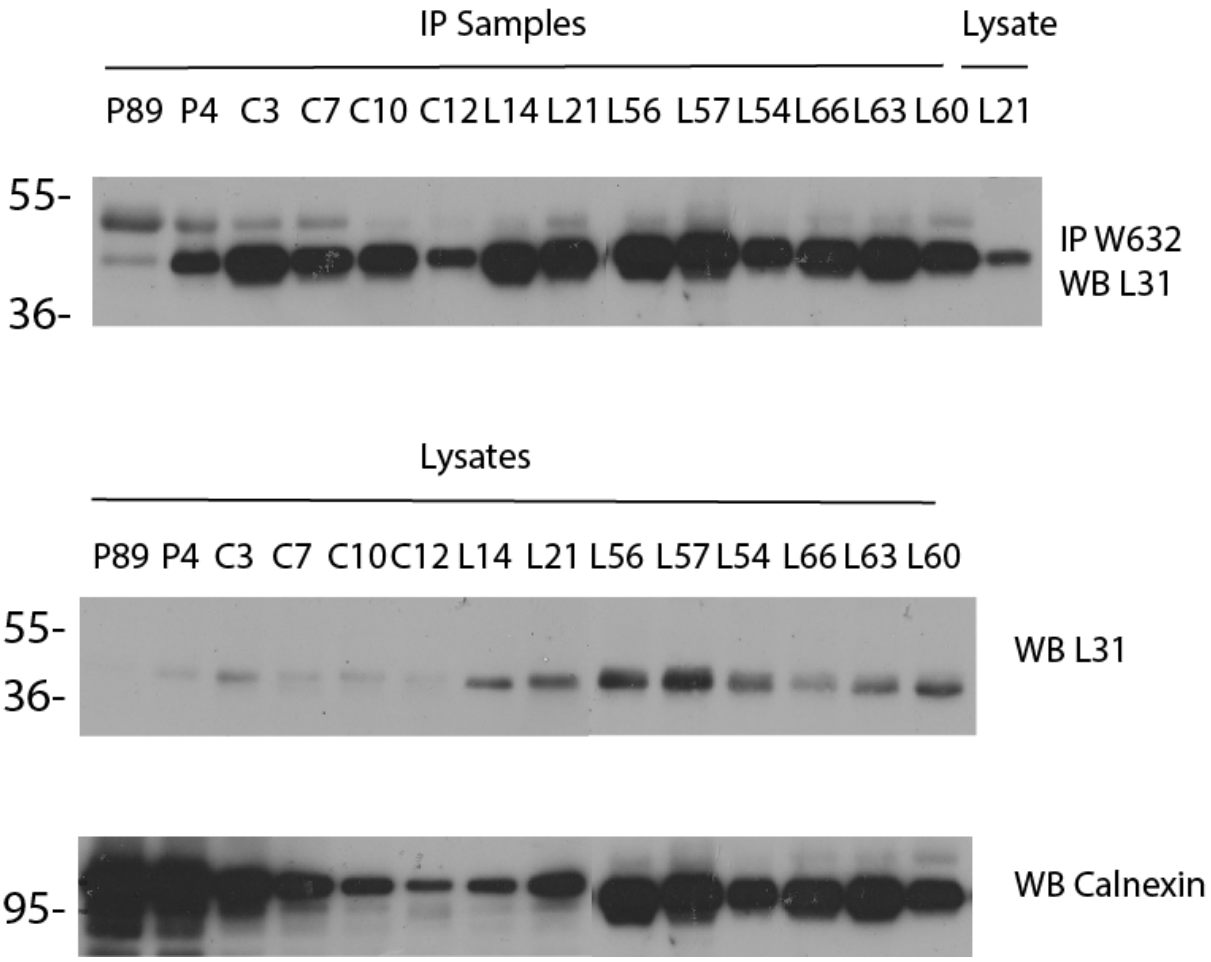

Figure 3.6 – Immunoprecipitation experiments confirm the presence of HLA-C in liver tissue. *Western blot analysis using L31 to detect the HLA-C on both W6/32 IP samples and on cell lysates from placenta (P), control liver (C) and cirrhotic (L14-L60) samples. The cirrhotic samples include patients with HCV (L14, L21, L56), HBV (L57), AIH (L66), PSC (L63), ARLD (L54) and NAFLD (L60). Western blotting for calnexin on lysates is included as a loading control.*

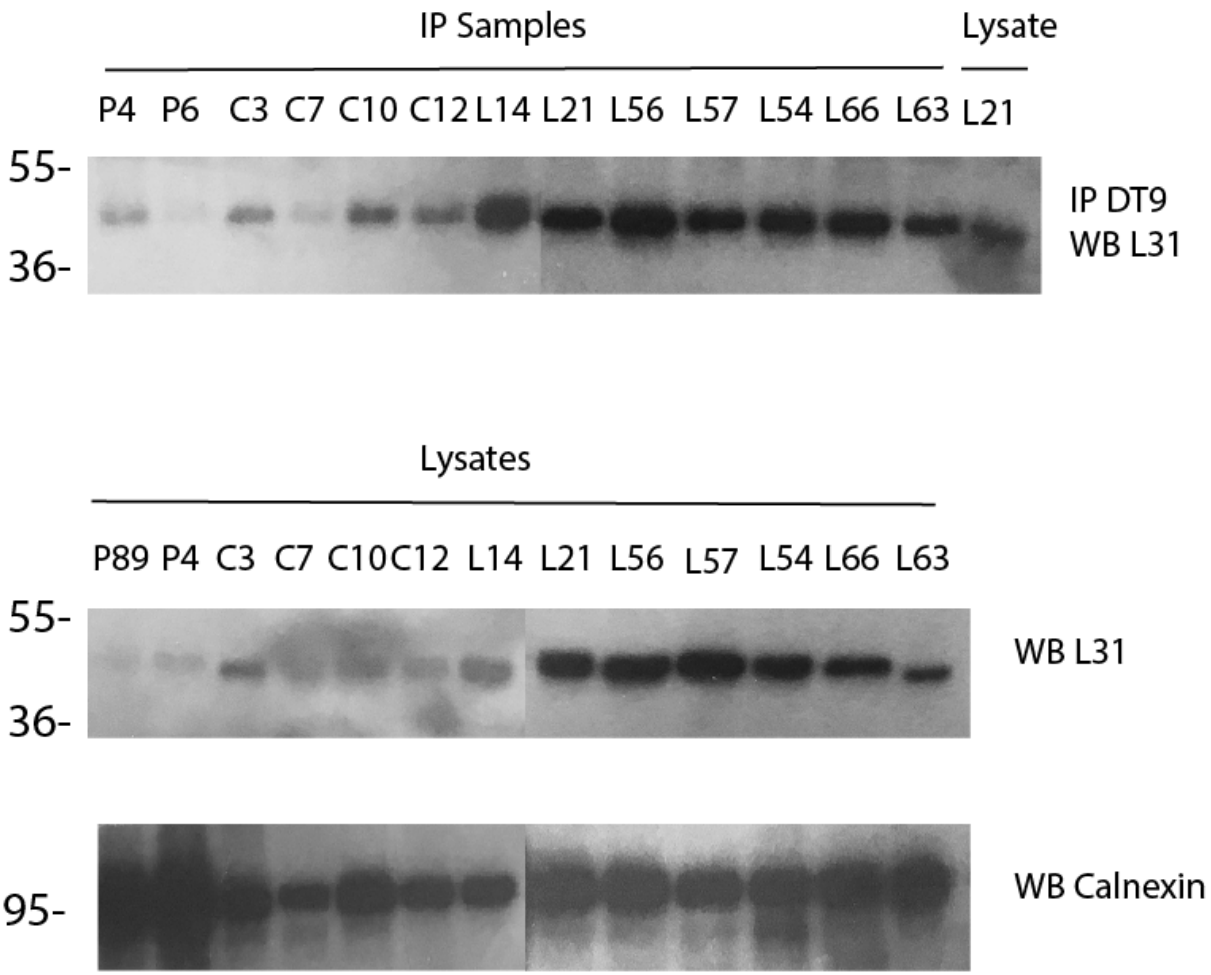

Figure 3.7 – Immunoprecipitation experiments with DT9 confirm the presence of HLA-C in liver tissue. *Western blot analysis using L31 to detect the HLA-C on both DT9 IP samples and on cell lysates from placenta (P), control liver (C) and cirrhotic (L14-L63) samples. The cirrhotic samples include patients with HCV (L14, L21, L56), HBV (L57), AIH (L66), PSC (L63) and ARLD (L54). Western blotting for calnexin on lysates is included as a loading control.*

Figures 3.6 and 3.7 both show a band at 41kDa, which represents HLA-C, but there is a further band identified at 50kDa. It appears that the commercial 'true blot' secondary antibody cross-reacts with a molecule of this size. Despite attempts to refine the immunoprecipitation by adding extra pre-clear and washing steps this band remained. As it is present in all immunoprecipitations undertaken with the liver samples it is likely that it is related to the protocol or reagents. It is possibly the heavy chain from the antibody used in the immunoprecipitation. The 50kDa band is not seen in the western blot when a different secondary antibody is used **(Figures 3.2 and 3.5)**.

3.4 Characterising the Expression of Non-Classical MHC Class I in Liver

The next set of experiments focused specifically on the non-classical MHC class I molecules to investigate their expression in healthy and diseased liver tissue. As discussed in both the introduction and above I am investigating whether they have a specific role in the development of cirrhosis.

HLA-E interacts with the CD94:NKG2 pathway and prevents NK cell activation and therefore destruction of the cell (Braud et al., 1998b). The hypothesis was to investigate the expression of HLA-E in health and disease as abnormal expression may allow senescent cells to accumulate (Lanier, 1997).

The role of HLA-F is still not fully understood but recent work has suggested it has a role in activating the immune system via NK cell receptors (Garcia-Beltran et al., 2016, Dulberger et al., 2017). Aberrant expression in cirrhosis may be contributing to disease.

Finally, HLA-G has a known role in pregnancy allowing the immune system to tolerate the developing foetus (McMaster et al., 1998). There is controversial work that suggests it may be expressed in pathological circumstances to help evade the immune system such as virus or cancer (Onno et al., 2000, Lin and Yan, 2018). The aim was to investigate whether expression of HLA-G in liver disease may mirror that of pregnancy and allow pathological senescent cells to accumulate contributing to disease.

3.4.1 Western Blot Analysis with MEME02 Reveals HLA-E is Present in Liver Tissue

In preliminary experiments, the antibody MEME07 was used to detect HLA-E **(Figure 3.1)**. However, in addition to recognising HLA-E, subsequent exploration of the literature revealed that MEME07 also cross-reacts with HLA-B7, -B8, -B27 and -B44 and therefore, in retrospect, was not a good choice of antibody for this purpose (Palmisano et al., 2005). This likely also explains the detection of a double protein band in three out of four liver samples **(Figure 3.1)**. Following a literature review, the antibody MEME02 was subsequently chosen to detect HLA-E for western blot analysis. This monoclonal antibody detects the denatured heavy chain of HLA-E and validation suggests it does not cross-react with HLA-A, -B, -C or -G (Menier et al., 2003). Western blot analysis of lysates using MEME02 revealed that HLA-E was present in liver tissue as well as placental tissue **(Figure 3.8)**.

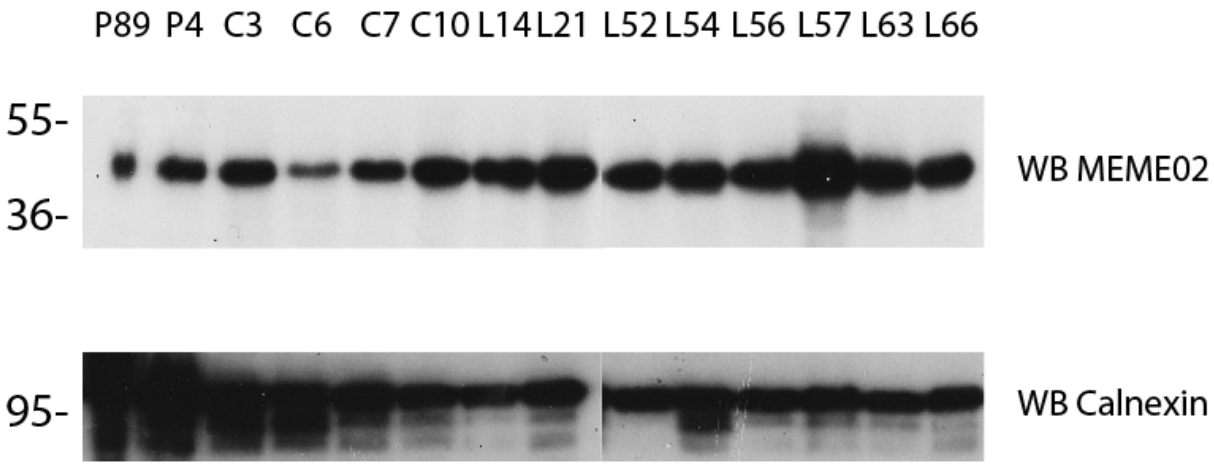

Figure 3.8 – Western blot analysis using MEME02 detects HLA-E in liver tissue. *Western blot analysis was performed on whole lysate samples from placental tissue (P89 & P4), healthy control liver (C3-C10) and cirrhosis (L14-L63) using the antibody MEME02 to detect HLA-E. Western blotting for calnexin was included as a loading control.*

3.4.2 HLA-E Expression Appears to be Higher in Cirrhosis than Healthy Control Liver using Immunoprecipitation

As mentioned above, several studies report that MEME02 does not cross-react with other HLA molecules. However, to improve the specificity and confirm the results shown in **Figure 3.8**, an immunoprecipitation was undertaken using three different antibodies.

First, a pan class I antibody W6/32 (Apps et al., 2009) was used to pull down HLA class I and then a specific western blot was undertaken using MEME02 to detect HLA-E **(Figure 3.9)**. The problem with this combination is that if MEME02 does cross-react with other HLA molecules then these would also have been precipitated by W6/32. Next, immunoprecipitation was undertaken with DT9, an antibody used to detect HLA-C that also isolates HLA-E, followed by western blotting with MEME02 and so was more specific for the final detection of HLA-E **(Figure 3.10)**. Finally, 3D12 a monoclonal antibody specific for HLA-E was used in immunoprecipitation followed by a western blot with MEME02, reducing cross-reactivity to a minimum (3D12 does not cross-react with HLA-A, -B, -C or -G by IP (Lee et al., 1998))**(Figure 3.11)**.

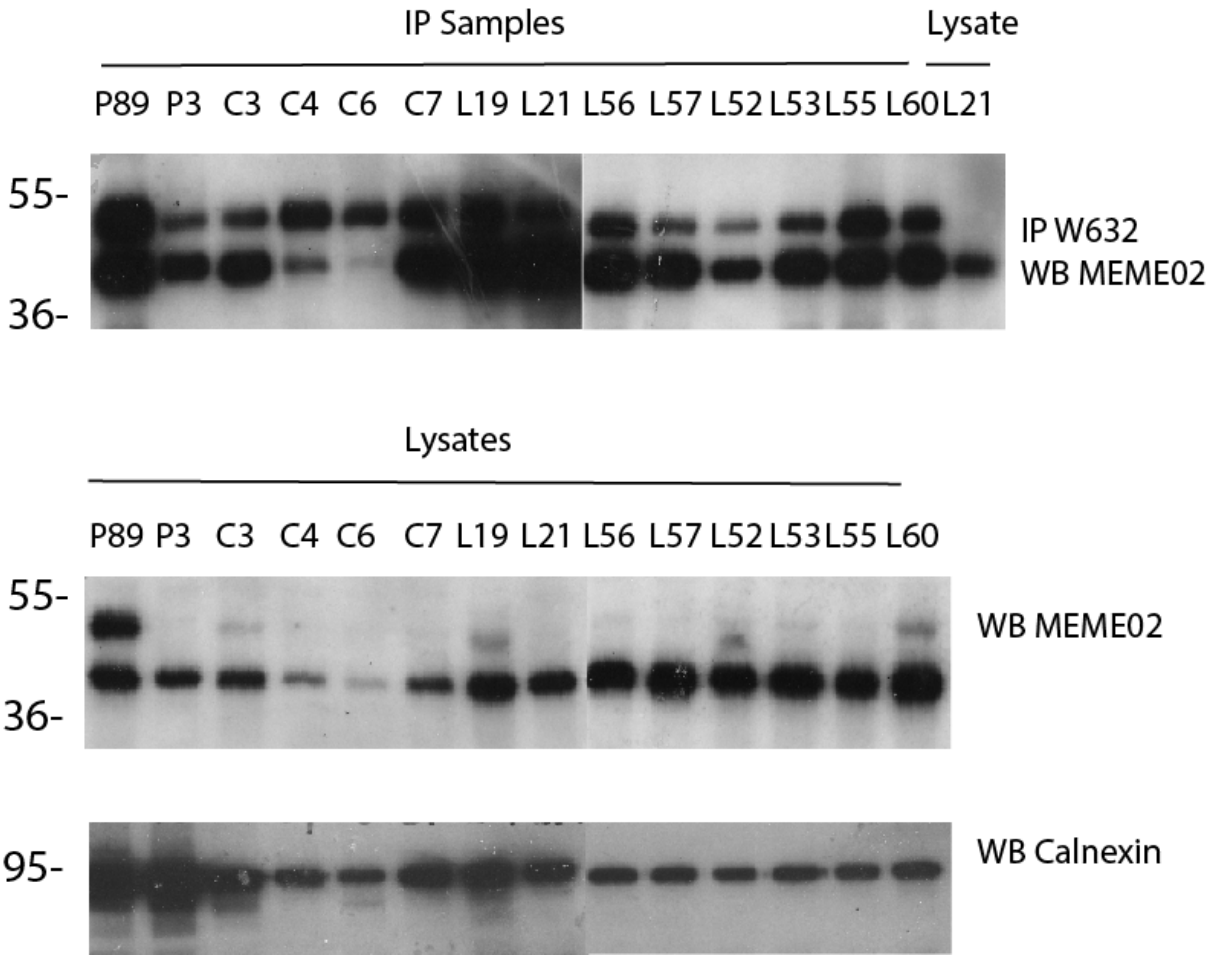

Figure 3.9 – Immunoprecipitation experiments with W6/32 suggest the presence of HLA-E in liver tissue. *Western blot analysis using MEME02 to detect the HLA-E on both W6/32 IP samples and on cell lysates from placenta (P), control liver (C) and cirrhotic (L19-L60) samples. The cirrhotic samples include patients with HCV (L19, L21, L56), HBV (L57), α1AT (L52), ARLD (L53) and NAFLD (L55 & L60). Western blotting for calnexin on lysates is included as a loading control. The band seen again at 50kDa in immunoprecipitations is believed to be due to cross reactivity of the secondary true-blot antibody, as noted previously.*

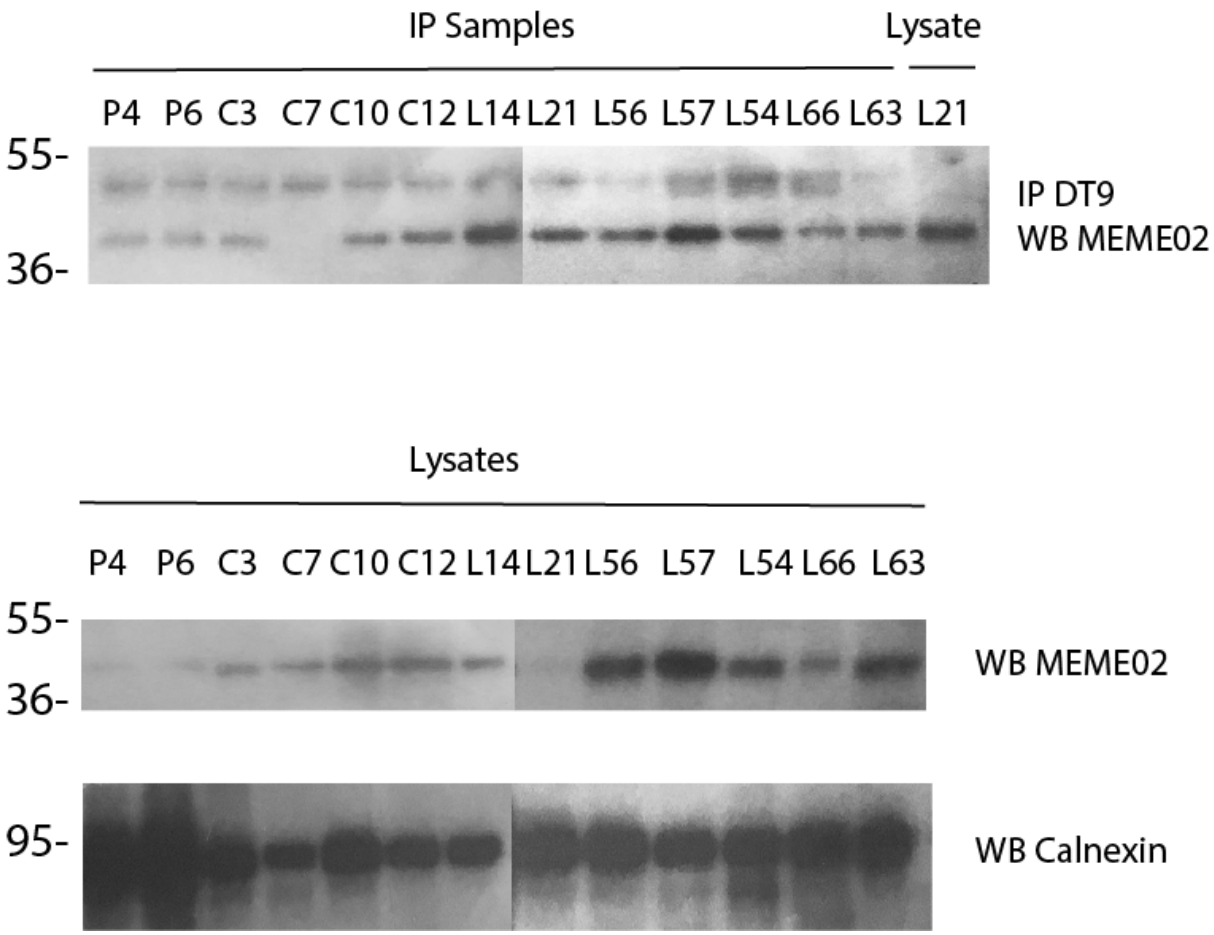

Figure 3.10 – Immunoprecipitation experiments with DT9 suggest the presence of HLA-E in liver tissue. *Western blot analysis using MEME02 to detect the HLA-E on both DT9 IP samples and on cell lysates from placenta (P), control liver (C) and cirrhotic (L14-L63) samples. The cirrhotic samples include patients with HCV (L14, L21, L56), HBV (L57), AIH (L66), PSC (L63), ARLD (L54) and NAFLD (L60). Western blotting for calnexin on lysates is included as a loading control.*

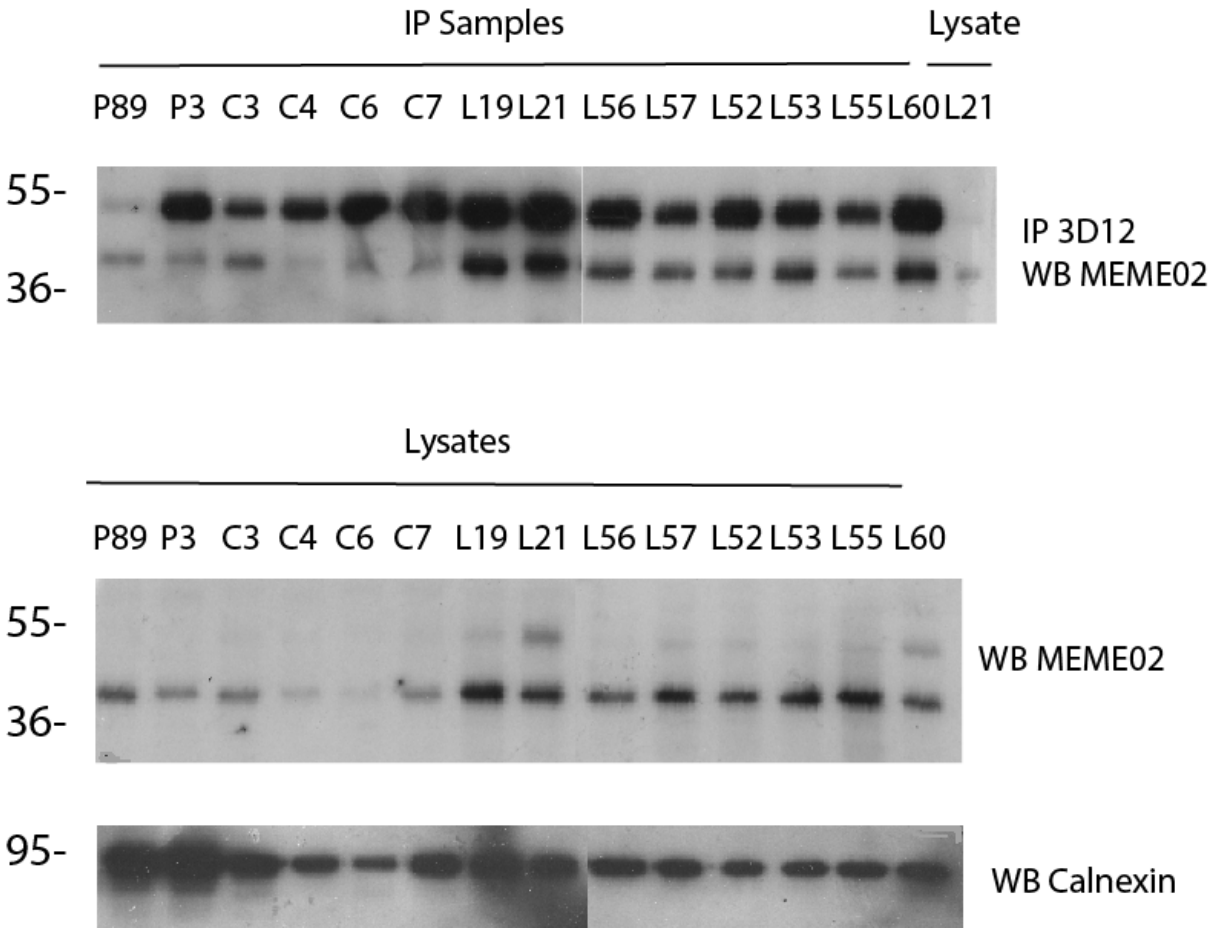

Figure 3.11 – Immunoprecipitation experiments with 3D12 suggest higher expression of HLA-E in cirrhotic tissue compared to control liver. *Western blot analysis using MEME02 to detect the HLA-E on both 3D12 IP samples and on cell lysates from placenta (P), control liver (C) and cirrhotic (L19-L60) samples. The cirrhotic samples include patients with HCV (L19, L21, L56), HBV (L57), α1AT (L52), ARLD (L53) and NAFLD (L55 & L60). Western blotting for calnexin on lysates is included as a loading control. The band seen again at 50kDa in immunoprecipitations is believed to be due to cross reactivity of the secondary true-blot antibody, as noted previously.*

The results in **Figure 3.9 – 3.11** show by several distinct approaches to immunoprecipitation that HLA-E is present in liver tissue and suggest that HLA-E is expressed at a higher level in cirrhotic samples compared to control liver or placenta samples. Using W6/32 to immunoprecipitate MHC class I, there was consistently higher expression of HLA-E detected using MEME02 in the cirrhotic samples compared with the control samples, while HLA-E appeared equal to the placenta samples **(Figure 3.9)**. The higher expression of HLA-E appeared uniform among the different cirrhotic samples and not affected by the different aetiologies. Blotting for calnexin revealed some unequal loading in the control samples, but this did not correlate with the HLA-E expression **(Figure 3.9)**.

Immunoprecipitation with DT9 antibody shows similar results **(Figure 3.10)**. Again, there was increased expression of HLA-E, shown as a band at 43kDa, following western blotting with MEME02 in the cirrhotic samples compared to the controls **(Figure 3.10)**. In this experiment the loading appeared more equal, supporting the concept that HLA-E might be expressed in higher levels in cirrhosis. Finally, immunoprecipitation with 3D12, also suggested increased expression of HLA-E in the cirrhotic samples compared to the control liver samples **(Figure 3.11)**. The loading control calnexin shows some unequal loading of the samples, slightly higher in placenta and lower in the C4 and C6 samples. However, this does not alter the overall conclusions as the other control samples were adequately loaded and showed reduced HLA-E expression.

3.4.3 HLA-F is Present in Liver Tissue Analysed by Western Blot

Investigation into the presence of HLA-F in liver tissue is more complex than with other HLA molecules, mainly because there are fewer commercial antibodies available. Also the expression and function of HLA-F in general is less well understood (Geraghty et al., 1990). Although initially I used the rabbit monoclonal antibody EPR6803, to determine expression of HLA-F **(Figure 3.1)**, there are no published studies using this antibody to determine cross reactivity with other HLA molecules. The presence of HLA-F in liver tissue was therefore investigated using antibodies that have been better characterised. The monoclonal antibody 3D11 is raised against the heavy chain of HLA-F (Lee and Geraghty, 2003). It has been reported not to cross-react with the classical MHC class I molecules, HLA-A, -B or-C (Ishitani et al., 2003).

Western blotting with 3D11 detected a band the predicted size of HLA-F in human liver and suggested that expression was increased in cirrhotic samples when compared with control liver **(Figure 3.12)**. No HLA-F was identified in the placenta samples **(Figure 3.12)**; the presence of HLA-F in trophoblast cells remains contentious (Lee and Geraghty, 2003). Blotting for calnexin suggested adequate loading of the placenta samples and indeed, this appears slightly higher than the liver samples. Sample C7 is under-loaded but otherwise the result is valid.

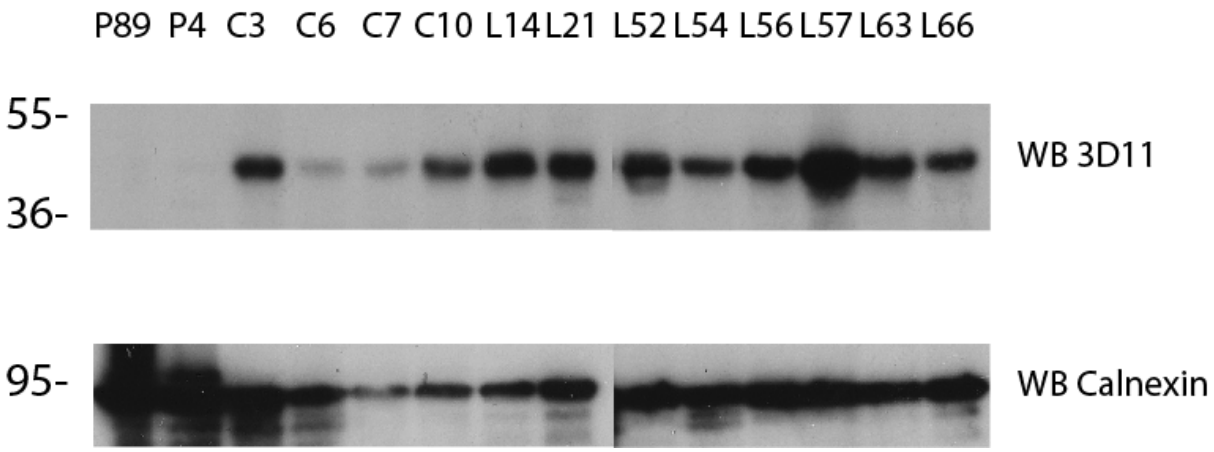

Figure 3.12 – Western blot analysis using 3D11 detects HLA-F in liver tissue*. Western blot analysis was performed on whole lysate samples from placental tissue (P89 & P4), healthy control liver (C3-C10) and cirrhosis (L14-L66) using the antibody 3D11 to detect HLA-F. Western blotting for calnexin was included as a loading control.*

3.4.4 Optimisation of HLA-F Immunoprecipitation

Other antibodies available to me included 4A11, a monoclonal antibody that also reacts with the HLA-F heavy chain but which is known to cross-react with HLA-Cw4 (Lee and Geraghty, 2003) and FG1, a monoclonal antibody that was generated against recombinant HLA-F in complex with β2m, and that has been tested to ensure no cross-reactivity with HLA-A2, -B7, -C, -E or -G (Lepin et al., 2000).

FG1, 4A11 as well as 3D11 can all be used to isolate HLA-F by immunoprecipitation, while 4A11 and 3D11 can be used in western blotting (Lee and Geraghty, 2003, Lepin et al., 2000). Optimisation experiments using the MHC class I deficient human lymphoblastoid cell line 721.221, which has been shown to express HLA-F as well as HLA-E (Shimizu et al., 1988, Lee et al., 1998, Tzeng et al., 1996) were undertaken to investigate which combination of antibodies would work best for further studies. While immunoprecipitation with W6/32, FG1, 3D11 and 4A11 followed by western blot analysis with either 3D11 or 4A11 all proved successful **(Figure 3.13)**, there were several notable differences in the results. Firstly, in western blot analysis 3D11 appeared superior to 4A11, in terms of signal intensity. It also detected numerous higher molecular weight products, which could be post-translationally modified HLA-F species (Boyle et al., 2006) (Louise Boyle, personal communication). Secondly, in immunoprecipitation experiments FG1 and 3D11 were superior to both W6/32 and 4A11 antibodies. No proteins bands were detected when western blot and immunoprecipitation were performed on HeLa cell lysates (Rahbari et al., 2009), which are believed

to be largely negative for HLA-F protein (Benham et al., 1998, Johnson and Mook-Kanamori, 2000) **(Figure 3.13)**. Based on this analysis, FG1 was chosen for immunoprecipitation of HLA-F, while 3D11 was selected for western blot analysis to avoid any cross-reactive with HLA-C molecules (Ishitani et al., 2003).

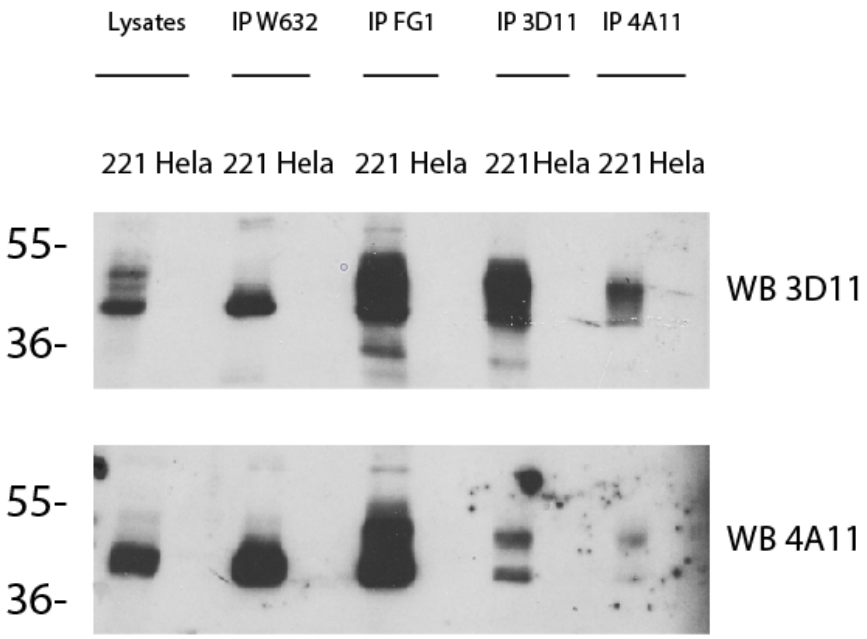

Figure 3.13 – Optimisation of the detection of HLA-F. *Western blot analysis using 3D11 or 4A11 to detect HLA-F on cell lysates and IP samples using W6/32, FG1, 3D11 and 4A11 from 721.221 cells that are known to express HLA-F and HeLa cells as a negative control.*

.

3.4.5 HLA-F Expression Appears to be Higher in Cirrhosis than Healthy Control Liver using Immunoprecipitation

To compare HLA-F expression levels between cirrhotic and control liver samples, immunoprecipitation experiments were performed using FG1 on a panel of liver samples. A dominant band at ~50kDa was observed in all immunoprecipitates and was believed to be the heavy chain of the antibody used in the immunoprecipitation cross-reacting with the horseradish peroxidase (HRP)-conjugated secondary antibody used in western blot analysis **(Figure 3.14)**. However, a band at ~40kDa, the predicted size of HLA-F, was also observed **(Figure 3.14)**. Furthermore, the ~40kDa was more intense in cirrhotic samples compared to control liver samples except for liver C3 **(Figure 3.14)**. The expression of HLA-F was higher in the cirrhotic samples but showed no association to aetiology. HLA-F was not detected in placental tissue using this method

(Figure 3.14). Furthermore, probing with 3D11 on W6/32 immunoprecipitates from the liver sample panel revealed similar findings **(Figure 3.15)**. Together, these data suggest HLA-F is expressed in liver tissue and implicate increased expression in cirrhotic samples compared with control liver samples.

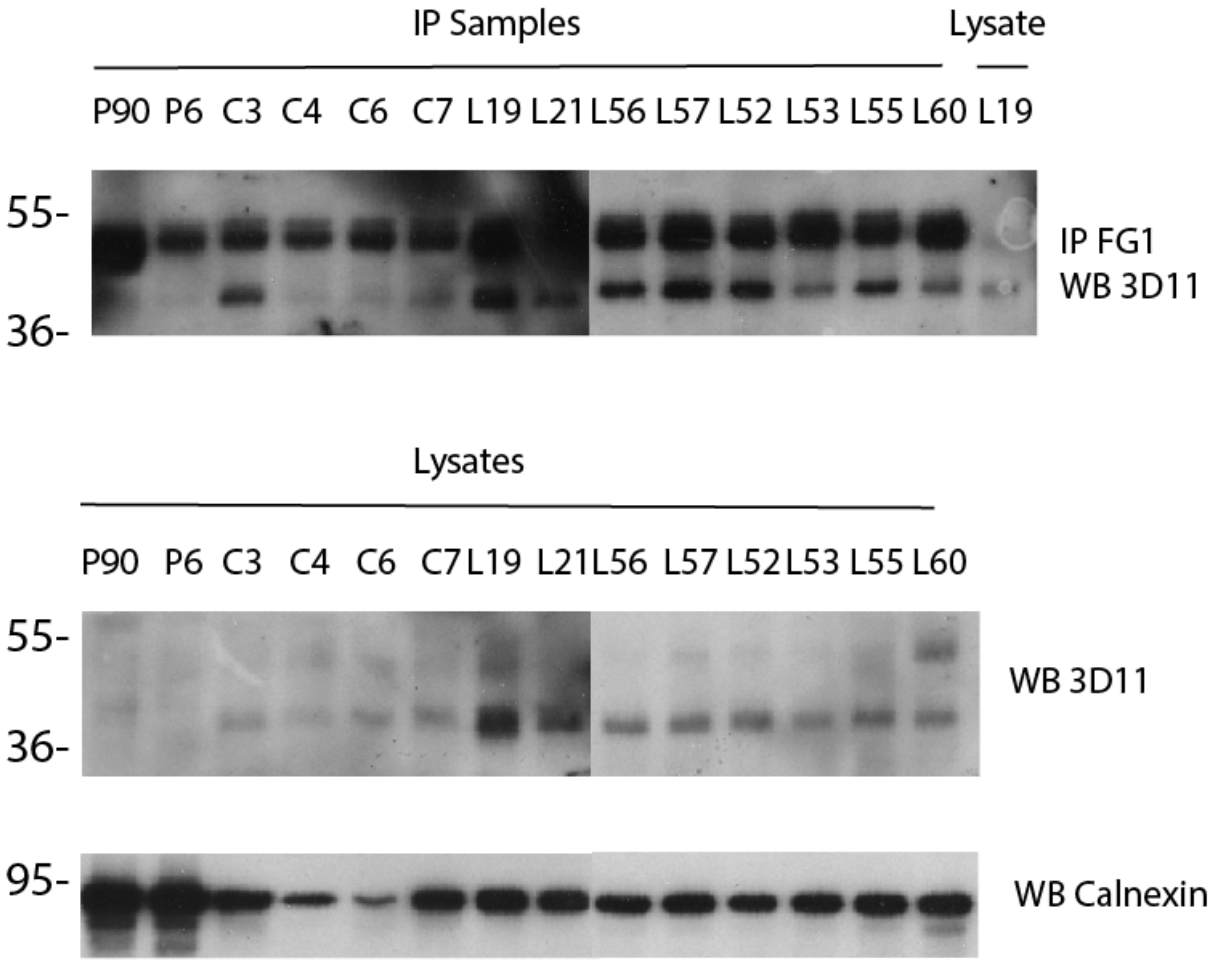

Figure 3.14 - Immunoprecipitation experiments with FG1 suggest higher expression of HLA-F in cirrhotic tissue compared to control liver. *Western blot analysis using 3D11 to detect HLA-F on FG1 IP samples and on cell lysates from placenta (P), control liver (C) and cirrhotic (L19-L60) samples. The cirrhotic samples include patients with HCV (L19, L21, L56), HBV (L57), α1AT (L52), ARLD (L53) and NAFLD (L55 & L60). Western blotting for calnexin on lysates is included as a loading control.*

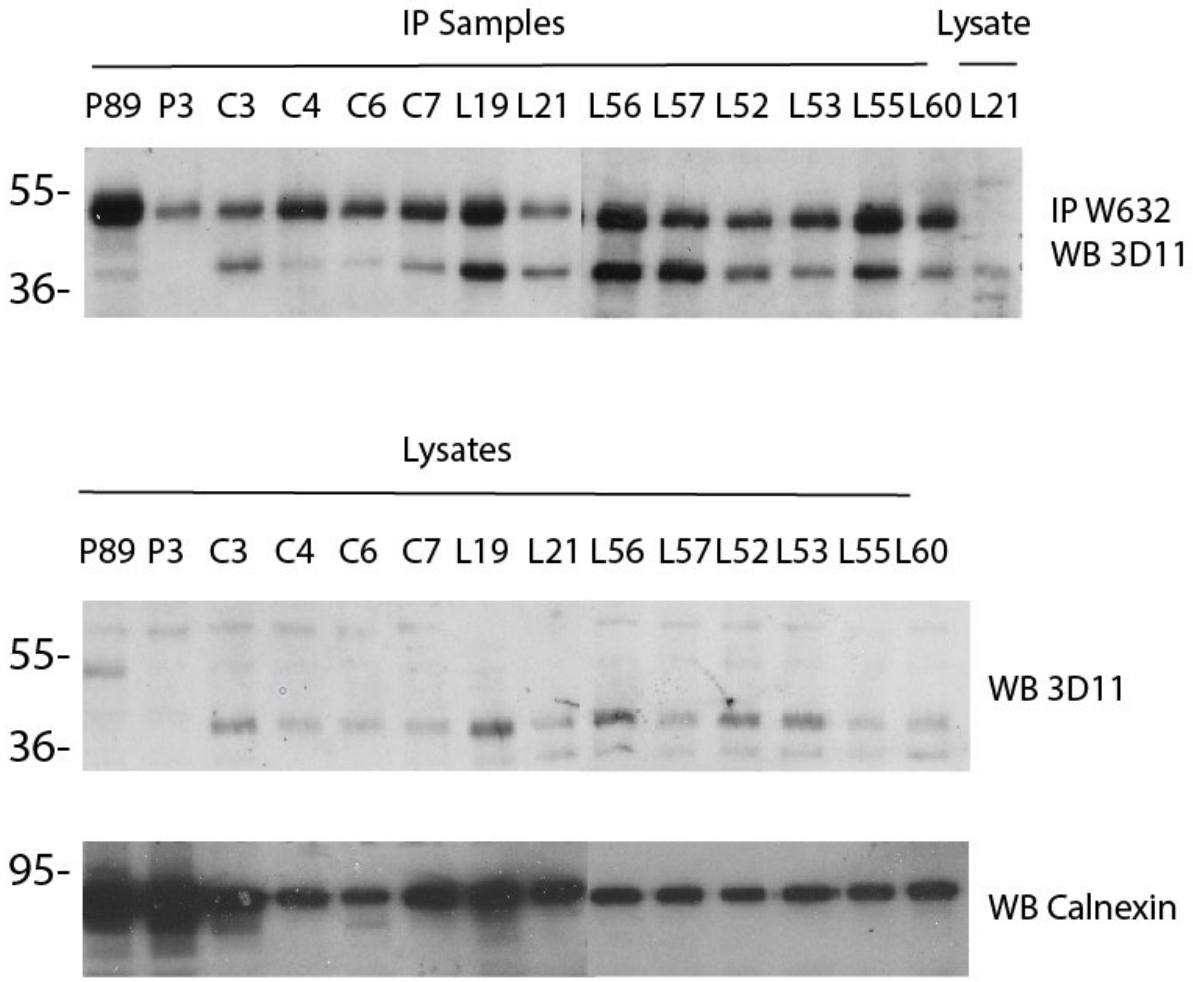

Figure 3.15 – Immunoprecipitation experiments with W6/32 suggest higher expression of HLA-F in cirrhotic tissue compared to control liver. *Western blot analysing using 3D11 to detect HLA-F on both W6/32 IP samples and on cell lysates from placenta (P), control liver (C) and cirrhotic (L19-L60) samples. The cirrhotic samples include patients with HCV (L19, L21, L56), HBV (L57), α1AT (L52), ARLD (L53) and NAFLD (L55 & L60). Western blotting for calnexin on lysates is included as a loading control.*

3.4.6 Analysis of HLA-G Expression in Liver

The physiological role of HLA-G is expression on the extra-villous trophoblast to protect the developing foetus during pregnancy (McMaster et al., 1998). Recent work has suggested that HLA-G may be expressed in liver tissue and liver disease (Moroso et al., 2015, Souto et al., 2011, Catamo et al., 2014). However, most of this later work was based on immunohistochemistry alone and is considered unreliable by some experts in the field (Apps et al., 2008b). The aim was to robustly investigate the presence of HLA-G using various biochemical techniques.

A review of the literature revealed that the original antibody I used, MEMG01, **(Figure 3.1)** was an appropriate antibody to continue to use to detect HLA-G in western blot analysis. This antibody reacts with the denatured heavy chain of HLA-G and is known to detect five isoforms of HLA-G (Menier et al., 2003). Two studies have tested this particular antibody for cross-reactivity by western blotting with HLA-A, -B, -C and -E and report there is none (Lozano et al., 2002, Hurks et al., 2001). Using MEMG01, I observed a band at 39kDa, the predicted size of HLA-G in the placental tissue (Loke et al., 1997). The extreme intensity of the signal observed is notable **(Figure 3.16)**. However, only a very faint band was seen in some liver samples **(Figure 3.16)**. Furthermore, I found the blot very hard to interpret (which was even more difficult in the cirrhotic samples) but this band appeared to be running a little higher at 42kDa than the expected 39kDa (Menier et al., 2003). There are smaller bands also seen including one at around 30kDa. This is seen more prominently in the L56 and L57 cirrhotic samples (HCV and HBV respectively) and in L66 (AIH). There are several plausible explanations including a different isoform of HLA-G in liver tissue or a soluble form of HLA-G but the literature indicates that the isoforms would be expected to be smaller (Riteau et al., 2001a). It has also been suggested that some HLA-G is not bound to β2m in the foetus; theoretically this could also occur in liver disease (Morales et al., 2007). Moreover, it has also been suggested that some isoforms of HLA-G can form dimeric complexes which could also be detected (Alegre et al., 2014).

Another explanation would be a cross-reaction with another HLA molecule, although this would be inconsistent with the published but limited literature. Western blot analysis for calnexin demonstrated that the western blot process had worked efficiently while suggesting there was less efficient loading of sample C6, this did not confound the results.

The results of the western blot differ from those obtained in the preliminary experiment **(Figure 3.1)**. However upon subsequent repeats I was unable to reproduce this first figure. One possible explanation is that the protein is somehow denatured by the western blot process and that this did not occur in the first experiement.

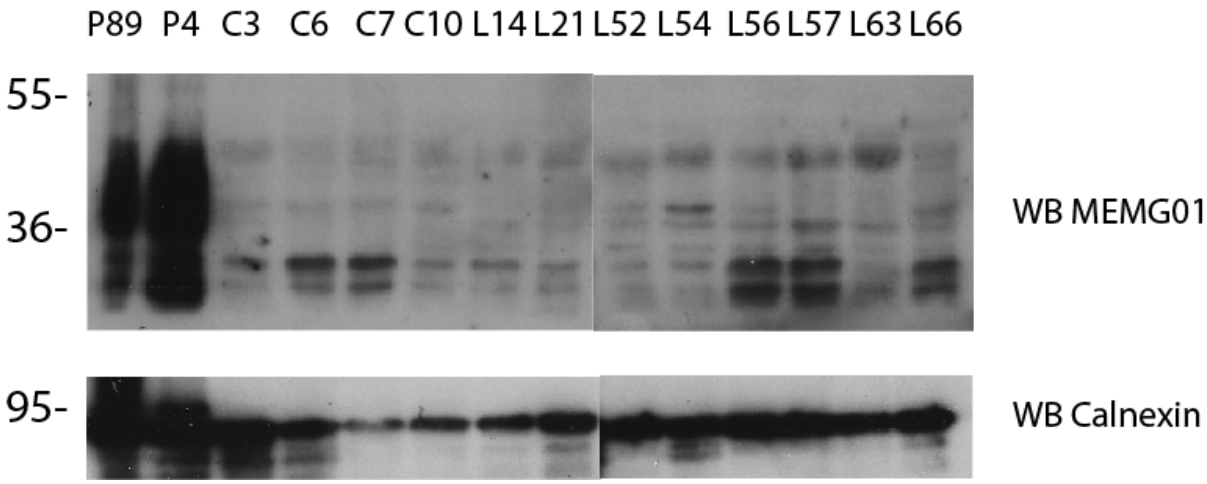

Figure 3.16 Western blot analysis using MEMG01 on liver tissue. *Western blot analysis was performed on whole lysate samples from placental tissue (P89 & P4), healthy control liver (C3-C10) and cirrhosis (L14-L66) using the antibody MEMG01 to detect HLA-G. Western blotting for calnexin was included as a loading control.*

3.4.7 Optimisation of the Detection of HLA-G by Immunoprecipitation

A small number of papers suggest that HLA-G is present in liver disease, but all the published studies have been based on detection by immunohistochemistry (Moroso et al., 2015, Souto et al., 2011, Catamo et al., 2014). Considering these studies, which contrast with my inconclusive results using western blotting to detect HLA-G, further investigation was required and to determine if the bands seen on the western blot gel were representative of HLA-G or because of cross reaction with another HLA molecule.

Immunoprecipitation for HLA-G in liver tissue has not been described previously. Therefore in the first instance, I optimised immunoprecipitation for HLA-G on JEG-3 cells, a choriocarcinoma cell line which are recognised to express HLA-G as well as HLA-C and represent the extravillous trophoblast (Burt et al., 1991) **(Figure 3.17)**, then on placenta samples **(Figure 3.18)** before using the liver samples.

As well as using the pan-class I monoclonal (mAb) W6/32 (Apps et al., 2009), there are a few antibodies which recognise conformational HLA-G and therefore appropriate to test in immunoprecipitation. These included G233, a monoclonal antibody raised against HLA-G in complex with β2m (Loke et al., 1997) which when tested against a panel of 96 classical HLA antigens only

exhibited minor cross-reactivity with HLA-B*54:01, HLA-B*55:01 and HLA-B*59:01 (Apps et al., 2009).

Furthermore, MEM09 (Menier et al., 2003), is an appropriate choice for immunoprecipitation as this monoclonal antibody, raised against conformational HLA-G in conjunction with β2m and reactive with isoforms HLA-G1 and -G5, has been shown not to react with HLA-A, -B, -C and -E in two studies using transfected cells lines (Riteau et al., 2001a).

Furthermore, I tested two antibodies in western blot analysis. These were MEMG01 (as discussed above) and 4H84, a monoclonal antibody against conformational HLA-G and the denatured heavy chain of HLA-G2, -G3 and -G4 (Riteau et al., 2001b) which is not thought to cross-react with other HLA antigens (McMaster et al., 1998). All attempted western blots with 4H84 failed to detect any signal of the correct size, so further experiments with this antibody were abandoned.

My results using lysates from JEG cells suggested that the three antibodies used for immunoprecipitation of HLA-G were effective, isolating a band at ~39kDa, the expected size of HLA-G upon western blotting with MEMG01 **(Figure 3.17)**. G233 and MEMG09 appeared more efficient than W6/32 at isolating HLA-G from JEG cells **(Figure 3.17)**. Using the placenta samples, the same antibody combinations yielded fairly similar results **(Figure 3.18)**. A band was seen at ~39kDa, which could represent HLA-G within these samples. Immunoprecipitation with W6/32, G233 and MEMEG09 revealed increased detection compared with lysates indicative of effective immunoprecipitation. Furthermore, immunoprecipitation with an isotype control antibody, failed to isolate HLA-G, as expected **(Figure 3.18)**. However, G233 appeared to be more efficient than MEM09 at isolating HLA-G in the placenta samples **(Figure 3.18)**. The band observed at 50kDa in all immunoprecipated samples is likely to represent detection of the heavy chain of the antibody used for immunoprecipitation. The monoclonal antibody to HLA class I heavy chain HCA2 is known to detect HLA-G (Seitz et al., 1998) so was used as alternative to MEMG01 in western blotting **(Figure 3.18-bottom panel)**. It showed similar results to those with MEMG01 in all samples but at lower intensity. However, as expected a strong band was seen in the W6/32 IP as observed with other HLA class I molecules.

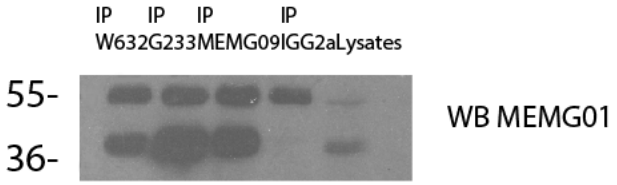

Figure 3.17 – Optimisation of the detection of HLA-G*. Western blot analysis using MEMG01 to detect HLA-G on cell lysates and IP samples using W6/32, G233, MEMG09 and an isotype control antibody (immunoglobulin G2a (IgG2a) from JEG cells that are known to express HLA-G. The band at ~39kDa is the predicted size of HLA-G while the 50kDa band is likely to be the heavy chain of the antibody used for immunoprecipitation.*

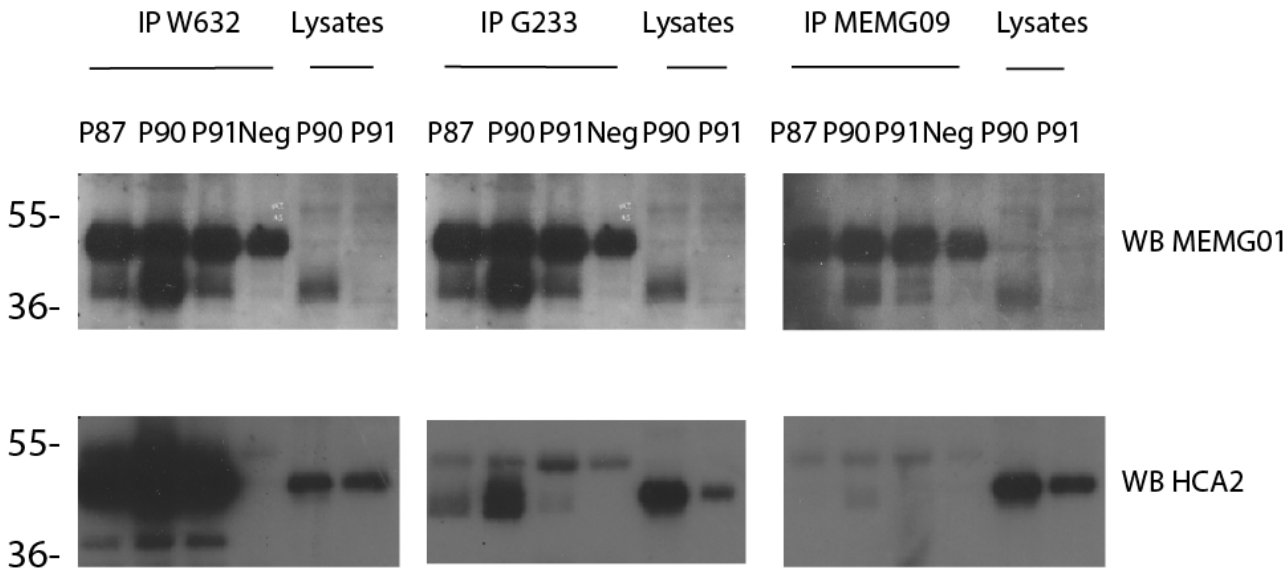

Figure 3.18 – Optimisation of the detection of HLA-G using placental samples*. Western blot analysis using MEMG01 (top panel) or HCA2 (bottom panel) to detect HLA-G on cell lysates and IP samples using W6/32, G233 and MEMG09 antibodies. A negative control for each antibody was run with the antibody and no placenta sample.*

3.4.8 HLA-G was Not Detected in Liver Tissue by Immunoprecipitation

Having established HLA-G isolation using the placenta samples, I next performed similar immunoprecipitation experiments on the liver samples. Initially, immunoprecipitation was undertaken with pan-class I antibody W6/32, followed by western blotting using MEMG01 antibody. While a 39kDa band was detected in placental samples, acting as positive controls, no band at the appropriate size was observed in any of the liver samples (healthy or diseased) suggesting that HLA-

G was not present **(Figure 3.19)**. When immunoprecipitation for HLA-G was performed using G233, followed by probing for HLA-G using either MEMG01 or HC10/HCA2, again, a 39kDa band corresponding to HLA-G was detected in the placenta samples but not in any of the liver samples **(Figure 3.20)**. When the lysates were probed with HC10/HCA2, which also identifies HLA-A, -B, -C as well as -E, -F and –G, bands corresponding to MHC class I were clearly detected in liver tissue **(Figure 3.20)**. However, probing the liver lysates with MEMG01 failed to detect a band corresponding to HLA-G **(Figure 3.20)**. A faint band running at a molecular weight higher than that expected for HLA-G was observed **(Figure 3.20)**, suggesting that the MEMG01 antibody may cross react with another HLA molecule. Based on these experiments, HLA-G did not appear to be present in any of the tested liver samples.

.

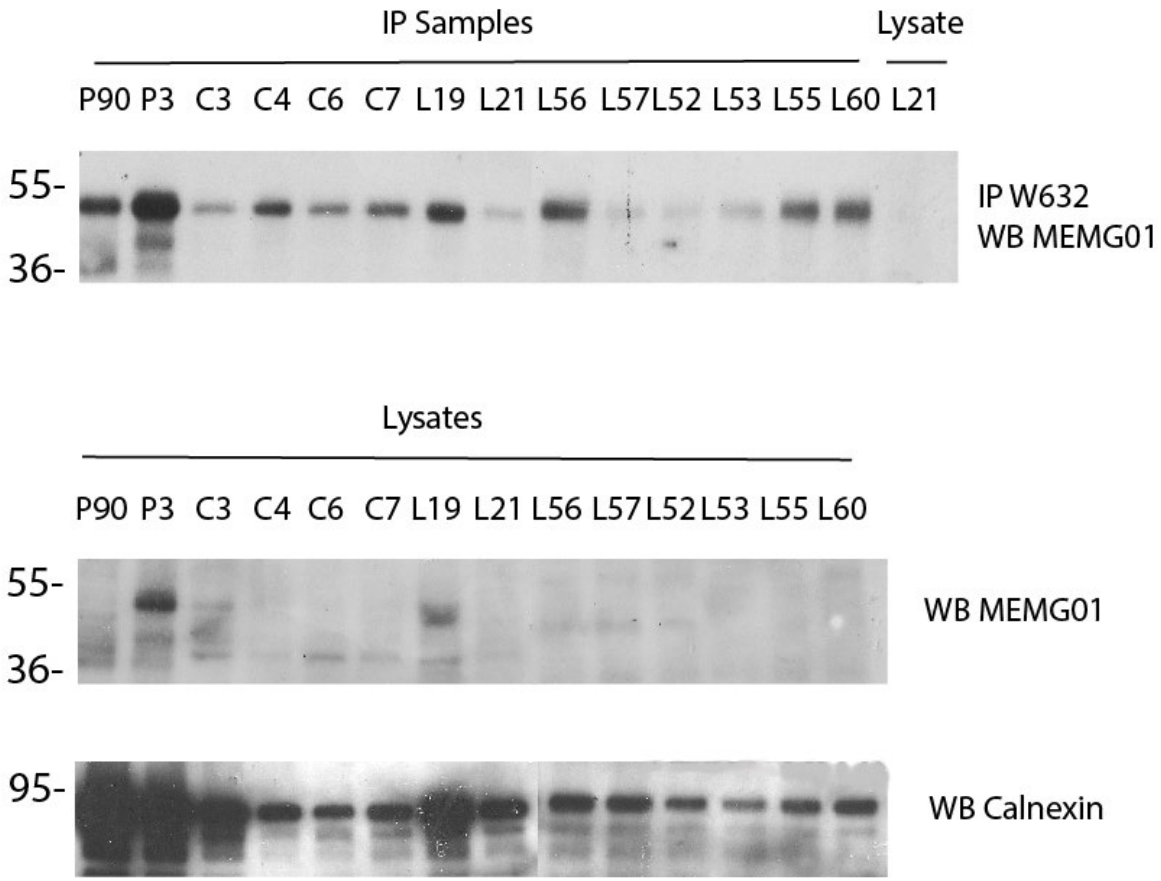

Figure 3.19 – Immunoprecipitation using W6/32 did not detect HLA-G in liver samples*. Western blot analysis using MEMG01 to detect the HLA-G on both W6/32 IP sample and on cell lysates from placenta (P), control liver (C) and cirrhotic (L19-L60) samples. The cirrhotic samples include patients with HCV (L19, L21, L56), HBV (L57), α1AT (L52), ARLD (L53) and NAFLD (L55 & L60). Western blotting for calnexin on lysates is included as a loading control.*

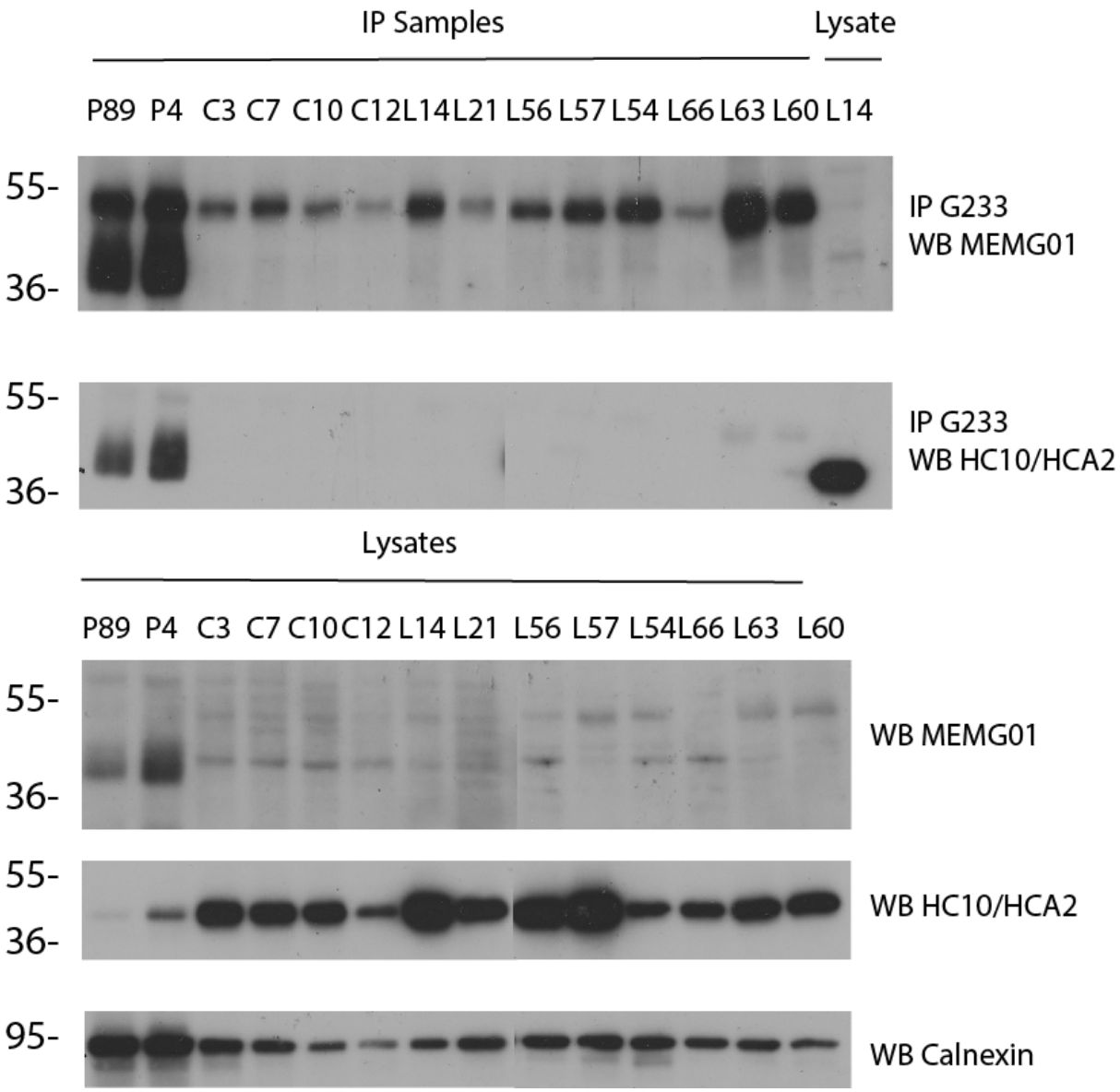

Figure 3.20 – Immunoprecipitation using G233 did not detect HLA-G in liver samples. Western blot analysis using MEMG01 to detect the HLA-G or HC10/HCA2 on both G233 IP samples and on cell lysates from placenta (P), control liver (C) and cirrhotic (L14-L63) samples. The cirrhotic samples include patients with HCV (L14, L21, L56), HBV (L57), AIH (L66), PSC (L63), ARLD (L54) and NAFLD (L60). Western blotting for calnexin on lysates is included as a loading control.

3.4.9 Validation of Non-Classical HLA Expression using Quantitative Real-Time PCR

My experiments above suggested that while the proteins for HLA-E and -F were expressed in liver samples, with higher expression in cirrhosis **(Figure 3.9-3.11 and 3.14-3.15)**, HLA-G was not detected **(Figure 3.19-3.20)**. To further support this conclusion qRT-PCR was employed to determine the RNA

transcript levels of HLA-E, -F and -G in liver tissue. The transcript level of HLA-C was included as a control.

Using this approach, HLA-C RNA was detected in the test liver tissues as well as the placenta sample **(Figure 3.21A)**. Furthermore, HLA-C transcript levels appeared higher in the cirrhotic samples than in the control tissue **(Figure 3.21A)**. The data are consistent with the protein expression observed in **Figure 3.6 and 3.7.** Similarly, HLA-E and HLA-F RNA were detected in the test liver samples and placenta **(Figure 3.21B and 3.21C, respectively)** and both appeared to be more abundantly expressed in cirrhosis compared to the control tissue. Of note, the level of expression of HLA-F RNA appeared to be much lower than that of HLA-E RNA, consistent with the protein work using immunoprecipitation **(Figures 3.9-3.11 and 3.14-3.15)**.

qRT-PCR for HLA-G RNA demonstrated high expression of HLA-G as expected in the positive control placenta sample **(Figure 3.21D)**. However, no HLA-G RNA was found in the control liver samples **(Figure 3.21D)**. In contrast, there was very low-level expression of HLA-G RNA in just one cirrhotic sample, L57 **(Figure 3.21D)**. This sample was derived from the single patient with HBV infection included in the study. Of note, in this patient, as with the others, the HLA-G immunoprecipitation/western blot experiments did not detect any HLA-G protein expression **(Figure 3.19-3.20)**.

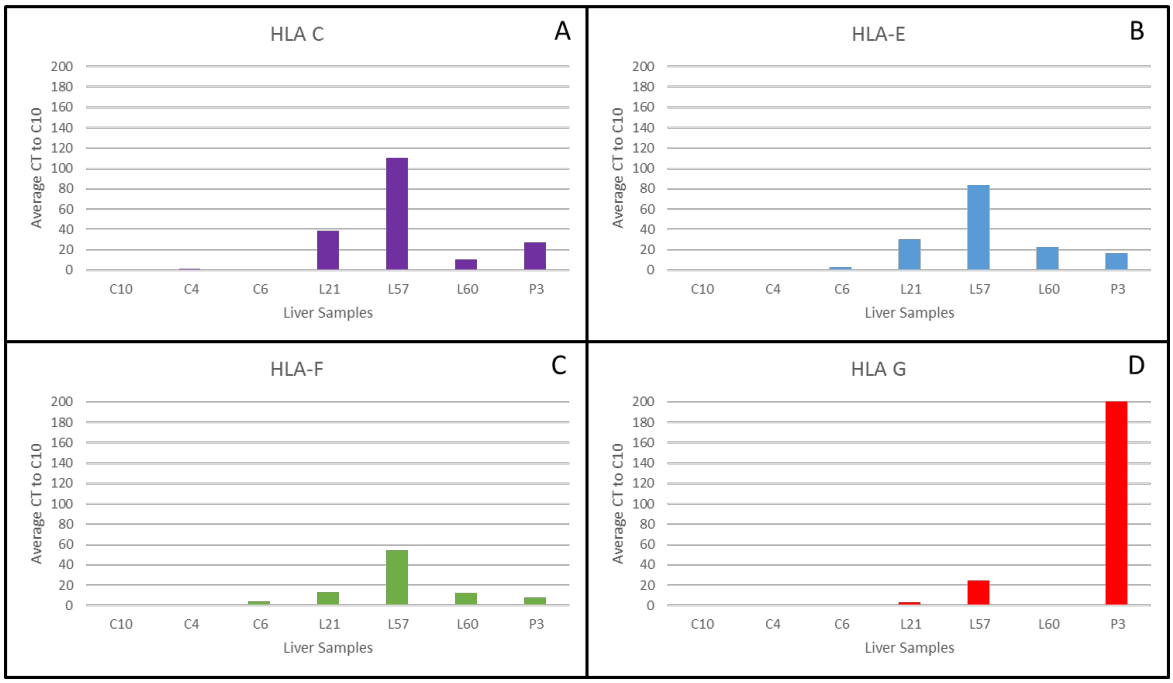

Figure 3.21 - Validation of MHC class I expression using qRT-PCR. *Expression of HLA-C (A), HLA -E (B), HLA-F (C), and HLA-G (D) RNA from control liver (C), cirrhosis (L) and placenta (P). The cirrhotic samples included HCV (L21), HBV (L57) and AIH (L60). Calnexin and hypoxanthine-guanine phosphoribosyltransferase (HPRT) housekeeping genes were used as a positive control and water was used as a negative control for all reactions to ensure validity. Each sample was run in triplicate and each experiment was performed three times. Mean results are shown with HPRT used for analysis. Sample C10 was used as a reference sample in all experiments and this value was then used for relative quantification.*

The presence of HLA-G RNA in the only HBV positive patient sample included prompted further experiments. A further two HBV positive liver samples were acquired from colleagues at The London Hospital (courtesy of Professor G. Foster & Dr U. Gill) and submitted to analysis **(Figure 3.22)**; the sample from L57 was tested again in the same run. All three HBV positive samples, including the two additional samples of HBV liver tissue L65 and T1 and the repeat sample from L57, were positive for HLA-G RNA; expression in L65 was marked, while T1 was positive but at lower levels **(Figure 3.22)**. The latter was a much smaller sample, and had also been stored in buffer, and while both factors may have influenced the quantitative analysis of this sample it was also found to contain HLA-E RNA validating the results **(Figure 3.22)**. In the same run L61, a cirrhotic control with PBC and two control liver samples (C5 & C15) were confirmed to be HLA-G RNA negative **(Figure 3.22)**. At the time of sample collection L57 was on antiviral therapy and was hepatitis B e-antigen (HBeAg) negative, hepatitis B e-antibody (anti-HBe) positive and HBV DNA negative. L65 was not on antiviral

therapy and was positive for both HBeAg and HBV DNA in serum. T1 was hepatitis B surface antigen (HBsAg) positive but the other clinical data is unknown.

Further experiments to pursue these interesting observations are planned in collaboration with colleagues at University College, London to determine whether chronic HBV carriers do have HLA-G RNA in liver tissue and if so, to try to understand why the associated protein was not detected. One explanation could be that the protein is excreted promptly; in HBV carriers with high level viral replication HBsAg cannot be detected easily in liver tissue but is present in plasma at enormous concentrations because of prompt secretion into plasma. Exposure to HBV in foetal life is associated with almost inevitable lifelong infection (unless the infant is vaccinated); in the first few decades of life, thereafter, characterised by high titre HBeAg and high-level viral replication, there is no liver injury and minimal hepatic inflammation a state that has been labelled immunotolerant; inflammation and fibrosis are triggered by the loss of HBeAg. The reason that exposure to HBV in foetal life leads to immune tolerance has never been explained; if further work confirmed a relation between HLA-G and chronic HBV infection this would be an exciting avenue to pursue.

In further experiments using a highly artificial situation in which human hepatocytes expressing HBV were isolated from the spleen of a humanised mouse model of hepatitis B virus infection (Billerbeck et al., 2016) were tested for HLA-G by PCR and found to be negative; these experiments in collaboration with Dr Marcus Dorner at Imperial College, London were curtailed by the sad, premature and unexpected death of Dr Dorner.

HLA-E is known to be present in liver tissue in patients with chronic HBV infection (Chen et al., 2006, Zidi et al., 2016) and the same samples were tested for the presence of HLA-E RNA **(Figure 3.22)** and all were positive, indicating adequate storage of these samples for qRT-PCR analysis. Different control and placenta samples were used for this experiment as there was no tissue remaining of the previous samples used in **Figure 3.21.** The relative copy number of the expression of both HLA-E and HLA-G in the placenta and control samples is lower in these samples.

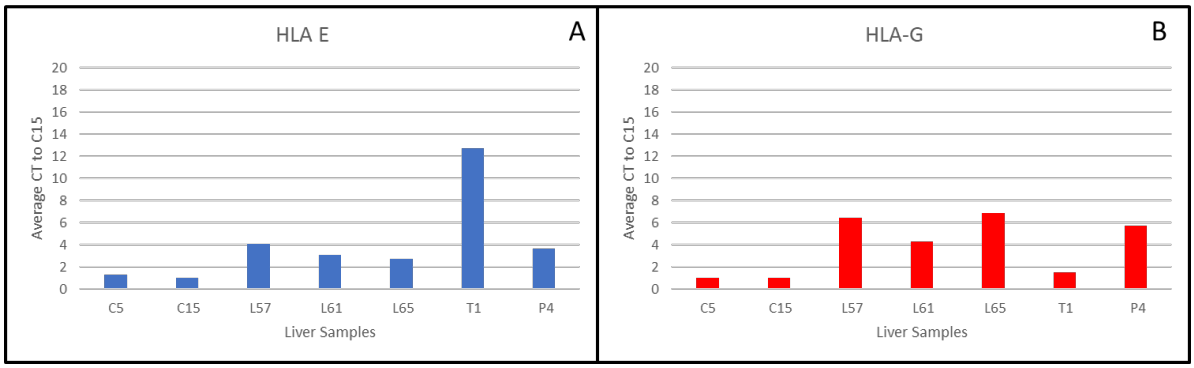

Figure 3.22 - HLA-G RNA appears to be present in hepatitis B liver samples. *Expression of HLA-E (A) and HLA-G (B) RNA from control liver (C), cirrhosis (L), Liver biopsy (T) and placenta (P). The cirrhotic samples included HBV (L57, L65 and T1) and PBC (L61). Calnexin and HPRT housekeeping genes were used as a positive control and water was used as a negative control for all reactions to ensure validity. Each sample was run in triplicate and each experiment was performed three times. Mean results are shown with HPRT used for analysis. Sample C15 was used as a reference sample in all experiments and this value was then used for relative quantification.*

A change in clinical practice with the introduction of fibroscan has reduced the number of patients undergoing diagnostic liver biopsy at the same time as the number of patients undergoing liver transplantation for HBV related liver failure has fallen substantially with the introduction of effective antiviral therapy with Adefovir, Entecavir and Tenofovir. Thus, the supply of HBV infected liver tissue in Cambridge has diminished almost to nothing, limiting the number of samples available to me for further study at this point. As mentioned in the introduction, HLA-G is a tolerogenic molecule and the presence of HLA-G may play a part in patients with chronic HBV infection by induction of tolerance (Lash et al., 2010). The lack of samples for study necessitates a different approach to confirm or refute his hypothesis.

3.4.10 Validation of HLA Expression using Mass Spectrometry

As a final test to validate the HLA expression results observed in this chapter using immunoprecipitation, selected immunoprecipitates were subjected to mass spectrometry analysis to confirm the isolation of the specific non-classical MHC class I molecules.

Secondly, an immunoprecipitation with the non-conformational antibody MEMG01 to HLA-G was also undertaken in an attempt to identify the 50kDa band with samples sent for mass spectrometry.

The data from the first samples sent was unusable. A second experiment to repeat the results was planned but has had to be postponed because of the SARS-Cov-2 outbreak.

3.5 Discussion

HLA class I is known to be present in both healthy and diseased liver tissue (Boegel et al., 2018). Western blot and immunoprecipitation experiments in this study support this and act as a test of the scientific techniques and quality of liver tissue samples.

The results suggest that HLA-E and -F RNA and the respective proteins are present in human liver tissue. Secondly, that both HLA-E and -F appear to be upregulated in cirrhosis compared to healthy control liver tissue. The presence of HLA-E and -F RNA is shown by the qRT-PCR results. The use of positive and negative control tissues and testing of the primers by sequencing confirms the validity of these results. The only published work to date on the presence of HLA-E RNA in liver disease was specifically looking at HBV and suggested it is downregulated (Chen et al., 2006). This is the opposite of my results but also contradictory to the other published literature on HLA-E (Araujo et al., 2018, Nattermann et al., 2005, Zidi et al., 2016). However, there are no reports of HLA-F RNA in liver disease to date.

The western blot and immunoprecipitation data also confirm the presence of HLA-E and -F in the liver tissue. Although it is difficult to quantify the level of expression from this method the images suggest there is higher expression in diseased liver. Liver tissue is known to contain HLA class I (Boegel et al., 2018) and so it is likely that HLA-E and -F would both also be present although this has not yet been reported specifically. The results are supported by using placenta as a positive control and the use of multiple antibodies for each molecule reporting the same results.

This is the first time that HLA-E and HLA-F have been shown to be present in liver tissue by immunoprecipitation. The results suggest that expression is higher in liver disease than in control liver tissue. The difference in the expression of HLA-E and -F in liver disease suggests that there may be a role for these molecules in the pathogenesis of cirrhosis.

HLA-E is a ligand for NK cells preventing their activation (Lanier, 1997). The presence of higher levels of HLA-E in cirrhosis may suggest that the NK cells are affected in liver disease and cannot function correctly. This overexpression in cirrhosis may mean that damaged cells in cirrhosis are not destroyed as they should be, leading to hepatocyte tolerance. In cirrhosis there is a known accumulation of senescent hepatocytes (Aravinthan et al., 2013a). I did not quantify the amount of senescent tissue in these samples which on reflection was an oversite, as the expression level can

vary which could confound the results (Meijnikman et al., 2021). However, we can presume there were some and the presence of high levels of HLA-E may prevent NK cells from removing these damaged cells, allowing this accumulation. If this is the case, then there may be the possibility of altering HLA-E expression in the future to act as a therapeutic option. This would be similar to current antibodies being investigated to block cancer cells in potential therapies (Hamid et al., 2019, Borst et al., 2020).

The true role of HLA-F is still unknown (Geraghty et al., 1990); however recent publications have suggested that it can be expressed on the plasma membrane and act as a ligand for KIR3DS1 and killer cell immunoglobulin like receptor with three immunoglobulin domains and long cytoplasmic tail (KIR3DL1) (Garcia-Beltran et al., 2016). The results herein suggest HLA-F is expressed in liver tissue and appears to be more highly expressed in liver disease. Again, the overexpression of HLA-F in cirrhosis may alter the immune response and NK cell activation in disease. As above this could tolerise hepatocytes and so allow the senescent cells to accumulate in liver disease leading to liver dysfunction.

The presence of HLA-G is more complex and requires further investigation. Previous published studies have reported the presence of HLA-G in liver disease (Moroso et al., 2015, Souto et al., 2011, Catamo et al., 2014) but these authors restricted investigations into the presence of HLA-G to immunohistochemistry and so these studies can be considered limited by the use of a single technique.

qRT-PCR analysis for HLA-G RNA did not detect identifiable RNA in all 20 liver samples tested apart from one HBV infected liver (and two later samples). Further work is being undertaken to investigate whether there is an association of HLA-G in HBV similar to that seen with HLA-E.

Western blot analysis identified a band which was larger than expected for HLA-G and running higher than that seen in the placenta positive controls suggesting a slightly different molecule. Immunoprecipitation was unable to identify any HLA-G present in the liver samples but did show abundant expression in the placenta control samples.

The results at this stage are inconclusive and suggest that conventional HLA-G is not present in cirrhosis. Options include cross reactivity of antibodies to another molecule or the expression of an aberrant form of HLA-G that is not recognised by conventional antibodies. The other HLA molecules are larger than HLA-G and the antibody could be identifying classical HLA class I. HLA-G has eight known forms (Apps et al., 2008b), it is possible that only one form is expressed in liver disease or in a modified or spliced form. Isotopes HLA-G2, G3 and G4 are known to be smaller and may not

therefore be detected by these antibodies (Wuerfel et al., 2020). The difficulties of identifying all HLA-G isoforms including soluble forms with conventional antibodies has been highlighted (Alegre et al., 2014). HLA-G can also form dimers and it has been questioned whether the antibodies would detect this form (Alegre et al., 2014) However, the lack of HLA-G RNA in the non-HBV infected liver samples suggests its presence to be unlikely. Although, there is a possibility that a spliced form may not be identified by the primers designed.

Many practice immunoprecipitation experiments were undertaken to polish the technique and control the results. However, in all IP results with all liver samples there was a 50kDa band. Despite adding extra wash steps, an altered volume of antibody and increased volume of beads this band remained. However, it was not present in the negative control or in the western blot analysis. The difference between the IP and western blot tests was the secondary antibody used. With all western blots the Dako anti-mouse secondary was used while in IP's the true blot anti-mouse antibody was used. This suggested that the liver tissue was reacting with the secondary antibody.

This work was all undertaken with liver lysate. The whole liver sample was broken down and formed into a lysate. Therefore, this sample does contain hepatocytes, but it also contains other cells present in the liver that could include some immune cells (although in small numbers). One must conclude that it is possible that the positive signal seen in the samples could be from circulating immune cells and not hepatocytes. Secondly, for these ligands to be having a significant effect there needs to be surface expression of these molecules to interact with the target cells. The next chapter aims to investigate the expression of the HLA molecules in liver tissue to identify what cells are expressing the molecules and whether there is any surface expression.

Chapter 4 Results - Localisation of MHC Class I Molecules in Liver Tissue

4.1 Introduction

In chapter 3 I described the presence of various MHC class I molecules in liver tissue and in addition demonstrated their increased expression in liver disease. However, qRT-PCR for the relevant RNA and western blotting for the relevant protein do not reveal the localisation of the molecules. The next stage was to determine the precise sites of MHC class I molecule expression i.e. which cells expressed these molecules and whether increased expression in liver disease was true for all cell types.

MHC class I molecules are ligands for NK cells, and they need to be expressed on the cell surface to bind with NK cells and thus alter their function (Iannello et al., 2008). MHC class I expression may be present on circulating immune cells within the liver tissue (Racanelli and Rehermann, 2006). The aim, therefore, was to determine whether these molecules were indeed expressed on hepatocytes, rather than cells infiltrating into the liver. To this end, the cellular localisation of specific HLA molecule and stress induced ligands was determined by performing immunohistochemistry. Furthermore, the surface expression of MHC class I molecules was investigated using biochemical techniques.

A hypothesis for the evolution of cirrhosis is that the failure to clear senescent hepatocytes in chronic liver injury is a form of tolerance. Altered expression of MHC class I molecules may prevent NK cell mediated killing, leading to the accumulation of senescent hepatocytes. For this reason, investigation of MHC class I expression was undertaken in conjunction with immunohistochemistry for the senescence marker p21.

4.2 Optimisation of Immunohistochemistry

Initial immunohistochemistry experiments were undertaken, first to gain experience with these techniques, then to optimise the various approaches and to identify the most suitable antibodies for detection of MHC class I molecules.

Anonymised liver tissue was provided by Addenbrooke's Hospital tissue bank as paraffin embedded slides of cirrhotic tissue from a broad range of liver disorders. **Figure 4.1** shows liver tissue from a patient with cirrhosis stained with an antibody to Mcm-2 which served as a positive control. This protein is present throughout the cell cycle and is therefore present in all replicating cells as well as those that have entered the cell cycle but in which there is cell cycle arrest.

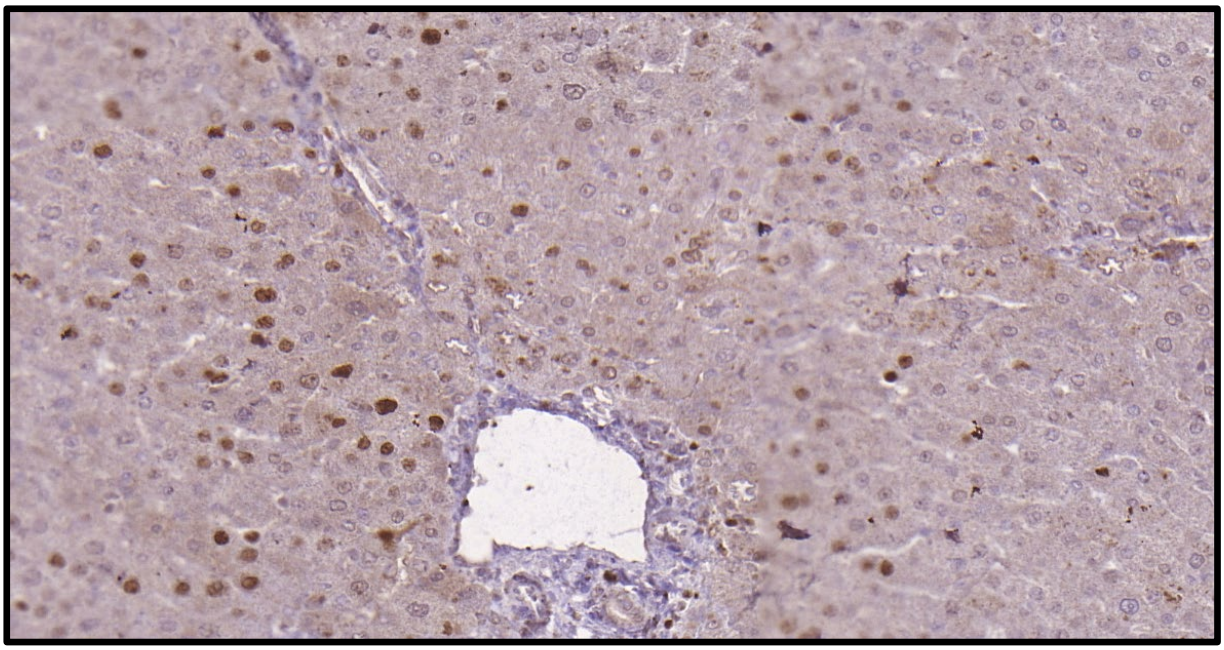

Figure 4.1 – Immunohistochemistry showing positive staining for Mcm-2 on paraffin embedded cirrhotic tissue. *Mcm-2, a marker of cell cycle entry, is seen within the nuclei; the secondary antibody is stained with DAB so positive cells are dark brown.*

Initial experiments used citrate antigen retrieval buffer, but as dual staining with p21 was planned, EDTA buffer was chosen for subsequent studies. EDTA buffer can enhance staining with low affinity antibodies or low affinity epitopes; however, this may be at the expense of increased background staining. The method used was based on previous work undertaken with p21 (a marker of cell cycle arrest and of senescence) (Marshall et al., 2005).

The following antibodies were trialled to detect various MHC class I molecules using immunohistochemistry:

W6/32, which reacts with peptide loaded MHC class I molecules associated with β2m. It is known to react with all subtypes of HLA-A, -B and -C (Apps et al., 2009). Unfortunately, I found this antibody did not work on paraffin embedded sections.

HC10 antibody, which is known to react with free heavy chains of the majority of HLA-B and -C molecule heavy chains and a well-defined series of HLA-A molecule heavy chains (HLA-A10, -A28, -A29, -A30, -A31, -A32, -A33) (Stam et al., 1986). Due to the high concentration of HLA class I in these samples the antibody was used at low concentration following preliminary work.

L31 was used for detection of HLA-C (Beretta et al., 1987). This antibody has been shown to cross-react with some HLA-B antigens including HLA-B7, -B8, -B35 and -B51 (Setini et al., 1996). Previous

citations and the manufacturers' instructions advised use at a concentration of 100µl per ml (Benevolo et al., 2007).

3D12, a monoclonal antibody to HLA-E (Lee et al., 1998) reported not to cross react with HLA-A, -B, -C and -G. I found this antibody did not work on paraffin embedded sections and on review of the manufacturers' guide it had not been validated for use in this technique.

MEME02, a monoclonal antibody to the denatured heavy chain of HLA-E has been tested to ensure it does not cross react with HLA-A, -B, -C or -G (Menier et al., 2003). This antibody has been used previously with paraffin embedded sections (Reimers et al., 2014); however the manufacturers' guide advises that concentrations should be optimised by preliminary testing. After preliminary experiments, a concentration of 1 in 100 (10µl per ml) was considered optimal.

FG1 is a monoclonal antibody generated to react with recombinant HLA-F complexed with β2m. It was assessed previously to ensure no cross-reactivity with HLA-A2, -B7, -C, -E and -G (Lepin et al., 2000) using the antibody at 30µl per ml concentration. Following further optimisation, the antibody was used at 1 in 200 (5µl per ml).

Finally, regarding HLA-G, published papers (Moroso et al., 2015, Cai et al., 2009) suggested it can be detected in cirrhosis using the MEMG01 antibody (Menier et al., 2003) which reacts with the denatured heavy chain of HLA-G and detects five isoforms of HLA-G. Previous studies report no cross-reactivity with HLA-A, -B, -C and -E (Lozano et al., 2002, Hurks et al., 2001) so this antibody was used at a concentration of 1 in 100 (10µl per ml). In addition, colleagues within the Department of Pathology in Cambridge advised the use of MEMG01 on paraffin embedded sections for investigating placental tissue.

In view of the possibility of cross-reactivity, an IgG2a control antibody to Aspergillus Niger glucose oxidase (an enzyme not present or inducible in mammalian tissues) was included as an additional control for each experiment.

4.3 Localisation of HLA Class I in Liver by Immunohistochemistry

4.3.1 HLA Class I is Detected Readily in Liver by Immunohistochemistry

Initially, the presence of HLA class I in both control liver and cirrhosis was confirmed by immunohistochemistry **(Figure 4.2)**. **Figure 4.2** is representative of four experiments testing 20 different cirrhotic and control liver samples. **Appendix Figure 4.1** shows a further example. HC10 antibody detected both plasma membrane localised and intracellular MHC class I in hepatocytes from both normal and diseased liver tissue, consistent with a previous publication (Paterson et al.,

1988). There was high expression of HLA class I in all liver tissue obtained from both control and cirrhotic samples; there was slightly higher expression of HLA class I consistently in cirrhosis when compared with control liver tissue. There was intense staining of HLA class I in the sinusoidal cells as expected, since these include kupffer cells (Poisson et al., 2017).

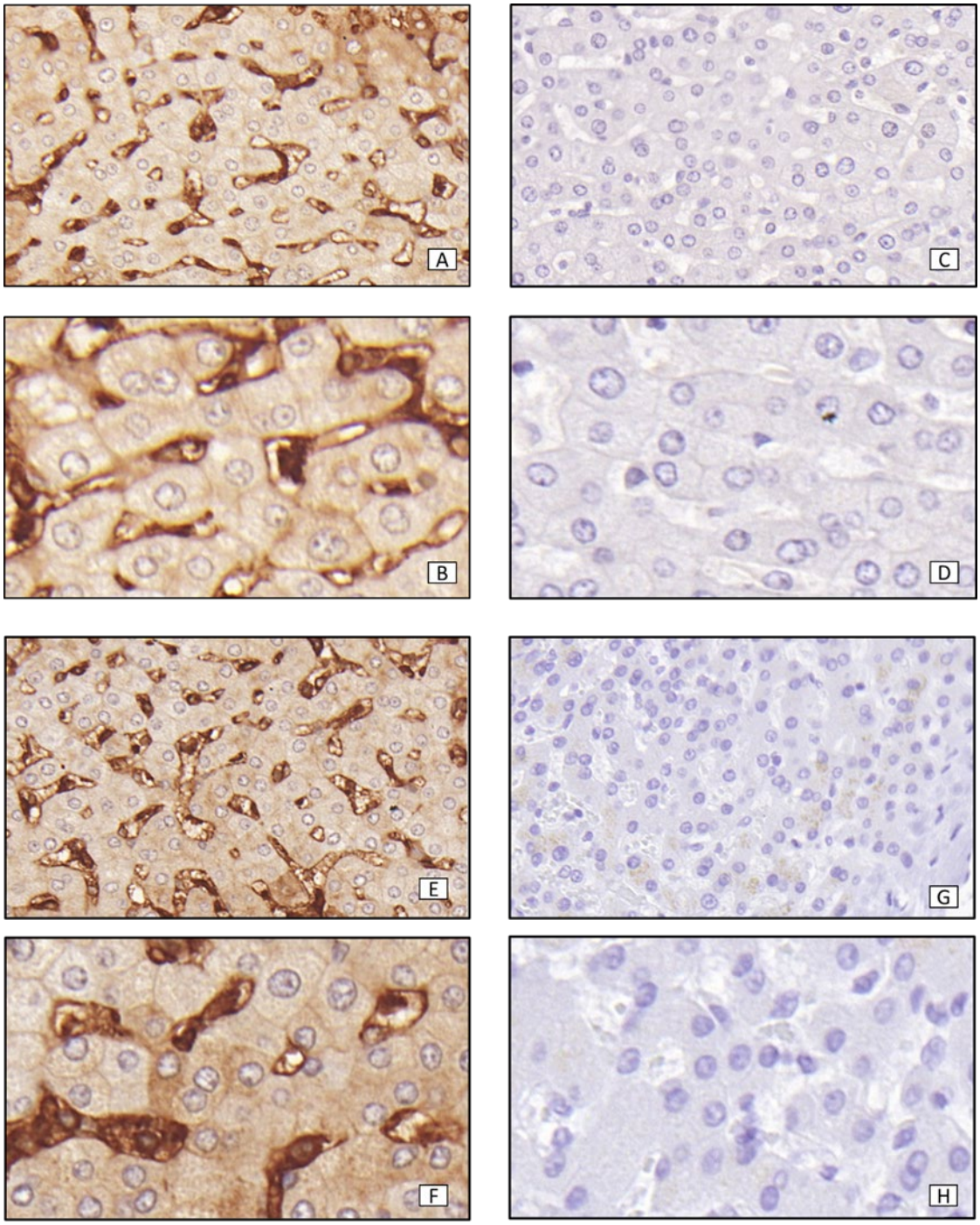

Figure 4.2 – Immunohistochemistry of HLA class I with HC10 antibody. *Antigen retrieval with EDTA buffer. Positive staining is seen as brown as the secondary antibody was tagged with DAB. Images A (20 times magnification (20x)) and B (40 times magnification (40x)) showing cirrhotic tissue with HLA class I. Images C (20x) and D (40x) showing cirrhotic tissue with an IgG2a control. Images E (20x) and F (40x) showing HLA class I staining in healthy control liver tissue and images G (20x) and H (40x) showing healthy control tissue with an IgG2a control antibody.*

4.3.2 HLA-C is Detected Readily in Liver Tissue by Immunohistochemistry

After reviewing some of the MHC class I results it was decided to investigate specifically for the presence of HLA-C within the liver tissue. As discussed in chapter I, HLA-C has a specific role during pregnancy, helping the developing foetus evade the immune system (Apps et al., 2008a) and could also play a role in cirrhosis. L31 antibody was used as described previously (Benevolo et al., 2007). My results suggested that in addition to intracellular HLA-C, cell surface expression of HLA-C was detectable on hepatocytes from both healthy and cirrhotic tissue; this was consistently of higher intensity in the cirrhotic specimens **(Figure 4.3)**. L31 staining also revealed the detection of HLA-C on immune cells found in the sinusoidal region. The staining observed for HLA-C shown in **figure 4.3** mirrors the staining pattern seen in **figure 4.2** for pan-HLA class I (using HC10), but there appears a greater difference between the cirrhotic and control tissues. **Figure 4.3** shows a representative image of the immunohistochemistry performed over three experiments and undertaken in 20 different cirrhotic and control liver samples. A further example is shown in **Appendix Figure 4.2**.

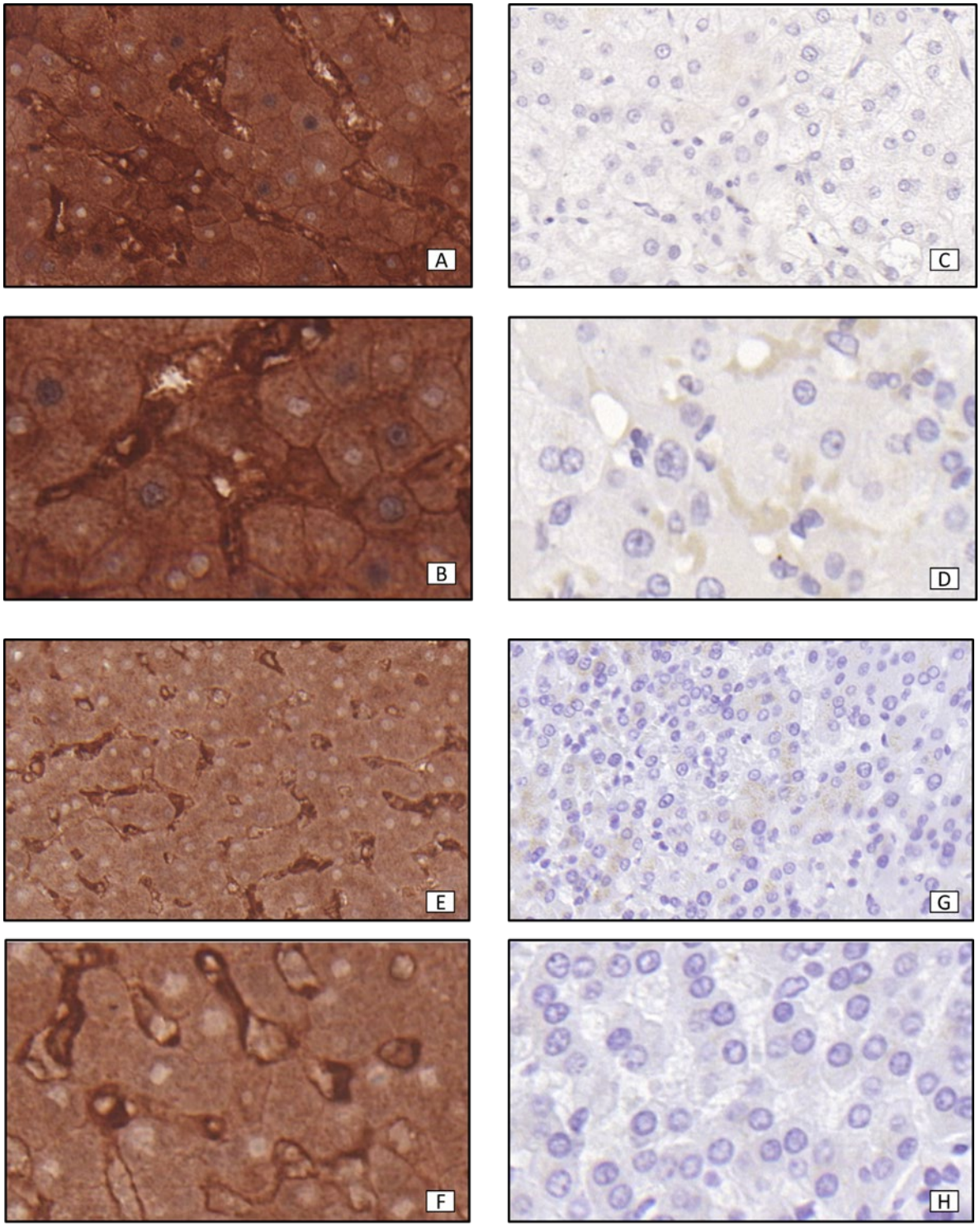

Figure 4.3 – Immunohistochemistry of HLA-C with L31 antibody. *Antigen retrieval with EDTA buffer. Positive staining was brown as the secondary antibody was tagged with DAB. Images A (20x) and B (40x) showing staining in cirrhotic tissue and images C (20x) and D (40x) staining in cirrhosis with an IgG2a control. Images E (20x) and F (40x) showing staining in healthy control liver tissue; G (20x) and H (40x) showing healthy control tissue with an IgG2a control antibody.*

4.3.3 HLA-E is Detected Readily in Liver Tissue by Immunohistochemistry

The next step was to investigate the distribution of non-classical HLA molecules. In chapter 3, I demonstrated the presence of HLA-E in control and diseased liver tissue. Staining for HLA-E was undertaken with MEME02 as described previously (Reimers et al., 2014) **(Figure 4.4).**

An interesting distribution of HLA-E when staining with MEME02 was seen in both cirrhotic and healthy liver tissue and this was more marked in the cirrhotic samples but with a similar distribution **(Figure 4.4)**. In both disease and health there was staining of both the infiltrating immune cells and hepatocytes. The hepatocyte staining showed a predominantly perinuclear and diffuse intracellular staining detection, consistent with retention of HLA-E within the ER. There was only minimal hepatocyte membrane expression; however, when detected this appeared to be stronger in the cirrhotic specimens. This was an unexpected distribution since interaction with the immune system would require surface rather than perinuclear expression. **Figure 4.4** shows a representative example of this staining from five experiments in at least 30 different cirrhotic and control liver sections. **Appendix Figure 4.3** shows a further example. On review, there was a shift from cytoplasmic localisation to nuclear staining in cirrhosis. Staining was also seen in the portal tracts with bile ducts often positive **(Figure 4.4 Images E & F)**. This again was more marked in the cirrhotic samples than control specimens.

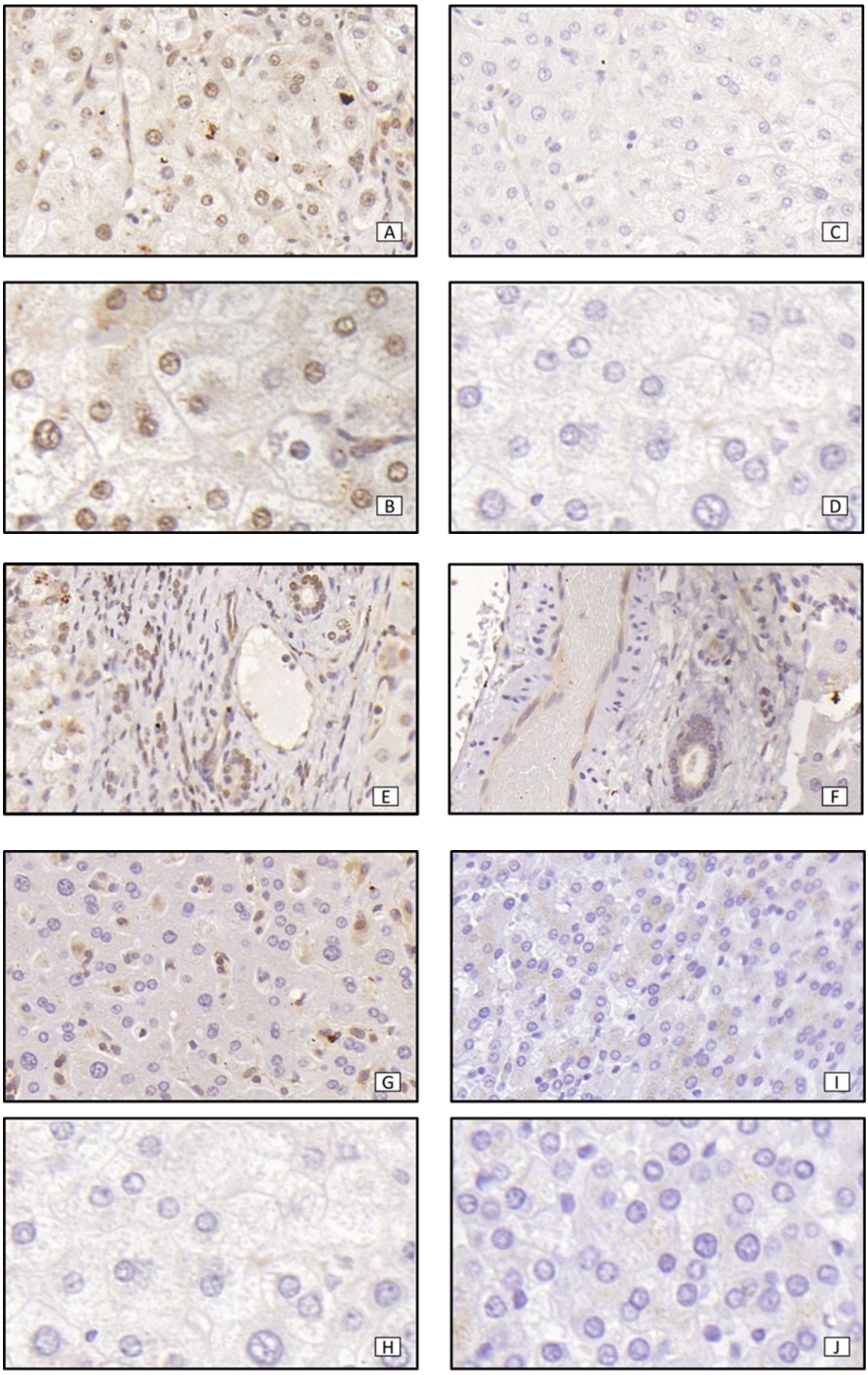
A
C
B
D
E
F
G
I
H
J

Figure 4.4 - Immunohistochemistry of HLA-E with MEME02 antibody. *Antigen retrieval with EDTA buffer. Positive staining is seen as brown as the secondary antibody was tagged with DAB. Images A (20x) and B (40x) showing staining of hepatocytes in cirrhotic tissue, while C (20x) and D (40x) show staining in cirrhosis with an IgG2a control. Images G (20x) and H (40x) show hepatocyte staining in healthy control liver tissue, while I (20x) and J (40x) show staining in healthy control tissue with an IgG2a control antibody. Images E and F showed portal and sinusoidal staining in the cirrhotic and control samples, respectively.*

4.3.4 HLA-F is Detected Readily in Liver Tissue by Immunohistochemistry

In chapter 3 I demonstrated that HLA-F is present in liver tissue using western blotting. Further work using immunohistochemistry was undertaken to identify which cells were expressing the molecule and to identify the subcellular distribution of HLA-F. The antibody used was FG1 as described previously (Lepin et al., 2000). My results suggest HLA-F was detected in both cirrhotic and healthy liver tissue **(Figure 4.5)**. Most of the staining with FG1 was detected intracellularly within the hepatocyte; however, membrane expression in specific areas was also seen on groups of hepatocytes **(Figure 4.5 section B, arrowhead)**. Perinuclear staining, suggestive of HLA-F retention within the golgi apparatus, was also observed using immunohistochemistry. There appeared to be more perinuclear localisation of HLA-F in healthy tissue than in cirrhotic tissue. Conversely, FG1 staining in cirrhosis appeared more diffuse, suggesting HLA-F may be localised in the ER. These appearances are consistent with a shift in HLA-F expression from the nucleus to the ER and eventually to the cell membrane in liver injury, as seen with HLA-E. **Figure 4.5** shows a representative example of HLA-F staining. Four experiments were undertaken in more than 20 different cirrhotic or control samples. A further example is shown in **Appendix Figure 4.4**.

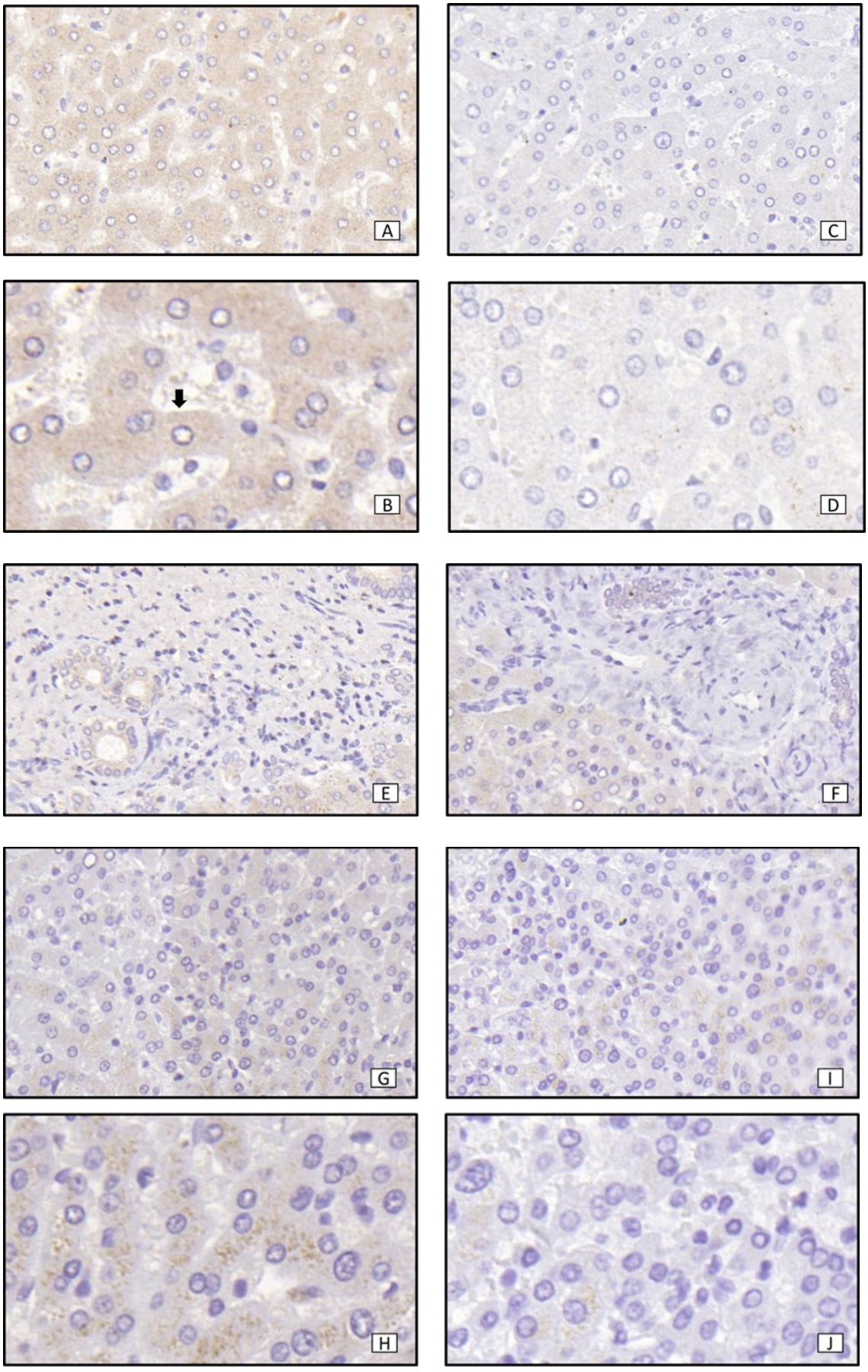
A
C
B
D
E
F
G
I
H
J

Figure 4.5 – Immunohistochemistry of HLA-F with FG1 antibody. *Antigen retrieval with EDTA buffer. Positive staining is seen as brown since the secondary antibody was tagged with DAB. Images A (20x) and B (40x) showing hepatocyte staining in cirrhotic tissue; C (20x) and D (40x) showing staining in cirrhosis with an IgG2a control. Images G (20x) and H (40x) showing staining in healthy control liver tissue and I (20x) and J (40x) showing no staining with an IgG2a control antibody. Images E and F show minimal portal staining in the cirrhotic and control samples, respectively.*

4.3.5 HLA-G is Detected Readily in Liver Tissue by Immunohistochemistry

Several published studies have reported that HLA-G is present in cirrhosis using MEMG01 antibody (Moroso et al., 2015, Souto et al., 2011). As discussed in the previous chapter there are concerns that this antibody reacts with something other than HLA-G. However, there have been no reports of cross reactivity with other HLA molecules (Lozano et al., 2002, Hurks et al., 2001).

The staining I observed with the MEMG01 antibody was congruent with the published studies (Lozano et al., 2002) **(Figure 4.6)**. **Figure 4.6** shows a representative sample of HLA-G staining over eight experiments testing 30 different cirrhotic and control liver samples. Although increased staining with MEMG01 was seen on the cirrhotic samples compared with healthy liver, the staining appeared diffuse, intracellular, and patchy across all liver tissues **(Figure 4.6)**. Furthermore, my findings demonstrated increased staining with MEMG01 on cirrhotic samples compared to placental tissue **(Figure 4.6)**, which was unexpected both from the literature (Moroso et al., 2015) and my own western blotting experiments **(Figure 3.16)**. The sinusoidal cells also stained positively using MEMG01.

The intensity of the staining observed using immunohistochemistry **(Figure 4.6)** appeared to be inconsistent with the immunoprecipitation experiments I undertook using liver samples in which I failed to detect HLA-G **(Figures 3.17 - 3.20)**. However, staining using MEMG01 on the placental samples was in line with the expected results **(Figure 4.6 sections K - N)**. For example, I observed intense staining using MEMG01 on cells thought to be Hofbauer cells (macrophages that should be positive for HLA-G) **(Figure 4.6 section L, arrowhead)**. The IgG2a control was also negative. In summary, although my immunohistochemistry experiments suggest that HLA-G may be present in liver tissue, the irregular staining pattern observed using this technique and its inconsistency with my other data makes me somewhat sceptical about these findings and they need to be considered with caution. A further example is seen in **Appendix Figure 4.5.**

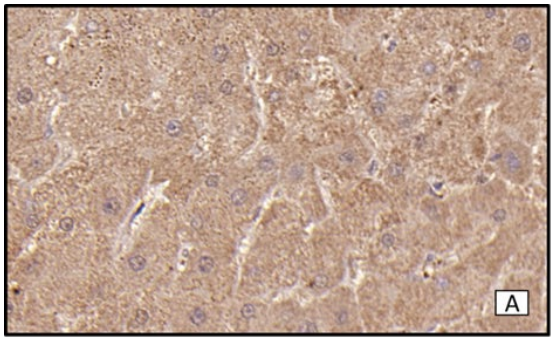
A

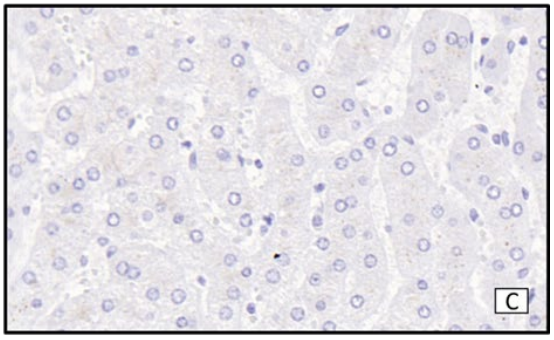
C

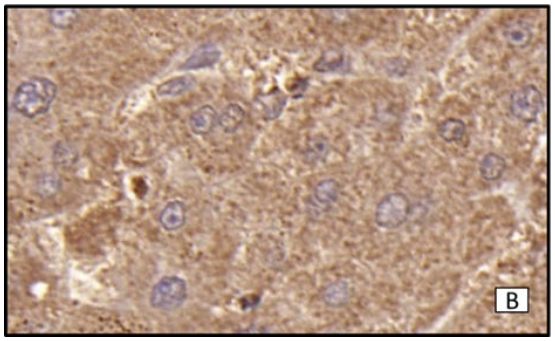
B

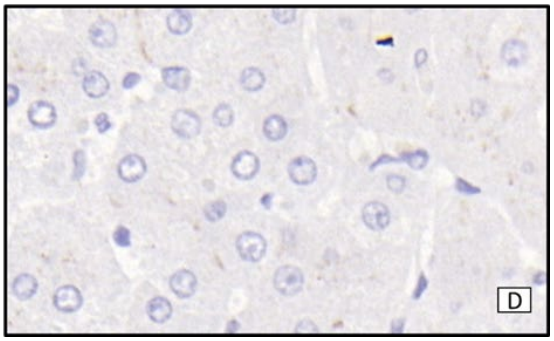
D

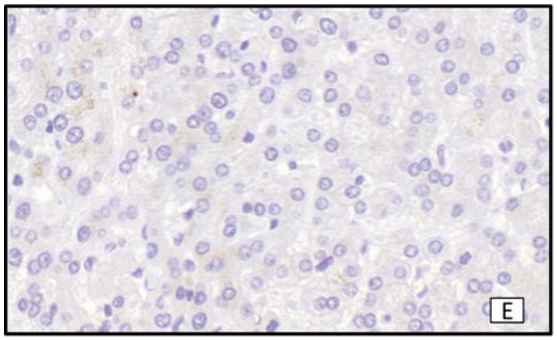
E

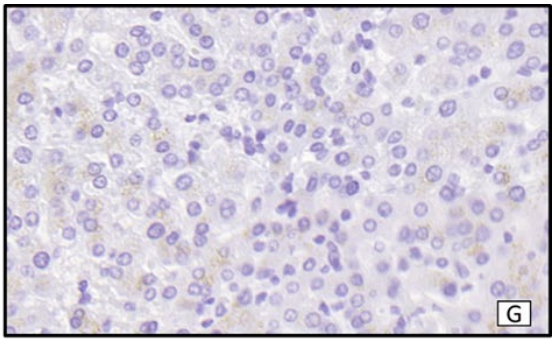
G

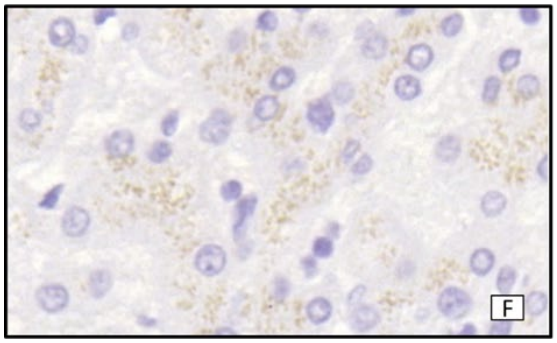
F

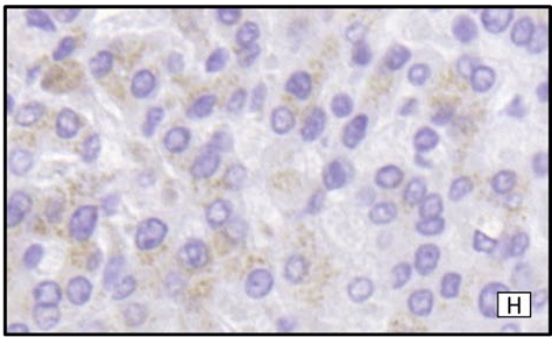
H

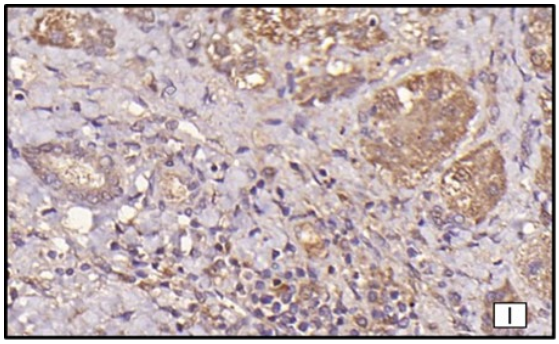
I

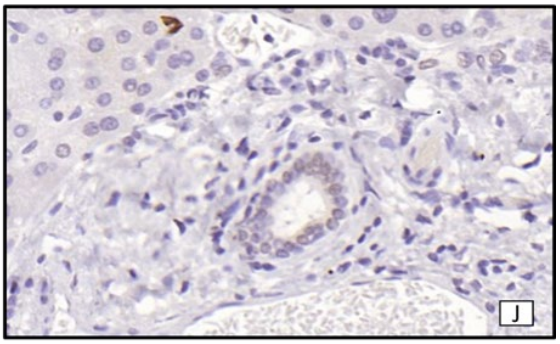
J

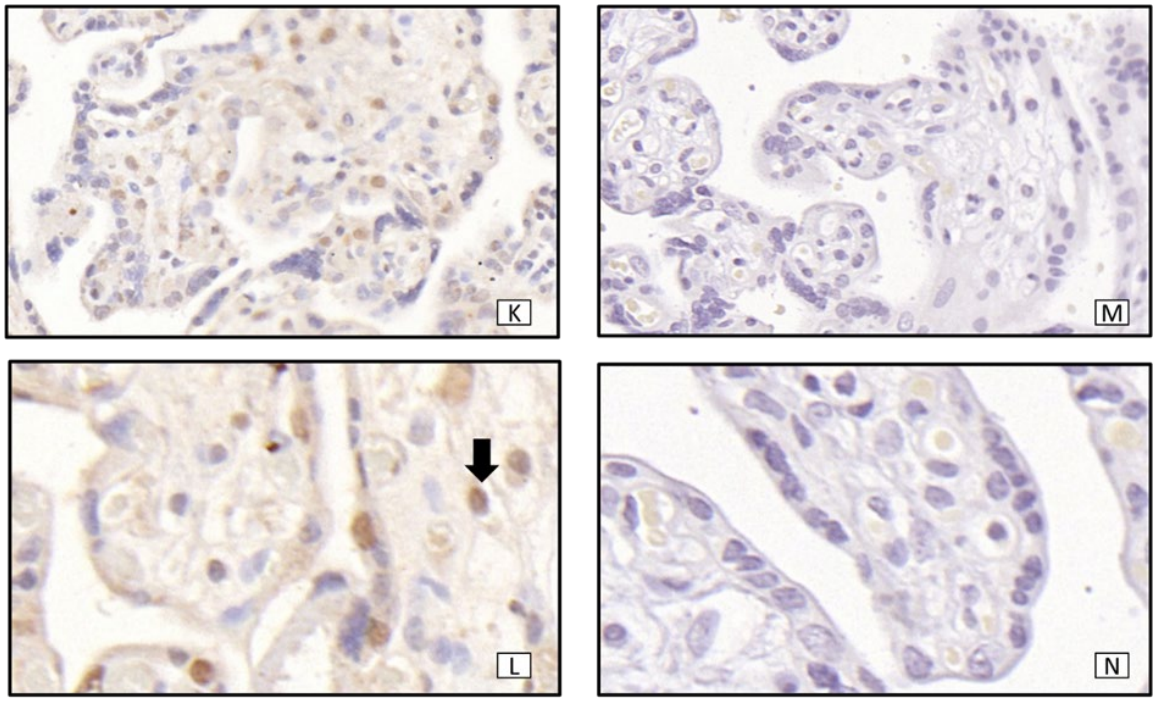

Figure 4.6 – Immunohistochemistry of HLA-G with MEMG01 antibody. *Antigen retrieval with EDTA buffer. Positive staining seen as brown since the secondary antibody was tagged with DAB. Images A (20x) and B (40x) showing staining in cirrhotic tissue; C (20x) and D (40x) showing staining in cirrhosis with an IgG2a control. Images E (20x) and F (40x) showing staining in healthy control liver tissue; G (20x) and H (40x) showing no staining of healthy control liver tissue with an IgG2a control antibody. Images K (20x) and L (40x) show staining of placenta tissue for HLA-G, while M (20x) and N (40x) again show the IgG2a control in the same placenta samples. Images I and J show minimal portal and sinusoidal staining in the cirrhotic and control samples, respectively.*

4.4 Localisation of HLA Class I in Liver Tissue by Immunofluorescence

Next, to further clarify the precise subcellular localisation of the HLA class I expression in the liver samples I turned to fluorescence microscopy. However, this technique proved to be incredibly challenging on paraffin embedded sections due to the substantial autofluorescence, such that interpretation was impossible. Autofluorescence in liver tissue has been reported previously (Bottiroli and Croce, 2004).

My attempts to optimise this included post staining washes with copper sulphate (Schnell et al., 1999) and ericrome T black (Davis et al., 2014). These both reduced autofluorescence, but the effect was minimal and still impaired interpretation of the subcellular localisation of HLA class I staining. Then further amplification of the signal from the target antibody was considered using extra layers of the secondary detection antibody. This did indeed improve my ability to distinguish the HLA

staining, but the background signal was still very high. Finally, UV radiation was used on the slides prior to antigen retrieval and staining (Viegas et al., 2007). This, in conjunction with the amplified antibody, allowed some useful images to be obtained, albeit in the presence of high background staining which prevented adequate negative control images to be obtained, which are critical to interpretation.

Figure 4.7 is representative of the images obtained with a second example in **Appendix 5.** Multiple experiments were undertaken while trying to reduce the background and the staining was consistent across these different cirrhotic and control sections. The final protocol was performed twice.

Membrane expression of HLA class I was observed on hepatocytes in cirrhosis using HC10 antibody **(Figure 4.7 images A and B)** as previously published (Paterson et al., 1988). Staining with MEME02 antibody revealed both a reticular and perinuclear localisation for HLA-E in hepatocytes, indicative of retention within the ER and golgi **(Figure 4.7 images C and D)**. However, it should be noted that a similar staining pattern was observed when staining using an isotype control **(Figure 4.7 images I and J).** Thus, it was difficult to discriminate the staining observed with MEME02 from the background staining observed on these tissues.

Staining using the FG1 antibody to detect HLA-F revealed a mainly intracellular staining, indicative of the ER, with some occasional cell surface staining **(Figure 4.7 images E and F)**. The strength of the staining appears lower than that of the other HLA molecules. Finally, HLA-G staining with MEMG01 antibody, appears diffusely within the cell and is difficult to distinguish from background staining **(Figure 4.7 Images G and H)**. The negative controls **(Figure 4.7 Images I and J)** for both control and cirrhotic liver show significant background staining. The staining for all molecules in the control liver shows a similar distribution but a lower intensity **(Figure 4.7 images O, P, Q)**.

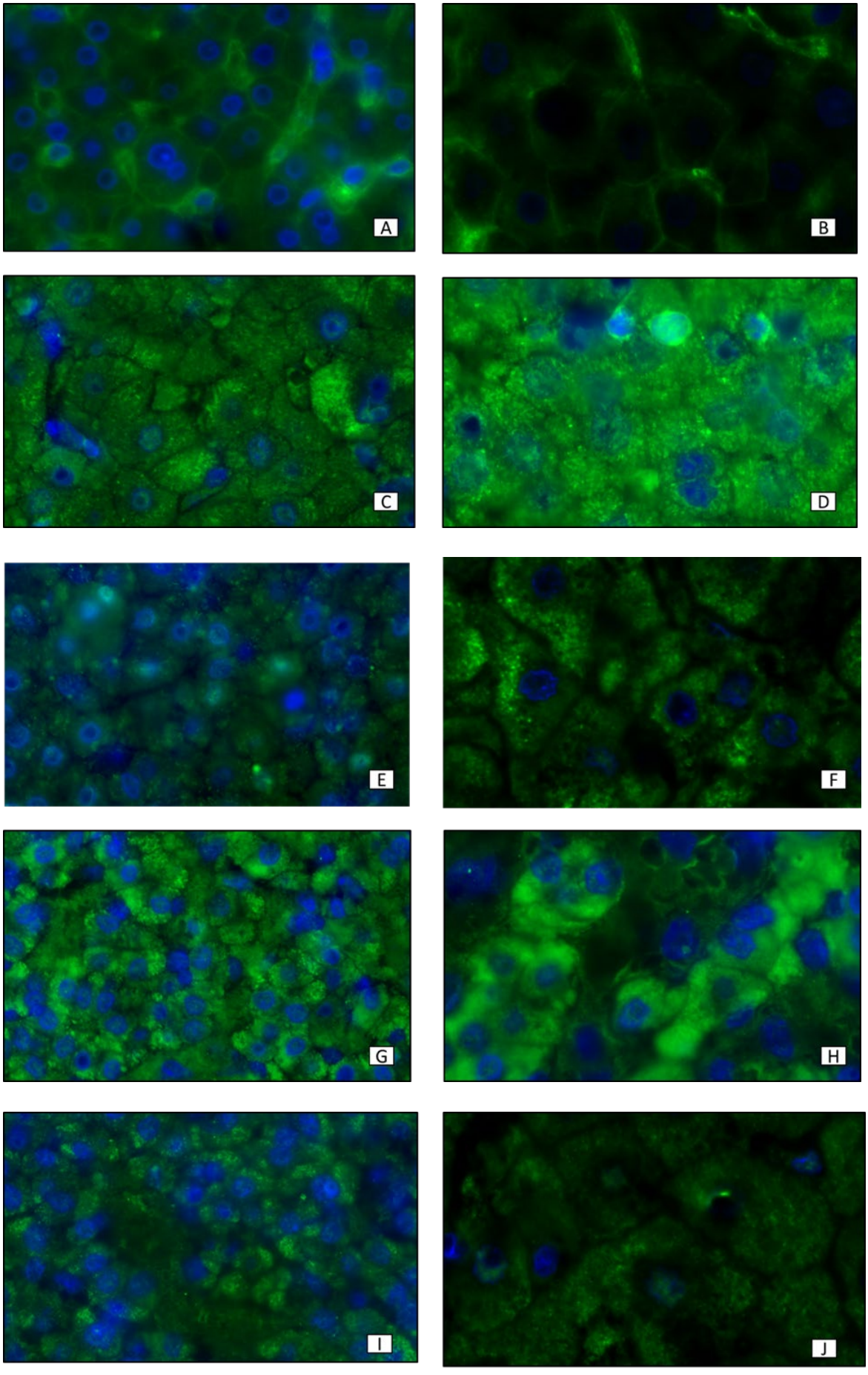
A
B
C
D
E
F
G
H
I
J

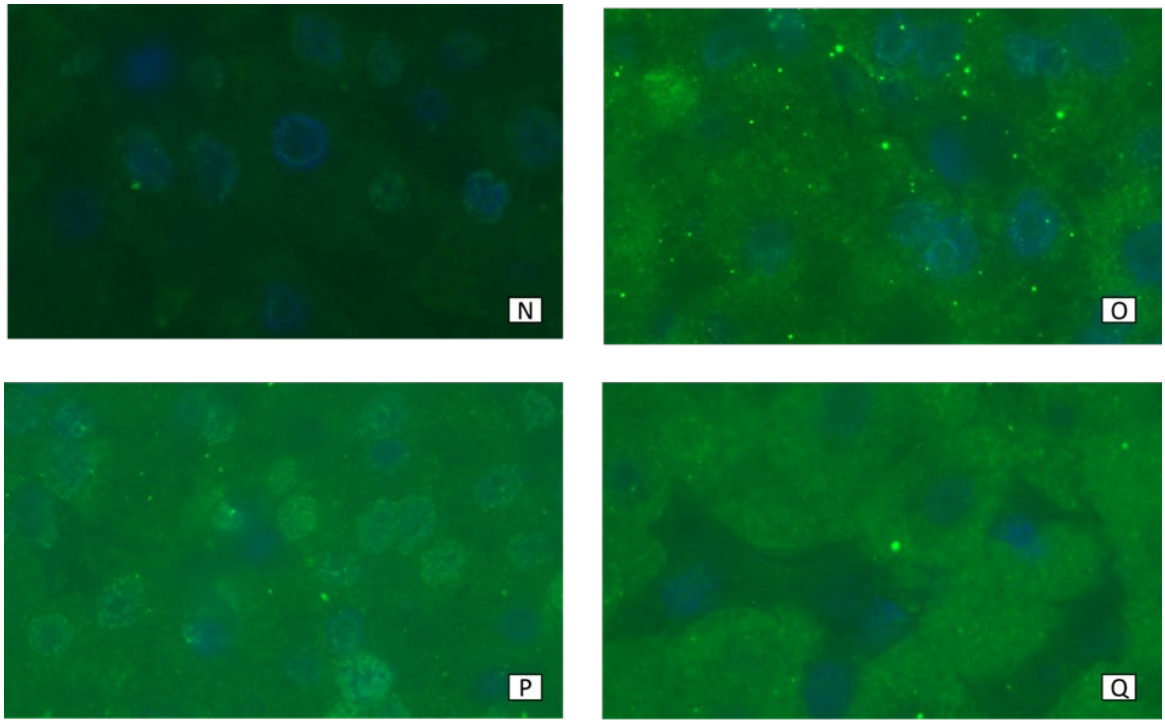

Figure 4.7 – Immunofluorescent staining of HLA class I and specially HLA-E, -F and -G using a green laser*. Nuclei are stained blue with Dapi. Images A (20x) and B (63 times magnification (63x)) show staining in cirrhotic tissue for HLA class I with HC10 antibody. Images C (20x) and D (63x) show staining of HLA-E with MEME02 antibody in cirrhosis. Images E (20x) and F (63x) show cirrhotic tissue HLA-F staining with FG1 antibody. Images G (20x) and H (63x) show staining of HLA-G with MEMG01 antibody in cirrhotic tissue. Images I (20x) and J (63x) show staining with the IgG2a, antibody used as a negative control in cirrhosis revealing prominent background auto-fluorescent staining of liver tissue. Image N (63x) shows prominent staining with the same negative control antibody in healthy control liver. Images O, P and Q (63x) show staining of HLA-E (MEM02), HLA-F (FG1) and HLA-G (MEMG01) respectively in healthy control liver.*

4.5 Investigation of Cell Surface Expression of MHC Class I using Endo H Digest

The results of both the immunohistochemistry and fluorescence microscopy suggested there was strong surface expression of HLA class I on hepatocytes, but the results were less conclusive for the non-classical HLA-E, -F and -G. Therefore, I performed a further set of experiments to explore membrane expression of HLA using a biochemical approach. An endo H digest was performed on the immunoprecipitate samples used in chapter 3. Endo H is an enzyme that breaks down proteins prior to modification in the golgi. Once proteins exit the golgi they are resistant to the effects of this enzyme and cannot be further cleaved (Alberts et al., 2002). Thus, when endo H is combined with

western blotting it can be used to visualise the proportion of a protein that is pre-medial golgi (i.e. endo H sensitive) or post-medial golgi (i.e. endo H resistant).

Figure 4.8 shows the results of the endo H digest for MHC class I, HLA-C, -E and -F. HLA-G was not tested using this approach since the immunoprecipitated samples were negative for this protein. The data shown are representative of two control and two cirrhotic samples studied with each antibody; a further eight samples were then tested to confirm these data **(Appendix 6)**.

Western blot analysis using HC10 on endo H treated W6/32 immunoprecipitate samples revealed most of the MHC class I protein was endo H resistant **(Figure 4.8A)**. This result is supportive of membrane expression of MHC class I. However, the high expression of MHC class I in these samples made it difficult to obtain clear images even with minimal exposure. Thus, bands were seen correlating with MHC class I at 41kDa, representing the surface molecule, as well as a smaller band of 39kDa representing the cleaved band. Similar findings were observed in both control liver and cirrhosis.

Western blot analysis using L31 on immunoprecipitated samples with DT9 showed a similar pattern with HLA-C, with most of the protein being endo H resistant shown as a band at 41kDa **(Figure 4.8B)**. Only a minimal amount of the HLA-C detected was endo H sensitive, a finding consistent with detection of membrane expressed protein.

In contrast, the results I observed for HLA-E were different **(Figure 4.8C)**. The endo H digest was undertaken on immunoprecipitated samples with 3D12 and western blot by MEME02. In the endo H treated samples, most of the protein was endo H sensitive and ran at 37kDa, while only a small fraction of endo H resistance protein was observed at 43kDa. Although more HLA-E was detected from the cirrhotic samples compared to healthy controls, the proportion of endo H resistance to sensitive HLA-E appeared to be similar between samples. These data suggest the majority of HLA-E is expressed within the ER, consistent with my observations using immunohistochemistry **(Figure 4.4)**.

Interestingly, my data for HLA-F were more suggestive that it might be expressed on the cell membrane and potentially at higher levels in the cirrhotic samples, given the increased expression of HLA-F in these samples **(Figure 4.8D)**. The immunoprecipitation was undertaken with FG1 antibody followed by western blot with 3D11. Upon endo H treatment, both endo H resistant and endo H sensitive pools of HLA-F were observed. The proportion of endo H resistant to sensitive material was similar in both healthy control and cirrhotic samples **(Figure 4.8D)**. If HLA-F is expressed on the surface of cirrhotic hepatocytes this may have a role in pathogenesis. However, the IP samples are made from whole liver lysate, and it is certain that there are cells other than hepatocytes in the

sample that may express HLA-F on the cell surface. As the immunohistochemistry results do not suggest significant hepatocyte surface expression this may be significant.

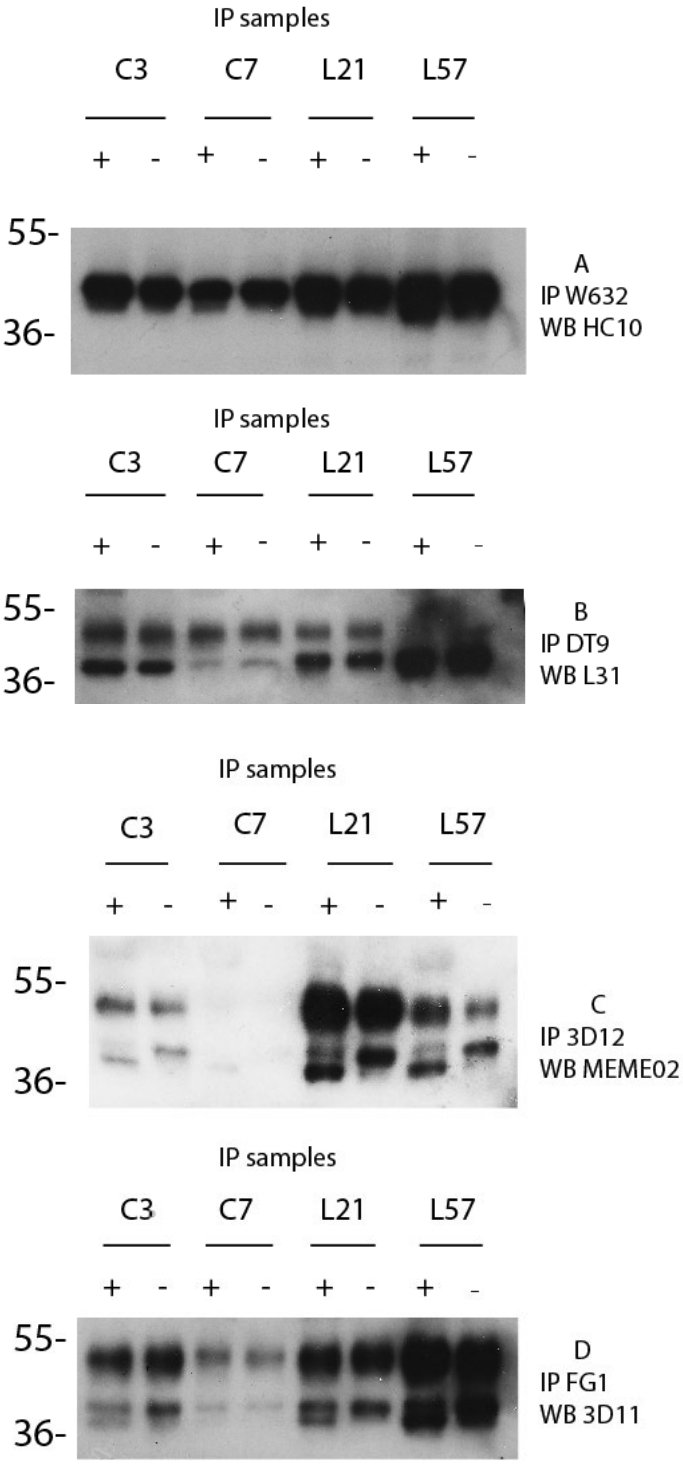

Figure 4.8 - Endo H digest investigating expression of HLA class I, HLA-C, -E and -F. *Immunoprecipitation samples using W6/32, DT9, 3D12 and FG1 for HLA class I, HLA-C, -E and -F respectively treated with endo H digest. Samples which received endo H (+) and a matched sample without endo H as a control (-). Western blots were performed with HC10, L31, MEME02 and 3D11 antibodies respectively in both control (C) and cirrhotic (L) lysates. In the HLA-C, -E and -F runs the*

staining for sample C7 appears to have failed. The band seen at 50kDa is a cross-reactive band as discussed in chapter 3 Pages 50 and 74.

4.6 Association Between HLA Class I Expression and Cellular Senescence

Finally, I explored whether there was any association between HLA class I expression, specifically HLA-E, -F or -G, and the process of cellular senescence in hepatocytes. There is no single marker of cellular senescence, but p21, a marker of cell cycle arrest, which is associated closely with this physiological process, (Campisi, 2001) (page 16) was used as a first measure of the association.

The initial plan was to use dual immunofluorescence; however, as discussed previously (page 88) there were significant and over-riding problems with auto-fluorescence. Multiple exploratory experiments were undertaken but dual staining based on fluorescence techniques failed ultimately. The HLA molecule was labelled with the green laser and p21 in red. Three different staining protocols were attempted (methods page 39), but all showed such strong background staining that it was impossible to identify the p21 positive cells with confidence against the background. **Figure 4.9** shows clear staining of p21 within the hepatocytes with single staining only.

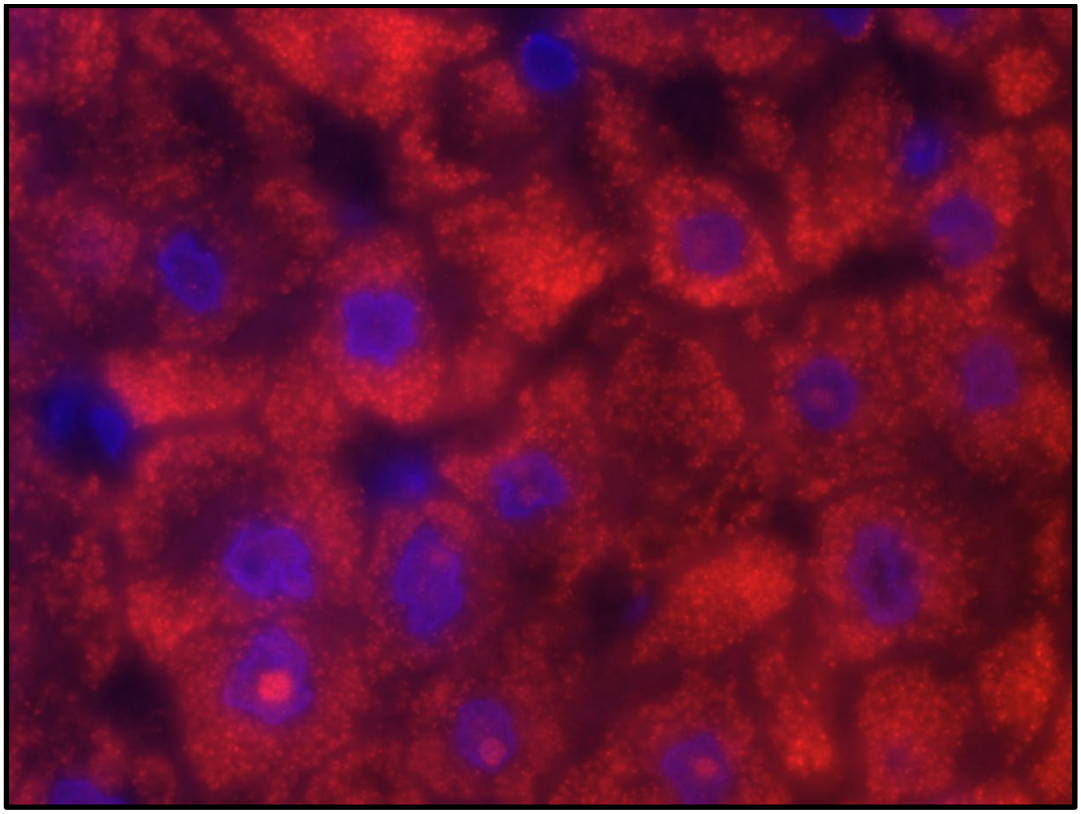

Figure 4.9 – Immunofluorescent staining of p21 stained by Cy3. *Hepatocytes with nuclear staining of p21 are seen in red within the nuclei-stained blue with Dapi. Note the substantial background staining of the hepatocyte cytoplasm, which prevented progress with this approach.*

Further investigations were undertaken using bright field dual staining immunohistochemistry. However, there were still numerous complications. The HLA antibodies described previously were all raised in mice. The p21 antibody, which had been used by colleagues working previously with Professor Alexander in liver senescence, was also raised in mice. The dual staining was performed with a dual staining kit which stated it was suitable for use with two antibodies of the same species. The kit included all the required blocking, secondary antibodies, and conjugates. However, significant cross-reactivity of both MHC class I and p21 was observed once more (data not shown).

In order to reduce the background staining other options were considered. It was highlighted that using two antibodies raised in mice could be contributing to the cross reactivity. So alternative p21 antibodies were sourced raised in different species. A rabbit antibody from Cell Signalling was trialled, but this did not work on paraffin embedded sections. However, an antibody from Abcam was successful, and despite marked background staining, can be seen. An example of the antibody testing is shown in **Figure 4.10**.

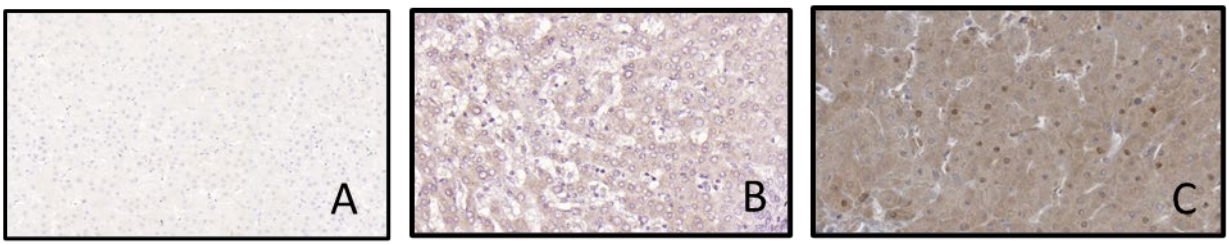

Figure 4.10 – Staining of p21 with three different antibodies. *Staining of p21 seen in brown using Dako p21 antibody (A), Cell Signalling p21 antibody (B) and Abcam p21 antibody (C).*

Once a suitable p21 antibody had been identified a different stain protocol was designed. Vectashield alkaline phosphatase kit was used for the p21 antibody. The Dako peroxidase kit discussed earlier continued to be used for the HLA class I. Further problems were encountered, the fast red label was too similar in colour to the DAB generating results that were difficult to interpret. **Figure 4.11** shows this dual staining with HLA markers in brown; significant background staining persists and the p21 positive nuclei, seen as red, were impossible to identify.

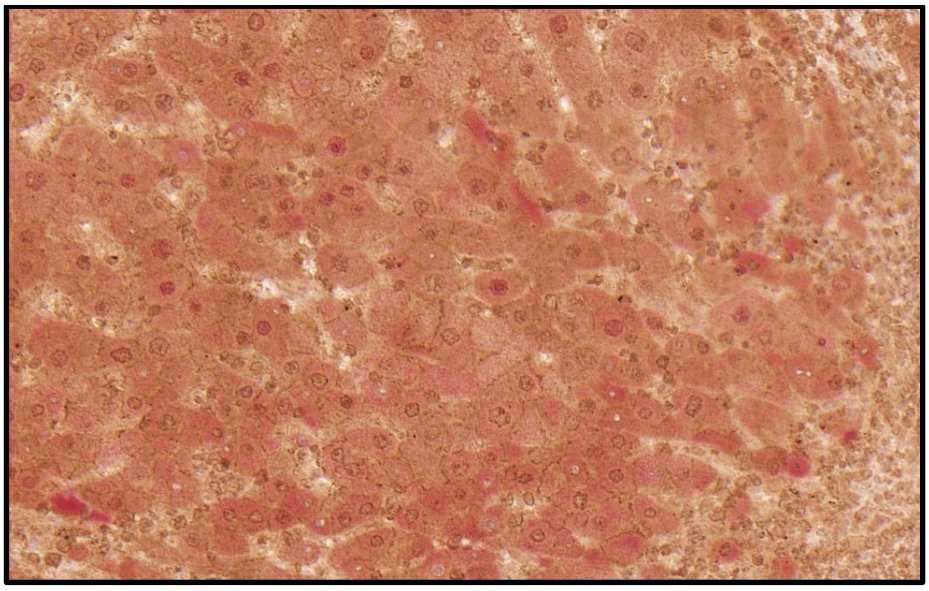

Figure 4.11 – Dual immunohistochemistry staining of HLA-F stained in brown and p21 antibody stained by fast red. *Nuclear hepatocyte staining of p21 is seen but impossible to fully identify from the background.*

To overcome this the substrate fast blue was used as a conjugate to the p21 staining while fluorescent dapi was used to identify the nuclei. This was less than ideal as the only way to fully

interpret these slides is to combine brightfield and immunofluorescence and that proved impractical.

For each HLA molecule a batch of ten cirrhotic sections and six normal liver sections were stained. **Figures 4.12 - 4.15** show representative staining of the HLA markers for HLA class I, HLA-E, -F and -G (brown stain) dual stained with p21 (blue nuclei). The fluorescent image shows the nuclear staining with Dapi.

As mentioned in the introduction, colleagues had shown that senescent cells were present and widespread immediately following transplantation but by 30 days these were no longer detected. This generated the assumptions firstly that the transplant process induced damage which increased expression of p21 and secondly that the p21 positive cells had been cleared within 30 days. The hypothesis was that acute wound injury was associated with expression of markers of acute senescence and that these cells could then be cleared by the innate immune system; it is noteworthy that acute rejection in the early post-operative period after liver transplantation is considered to be NK mediated. Sections of these same transplant biopsies used for this study were dual stained for p21 and the HLA markers.

Figures 4.12 - 4.15 show similar staining for HLA class I, HLA-E, -F and -G as discussed above and seen in **Figures 4.2 - 4.6.** As expected, there is more p21 staining in the cirrhotic samples than control samples, particularly in hepatocytes, consistent with previous studies showing senescence of hepatocytes in cirrhosis. However, there is also high p21 expression in the acute rejection samples, particularly in vascular tissues, consistent with cell cycle arrest (and perhaps with senescence, which for a more confident diagnosis would require a second marker).

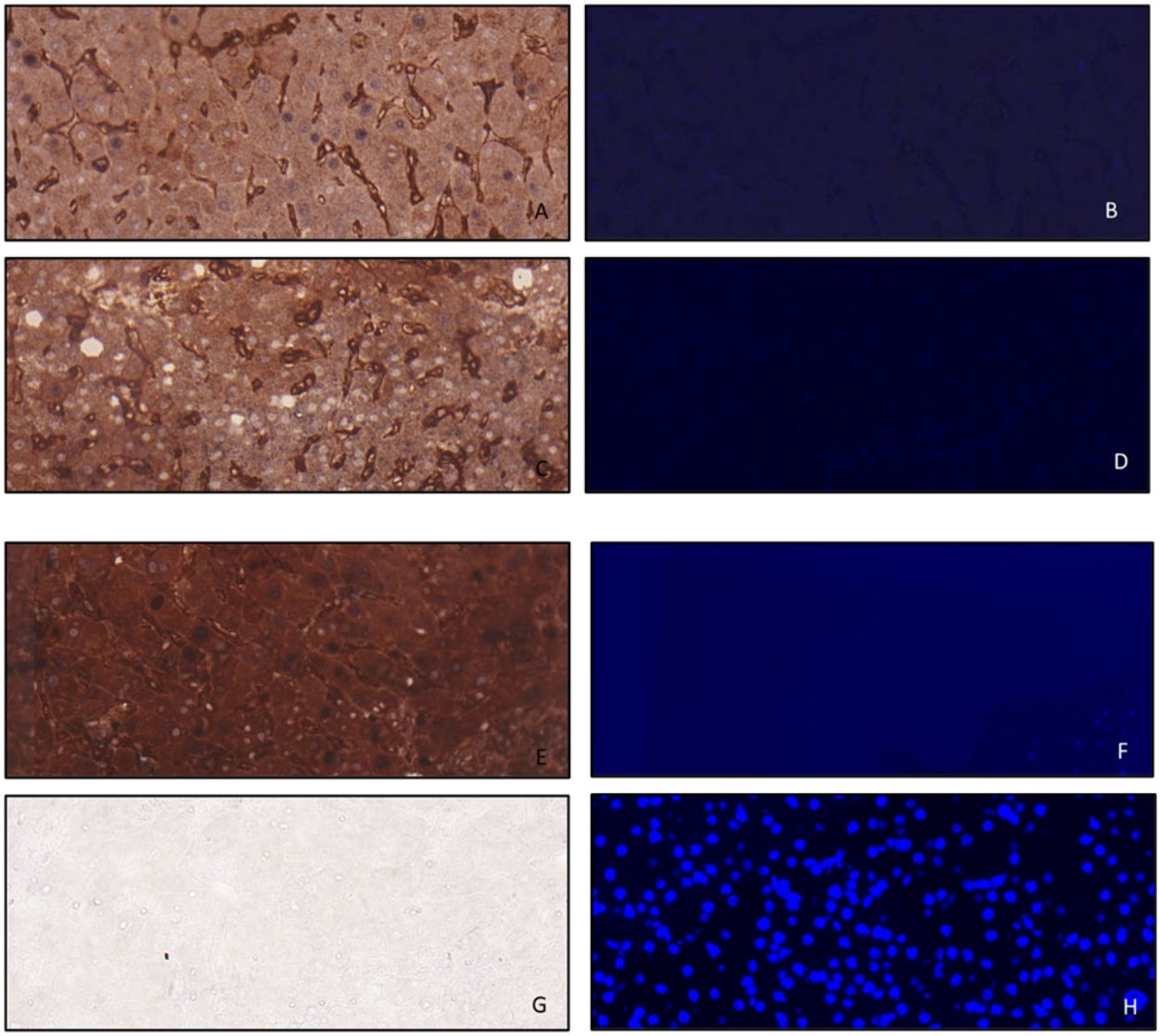

Figure 4.12 – Immunohistochemistry of HLA class I with HC10 antibody and the senescence marker p21. *Antigen retrieval with EDTA buffer. Positive staining of HLA class I is seen as brown since the secondary antibody was tagged with DAB (Images A, C, E and G). Positive staining of p21 is seen in blue since the secondary antibody was tagged with fast blue (Images A, C, E and G). Positive staining of nuclei seen in blue on fluorescence images as tagged with Dapi (Images B, D, F and H). Images A and B showing cirrhosis, Images C and D showing control liver, Images E and F showing an acute rejection biopsy and Images G and H are a negative control slide (no antibody used).*

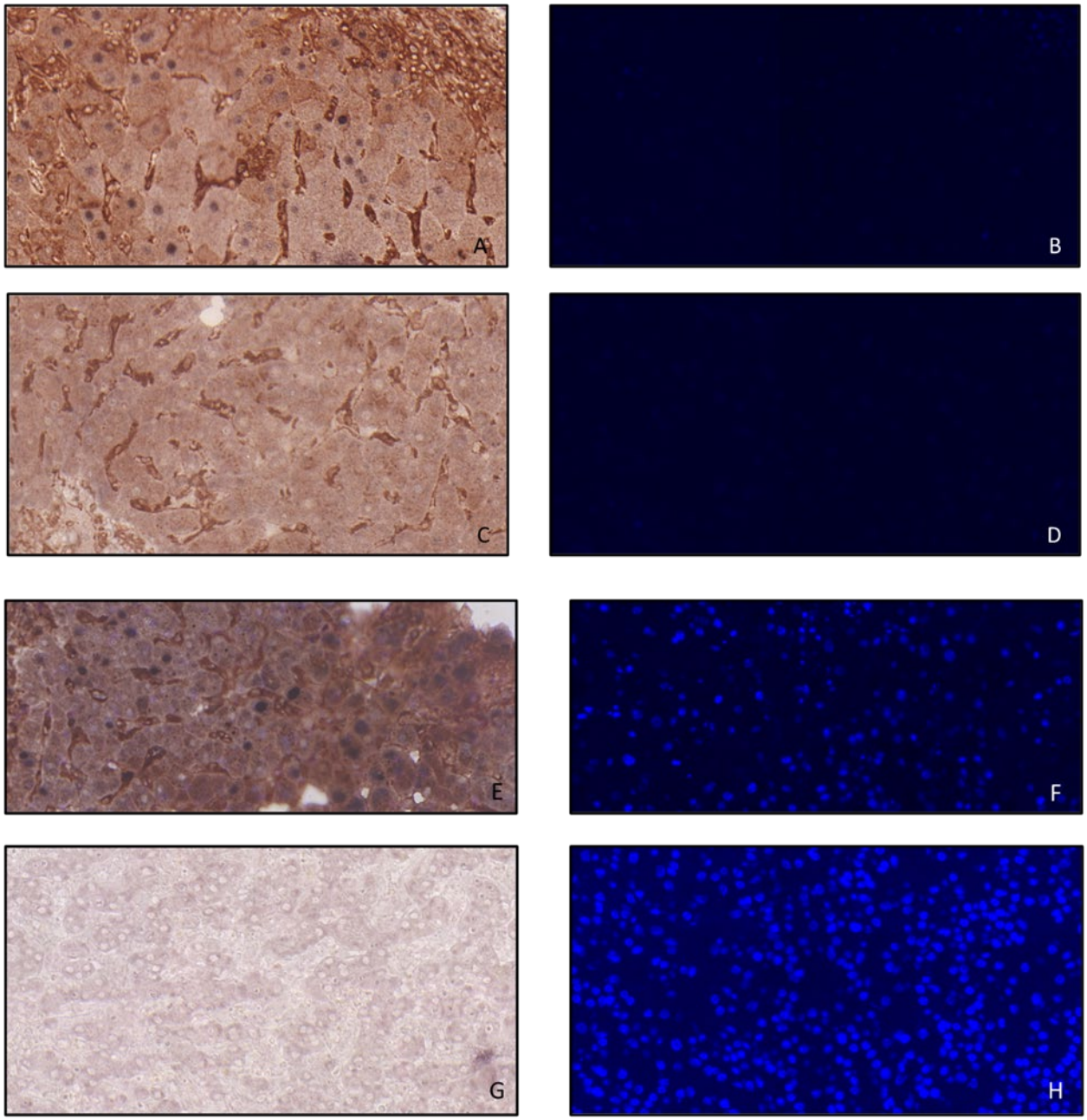

Figure 4.13 – Immunohistochemistry of HLA-E with MEME02 antibody and the senescence marker p21. *Antigen retrieval with EDTA buffer. Positive staining of HLA-E is seen as brown since the secondary antibody was tagged with DAB (Images A, C, E and G). Positive staining of p21 is seen in blue since the secondary antibody was tagged with fast blue (Images A, C, E and G). Positive staining of nuclei seen in blue on fluorescence images as tagged with Dapi (Images B, D, F and H). Images A and B showing cirrhosis, Images C and D showing control liver, Images E and F showing an acute rejection biopsy and Images G and H show a negative control slide (no antibody used).*

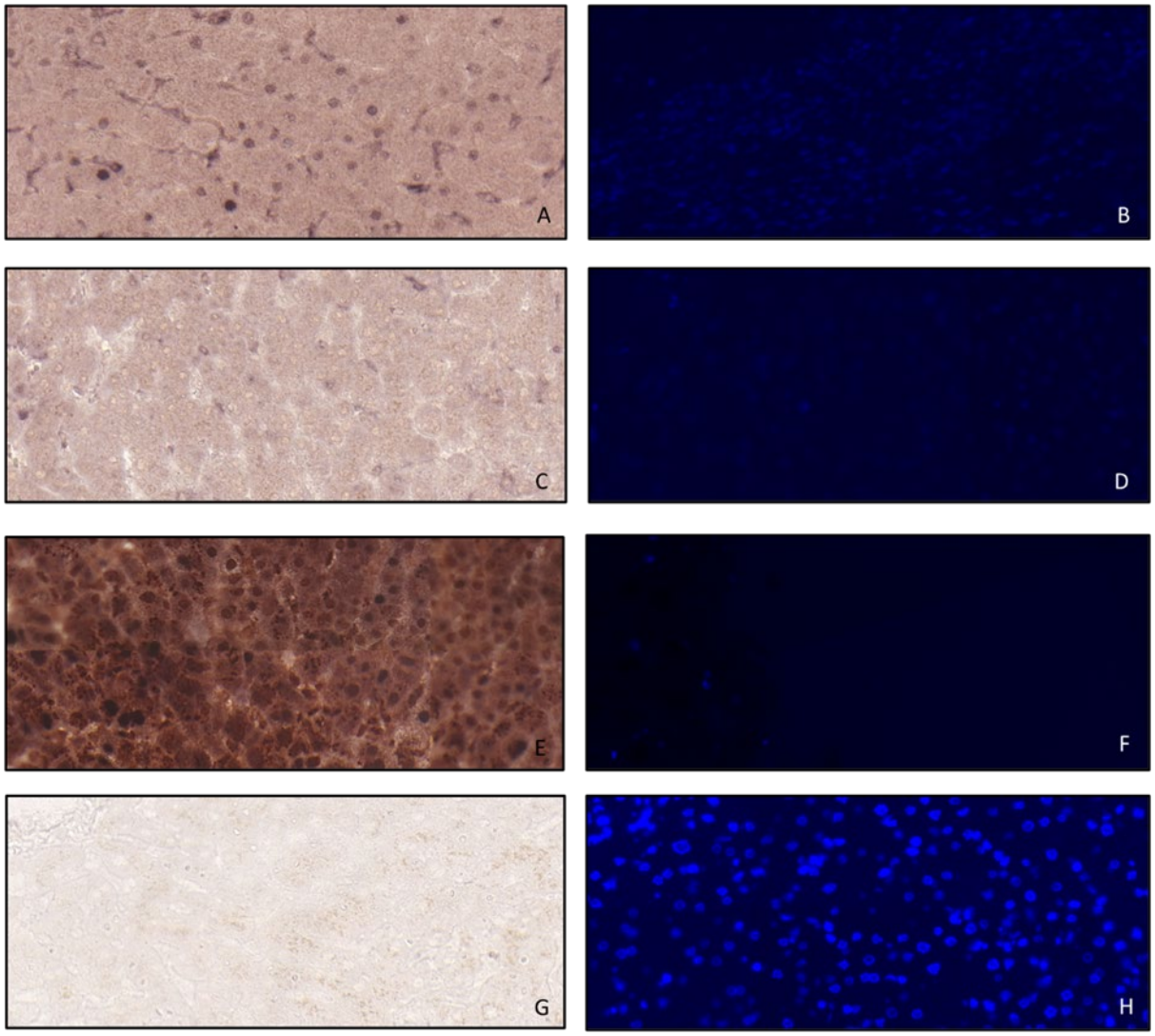

Figure 4.14 – Immunohistochemistry of HLA-F with FG1 antibody and the senescence marker p21. *Antigen retrieval with EDTA buffer. Positive staining of HLA-F is seen as brown since the secondary antibody was tagged with DAB (Images A, C, E and G). Positive staining of p21 is seen in blue since the secondary antibody was tagged with fast blue (Images A, C, E and G). Positive staining of nuclei seen in blue on fluorescence images as tagged with Dapi (B, D, F and H). Images A and B showing cirrhosis, Images C and D showing control liver, Images E and F showing an acute rejection biopsy and Images G and H show a negative control slide (no antibody used).*

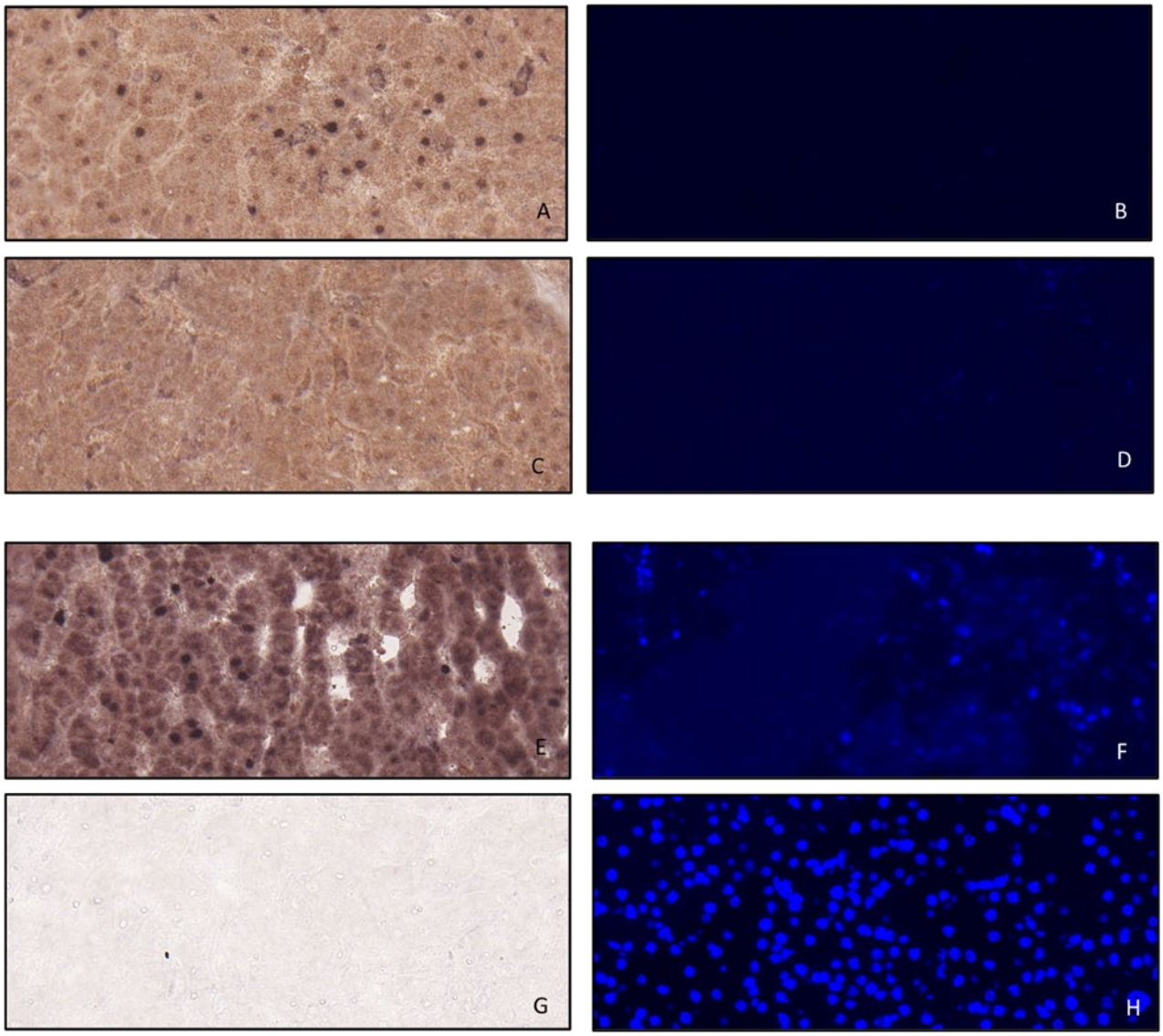

Figure 4.15 – Immunohistochemistry of HLA-G with MEMG02 antibody and the senescence marker p21. *Antigen retrieval with EDTA buffer. Positive staining of HLA-G is seen as brown since the secondary antibody was tagged with DAB (Images A, C, E and G). Positive staining of p21 is seen in blue since the secondary antibody was tagged with fast blue (Images A, C, E and G). Positive staining of nuclei seen in blue on fluorescence images as tagged with Dapi (Images B, D, F and H). Images A and B showing cirrhosis, Images C and D showing control liver, Images E and F showing an acute rejection biopsy and Images G and H showing a negative control slide (no antibody used).*

Further analysis of the data was then undertaken to assess the expression of both p21 and the HLA markers within these tissues and secondarily to assess for co-expression of these markers.

For each HLA marker a Likert scale was designed to assess the level of HLA and p21 expression within the sample. Five represents the highest level of staining and one correlates with the

background staining seen on the negative control samples. **Figures 4.16 - 4.20** show examples of the scale for p21, HLA class I, HLA-E, -F and -G respectively. **Table 4.21** Shows the mean and median values while the full data is included in **Appendix 7.**

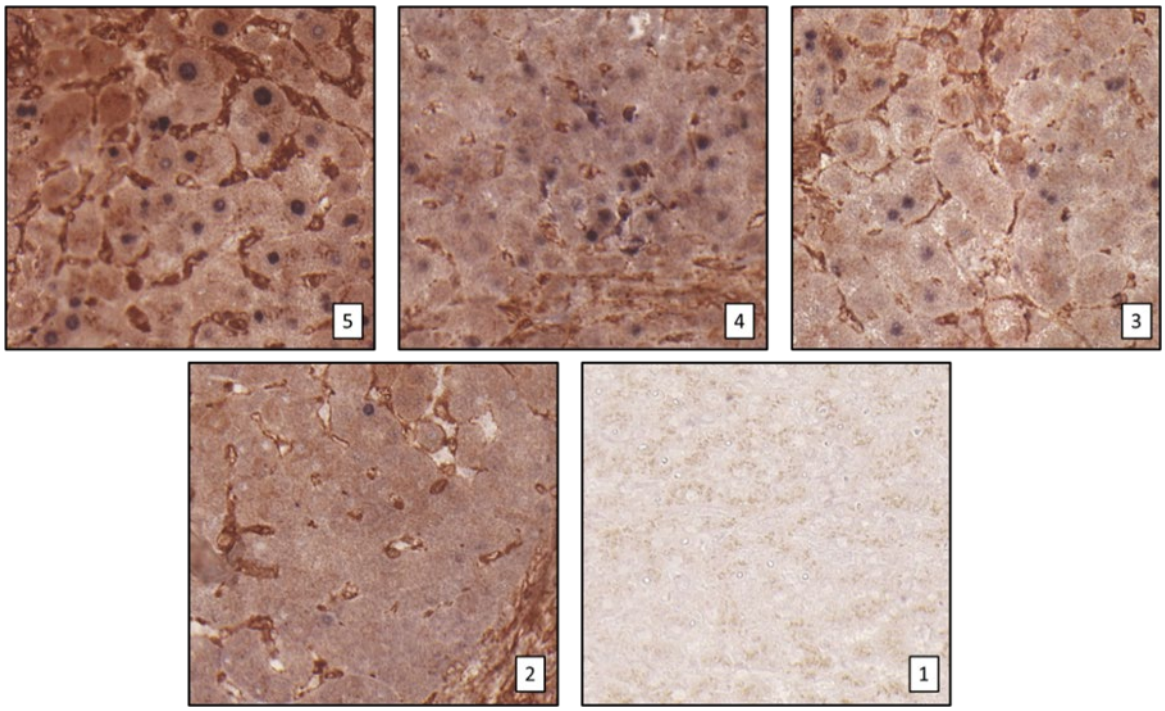

Figure 4.16 - Likert scale showing the range of p21 expression in the cirrhotic samples. *5 = Majority of nuclei p21 positive, 4 = More nuclei p21 positive than negative, 3 = Positive patchy areas of p21 staining, 2 = Occasional p21 positive and 1 = Background staining of negative control.*

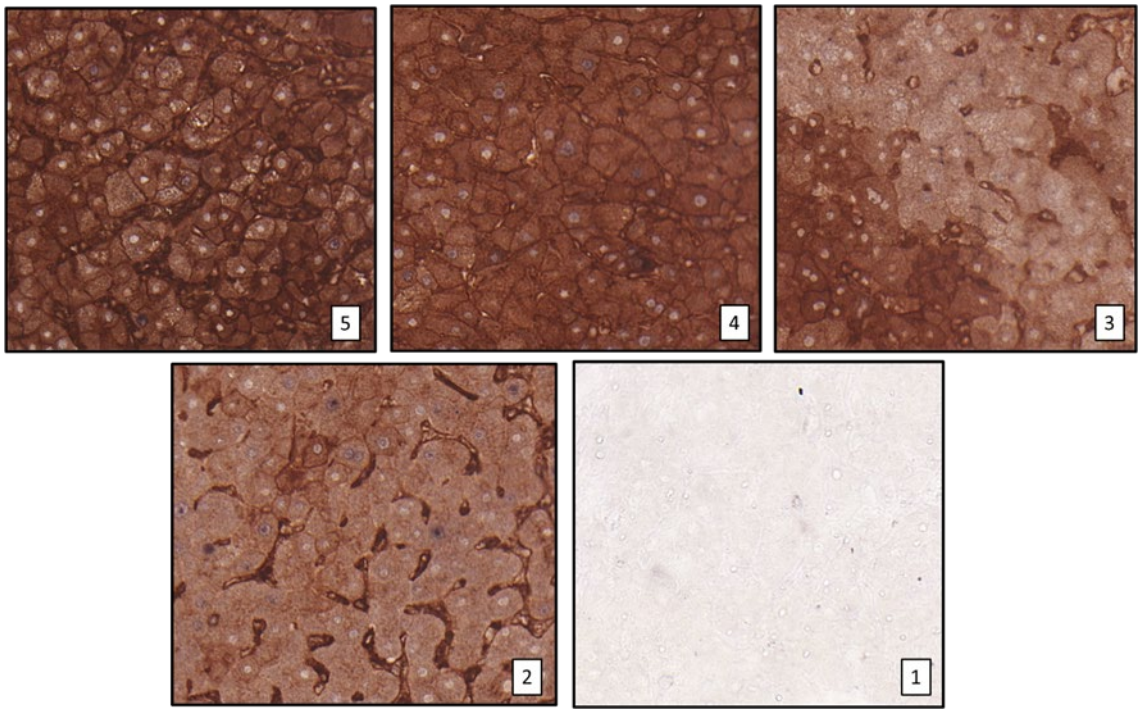

Figure 4.17 - Likert scale showing the range of HLA class I expression in the cirrhotic samples. *5 = Dense sinusoidal, membranous, and intracellular staining, 4 = High volume membranous and intracellular staining, 3 = Patchy higher and lower areas of membranous and intracellular staining, 2 = Mainly intracellular and sinusoidal staining only, 1 = Background staining of negative control.*

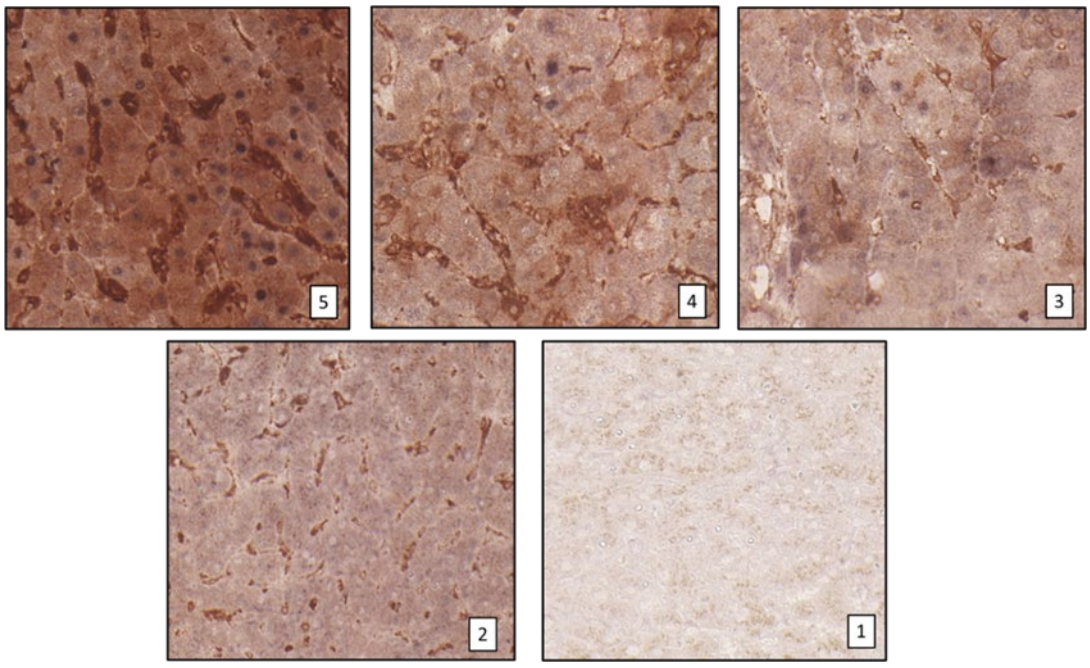

Figure 4.18 - Likert scale showing the range of HLA-E expression in the cirrhotic samples. *5 = Dense sinusoidal and intracellular staining, 4 = Moderate sinusoidal and intracellular staining, 3 = Patchy sinusoidal and intracellular staining, 2 = Sinusoidal staining only, 1 = Background staining of negative control.*

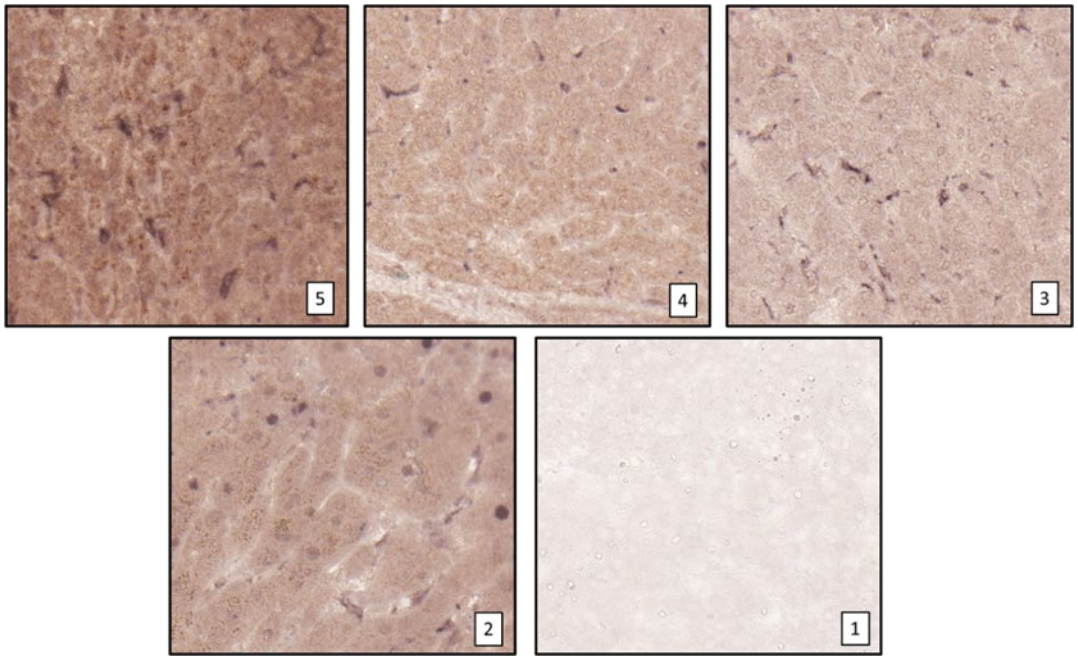

Figure 4.19 - Likert scale showing the range of HLA-F expression in the cirrhotic samples. *5 = Strong reticular and intracellular staining, 4 = Moderate intracellular staining, 3 = Patchy intracellular staining, 2 = Low reticular and intracellular staining, 1 = Background staining of negative control.*

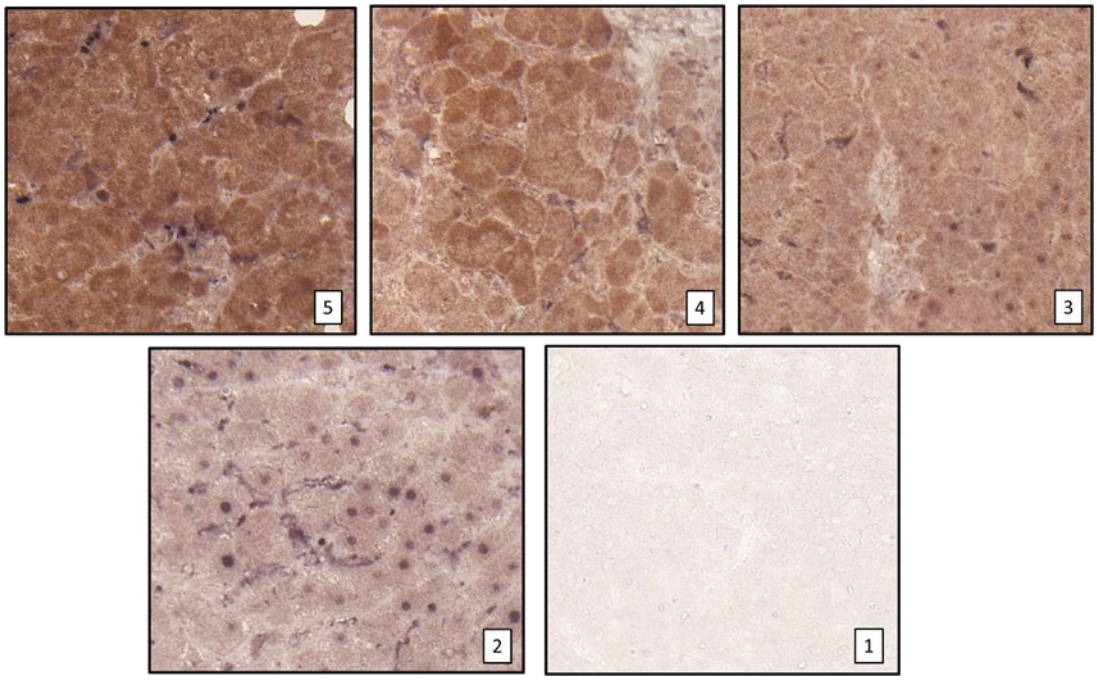

Figure 4.20 - Likert scale showing the range of HLA-G expression in the cirrhotic samples. *5 = Dense reticular, perinuclear, and intracellular staining, 4 = Moderate intracellular staining, 3 = Patchy intracellular staining with perinuclear delineation, 2 = Low reticular and intracellular staining, 1 = Background staining of negative control.*

HLA class I	Mean HLA	Median HLA	Mean p21	Median p21
Cirrhotic	3.3	3	2.8	3
Normal	3	2.5	2	2
Acute Rejection	3.76	4	3.52	3.5
P-value	0.12		0.01	
HLA-E				
Cirrhotic	3.5	4	3.2	3
Normal	3.2	3	2.4	2
Acute Rejection	3.76	4	2.9	3
P-value	0.04		0.32	
HLA-F				
Cirrhotic	3.4	4	2.7	2.5
Normal	2.8	3	2	2
Acute Rejection	3.6	4	3.5	3
P-value	0.46		0.02	
HLA-G				
Cirrhotic	3.3	3.5	2.4	2
Normal	2.4	2	1.8	2
Acute Rejection	3.1	3	2.6	2
P-value	0.81		0.28	

Table 4.21 – The mean and median expression of p21 and HLA class I in the histology samples. *Samples are from cirrhosis and healthy control liver as well as post-transplant biopsies representative of acute rejection. Each sample scored on the Likert scale (1-5) before both a median and mean were calculated.*

Higher expression of HLA class I is seen in the cirrhotic samples than the control samples with a median Likert score of three compared to two and half. The expression is significantly higher in acute rejection which is an immune process. Secondly the expression of p21 is also higher in the cirrhotic samples compared to the control samples (Likert three and two respectively) suggesting that that

the presence of p21 is associated with the presence of HLA class I. This is supported by a higher expression of p21 in the acute rejection samples also. Some co-expression is seen within the samples and examples are shown in **Figure 4.22.** Hepatocytes which express p21 appear to also have higher expression of HLA class I.

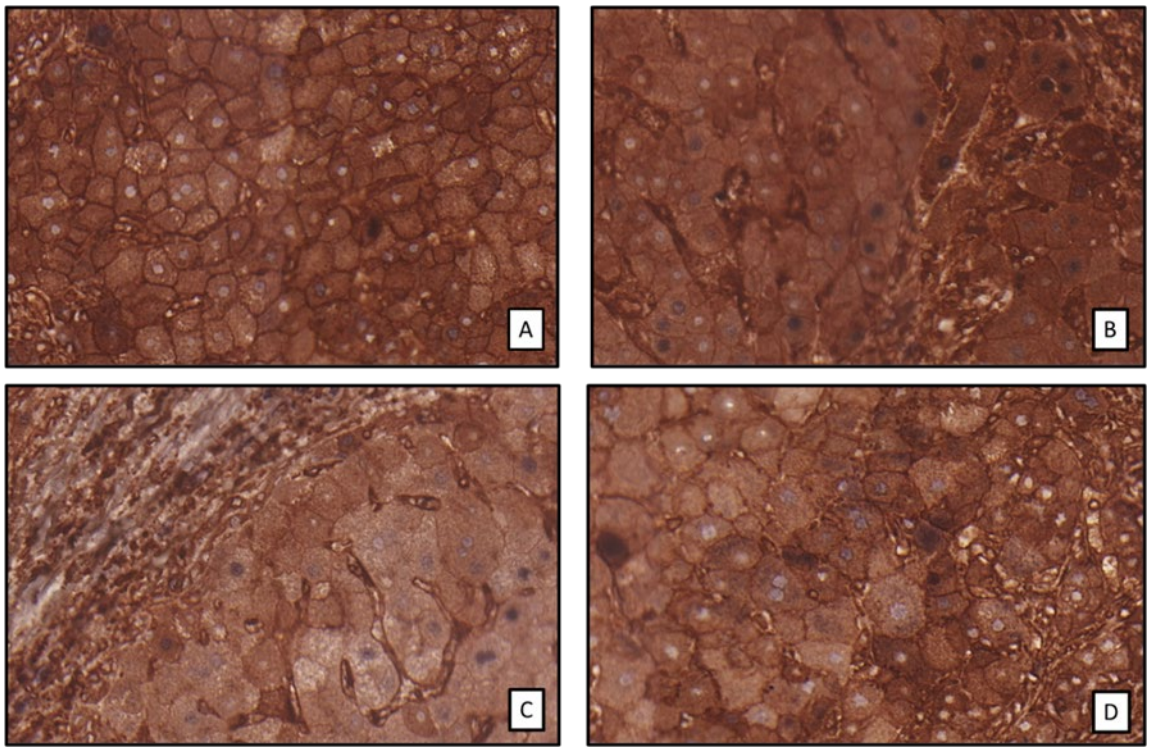

Figure 4.22 - An example of co-staining of HLA class I with p21. *Staining of HLA class I with HC10 antibody and stained brown with DAB. p21 positive nuclei stained with blue dye.*

There is higher HLA-E expression in the cirrhotic samples compared to the control with a median Likert score of four compared to three. The post-transplant biopsies, representative of acute rejection, show moderate p21 expression with median three on the Likert scale. However, the expression of HLA-E in these samples is high (median Likert score four). However, there is some p21 expression in the control samples (median score two compared to three in cirrhosis) so they may not (indeed cannot) be entirely representative of normal liver tissue. The HLA-E staining is patchy with areas of high expression of HLA-E and areas of low expression. However, on review the areas with higher HLA-E expression also seem to have higher p21 expression. There are a few areas of co-expression in some samples and examples are shown in **Figure 4.23**. This along with the higher expression of HLA-E in areas with higher p21 expression may suggest a relationship with senescence. Although it is inconsistent and sometimes near to the edge of samples so could be an artefact effect.

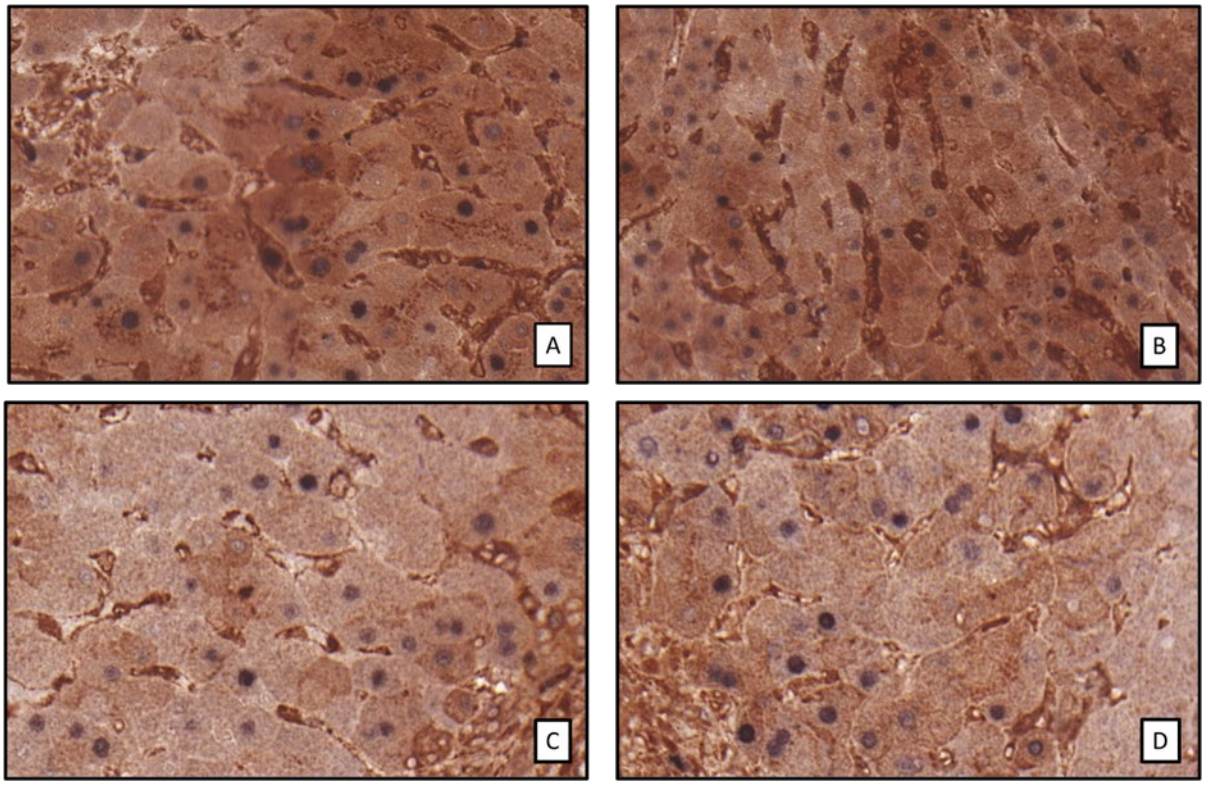

Figure 4.23 - An example of co-staining of HLA-E with p21. *Staining of HLA-E with MEME02 antibody and stained brown with DAB. p21 positive nuclei stained with blue dye.*

The staining of HLA-F showed diffuse reticular staining throughout the samples. There was higher expression seen in the cirrhotic compared to the control samples. The median Likert score in the cirrhotic samples was four compared to three in the control liver samples and four in the acute rejection samples. The staining of p21 also showed higher staining in cirrhotic and acute rejection samples. There is higher HLA-F staining in patches with higher p21, however, the correlation seen between the higher HLA-F staining and specific p21 staining was markedly less than that seen with HLA-E. The staining of HLA-F was very uniform, and this staining does not report a strong relationship with p21. **Figure 4.24** shows examples of the co-staining.

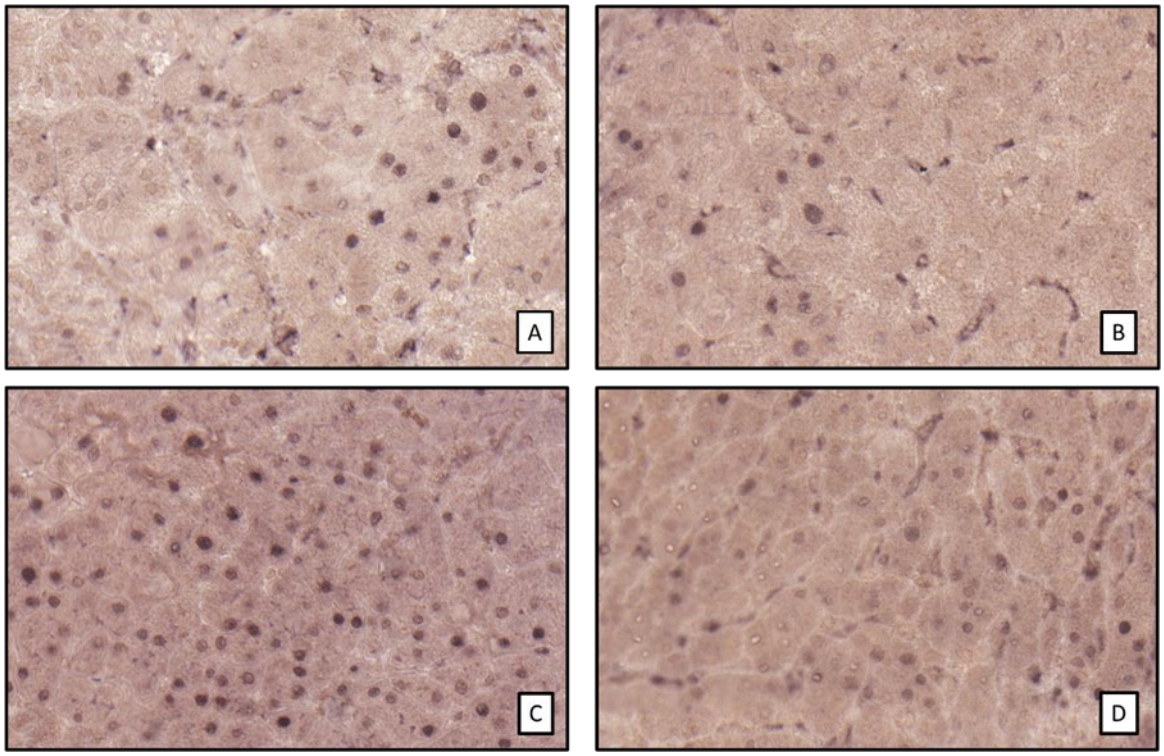

Figure 4.24 - An example of co-staining of HLA-F with p21. *Staining of HLA-F with FG1 antibody and stained brown with DAB. p21 positive nuclei stained with blue dye.*

As discussed previously in this section the staining of HLA-G showed a very diffuse reticular form with less variation between areas of high and low staining and a more uniform global stain. As previously there is higher staining in the cirrhotic and acute rejection patients compared to controls although the staining of p21 was lower (Likert three and half, three and two and half respectively). Areas showing higher p21 staining did appear to show increased HLA-G staining and examples are seen in **Figure 4.25**. Interestingly the expression of p21 was the same across the cirrhotic, control and acute rejection samples for the HLA-G staining. This could confound these results if the control samples are less reliable.

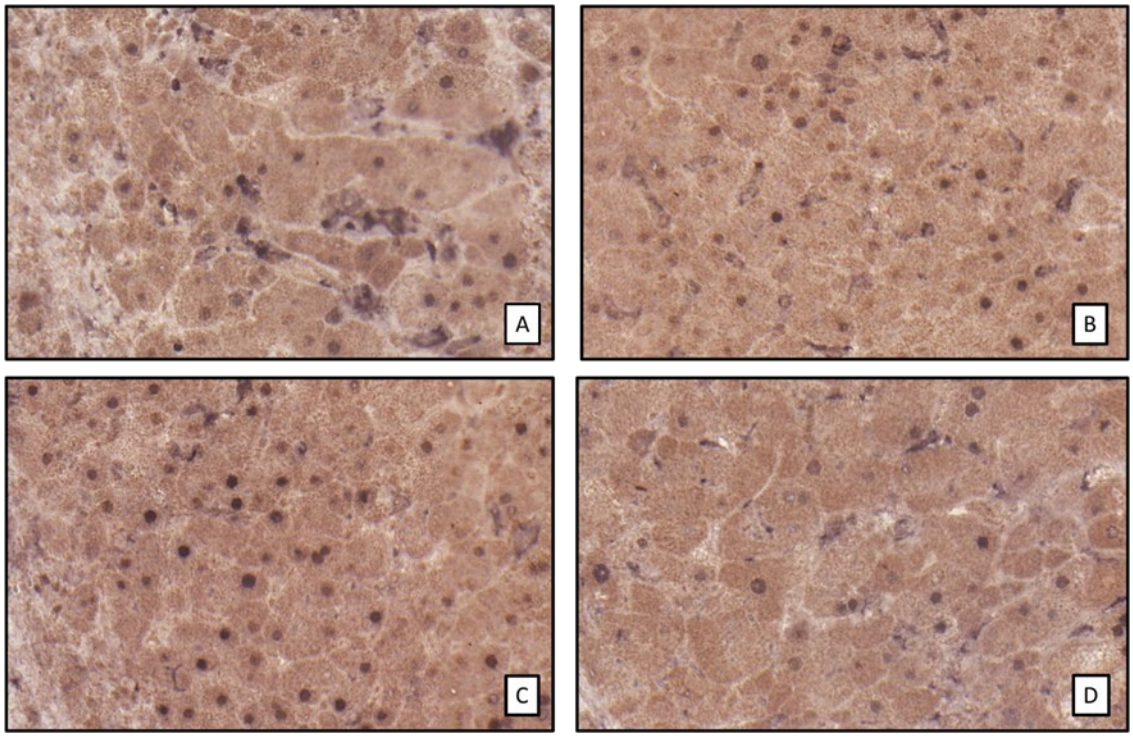

Figure 4.25 - An example of co-staining of HLA-G with p21. *Staining of HLA-G with MEMG01 antibody and stained brown with DAB. p21 positive nuclei stained with blue dye.*

4.7 Discussion

Despite numerous technical problems encountered during this section of the study, some significant results were obtained, and conclusions can be drawn.

Firstly, classical HLA class I was identified within the liver tissue both in health and disease in agreement with the reported literature (Paterson et al., 1988). The immunohistochemistry results suggested this staining was on the cell membrane of hepatocytes as well as in the immune cells within the liver tissue. Globally there appears to be higher expression of HLA class I in disease than health suggesting a role in the pathology. The endo H digest identified an uncleaved band, consistent with membrane expression.

The findings for HLA-C are similar. Immunohistochemistry staining suggests that HLA-C is expressed on the hepatocyte membrane. Immune cells are again positive within the hepatic sinusoids on immunohistochemistry. The expression appears greater in the cirrhosis compared to control tissue. Again, using endo H digest, resistant protein was detected suggestive of these molecules being expressed on the cell membrane.

Regarding HLA-E the results are somewhat different. The immunohistochemistry staining appeared to show some HLA-E staining within the cells in a peri-nuclear and intracellular reticular fashion. This was unexpected as HLA-E cannot interact with a receptor if it is not on the cell membrane. Strong staining was also seen in the sinusoidal immune cells. The expression of HLA-E was higher in cirrhotic patients than the control liver samples. The endo H digest results further supported the immunohistochemistry findings demonstrating that the majority of the HLA-E protein was sensitive to cleavage and therefore indicative of localisation in the ER and cis-golgi, without passage beyond the medial-golgi or to the cell surface. In conclusion, my results suggest that expression of HLA-E is higher in cirrhosis but its function at this stage is less clear as it remains intracellular. In this context it may be that hidden HLA-E lacks any effect on the local immune system.

There were more varied results for HLA-F. The immunohistochemistry findings were like those with HLA-E. Most of the staining was detected intracellularly within the hepatocyte, but some membrane expression in specific areas was also seen in groups of hepatocytes. There was also peri-nuclear staining. However, the endo H findings suggest there was some cell surface expression of HLA-F, that was increased in the cirrhotic compared with the control samples. The peri-nuclear staining could be indicative of retention within the golgi or endosomes. This could represent material that had been at the cell surface, then recycled into endosomes in the peri-nuclear region, which would fit with the endo H digest results.

Finally, HLA-G showed florid staining in the cirrhotic samples in agreement with the published literature (Moroso et al., 2015, Souto et al., 2011). However, the staining was diffuse throughout the cell cytoplasm showing no specific distribution. This is likely to represent cross-reactivity or background staining rather than positively identifying HLA-G. The potential cross reactivity of the MEMG01 antibody is discussed on page 73.

Another aim was to investigate any relationship between the expression of HLA molecules and senescent cells. The results show that there is increased p21 expression representative of senescence in hepatocytes which express the HLA molecules. When comparing the total expression of HLA molecules with p21 there is a relationship between increased expression seen in correlation with p21. This is more marked with HLA class I and HLA-E but is also seen with a lesser extent with HLA-F and -G. There is also co-expression seen with HLA class I and HLA-E whereby cells expressing p21 show greater expression of HLA class I or HLA-E. This suggests that there might be a causal link between these molecules, or alternatively that both proteins are induced by inflammation. What the study does not identify is whether senescent cells induce HLA class I or HLA-E expression or whether the expression of these molecules helps to induce senescence. The hypothesis is that the expression

of HLA-E prevents the clearance of senescent cells similar to the pregnancy model (Moffett-King, 2002, Rajagopalan, 2014). Further attempts to investigate this area failed via flow cytometry but tentative conclusions can be made. Further work may involve invitro experiments where the response of senescent cells to the expression of MHC class I could be studied.

The upregulation of HLA-E and -F in cirrhosis suggests that these molecules do have a role in the pathogenesis. More work needs to be undertaken to establish this role. This was undertaken by an investigation into the ligands to which they may bind in the next chapter.

Chapter 5 Results - Expression of NK Cell Receptors in Chronic Liver Disease

5.1 Introduction

The previous two chapters have shown that non-classical MHC class I molecule expression is increased within hepatocytes in cirrhosis and potentially has a role in the pathogenesis of disease. However, to have a biological effect a non-classical HLA molecule needs a ligand to be present with which to interact. HLA-E interacts with the CD94:NKG2 pathway (Braud et al., 1998a), while HLA-G has been reported to interact with KIR2DL4 (Rajagopalan and Long, 2012) and a recent paper suggests an interaction between HLA-F and both KIR3DL1/3DS1 (Garcia-Beltran et al., 2016). Other receptors identified as potentially interacting with the innate immune system include the LILRBs (Katz, 2006) as well as the activating and inhibitory KIRs which interact with HLA-C including KIR2DL1 and killer cell immunoglobulin like receptor with two immunoglobulin domains and short cytoplasmic tail 1 (KIR2DS1) (Rajagopalan and Long, 2005). The aim was to characterise NK receptor expression in health and liver disease.

Since NK cells express different receptors as they become more mature (Abel et al., 2018) further work was undertaken to investigate whether there was an age difference in the liver infiltrating or circulating NK cells in health and disease by assessing the maturity sensitive receptors cluster of differentiation cells 57 (CD57), CD69 and NKG2A.

5.2 Flow Cytometry to Investigate NK Cell Receptors in Chronic Liver Disease

5.2.1 Identification of NK Cell Receptors on Circulating NK Cells in Health and Liver Disease

Flow cytometry staining was undertaken in the laboratory and analysed using LSRFortessa (BD biosciences). Care was taken to plan a detection panel to identify the appropriate markers. Advice regarding the selection of antibodies was taken from the experts within the department of pathology. All the antibodies used in these experiments had been tested previously, were known to be effective and stored within the laboratory library.

PBMCs from whole blood was donated with informed consent from 12 patients with cirrhosis as well as five healthy volunteers (Ethics number 11/NE/0356). In addition, stored PBMCs were kindly donated by Dr William Gelson (Addenbrooke's Hospital, Cambridge) that had been collected from patients suffering acute rejection following liver transplantation (Ethics number 05/Q0104/38).

Five healthy volunteers were used for control samples (male = four and female = one, median age 21, interquartile range (IQR) 14), nine cirrhotic samples (male = six and female = three, median age

56, IQR 10) and six acute rejection samples (male = two and female = four, median age 51.5, IQR 18.25).

NK cells were identified as follows: protein tyrosine phosphatase receptor type C (CD45) positive (a marker of immune cells (Desai et al., 1994)), DCM negative, thus identifying live only cells. These were then gated cluster of differentiation 4 (CD4), cluster of differentiation 14 (CD14) and B-lymphocyte surface antigen B4 (CD19) negative cells thus removing T-cells (Crocker et al., 1987), macrophages (Crocker et al., 1987), monocytes (Ong et al., 2019) and B cells (Bradbury et al., 1992) respectively. Finally, NK cells were identified as cluster of differentiation 3 (CD3) negative (Abel et al., 2018). The gating strategy is shown in **figure 5.1.** The antibodies used are listed in materials and methods (chapter 2, page 32).

The NK cells were then sub-divided in to $CD56^{bright}$ or $CD56^{dim}$. The $CD56^{bright}$ subset was cluster of differentiation 16 (CD16) negative. The expression of NKG2A and NKG2C was assessed on $CD56^{bright}$ NK cells **(Figure 5.2A)**. The expression of leukocyte immunoglobulin like receptors B1 and B2 (LILRB1 and LILRB2) were assessed on $CD56^{dim}$ NK cells **(Figure 5.2B)**. The KIR receptors were assessed on both $CD56^{dim}$ and $CD56^{bright}$ NK cells **(Figure 5.3).**

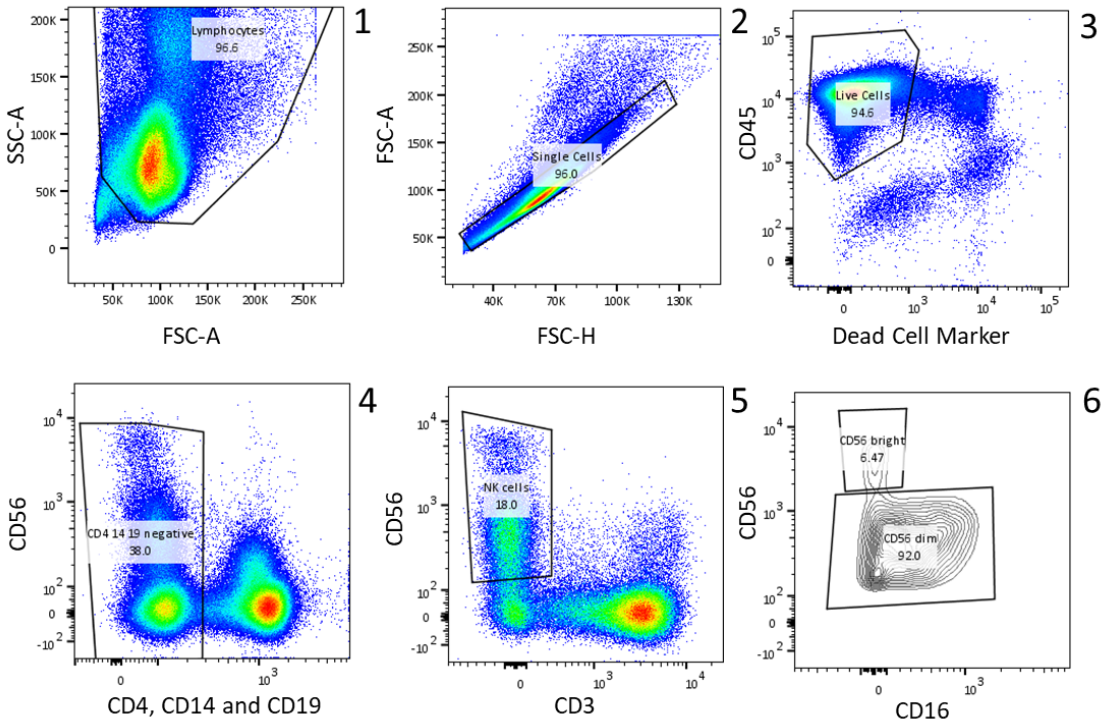

Figure 5.1 – An example of the gating strategy used to identify NK cells from PBMC. *Dot plots show the sequential gating strategy used to identify NK cells from previously frozen PBMCs from a healthy volunteer. First, lymphocytes were gated based on forward scatter (FSC-A) and side scatter (SSC-A) (1). After gating on single cells and live cells using a dead cell marker (2, 3), a gate was applied to CD4, CD14 and CD19 negative cells (4). NK cells were subsequently identified as neural cell adhesion molecule (CD56) positive and CD3 negative cells (5). Finally, a gate was applied to split* $CD56^{bright}$ *and* $CD56^{dim}$ *NK cells (6).*

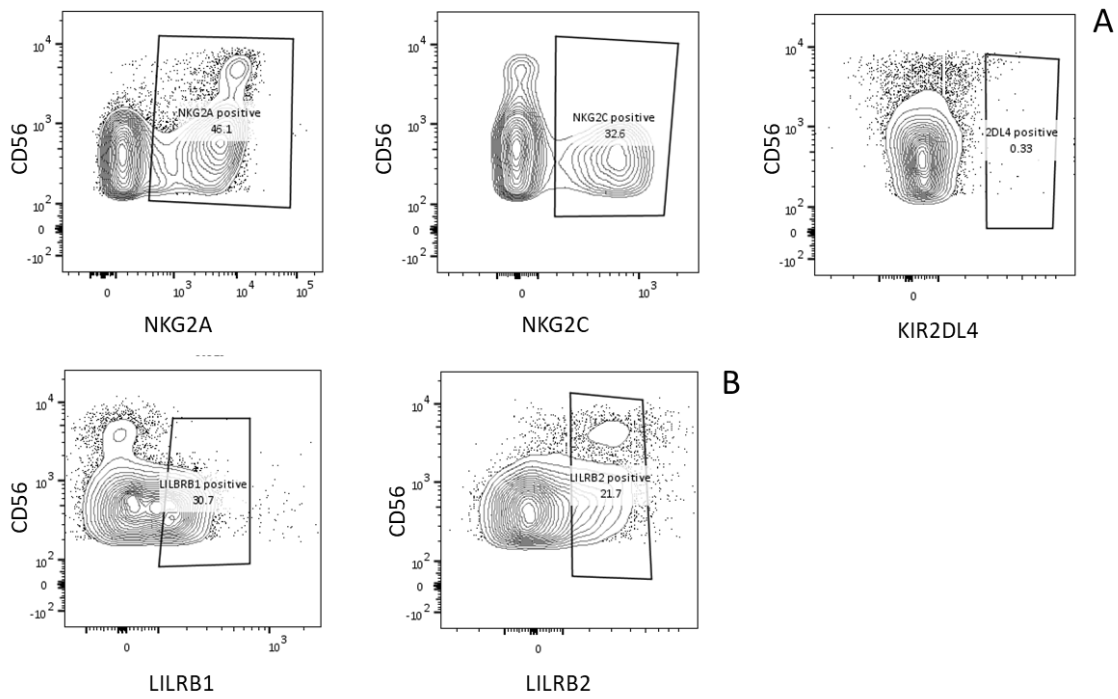

Figure 5.2 – An example of the gating strategy of the target NK cell receptors. *Dot plots show the gating strategy used to identify target NK cell receptors from previously frozen PBMC from a healthy volunteer. NKG2A, NKG2C and KIR2DL4 were identified on CD56^{bright} cells (A). LILRB1 and LILRB2 were identified on CD56^{dim} cells (B).*

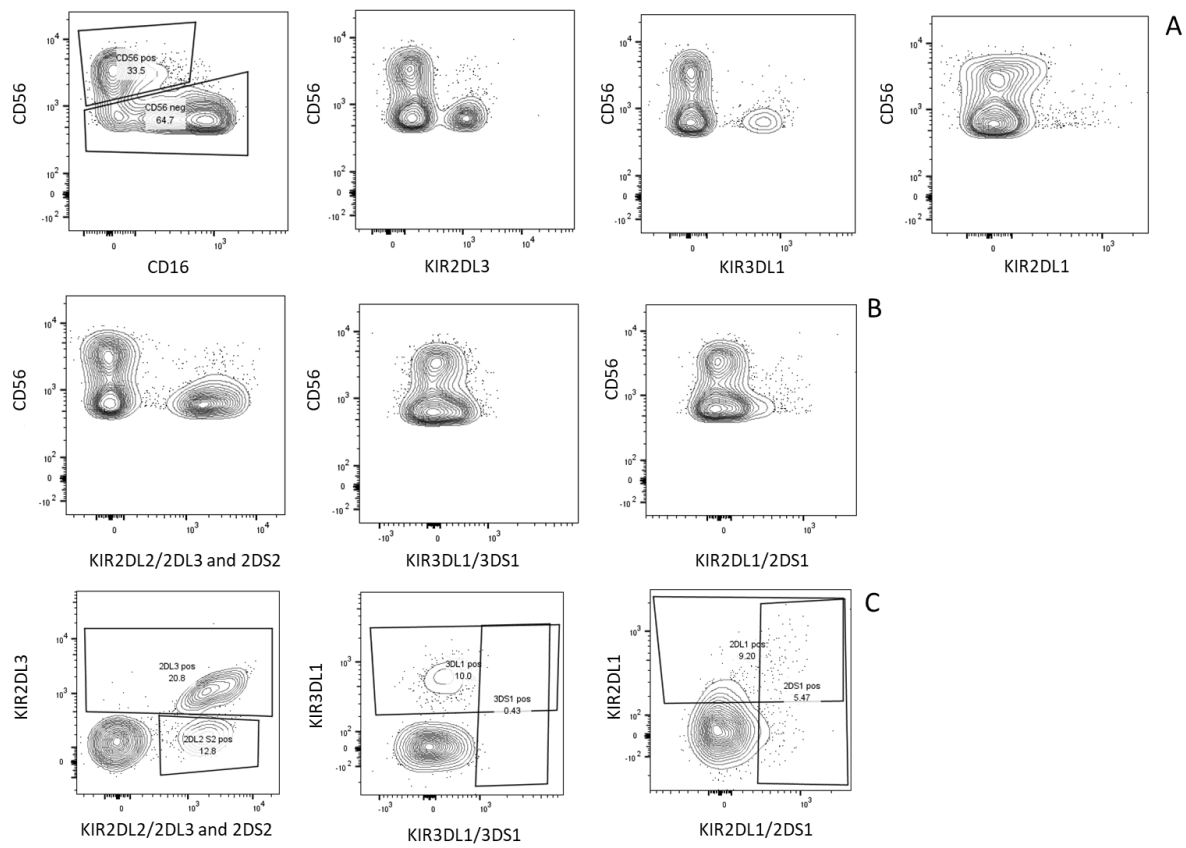

Figure 5.3 – An example of the gating strategy of the target KIR receptors. *Dot plots show the gating strategy used to identify target KIR receptors from previously frozen PBMC from a healthy volunteer. Section A shows individual antibodies for KIR receptors KIR2DL3, 3DL1 and 2DL1. Section B shows combination antibodies for multiple KIR receptors. Section C shows further gating to identify individual KIR receptors using a combination of single and multi-KIR antibodies.*

The proportion of cells expressing each individual marker for each patient or control sample are shown below as a percentage of the parent population (NK cells). All results obtained are shown in **figures and tables 5.4 and 5.6**. The original data is shown in **Appendix 8.** Statistical analysis was then performed where numbers were sufficient on the mean percentage of positive cells for each marker to compare between the cirrhotic, control and acute rejection samples. Caution needs to be considered with the acute rejection samples as these had been stored for a longer period and the number of cells was lower than expected consistent with cell loss. The results were then analysed with a Kruskal-Wallis test to check for significant differences between the three groups – control, cirrhotic and acute rejection. The median results and p-values are included in **figures and tables 5.5 and 5.7.**

There was a significant difference in the total number of NK cells between the three groups (p=0.0015). The lowest number was in the acute rejection group (mean = 7.315) **(Figure and Table 5.5)** with the highest number seen in the cirrhotic group (mean = 25.2). The NK cell population was also high in the control group but not reaching the level of the cirrhotic samples (mean = 18.6). This may have been due to a lower total number of cells in this group due to the age of the samples (Min et al., 2018), or infiltration of the liver as part of the acute rejection process (Obara et al., 2005). The ratio of $CD56^{bright}$ to $CD56^{dim}$ NK cells was also different between the control group compared to the cirrhotic or acute rejection group, but this did not reach significance (p>0.05, **Table 5.5**). Similarly, the proportion of cells NKG2A positive is higher in the acute rejection group compared to the cirrhotic and control but this is also not significant (p>0.05). Globally on review of the data there was a lower proportion of cells expressing all KIR receptors in the acute rejection samples compared to control and cirrhotic samples. There was a significantly higher proportion of cells expressing KIR2DL2 or killer cell immunoglobulin like receptor with two immunoglobulin domains and short cytoplasmic tail (KIR2DS2) in the cirrhotic group (p=0.035). Also, a significantly lower proportion of cells expressing KIR3DL1 was seen in the acute rejection group compared to cirrhotic and control groups (p=0.049) **(Table 5.5)**.

The mean fluorescence intensity (MFI) of the results did not mirror the percentage populations. In the $CD56^{bright}$ group the expression of CD56 was significantly lower in the acute rejection samples (p=0.035) **(Figure and Table 5.7)**. There was also a significantly lower expression of NKG2C the acute rejection samples (p=0.012) **(Figure and Table 5.7)**. The only significant difference in the MFI of the KIR receptors was in the expression of KIR3DS1 which was very low in the acute rejection samples (p=0.008) **(Figure and Table 5.7)**. This is mirrored in the percentage positive population of KIR3DS1 but the total numbers are very low.

However, on review of the data does show some variance. It is known that the NK cell repertoire differs between individuals and, although not fully understood, may be established during NK cell development rather than influenced by later disease (Carrillo-Bustamante et al., 2016). In addition, some NK cell receptors are not expressed on the cell membrane in all individuals; one example is KIR2DL4 (Kikuchi-Maki et al., 2003). Variation in the results is addressed further in the discussion.

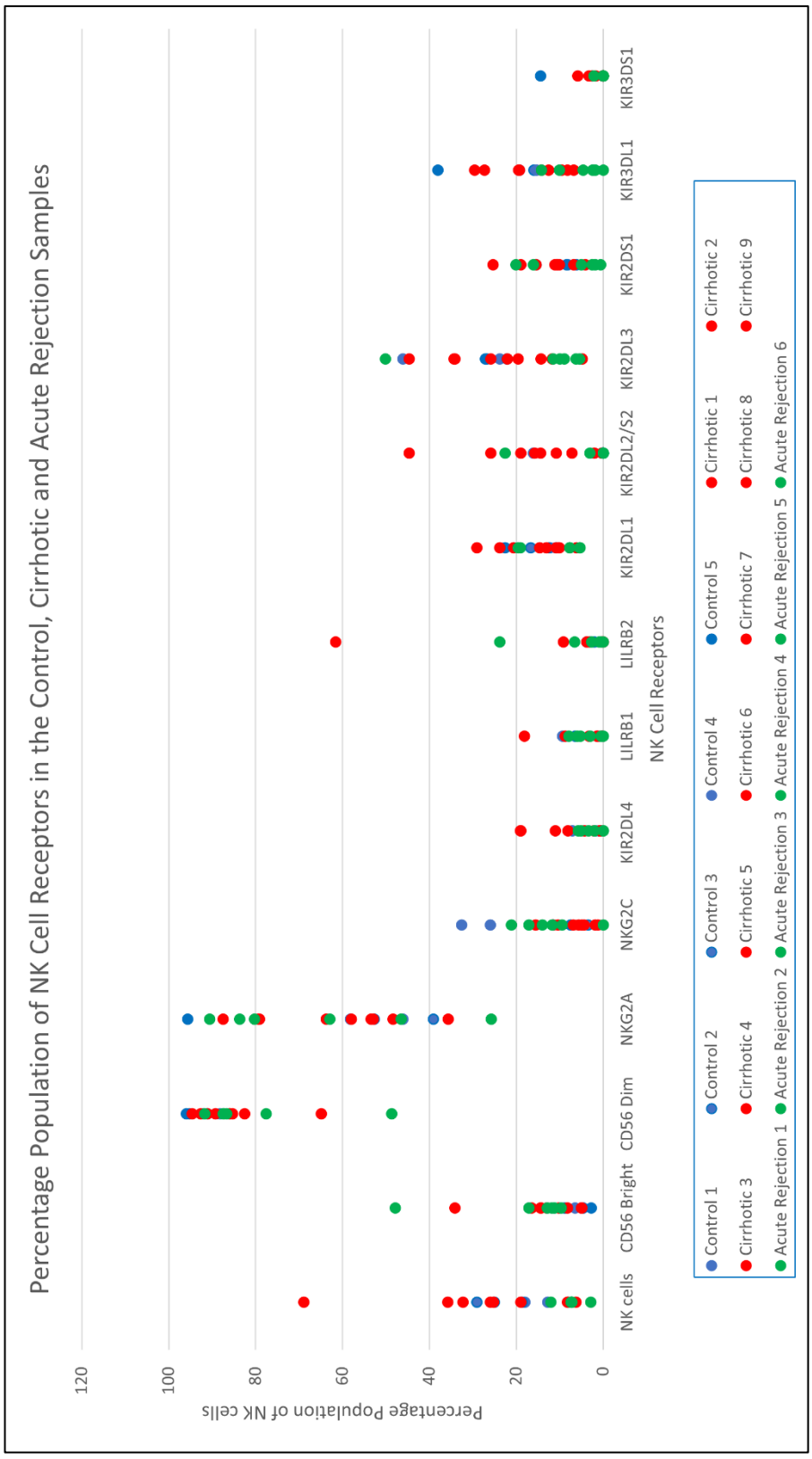

Figure 5.4 – Percentage population of NK cell receptors expressed on NK cells in the control, cirrhotic and acute rejection samples*. Control samples are shown in blue, cirrhotic samples in red and acute rejection samples in green.*

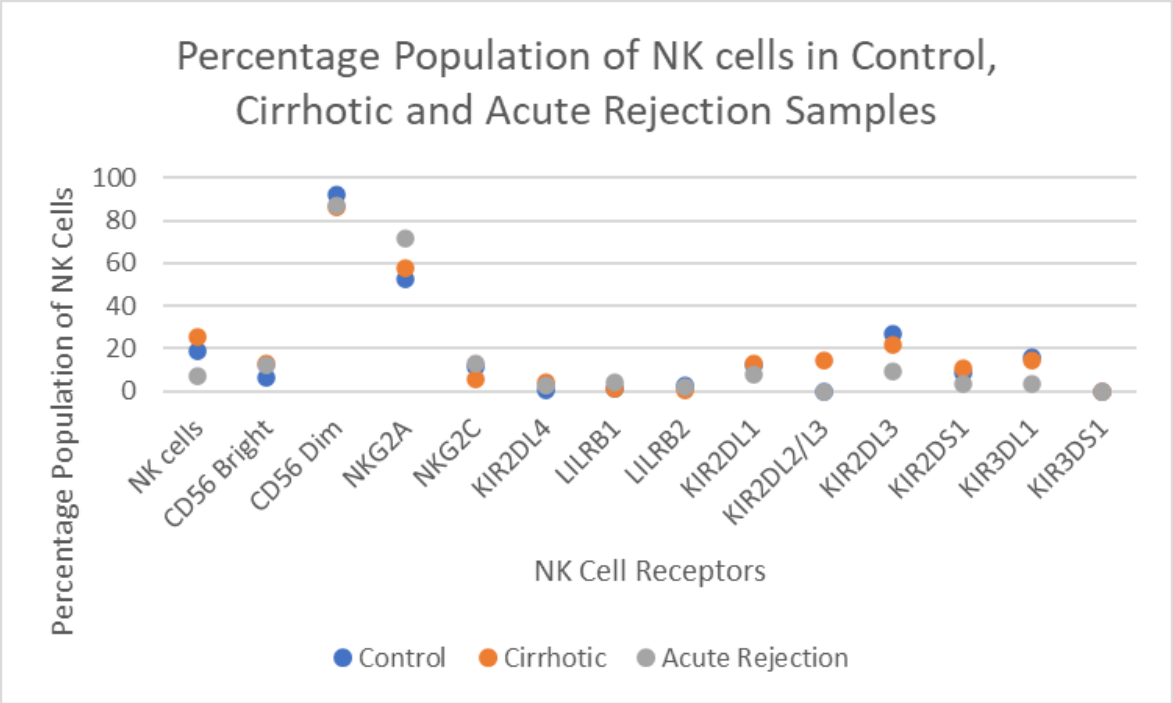

Figure 5.5 – Median percentage population of NK cell receptors expressed on NK cells in the control, cirrhotic and acute rejection samples.

	NK cells	CD56 Bright	CD56 Dim	NKG2A	NKG2C	KIR2DL4	LILRB1	LILRB2
Control	18.6	6.47	92	52.7	11.5	0.89	1.22	2.72
Cirrhotic	25.2	13	86	58	5.68	4.33	1.41	0.37
Acute Rejection	7.315	12.35	87	71.6	12.85	2.69	4.1	1.735
P-value	**0.0015**	**0.055**	**0.053**	**0.757**	**0.188**	**0.229**	**0.968**	**0.860**

	KIR2DL1	KIR2DL2/S2	KIR2DL3	KIR2DS1	KIR3DL1	KIR3DS1
Control	12.5	0.055	26.8	8.43	16	0.05
Cirrhotic	13.1	14.4	22	10.7	14.2	0.088
Acute Rejection	7.68	0	9.47	3.805	3.535	0
P-value	**0.250**	**0.035**	**0.103**	**0.298**	**0.041**	**0.068**

Table 5.5 – Median percentage population of NK cell receptors expressed on NK cells in the control, cirrhotic and acute rejection samples. *Median and p-values are included within the table.*

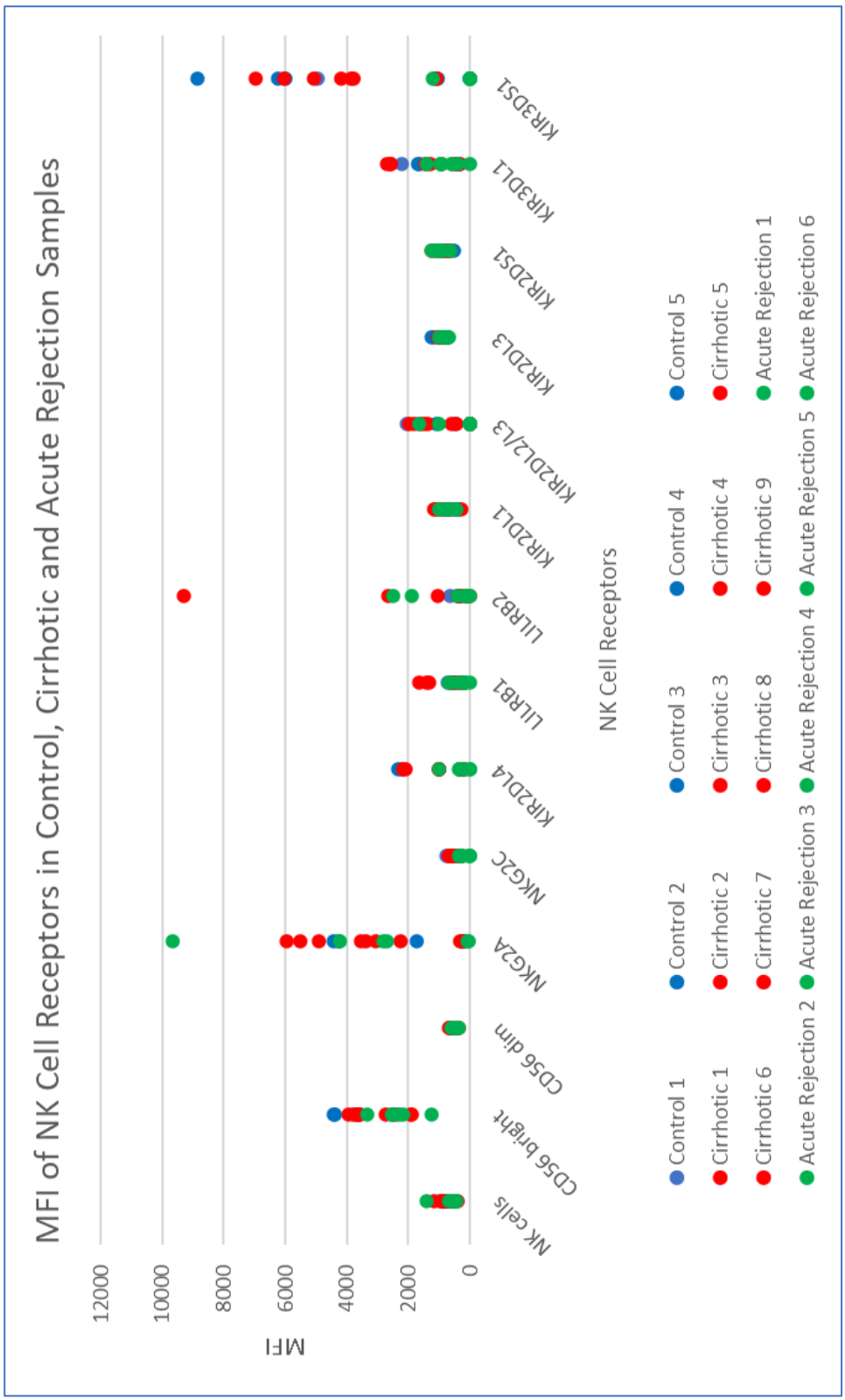

Figure 5.6 – MFI of NK cell receptors expressed on NK cells in the control, cirrhotic and acute rejection samples*. Control samples are shown in blue, cirrhotic samples in red and acute rejection samples in green.*

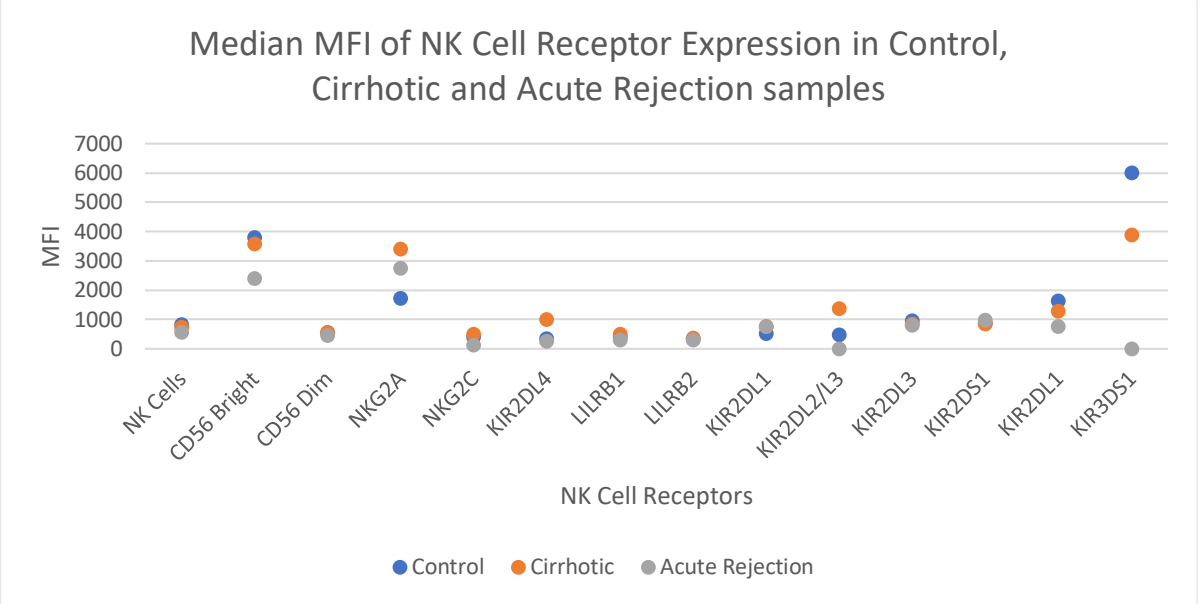

Figure 5.7 – Median MFI of NK cell receptors expressed on NK cells in the control, cirrhotic and acute rejection samples*. Median and p-values are included within the table.*

	NK cells	**CD56 Bright**	**CD56 Dim**	**NKG2A**	**NKG2C**	**KIR2DL4**	**LILRB1**	**LILRB2**
Control	821	3789	533	1715	407	340	393	330
Cirrhotic	747	3570	567	3403	506	995	506	355
Acute Rejection	561	2403	458.5	2745.5	123.05	265.5	308.5	296
P-value	**0.319**	**0.035**	**0.319**	**0.636**	**0.012**	**0.230**	**0.448**	**0.844**

	KIR2DL1	**KIR2DL2/S2**	**KIR2DL3**	**KIR2DS1**	**KIR3DL1**	**KIR3DS1**
Control	519	475	945	862	1642	5998
Cirrhotic	754	1376	842	853	1276	3882
Acute Rejection	754.5	0	804.5	973.5	758.5	0
P-value	**0.281**	**0.352**	**0.392**	**0.599**	**0.448**	**0.008**

Table 5.7 – Median MFI of NK cell receptors expressed on NK cells in the control, cirrhotic and acute rejection samples*. Median and p-values are included within the table.*

5.2.2 Assessment of NK Cell Maturity on Circulating NK Cells in Health and Liver Disease

Secondly, an assessment of NK cell maturity was undertaken in health, cirrhosis, and acute rejection. The hypothesis to be tested was that in cirrhosis NK cells are more mature and so less able to remove the senescent hepatocytes compared to those in either health or acute rejection (both scenarios in which the liver has not been exposed to chronic inflammation). The expression of NKG2A, CD57 and CD69 as markers of NK cell maturity were identified **(Figure 5.8)**.

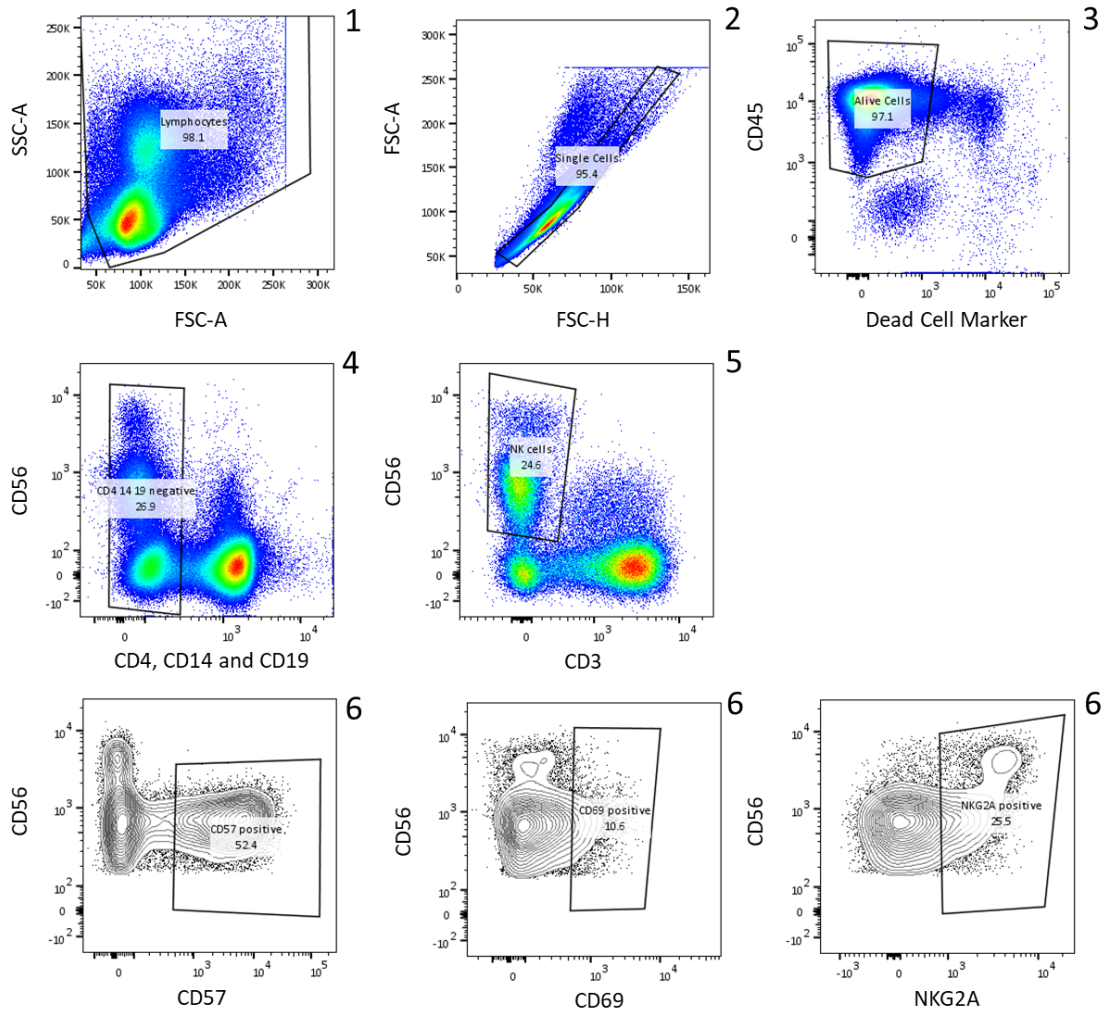

Figure 5.8 – An example of the gating strategy used to identify NK cells from PBMC and the NK cell maturity markers. *Dot plots show the sequential gating strategy used to identify NK cells from previously frozen PBMCs from a healthy volunteer. First, lymphocytes were gated on based on forward scatter (FSC-A) and side scatter (SSC-A) (1). After gating on single cells and live cells using a DCM (2, 3), a gate was applied to CD4, CD14 and CD19 negative cells (4). NK cells were subsequently identified as CD56 positive and CD3 negative cells (5). CD57, CD69 and NKG2A positive cells were then identified on the NK cells.*

The results were analysed with a Kruskal-Wallis test to check for significant differences between the three groups: control, cirrhotic and acute rejection. The individual results are shown in **figures 5.9 and 5.11** and the full data is shown in **Appendix 9.** The median results and p-values are included in **figures and tables 5.10 and 5.12.**

A statistical significance was seen with a lower proportion of cells expressing CD57 in the acute rejection group (p=0.007) **(Figure and Table 5.10)**. This may suggest that these NK cells are younger and less mature in the acute rejection population compared to the cirrhotic and control. CD57 positive cells are known to have less replicative potential (Lopez-Verges et al., 2010). The expression of CD57 was also statistically significantly lower (p=0.019) in the acute rejection group **(Figure and Table 5.12)**. The expression of the other maturity NK cell receptors CD69 and NKG2A was not statistically different between the three groups (p>0.05) **(Figure and Table 5.10 and 5.12)**. In this panel the NKG2A stain was undertaken on all NK cells rather than a gated $CD56^{bright}$ NK cell group which may account for the different data to that seen in **figures 5.4 and 5.6.**

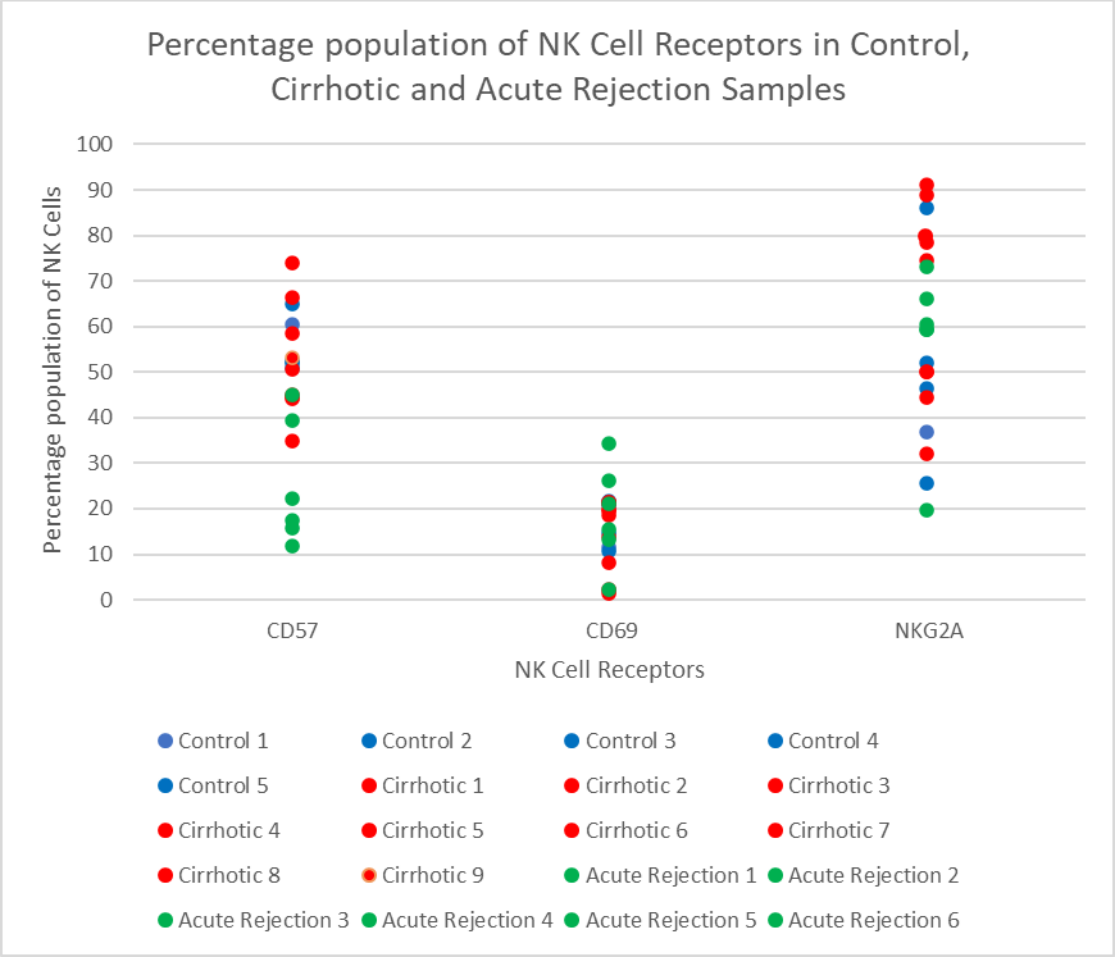

Figure 5.9 – Percentage population of NK cell maturity markers expressed on NK cells in the control, cirrhotic and acute rejection samples*. Control samples are shown in blue, cirrhotic samples in red and acute rejection samples in green.*

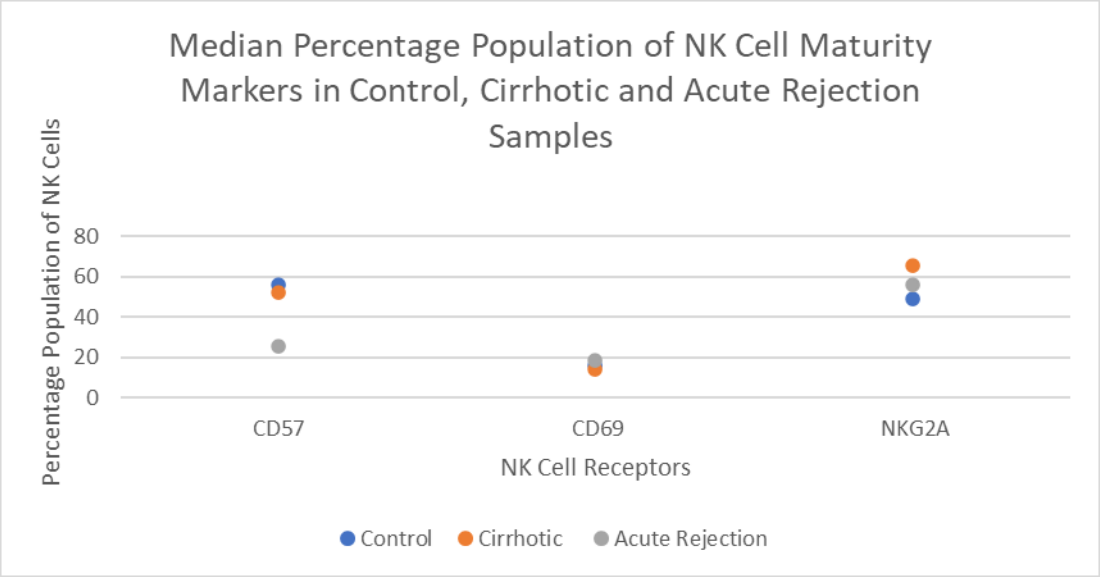

Figure 5.10 – Median percentage population of NK cell maturity markers expressed on NK cells in the control, cirrhotic and acute rejection samples*. Median and p-values are included within the table.*

	CD57	**CD69**	**NKG2A**
Control	56.1	15.84	49.34
Cirrhotic	52.28	14.09	65.49
Acute Rejection	25.32	18.74	56.3
P-value	**0.007**	**0.682**	**0.401**

Table 5.10 – Median percentage population of NK cell maturity markers expressed on NK cells in the control, cirrhotic and acute rejection samples*. Median and p-values are included within the table.*

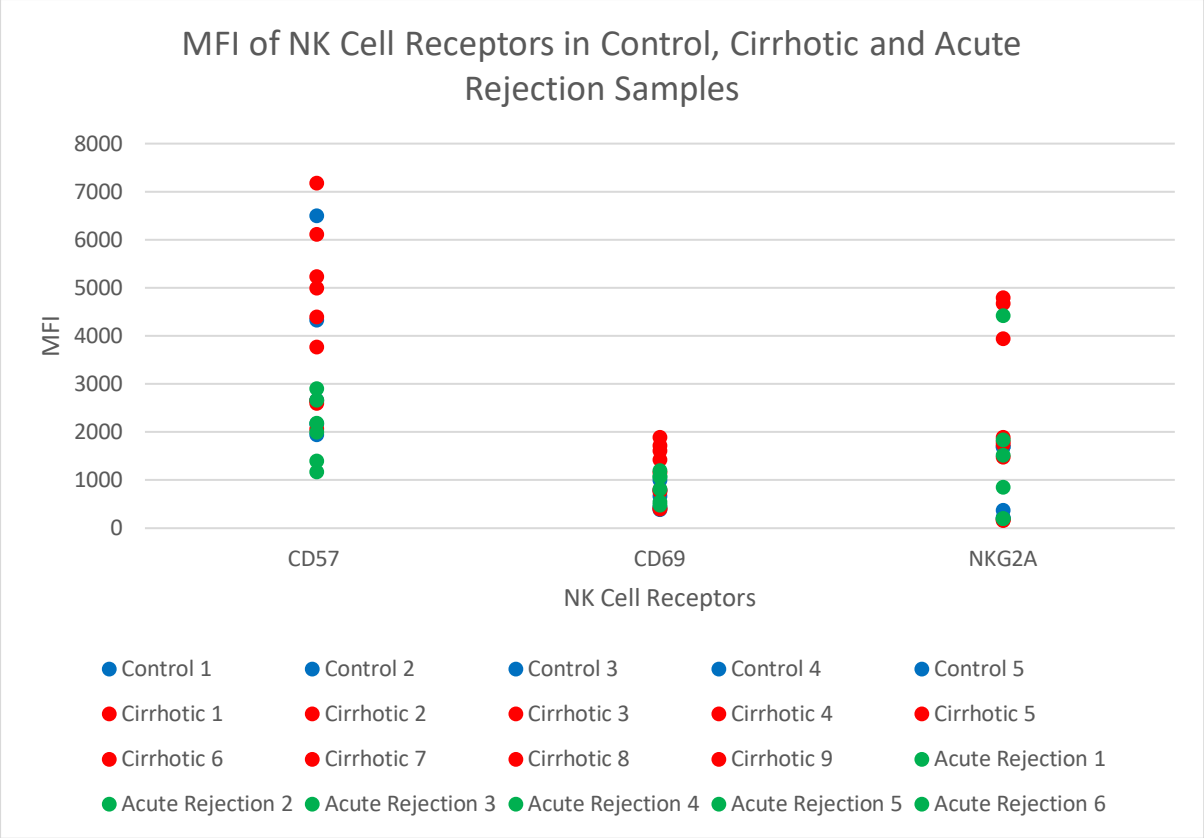

Figure 5.11 – MFI of NK cell maturity markers expressed on NK cells in the control, cirrhotic and acute rejection samples*. Control samples are shown in blue, cirrhotic samples in red and acute rejection samples in green.*

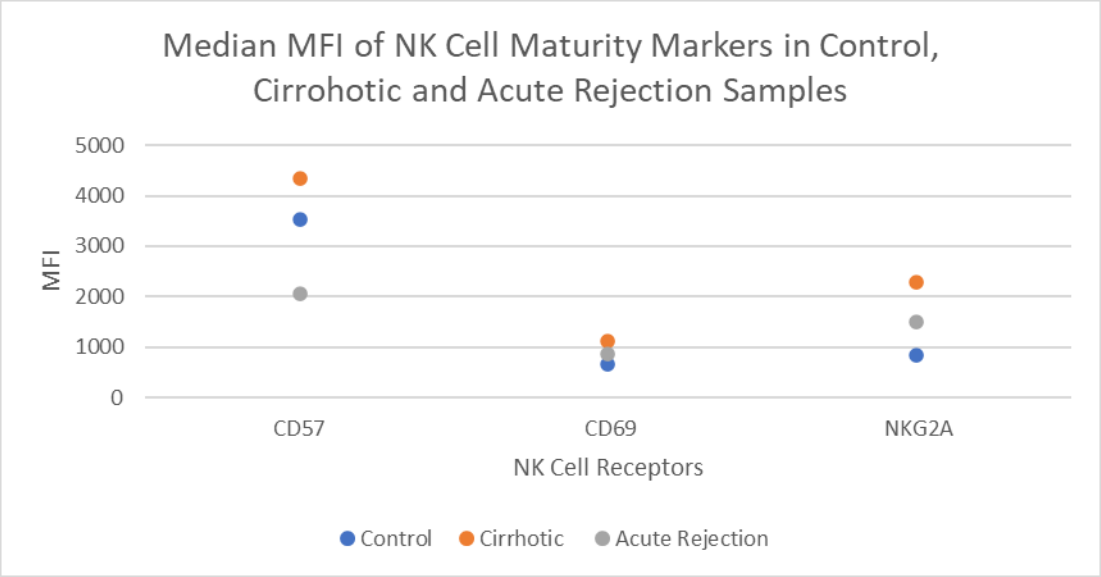

Figure 5.12 – Median MFI of NK cell maturity markers expressed on NK cells in the control, cirrhotic and acute rejection samples*. Median and p-values are included within the table.*

	CD57	**CD69**	**NKG2A**
Control	3522.8	655.6	835.4
Cirrhotic	4333.7	1130.8	2293.3
Acute Rejection	2052.2	860.83	1503.7
P-value	**0.019**	**0.205**	**0.389**

Table 5.12 – Median MFI of NK cell maturity markers expressed on NK cells in the control, cirrhotic and acute rejection samples*. Median and p-values are included within the table.*

5.3 Identification of NK Cell Receptors on Hepatocytes in Health and Liver Disease

Further investigation was planned to investigate expression of the NK cell receptors on hepatocyte membranes. However numerous problems were encountered. This technique cannot be undertaken with frozen tissue and fresh liver tissue was required. Initial experiments were undertaken using fresh liver taken from routine diagnostic or staging liver biopsy samples and from theatre during liver transplantation or liver resections.

Liver biopsy samples were more often available and undertaken at a planned time, so were therefore easier to collect, but the volume of cells available after the sample was split between research and pathology was almost too small for analysis. A second pass for research to obtain more sample was not permitted in the ethics application at the time of this study.

Sadly, the opposite was true with the explant samples provided, which were very large and contained much tissue other than hepatocytes. Liver transplant operations are rarely pre-planned so take place at short notice and often occur at night meaning that sample collection with immediate processing was very difficult. Isolating hepatocytes from these samples caused significnt trauma and then passing through cells the fortessa led to destruction.

Hepatocyte isolation and identification was attempted using several antibodies but all failed. The asialoglycoprotein receptor (ASGPR) was tried initially. ASGPR is expressed in sinusoidal cells and on the surface of the plasma hepatocyte membrane (Spiess, 1990), and is upregulated in cirrhosis (Nakaya et al., 1994). No staining was seen in the samples. Cytokeratin 18 (CK18) was also trialled, it is a protein found in the intracytoplasmic cytoskeleton of epithelial tissue (Schweizer et al., 2006). Mallory bodies are seen in cirrhosis and are abnormally phosphorylated and cross-linked to keratins such as CK18 (Matteoni et al., 1999). Staining was seen but this was non-specific for hepatocytes. A donation of unconjugated antibody to albumin (a protein synthesized by hepatocytes) was provided by Dr Fotios Sampaziotis (University of Cambridge). Again, no positive staining was seen with this antibody (Data not shown). Further experiments were abandoned.

5.4 Discussion

There are some significant differences seen between the NK cell receptor expression in the three groups, although they need to be assessed with caution. There was a significant difference in the expression of CD57 in the acute rejection group as well as a total lower number of NK cells in this group. There was also a significantly higher proportion of cells expressing KIR2DL2/2DS2 in the cirrhotic group and a lower proportion expressing KIR3DL1 in the acute rejection group.

Regarding the maturity of the NK cells there was a lower proportion of cells expressing CD57 in the acute rejection group compared to the cirrhotic and control samples. CD57 is a marker of NK cell maturation, identifying cells with cytotoxic potential but decreased sensitivity to cytokines and reduced replicative ability (Lopez-Verges et al., 2010). This might suggest that in acute rejection a less mature, younger, and more active set of NK cells are present which can act and cause the clinical effects. In both the control and cirrhotic groups, the NK cells are more mature, less responsive to cytokines and may therefore allow the senescent cells to accumulate.

The finding of less NK cells in the acute rejection group may be due to the age of the acute rejection samples; an alternative, more likely, explanation is that in acute rejection of severity to prompt liver biopsy these cells are infiltrating the tissue (Obara et al., 2005). If this project was to be undertaken

again or investigated further then acute rejection samples would be collected prospectively in the same time frame as the study samples and simultaneous analysis with tissue could resolve the issue of reliabilty in this sample set. For my own study, this would have extended the study period beyond that planned as it would take months to collect acute rejection samples. NK cells have been shown to be functional after 12 months cryopreservation (Lapteva et al., 2012); however another paper suggested altered NK cell receptor function and reduced NK cell survival after NK cell cryopreservation (Min et al., 2018). The process of freezing and thawing the cells has not been shown to effect NK cells (Domogala et al., 2016) and since all my samples were processed in similar fashion I feel that sample storage can not explain these differences.

There is a significantly higher proportion of cells expressing KIR2DL2/2DS2 in the cirrhotic group compared with both the acute rejection and control samples. KIR2DL2/2DS2 interact with HLA-C predominantly (David et al., 2013) and the expression has been associated with better outcomes from viral infections (Lin et al., 2016, Seich-Al-Basatena et al., 2011). They report that viral replication is suppressed by the expression of inhibitory KIR2DL2 via interaction with the HLA system. It is possible that in some manner this may also inhibit hepatocyte regeneration in liver disease contributing to cirrhosis. Although, to my knowledge not studied in cirrhosis, the presence of a HLA-C and killer cell immunoglobulin like receptor with two immunoglobulin domains (KIR2D) interaction has been associated with a reduced acute rejection rate and increased liver graft tolerance (Moya-Quiles et al., 2003, Hanvesakul et al., 2008). If there is both a higher expression of HLA-C in cirrhosis and KIR2D on peripheral NK cells a similar phenonmen could be seen. This could allow increased tolerance of the senescent hepatocytes contributing to cirrhosis. However, as I was unable to investigate the expression on the liver resisdent NK cells I can not confirm this hypothesis. This interaction would correlate with my work from chapter 3 showing increased expression of HLA-C in cirrhosis and now there is also higher expression of a partner ligand on the NK cells.

There is a significantly lower proportion of cells expressing KIR3DL1 in the acute rejection group compared with the cirrhotic and control groups. KIR3DL1 is an inhibitory KIR and therefore lower expression would lead to increased NK cell activity which would be associated with increased NK cell activation in acute rejection. On review the presence of inhibitory KIRs has been associated with a better outcome in acute rejection and graft survival in renal transplantation (Alam et al., 2015, Lopez-Botet et al., 2017). KIR3DL1 has been shown to interact with HLA-F as well as KIR3DS1 (Garcia-Beltran et al., 2016). The proportion of cells expressing KIR3DS1 was also lower in the acute rejection group but did not reach significance. Therefore we know that the necessary NK cell receptor is present to interact with the HLA-F expressed in liver disease and once this ligand is upregulated in cirrhosis may lead to higher activation.

The ratio of $CD56^{bright}$ to $CD56^{dim}$ cells may be higher in the two disease groups when compared to controls, although the difference did not reach statistical significance. If time had allowed it would have been helpful to increase the numbers of patients studied. It is possible that the higher number of $CD56^{bright}$ NK cells in the cirrhotic and acute rejection groups has a role in disease. A larger series may suggest over expression or reduced maturation of NK cells in disease as over expansion of the $CD56^{bright}$ subset has been reported previously in hepatocellular carcinoma (Cai et al., 2008) and hepatitis B (Zhao et al., 2012a).

Chapter 3 also showed an increased expression of HLA-E in cirrhosis compared to control liver samples. HLA-E interacts with the CD94:NKG2 pathway, but this work did not show a significant difference in the expression of these receptors in cirrhosis. There was higher expression in the acute rejection samples which did not reach significance. What the data does show is that these receptors are expressed and could interact with the overexpressed HLA-E in cirrhosis. There was minimal expression of KIR2DL4 in any samples which could interact HLA-G if it was actually present in the liver tissue (chapter 3 and 4 discuss this further).

On review of the data obtained there is some variation in the results of both percentage population and MFI within the same group (control, cirrhotic and acute rejection). The number of subjects studied was small and with the opportunity for a bigger sample variation may be reduced. However, the expression of NK cell receptors can be influenced by a number of factors and it is not unexpected that the reportoire of NK cell receptors expressed is different in different individuals (Carrillo-Bustamante et al., 2016). Secondly, I studied cirrhotic samples versus control but NK cell receptor expression has been shown to be affected by hepatocellular carcinoma or viral infection and therefore the underlying aetiology may have affected the results (Liu et al., 2018). For example KIR2DS1 has been associated with autoimmune hepatitis (Littera et al., 2016) and upregulation of LILRs has also been reported in autoimmune diseases, cancers and viral infections (Zhang et al., 2017).

Finally, this work focused on circulatory NK cells isolated from periperal blood due to the difficulties in isolating cells from human liver tissue. As discussed in the introduction liver resident NK cells are known to be phenotypically different to circulatory NK cells and therefore they could have a different expression profile to the peripheral NK cells I have studied. It would be important to assess the intrahepatic population in future studies. An option in future would be to collect blood from intra-hepatic sources for example during TIPSS (transjugular intrahepatic portosystemic shunt) or PTC (percutaneous transhepatic cholangiogram) procedures. However, to date it is not known which

NK cell population is affecting the liver in response to damage or disease (Mikulak et al., 2019, Peng and Sun, 2017).

Chapter 6 Results - Investigation of the Antigen Presentation Pathway in Liver Tissue

6.1 Introduction

The work in chapter 3 and 4 demonstrates that HLA class I is present within liver tissue and that there is differential expression between health and disease, with HLA class I molecules upregulated in cirrhosis. One interpretation is that cirrhosis or liver disease per se leads to an alteration in the MHC class I antigen presentation pathway. To my knowledge, the details and specific molecules of the MHC antigen presentation pathway have not been studied in patients with liver disease. The aim in this chapter, therefore, was to characterise the expression of three key accessory proteins of the MHC class I antigen presentation pathway, tapasin (Lehner et al., 1998), TAPBPR (Boyle et al., 2013) and TAP (Tan et al., 2002) in liver tissue during both health and disease. Further investigation would examine interactions with known association partners.

6.2 Investigation into the Components of the Antigen Presentation Pathway by Western Blot

In the first instance the antigen presentation pathway proteins were sought by western blot analysis using liver lysates. Both cirrhotic and control liver samples were used for comparison.

Exploratory experiments were undertaken by Jessica Clifton, an undergraduate student working with the group under my guidance. Using previously characterised cell lines to act as a positive and negative controls, she examined whether the expression of components of the antigen presentation pathway could be detected in frozen human liver tissue **(Figure 6.1)**. Subsequent work in this chapter was undertaken by me, unless otherwise stated. Jessica Clifton also undertook some further experiments as part of her own studies, again in collaboration with me.

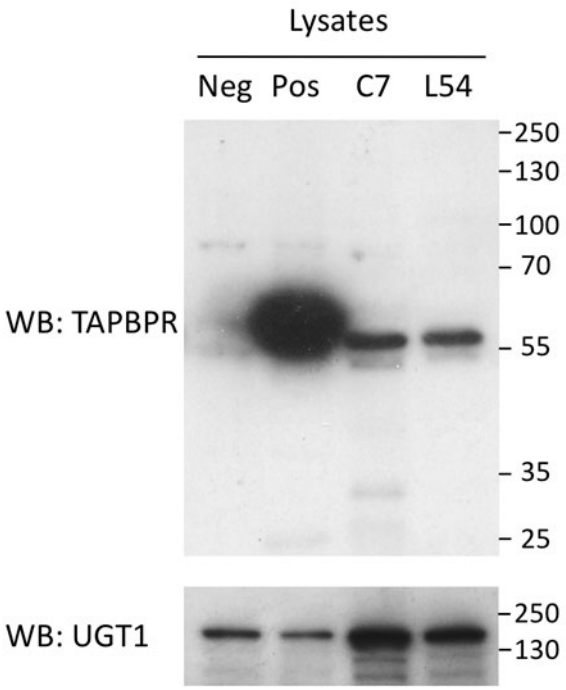

Figure 6.1 – TAPBPR can be detected in liver samples by western blot analysis. *Lysates from HeLaM-TAPBPR^{KO} cells (neg), HeLaM overexpressing a glycosylated form of TAPBPR (pos) as well as lysates from healthy control liver (C7) and diseased liver (L54) were probed using an antibody specific for TAPBPR (R021) and UGT1 as a loading control. Note, this figure was supplied by Miss Jessica Clifton.*

Western blot analysis of control liver (C7) and diseased liver (L54) were compared to cell lines generated and supplied by Dr Andreas Neerincx, comprising a HeLa cell line in which TAPBPR had been knocked out (7-9) (Neerincx et al., 2017) and which served as a negative control and one from a HeLa cell line overexpressing TAPBPR (HeLa m-glycTAPBPR cells), which functioned as a positive control.

A 55kDa band corresponding to TAPBPR (the approximate predicted size of TAPBPR) was seen in both liver samples as well as the positive control **(Figure 6.1)**. In contrast, this protein band was not observed in the TAPBPR knockout cell line, although this lane is partially obscured due to the high TAPBPR expression in the positive control line **(Figure 6.1)**. In addition, a smaller band is seen at a lower molecular weight when probing with the TAPBPR-specific mAb (for example, in C7), which may be a degradation product of TAPBPR **(Figure 6.1)**. Western blotting for UGT1 suggested equal sample loading between the liver samples and slightly lower protein levels in the HeLa cell lines.

Following the successful detection of TAPBPR in two liver samples, I next explored the expression pattern of TAPBPR and two other key components of the MHC class I antigen presentation pathway, tapasin and TAP, on a larger panel of liver samples. Western blot analysis suggested TAPBPR was expressed in all liver samples tested and appeared to be in higher concentration in cirrhosis compared to healthy control liver tissue **(Figure 6.2)**. A similar expression pattern was observed for tapasin **(Figure 6.2)**. Unfortunately, western blot of TAP was not particularly successful, although a weak band at 70kDa (the size of transporter associated with antigen presentation 1 (TAP1)) was observed in the cirrhotic samples **(Figure 6.2)**.

The apparent increase in the expression of TAPBPR, tapasin and possibly TAP, in the cirrhotic samples compared to the healthy control tissue is intriguing and is in keeping with my observations in chapter 3 and 4 for HLA class I molecules in general.

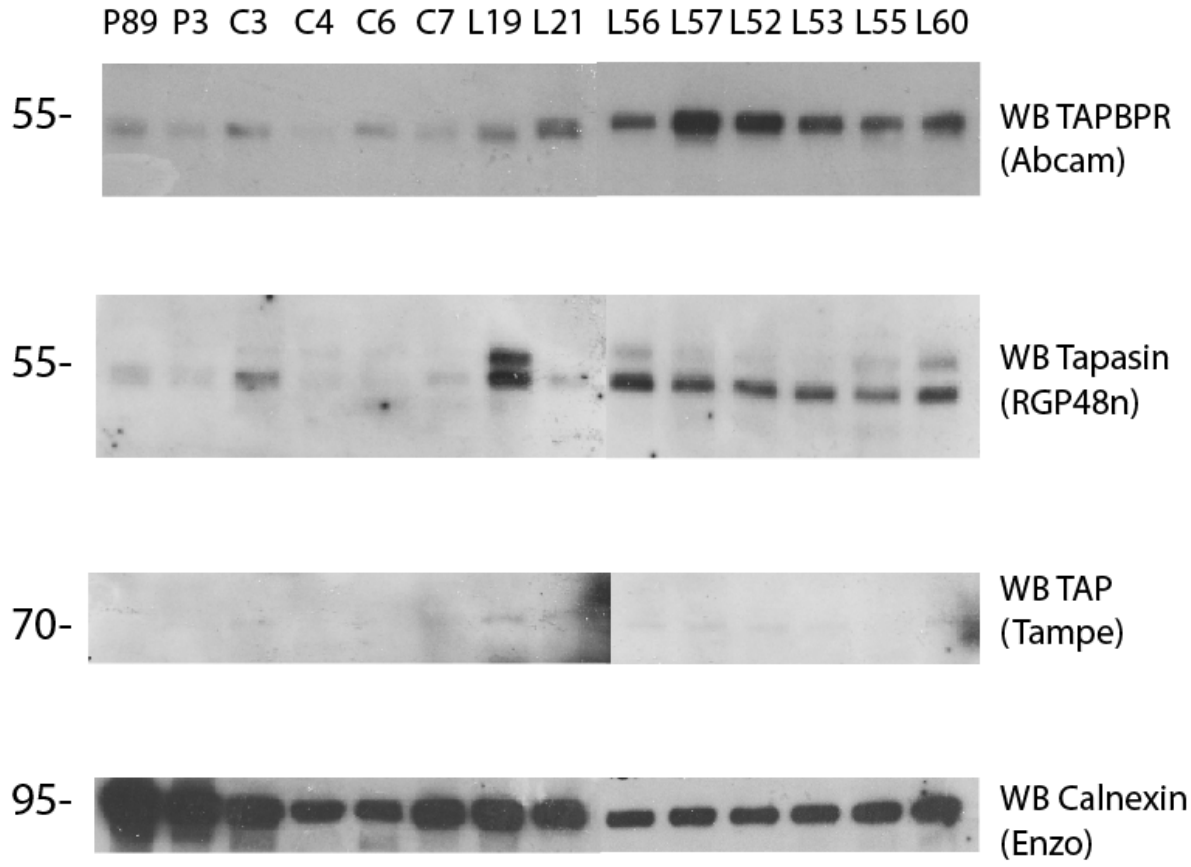

Figure 6.2 – Western blot analysis of whole lysate samples suggests tapasin and TAPBPR are upregulated in liver disease. *Lysates from placenta (P89 & P3), control liver (C3-C7) and diseased liver (L19-L60) tissue were probed using antibodies specific for TAPBPR (Abcam), Tapasin (RGP48n) and TAP (Tampe) as indicated. Western blot analysis for calnexin is included as a loading control. Of note a different antibody from that in* ***Figure 6.1*** *was used for TAPBPR which appears to detect with lower affinity.*

6.3 Investigation into TAPBPR in Human Liver by Immunoprecipitation

6.3.1 Immunoprecipitation Experiments Confirm TAPBPR Expression in Human Liver

To confirm these results and for further analysis, immunoprecipitation experiments were undertaken. No similar work on TAPBPR expression in human liver appear to have been published previously. Therefore, initial titration experiments were performed to assess the available antibodies for immunoprecipitation for TAPBPR. PeTe4, a mouse monoclonal antibody specific for the native conformation of TAPBPR (Hermann et al., 2013) and R014, a rabbit polyclonal raised to the luminal domains of TAPBPR (Hermann et al., 2015), were tested for immunoprecipitation. The Abcam TAPBPR monoclonal antibody and R021, a rabbit polyclonal raised to the cytoplasmic tail of TAPBPR (Hermann et al., 2013) were used for western blotting.

Using PeTe4 to immunoprecipitate TAPBPR, followed by western blotting using R021, TAPBPR expression was confirmed in human liver samples **(Figure 6.3)**. Furthermore, TAPBPR expression appeared to be increased in cirrhosis compared to control liver tissue **(Figure 6.3)**. However, the results are confounded by the presence of the 50kDa band present in the human liver immunoprecipitates as observed in chapter 3. Subsequent immunoprecipitation using R014 showed much clearer results, confirming the presence of TAPBPR in human liver **(Figure 6.4)**. Again, expression appeared to be increased in cirrhosis compared to control liver samples **(Figure 6.4)**.

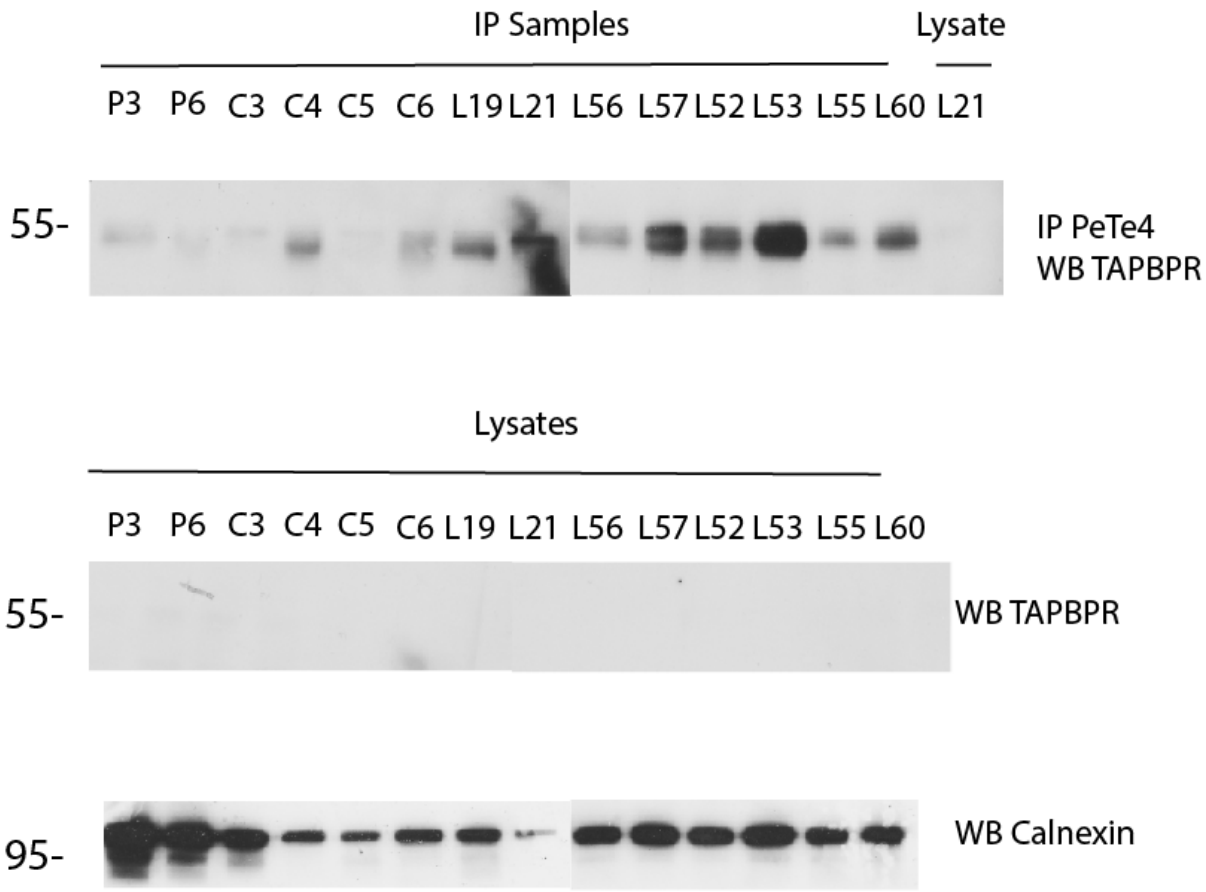

Figure 6.3 – Immunoprecipitation using the TAPBPR specific monoclonal antibody PeTe4 confirms TAPBPR expression in liver*. TAPBPR was immunoprecipitated from placenta (P89 & P3), control liver (C3-C7) and diseased liver (L19-L60) lysates using the TAPBPR specific mAb PeTe4. TAPBPR-immunoprecipates (top panel) and tissue lysates (middle panel) were subsequently probed using the abcam TAPBPR antibody. Western blot analysis for calnexin on tissue lysates is included as a loading control (bottom panel) and revealed some unequal loading of the samples (slightly higher in placenta and lower in the C4, C5 and L21 samples). Note: blotting for TAPBPR on lysates using abcam the antibody failed for this experiment.*

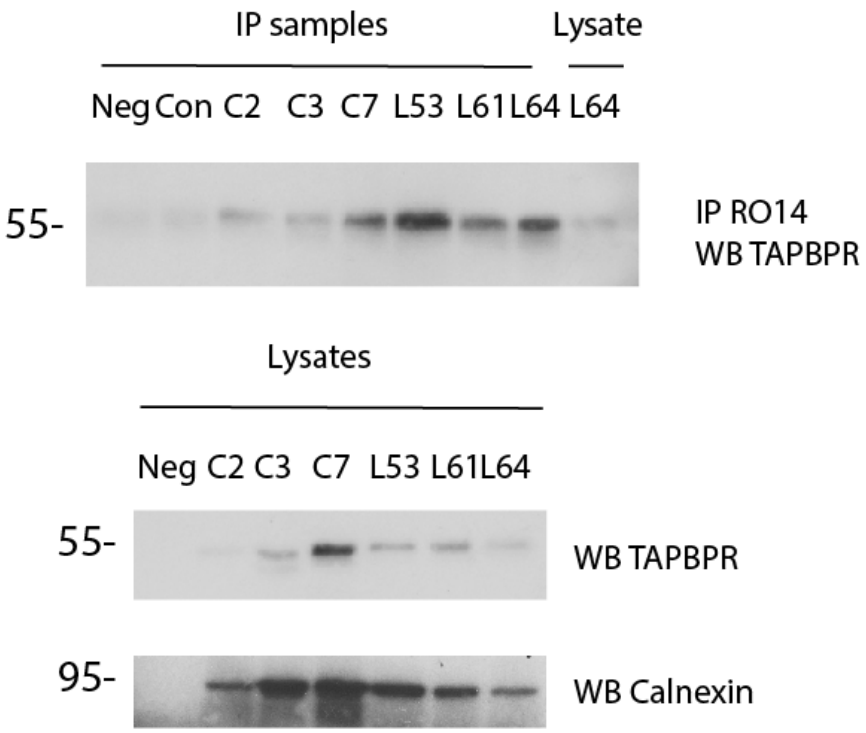

Figure 6.4 – Immunoprecipitation using the TAPBPR specific monoclonal antibody R014 confirms TAPBPR expression in liver. *TAPBPR was immunoprecipitated from control liver (C2-C7) and diseased liver (L53-L64) lysates using R014, a polyclonal antibody raised to the luminal domain of TAPBPR. TAPBPR-immunoprecipates (top panel) and tissue lysates (middle panel) were subsequently probed using the TAPBPR mAb from Abcam. Western blot analysis for calnexin on tissue lysates is included as a loading control (bottom panel). The control sample (Con) was a sample which underwent an IP with no antibody while the negative sample (Neg) was running buffer only with no IP or lysate sample.*

6.3.2 TAPBPR Interacts with MHC Class I in Human Liver

TAPBPR is an MHC class I chaperone and peptide editor (Boyle et al., 2013, Morozov et al., 2016, Hermann et al., 2015). So far, the interaction between TAPBPR and MHC class I has only been demonstrated in mammalian cell lines such as HeLa cells and KBM-7 cells or in vitro experiments using recombinant proteins. To date, the interaction between TAPBPR and MHC class I has not been explored directly in human tissue. Therefore, next I investigated whether TAPBPR associates with MHC class I in liver tissue. Following immunoprecipitation of TAPBPR, western blot analysis was performed for MHC class I. A band can be seen at 42kDA suggestive of MHC class I. The results show that there is an interaction between MHC class I and TAPBPR in liver **(Figure 6.5)**. Furthermore, there appears to be increased interaction in the cirrhotic samples compared with the control samples **(Figure 6.5)**.

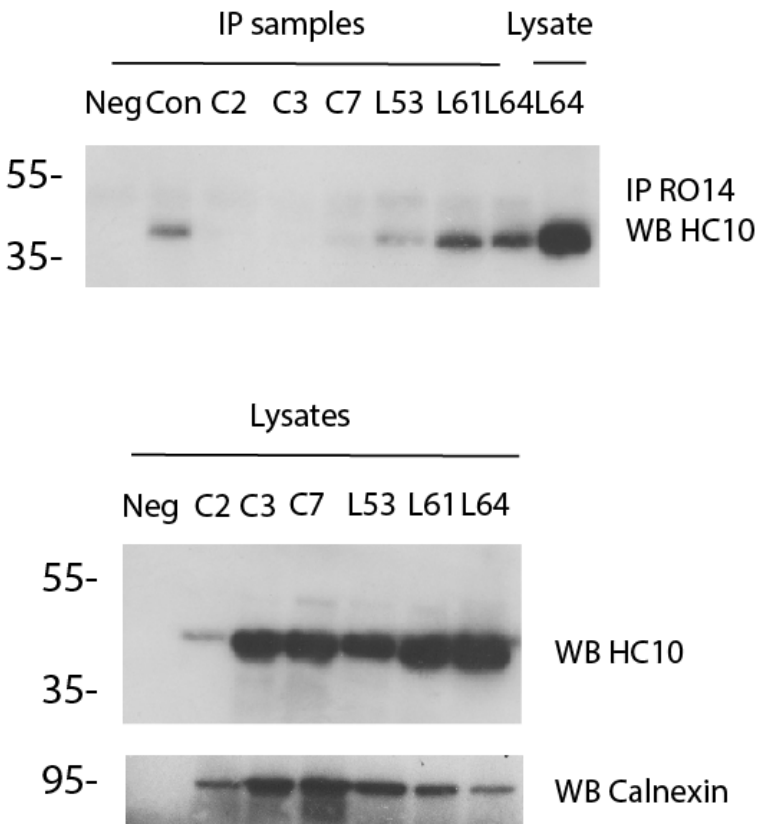

Figure 6.5 – TAPBPR interacts with MHC class I in human liver. *TAPBPR was immunoprecipitated from control liver (C2-C7) and diseased liver (L53-L64) lysates using R014, a polyclonal antibody raised to the luminal domain of TAPBPR. TAPBPR-immunoprecipitates (top panel) and tissue lysates (middle panel) were subsequently probed using HC10, a monoclonal antibody which reacts with HLA heavy chain particularly from HLA-B and -C molecules. Western blot analysis for calnexin on tissue lysates is included as a loading control (bottom panel) and suggests unequal loading of the samples with less in C2 and L64. However, this does not hamper the overall outcome of the results as the other control samples were adequately loaded. A negative control (Neg) using running buffer only was run as well as a control liver sample with no antibody included (Con). This sample is detected on the blot and suggests some minor contamination from the antibody in the neighbouring lane.*

6.4 Immunoprecipitation Experiments Confirm Tapasin Expression in Human Liver

Immunoprecipitation was also undertaken to investigate the presence of tapasin in healthy and diseased human liver and in addition, the interaction with MHC class I. Immunoprecipitation was undertaken with Pasta 1 antibody, a monoclonal antibody to tapasin by our student Jessica Clifton (Dick et al., 2002). The results confirm tapasin expression in liver tissue **(Figure 6.6, arrowhead)**. Furthermore, the findings suggest tapasin expression may be lower in control liver compared to

cirrhotic samples **(Figure 6.6)**. Subsequent probing of the tapasin immunoprecipitates for MHC class I was consistent with an association between tapasin and MHC class I in liver tissue and so potentially indicates increased association between these two proteins in the cirrhotic samples **(Figure 6.6)**. However, it is worth noting that although tapasin appears to have been successfully isolated by immunoprecipitation, the efficiency of the immunoprecipitation is somewhat questionable given that more tapasin is detected in the straight lysate lane compared to the immunoprecipitates. Therefore, this experiment will require further optimisation before firm conclusions can be drawn.

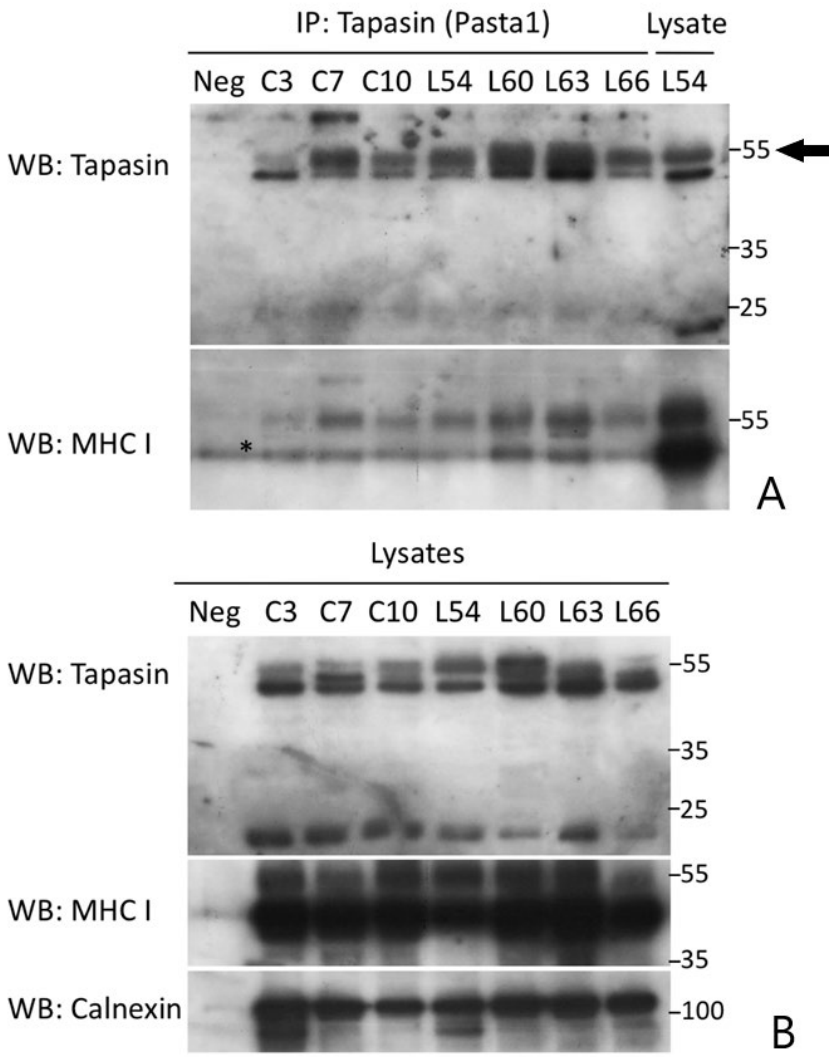

Figure 6.6 – Immunoprecipitation using the tapasin specific monoclonal antibody Pasta1 confirms tapasin expression in liver. *Tapasin was immunoprecipitated from control liver (C3-C10) and diseased liver (L54-L66) lysates using Pasta1, a mAb raised to the luminal domain of tapasin. Tapasin-immunoprecipitates (A) and tissue lysates (B) were probed using Rgp48N for tapasin and HC10 for the HLA class I heavy chain. Western blot analysis for calnexin on tissue lysates is included as a loading control and a negative control (Neg) using running buffer only. Note, this figure was supplied by Miss Jessica Clifton.*

6.5 TAP is Expressed in Human Liver by Immunoprecipitation

An immunoprecipitation was undertaken to identify TAP within the liver samples using Ring4C, a rabbit polyclonal antibody raised to the C-terminal region of TAP1 (Ortmann et al., 1997). A very faint band is detected at 70kDa **(Figure 6.7, arrowhead)** and was consistent with the detection of

TAP, but the strength of the signal does not yet support this observation with confidence. Secondly the lysate blot also failed casting doubt on the results. A band is seen at 50kDa as in previous studies, possibly related to cross-reactivity of the secondary antibody **(Figure 6.7)**.

This experiment was repeated by Jessica Clifton the student I was supervising within the department using a different antibody Tampe (Meyer et al., 1994) to undertake the immunoprecipitation. Again, the results were not convincing for the presence of TAP in liver tissue. The IP shows no obvious band at 70kDa the molecular weight of TAP **(Figure 6.8A arrowhead)**. However, the lysates do suggest expression in liver tissue **(Figure 6.8B arrowhead)**. This suggests that the immunoprecipitation itself failed. The results do not allow a firm conclusion for the presence of TAP in liver disease and further optimisation and work is required on this area.

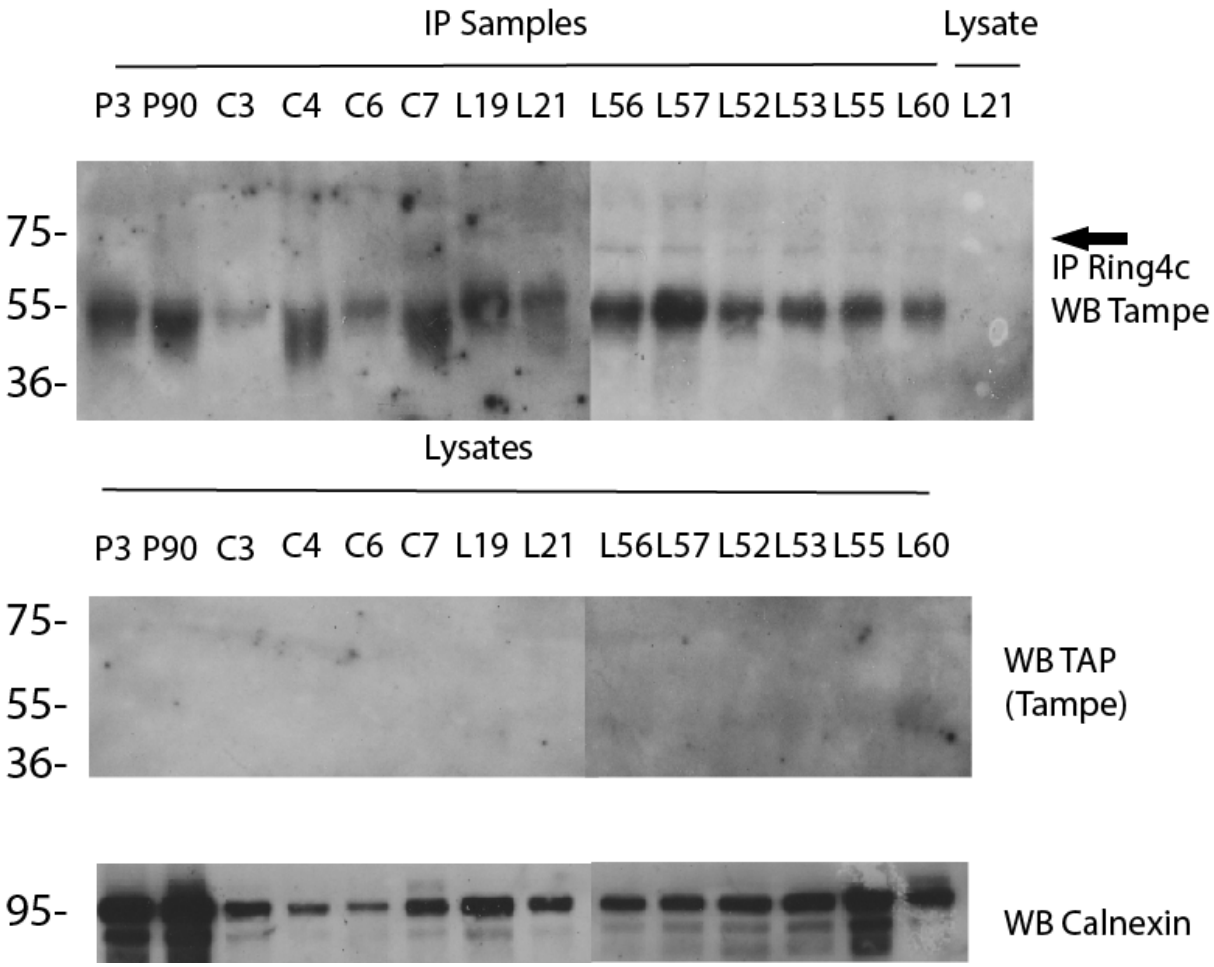

Figure 6.7 – Immunoprecipitation using the TAP specific monoclonal antibody Ring4c and subsequent western blot analysis with Tampe antibody*. TAP was immunoprecipitated from control liver (C3-C7) and diseased liver (L19-L60) lysates using Ring4c, a rabbit polyclonal antibody raised to the C-terminal region of TAP1. TAP-immunoprecipitates and tissue lysates were probed using Tampe for TAP. Western blot analysis for calnexin on tissue lysates is included as a loading control.*

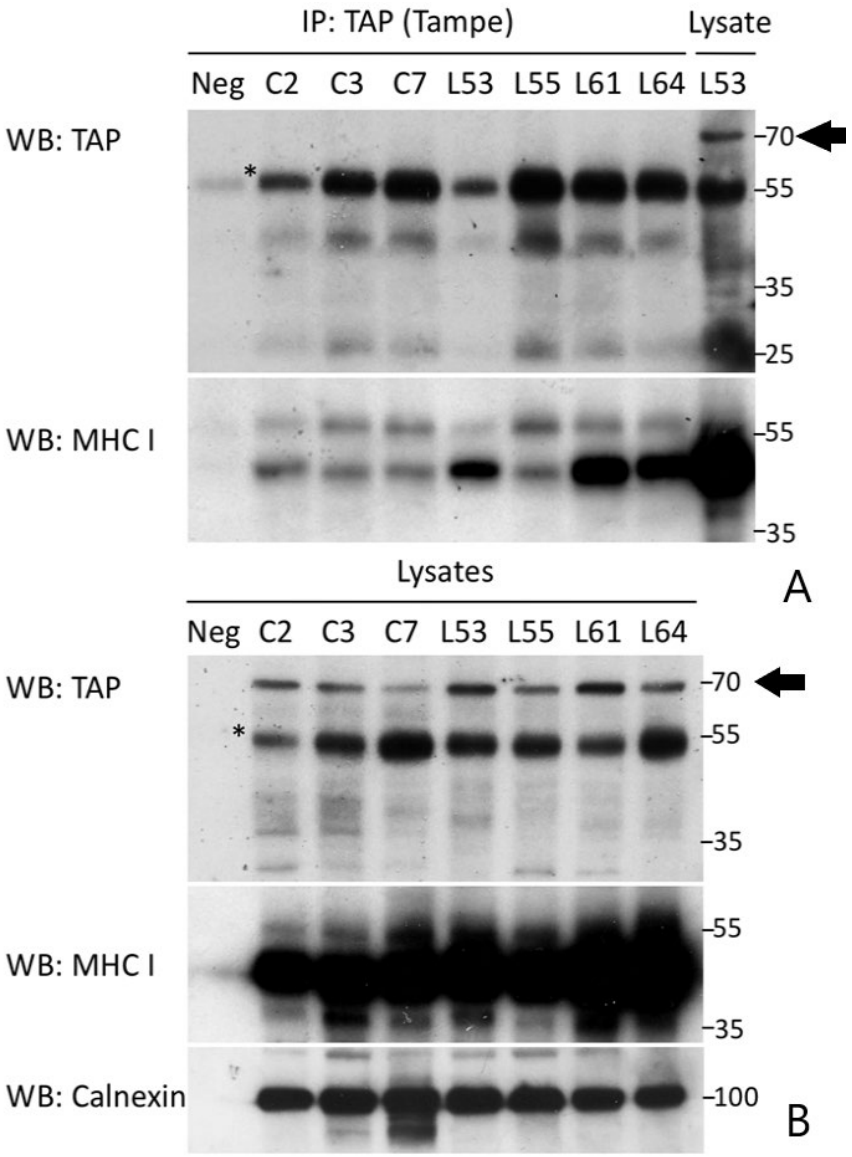

Figure 6.8 – Immunoprecipitation using the TAP specific monoclonal antibody Tampe inconclusive for TAP expression in liver. *TAP was immunoprecipitated from control liver (C2-C7) and diseased liver (L53-L64) lysates using Tampe, antibody for TAP (A). TAP-immunoprecipitates and tissue lysates (B) were probed again using Tampe for TAP and HC10 for the HLA class I heavy chain. Western blot analysis for calnexin on tissue lysates is included as a loading control and a negative control (Neg) using running buffer only. Note, this figure was supplied by Miss Jessica Clifton.*

6.6 Localisation of TAPBPR

Immunohistochemistry was undertaken to investigate the localisation of the TAPBPR molecule within the liver. Initial titration experiments showed PeTe4 antibody to be effective at a concentration of 1:100. **Figure 6.9** shows the presence of TAPBPR in hepatocytes. The staining

appears as small spicules within the hepatocytes, and this could represent expression of TAPBR in the golgi or vesicles. There was heterogeneous expression. The staining in both healthy and diseased liver is very similar; however globally, there was slightly increased staining in cirrhotic compared to control samples. A further example is shown in **Appendix 10.**

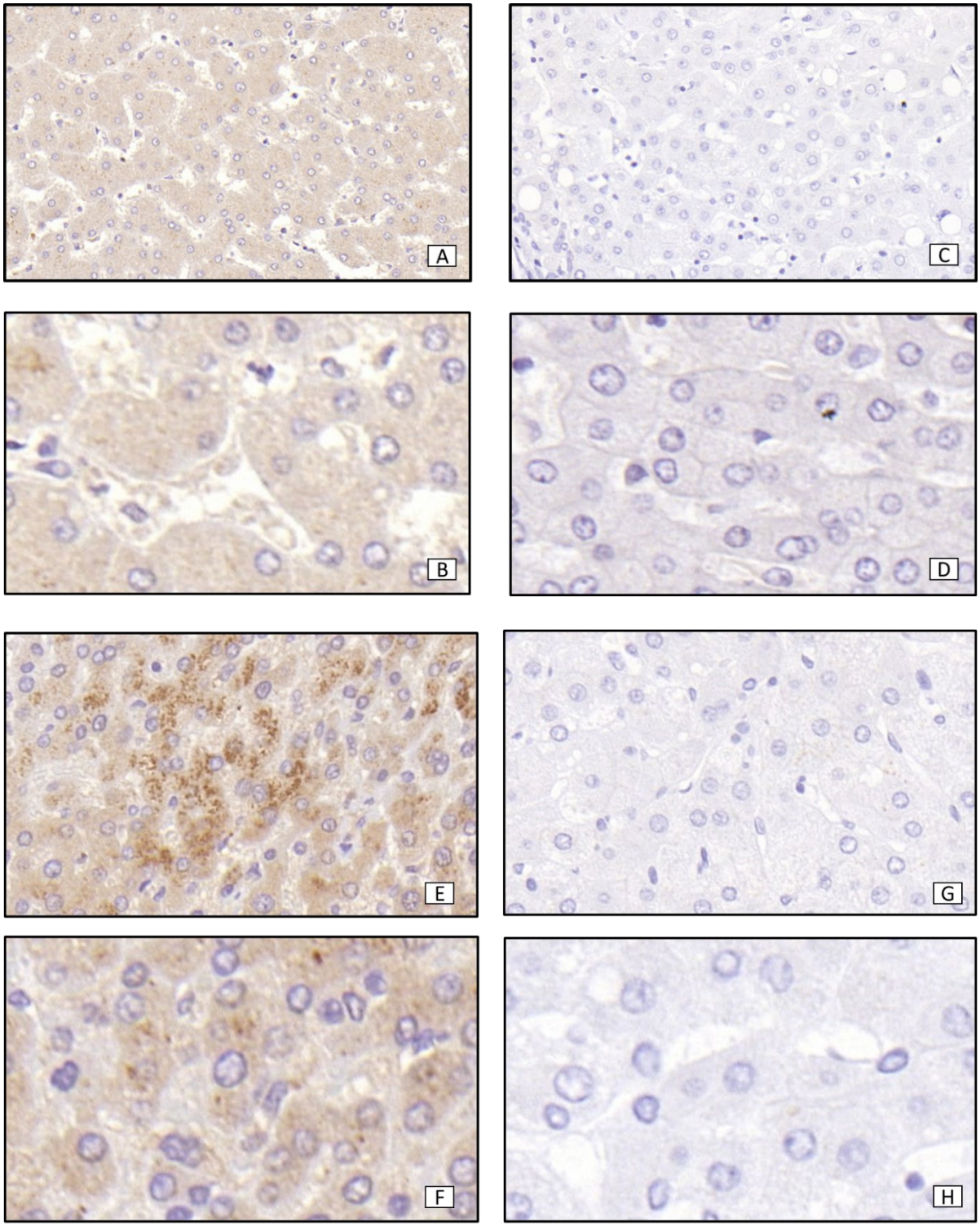

Figure 6.9 – Immunohistochemistry of TAPBPR with PeTe4 antibody in liver tissue*. Antigen retrieval with EDTA buffer. Positive staining is seen as brown as the secondary antibody was tagged with DAB. Images A (20x) and B (40x) showing hepatocyte staining in cirrhotic tissue. Images C (20x) and D (40x) were negative for staining in cirrhosis with an IgG2a control. Images E (20x) and F (40x) showed hepatocyte staining in healthy control liver tissue. Images G (20x) and H (40x) showed no staining in healthy control tissue with an IgG2a control antibody.*

Further experiments were conducted as part of preliminary work for future studies on the expression of TAPBPR in normal and diseased tissue as well as hepatocellular carcinoma. **Figure 6.10** shows a representative example of staining of TAPBPR in cirrhotic and normal livers as well as hepatocellular carcinoma. There appears to be increased expression in liver disease and associated with hepatocellular carcinoma although the results are not qualitative. Further work is being undertaken by my colleagues within the department.

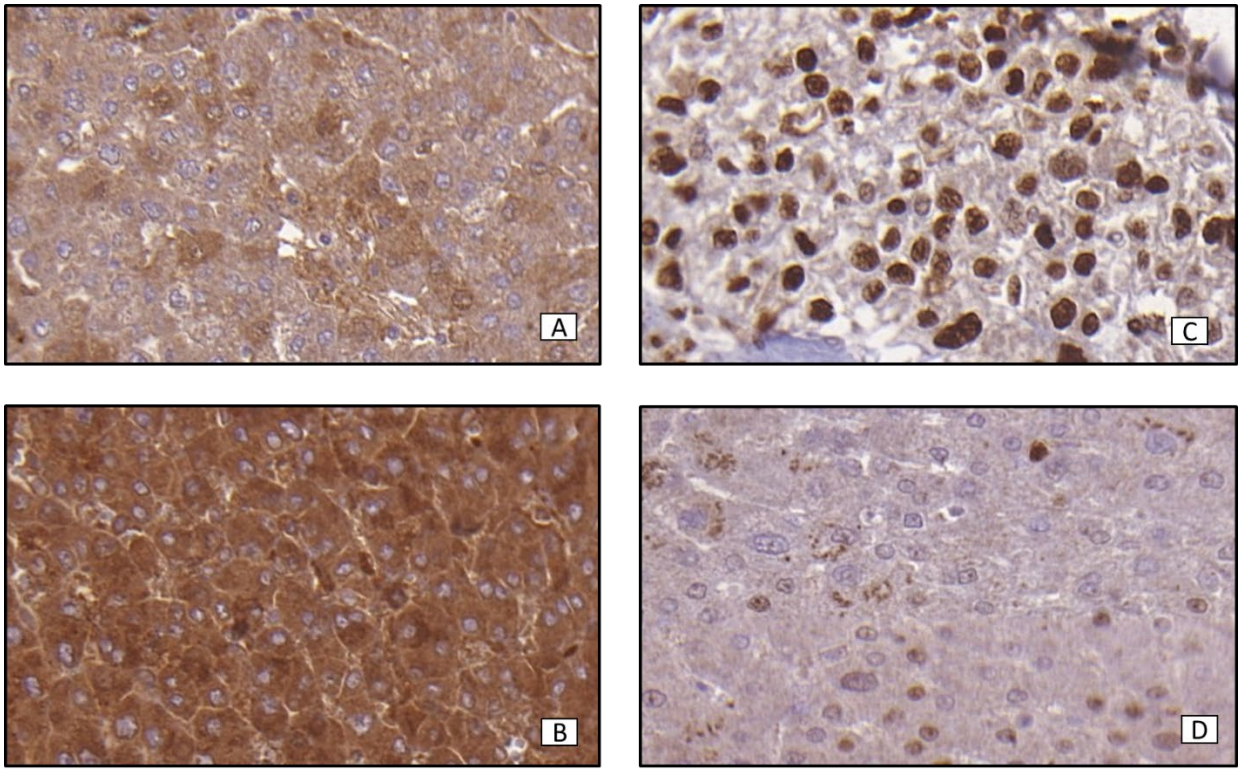

Figure 6.10 – Immunohistochemistry of TAPBPR with PeTe4 antibody in hepatocellular carcinoma*. Antigen retrieval with EDTA buffer. Positive staining is seen as brown as the secondary antibody was tagged with DAB. Image A (20x) showing staining in hepatocellular carcinoma. Image C shows a positive control with Mcm-2 antibody showing high nuclear expression within the cancer cells on this same sample. Image B shows staining in a control liver sample. (High background staining was seen in this case, but similar patchy staining is seen). Image D (20x) shows Mcm-2 staining in this healthy control tissue.*

6.7 Discussion

Firstly, human TAPBPR was identified within the liver tissue both in health and disease which is a novel finding. The immunohistochemistry staining suggested this staining was within the cell and

may be localised to the golgi, which concurs with the current literature in cell lines (Boyle et al., 2013).

The western blots and immunoprecipitation experiments appear to suggest that the expression of TAPBPR is increased in cirrhosis compared with control liver tissue. In addition, the interaction of the TAPBPR with HLA class I appeared to be increased in the cirrhotic tissue relative to healthy liver, suggesting there is altered regulation of TAPBPR in liver injury. This observation needs to be explored in further studies. Similar findings were seen with tapasin, suggesting that although the expression of the molecules is similar in healthy and diseased tissue there may be increased activation or use of this pathway which is contributing to the disease. The data I have obtained to date are inconclusive regarding the presence of TAP in liver tissue or liver disease and further work is needed before firm conclusions can be drawn.

Parallels can be drawn between this work and the results I obtained and described in chapter 3. The same mechanisms which are leading to overexpression of HLA class I molecules in liver disease appear also to be upregulating components of the antigen presentation pathway.

Both TAPBPR and tapasin act in the presentation and optimisation of peptides within the antigen presentation pathway (Lehner et al., 1998, Boyle et al., 2013). If these are being overexpressed in disease, then this would lead to the optimisation of the peptide presentation pathway and would also suggest that the HLA class I expression is playing a role in the disease pathology.

The role of TAPBPR and other components of the antigen presentation pathway in liver disease is under further investigation by the department.

Chapter 7 Final Discussion

7.1 Introduction

Cells become senescent as a protective mechanism to prevent the replication of damaged cells (Collado et al., 2007). However, in liver disease long standing cellular senescence in hepatocytes also drives fibrosis, where the number of senescent hepatocytes determines prognosis. I embarked upon this study with several aims but with an overriding plan to investigate the role of the immune system in hepatocyte senescence and cirrhosis. Specifically, to confirm the presence of a more complete range of HLA class I molecules in liver tissue and to investigate their role in disease, and to specifically investigate the presence and role of the non-classical MHC class I molecules in liver disease. Furthermore, to investigate any relation between the expression of MHC class I and the development of cellular senescence and the accumulation of senescent cells in cirrhosis.

The hypothesis was that senescent hepatocytes accumulate due to a failure of the innate immune system in liver disease analogous to the situation in pregnancy when maternal NK cells become senescent to protect the developing foetus (Rajagopalan, 2014). I hypothesise that cell surface expression of stress induced ligands and MHC class I molecules are altered in damaged hepatocytes which in acute injury results in their clearance via NK cells. However, I suggest that in chronic liver disease hepatocytes become senescent and therefore express a different signature of ligands on their cell surface which results in resistance to NK cell clearance and consequently leads to accumulation of hepatocytes with altered function. As such cells accumulate it leads eventually to impaired organ function.

Another aim was to investigate the antigen presentation pathway including TAPBPR, a novel peptide editor which has not previously been studied in liver disease. The expression of the HLA molecules under investigation would be affected by the expression of this presentation pathway. The plan was to investigate whether it is expressed in human liver and whether it has a role in disease. As a novel protein it may have an aberrant function in the pathogenesis of cirrhosis.

The previous chapters outline the work I have undertaken in the investigation of this hypothesis, and I will discuss the results in more depth below.

7.2 Discussion

7.2.1 HLA Class I

HLA class I was present in the liver tissue which concurs with literature published during the course of my studies (Boegel et al., 2018). This paper provides a genomic sequencing map of human tissue. I explored HLA class I using multiple techniques including western blot, immunoprecipitation, and immunohistochemistry. The immunohistochemistry suggested hepatocyte cell surface expression, which was confirmed by the endo H digest. Again, this is consistent with the current literature (Barbatis et al., 1981). By undertaking these studies, I could confirm the published findings as well as ensure that the biochemical techniques were robust for my planned work.

Interestingly, there appears to be increased expression of HLA class I across all the techniques I deployed in liver tissue from patients with cirrhosis. This suggests that the hepatocyte is behaving differently in cirrhosis compared to healthy liver tissue and that this might have the knock-on effect of altering immune responses.

7.2.2 HLA-E and -F

My work shows the presence of HLA-E and -F in liver tissue by western blot and immunoprecipitation. These are new findings, as previous work was limited to immunohistochemistry and RNA expression (Chen et al., 2006, Araujo et al., 2018, Zidi et al., 2016). Consistent with these findings, HLA-E and -F RNA were both identified in the liver tissue also. Finally, immunohistochemistry was also performed which showed expression in liver tissue.

Expression of HLA-E and -F using all the above techniques appeared to be increased in patients with cirrhosis compared to the healthy controls. This suggests that an upregulation in these molecules is related to the development or progression of liver disease and cirrhosis; although experiments performed at a single time point cannot distinguish cause from effect.

Classical HLA class I molecules HLA-A, -B and -C are expressed on the cell surface and if in conjunction with antigenic peptides can lead to attack and destruction by the immune system (Carrillo-Bustamante et al., 2016). The expression of the non-classical HLA-E molecule is another protective mechanism. HLA-E is expressed when HLA-A, -B and -C are present and prevents killing of cells through engagement with inhibitory receptors expressed on NK cells and cytotoxic T-cells known as KIRs. NK cells recognise ligands on a healthy cell membrane which prevents the lysis of normal cells (Colonna and Samaridis, 1995, Lanier, 1997). Higher levels of HLA-E in cirrhosis may

suggest that the NK cells would be inhibited or prevented from functioning correctly i.e. by eliminating the target cell. Over expression of HLA-E in cirrhosis may mean that damaged hepatocytes or other liver cells are not destroyed. In cirrhosis there is an accumulation of senescent hepatocytes (Aravinthan et al., 2013a) and higher levels of HLA-E may prevent NK cells from removing these damaged cells. The expression of HLA-E in pregnancy and subsequent inhibition of NK cell function to protect the developing foetus would mirror this hypothesis (Ishitani et al., 2006, Tripathi et al., 2007). The mechanism used physiologically during pregnancy may be exploited in the liver disease state. Recently senescent cells have been shown to upregulate HLA-E (Pereira et al., 2019).

The immunohistochemistry did confirm the presence of HLA-E in liver tissue and an upregulation in cirrhosis. However, the expression was intracellular and peri-nuclear in patients with cirrhosis; with a similar distribution seen in healthy tissue but to a lesser extent. As I have discussed, immunohistochemistry can sometimes be inaccurate, but the conclusions are supported by the endo H digest results. My attempts at assessing cell surface expression on hepatocytes by flow cytometry were unsuccessful but that would be another option for further investigation.

Further work needs to be undertaken to assess whether the function of HLA-E is retained if the molecule is not expressed on the cell surface. I have two potential ideas for this which would need further investigation.

The first, is that the HLA-E inside the cell can still somehow prevent NK cell killing, leading to an accumulation of damaged or potentially senescent cells in cirrhosis. Options for this might include the secretion of local substances or interaction with other molecules to be presented on the surface. HLA-E is now known to function as an antigen presenting cell to specific HLA-E restricted CD8+ T-cells (Joosten et al., 2016). Studies have identified a role in viral infections including HIV (D'Souza et al., 2019) and autoimmune diseases including multiple sclerosis (Sinha et al., 2015) and rheumatoid arthritis. This restricted population of cells is now a target for vaccine development (Yang et al., 2021). Similarly, it has been suggested that the HLA-E molecules within macrophages may reside within autophagy-lysosomal vesicles and act from this site (Camilli et al., 2016). The intracellular hepatocyte HLA-E may have a novel unknown function. Another suggestion is that Hsp60 can bind to the HLA-E in stressed cells (cirrhosis or senescence) which leads to NK killing (Michaelsson et al., 2002). By remaining intracellular this could be prevented. Ultimately, if the HLA-E molecules remain intra-cellular in senescence, then this may prevent cell destruction via a different pathway that the classical NK cell mediated destruction via the CD94/NKG2 pathway.

My second hypothesis is that some HLA-E is expressed on the cell surface but in a transient manner returning into the cell. Melanoma cells also showed high levels of HLA-E intracellularly with limited cell surface expression. However, this surface expression was inducible with IFNγ (Derré et al., 2006). More recently a study linking the expression of HLA-E with the persistence of senescent skin fibroblasts suggested that the expression of HLA-E on the cell surface altered following injury (Pereira et al., 2019). Over a 14-day time course the expression was seen to vary. This supports the possibility that any surface expression may be transient, or it may be that skin cells behave differently to hepatocytes. A brefeldin A (BFA) decay assay could be undertaken to investigate this further (Ilca et al., 2019).

Recently, specific variants of HLA-E have been associated with severe disease in SARS-Cov2 infection (Vietzen et al., 2021). My work has not focused on the genetic variants of the HLA-E molecule, but this may be an avenue to explore as it may leave patients at a greater risk of cirrhosis than others.

Expression of HLA-F was identified in liver tissue. The pattern of expression was almost identical to that seen with HLA-E and was also upregulated in cirrhosis. As discussed in earlier chapters the full role of HLA-F is not fully understood (Geraghty et al., 1990). However, recent studies suggest it may be a ligand for NK cell KIR receptors (Garcia-Beltran et al., 2016). So, in similar fashion to HLA-E it may be that the overexpression in cirrhosis might influence the activation of NK cells in the pathological process. Similarly, to HLA-E and HLA-G the hypothesis is that expression of HLA-F may prevent NK mediated attack during pregnancy (Ishitani et al., 2006). My hypothesis is the overexpression of HLA-F prevents the NK cell mediated killing of damaged cells and therefore they accumulate in cirrhosis. We know that senescent hepatocytes accumulate in cirrhosis and contribute to the disease process (Aravinthan et al., 2013a).

The immunohistochemistry findings for HLA-F show that most of the expression is reticular and intracellular. However, there was some patchy hepatocyte cell surface staining seen in localised areas in cirrhosis. This was confirmed by the endo H findings, which also suggest there was some cell surface expression of HLA-F and that this was also increased in the cirrhotic compared with the control samples. This finding is different to the results for HLA-E suggesting they may have a slightly different role.

The peri-nuclear staining could be indicative of retention within the golgi or endosomes which could represent material that had been at the cell surface, then recycled into endosomes in the peri-nuclear region. I surmise that this hepatocyte surface expression is present in areas of senescent hepatocytes which prevents the NK mediated killing of these cells leading to their accumulation is cirrhosis as suggested by my hypothesis.

My work shows that expression of HLA-E and HLA-F is increased in cirrhosis which supports my hypothesis. Further work needs to be undertaken into the specific function of these molecules in disease to establish how this may link to senescence. My focus was that the senescent hepatocytes accumulate due to a failure of NK cells, but it may be other immune cells responsible. The liver is now known to have several specific populations of tissue resident cells with phenotypic differences to circulating cells including NK cells, T-cells, mucosal associated T-cells (MAIT) cells, intra-epithelial lymphocytes and innate lymphoid cells (Wang and Zhang, 2019). Little is known yet of the different functions of these cells, but they could be interacting with the over-expression of HLA-E and -F seen in cirrhosis contributing to the pathology.

This work shows that HLA-E and HLA-F as well as HLA class I are upregulated in cirrhosis. During the development of cirrhosis, the liver is subject to both acute and chronic inflammation due to liver damage. This would release cytokines including IFNγ that could lead to the upregulation of these HLA molecules (Keskinen et al., 1997). Another possible mechanism is due to the relationship with senescence. Senescent cells release substances in the local area which is known as the SASP (Coppé et al., 2010). Many of these are interleukins and chemokines which would also lead to the upregulation of HLA class I molecules as well as HLA-E and HLA-F (Carbotti et al., 2017, Morandi et al., 2014).

7.2.3 HLA-G

The results I have obtained for HLA-G are more complex. HLA-G has been demonstrated in cirrhotic tissue previously (Moroso et al., 2015, Souto et al., 2011, Catamo et al., 2014); however, all of the studies were undertaken with immunohistochemistry and experts in the field have doubts about the value of these data (Alegre et al., 2014).

My intention was to fully investigate the presence of HLA-G using several more robust techniques. The results were also inconclusive. Immunohistochemistry suggested high expression of HLA-G in the cirrhotic samples, in agreement with the published studies (Moroso et al., 2015, Souto et al., 2011, Catamo et al., 2014), but this staining was diffuse throughout the cell cytoplasm and showed no specific distribution. In my opinion, this pattern of staining is more likely to be due to cross reactivity of the antibody MEMG01 with other HLA class I molecules rather than specifically identifying HLA-G. This view is supported by the results using other approaches to identify the expression of HLA-G, approaches that are more robust than any in the literature. I was unable to conclusively detect HLA-

G in the liver tissue by either western blotting or immunoprecipitation despite overt expression in the positive control placenta samples.

Similarly, I did not detect identifiable HLA-G RNA in any liver tissue except HBV infected samples. This suggests any expression in these samples may be related to the HBV virus rather than cirrhosis. Further study is required in this area as the numbers are small but there does appear to be a promising link between the hepatitis B virus and the expression of HLA-G which warrants further investigation. HLA-G is expressed during pregnancy to protect the foetus from NK cell attack (McMaster et al., 1998). Hepatitis B is a virus which hides within the immune system for many years (Protzer and Schaller, 2000) and could be using the expression of HLA-G to help its survival.

Overall, I feel the results suggest that conventional HLA-G is not present in cirrhosis. Therefore, we need to explore the other options for the positive results seen by others. As discussed, my suspicion is that the antibody MEMG01 has cross reactivity to another HLA class I molecule. This would explain why in all the published studies in immunohistochemistry, and in my own work, positive staining was seen in cirrhosis. Notably, all the published studies have used this antibody.

Another possibility is that the expression of HLA-G in cirrhosis is in an aberrant form that is not recognised by conventional antibodies used in blotting or immunoprecipitation but is detected by the MEMG01. HLA-G has seven known isoforms (Apps et al., 2008b) and it is possible that only one form is expressed in liver disease or that the HLA-G expressed is in a modified or spliced form. Dimers can form with HLA-G molecules which may also not be detected (Alegre et al., 2014). Similarly the isoforms G2-G4 are known to be of smaller kDa and may not be detected by conventional antibodies (Wuerfel et al., 2020) However, the lack of HLA-G RNA in all the non-HBV infected liver samples suggests its presence to be unlikely, although, there is a less likely possibility that spliced forms of HLA-G RNA may not be identified by the primers designed. Against this possibility is the observation that the positive control for HLA-G RNA was indeed positive and, in addition, HBV positive liver tissue contained HLA-G RNA in three patients. This latter observation is being followed up.

Finally, it could be possible that the antibodies are detecting other HLA molecules. These are larger than HLA-G and potentially could be the faint band seen on the western blot which used the same antibody as immunohistochemistry which showed positive staining.

The intention was to undertake mass spectroscopy to investigate this further, but I was unable to obtain these results prior to thesis submission because of the SARS-Cov-2 outbreak.

7.2.4 Senescence and the Innate Immune System

The dual immunohistochemistry does show a relationship between the expression of HLA class I, HLA-E, -F and -G with the expression of p21 in hepatocytes and therefore senescent cells. The hypothesis is that the expression of these molecules is preventing the removal of these senescent cells allowing their accumulation in senescence. The study shows that higher p21 expression correlates to higher expression of these molecules. The co-expression of these molecules is more convincing for HLA class I and HLA-E than HLA-F or -G. Further work needs to be undertaken to investigate whether there is a functional effect.

7.2.5 TAPBPR and the Antigen Presentation Pathway

I have identified the presence of TAPBPR in both healthy and diseased liver, another novel finding and not published previously to my knowledge. This was confirmed by western blot, immunoprecipitation, and immunohistochemistry. The immunohistochemistry suggested the staining was within the cell and may be localised to the golgi, as suggested by the current literature (Boyle et al., 2013).

My experiments suggest that the expression of TAPBPR is increased in cirrhosis compared with control liver tissue. Secondly, the interaction of the TAPBPR with HLA class I appears to be increased in the cirrhotic tissue relative to healthy liver, which suggests there is altered regulation of TAPBPR in liver injury. Again, it is impossible to distinguish the cause from effect in experiments undertaken at a single time point.

Tapasin was also identified in both healthy and diseased liver tissue but at similar levels of expression. However, there was an interaction seen with MHC class I, so it is possible that there is increased activation or use of the antigen presentation pathway, which is contributing to the disease. At present the data are inconclusive on the expression of TAP in liver tissue as expression was seen with western blotting but immunoprecipitation failed. Further work is underway.

It is possible that similar mechanisms which are leading to overexpression of HLA class I molecules in liver disease may also to be upregulating components of the antigen presentation pathway. Both TAPBPR (Boyle et al., 2013) and tapasin (Lehner et al., 1998) act in the presentation and optimisation of peptide presentation within the antigen presentation pathway. If TAPBPR is overexpressed in disease, then this could be optimising or altering the peptide presentation pathway. This would also suggest that HLA class I expression is playing a role in the disease pathology which needs further investigation.

7.2.6 NK Cell Receptors

As the data obtained for this chapter were incomplete the conclusions are drawn with caution but do highlight aspects which could be followed up with further study. The significant findings were that there was higher expression of KIR2DL2/2DS2 in the cirrhotic group, but in contrast, the acute rejection samples showed a lower expression of KIR3DL1 and lower expression of CD57. The implications are discussed below.

The study showed a lower expression of the maturity marker CD57 in the acute rejection group compared to the cirrhotic and control samples. This might suggest that the population of NK cells in acute rejection are younger, less mature, and more active. I suggest therefore that they would be more effective in clearing damaged or senescent cells. In the cirrhotic group, the NK cells are more mature and less active, and I suggest this would allow the senescent cell accumulation as seen in cirrhosis. Similarly, the ratio of $CD56^{bright}$ to $CD56^{dim}$ cells was higher in both rejection and cirrhosis compared to controls but did not reach significance. This would also suggest that the cells in cirrhosis are more mature and therefore less active or effective at removing damaged or senescent cells.

I identified a significantly higher expression of KIR2DL2/2DS2 in the cirrhotic group compared with both the acute rejection and control samples. KIR2DL2/2DS2 interacts with HLA-C predominantly (David et al., 2013) and the expression of this receptor has been linked to better outcomes from viral infections (Lin et al., 2016, Seich-Al-Basatena et al., 2011). The suggestion is that viral replication is suppressed by the expression of KIR2DL2, an inhibitory KIR. My suggestion is that expression of this KIR receptor may also inhibit hepatocyte regeneration in cirrhosis. In the control and acute rejection samples the patients fully recovered from injury. The hepatocytes had the ability to recover from the injury but in cirrhotic samples this function is lost. This may be due to the expression of this inhibitory KIR. The presence of HLA-C and KIR2D interaction has been associated with a reduced acute rejection rate and increased graft tolerance following liver transplantation (Moya-Quiles et al., 2003, Hanvesakul et al., 2008). If there is higher expression of HLA-C in hepatocytes in cirrhosis and KIR2D on the peripheral NK cells this could allow increased accumulation of senescent hepatocytes contributing to cirrhosis.

I identified a significantly lower expression of KIR3DL1 in the acute rejection group compared with the cirrhotic and control groups. KIR3DL1 is an inhibitory KIR and lower expression would lead to NK cell activation and increased activity in acute rejection. The presence of inhibitory KIRs has been associated with a better outcome in acute rejection and graft survival in renal transplantation (Alam et al., 2015, Lopez-Botet et al., 2017) and it seems likely that similar association would be seen in

liver disease if studied. Finding a reduction in an inhibitory KIR, KIR3DL1, in the group which suffered acute rejection concures with the current literature and helps to support the conclusions drawn from this study.

As disussed previously this work was undertaken with small numbers and to investigate this area further increased numbers of samples would help to confirm or refute the above conlusions. Secondly, this work focused on peripheral NK cells and not tissue-resident NK cells. There are known phenotypic differences and potential differences in functionality.

7.3 Limitations

With any large research project many lessons are learnt along the way and knowledge gained. I started this project with no laboratory-based experience and therefore have had to learn all the scientific techniques required. I now have three years of laboratory experience and looking back over the project there are, as expected, some things which could be undertaken differently a second time.

The western blot and immunoprecipitation experiments were undertaken on whole tissue lysate. Therefore, this would contain all cells including immune cells as well as hepatocytes. Conclusions drawn from this data must include the caveat that the molecule was expressed in liver tissue, but it does not define which cell type. The immunohistochemistry does help to investigate this, but the aim was to overcome this using flow cytometry. I planned to isolate hepatocytes by flow cytometry and then assess the HLA class I expression on these cells. However, as discussed in chapter 5 I failed to isolate hepatocytes effectively to complete this part of the study.

At the start of the project a decision was made to use all cirrhotic tissue collected including all aetiologies. The reasoning behind this was that tissue collection was difficult and time consuming (need for consent, tissue collection from theatre out of hours, unpredictability of liver transplantation surgery) and the concern was that not enough tissue would be available if only specific conditions were used. However, this means that the study samples have undergone different disease processes although all which ultimately led to cirrhosis. It is possible that differences in the HLA expression are due to the disease type (for example viral infection or autoimmunity) rather than cirrhosis. Despite obtaining a good amount of tissue throughout the project I do not have enough numbers of each specific disease type to compare them individually and make definitive conclusions on their relationship with HLA expression.

The control tissue used was obtained from hepatic resections. The histology was reviewed to ensure the tissue was as 'normal' as possible. No samples with any documented steatosis were studied although they were collected. At the start of the project with limited samples available some samples were used which had documented surgical handling changes or atrophy. In retrospect this was a mistake as these abnormalities could have confounded the results if the tissue was not completely normal. If this project were to continue an alternative source of control tissue could be explored including donor livers not used for transplantation or tissue banks available for research.

The immunohistochemistry work was successful in HLA molecule cellular location and sub-cellular location. Much time was spent following this trying to undertake immunofluorescence and dual-staining immunofluorescence on paraffin embedded liver sections. I struggled with auto-fluorescence despite many attempts to overcome this. The autofluorescence may have been less of a problem with frozen sections, however, by the time this was considered it was too late to re-start the project. Secondly, the liver samples collected were not sufficient for the volume of tissue required.

As discussed in chapter 3 the amount of senescent tissue can vary in different cirrhotic samples (Meijnikman et al., 2021). This is accounted for in the immunohistochemistry work where I stained for p21 alongside the MHC class I marker and the results do show a variation in the level of p21 expression. However, I did not quantify the volume of senescent tissue within the collected cirrhotic or control liver samples. This could have confounded my results if the levels were at the extreme high or low end. However, in support of the results a total of 33 cirrhotic samples were tested showing similar results. In retrospect I should have included a western blot for p21 or a similar senescence marker.

I used p21 as a marker of senescence however p16 may have been a more reliable marker. Although levels of both p21 and p16 would be raised in senescence, it is suggested that p16 is required for the maintenance of senescence and that levels of p21 could start to diminish (Stein et al., 1999). Initially I used p21 as this had been used previously in the laboratory and I followed established protocols. However, if further studies were undertaken the possibility of a suitable p16 antibody could be explored.

Chapter 5 assessed the NK cell receptors which would interact with the MHC class I molecules. Due to a failure to obtain meaningful results from flow cytometry with liver tissue the conclusions are drawn from the results of peripheral NK cells. These cells would have adequate opportunity to interact with the hepatocytes and affect their functionality. However, there is known to be a population of liver resident NK cells which have a different phenotype to circulating NK cells

(Marquardt et al., 2015). These may have other effects on the hepatocytes and further work should be undertaken to assess this NK cell population to confirm the findings. An option to obtain this tissue would be to collect blood rather than liver tissue but from directly inside the liver either during PTC or TIPSS procedures.

Time constraints and the SARS-Cov-2 pandemic have prevented the completion of some parts of the research. I was unable to obtain the mass spectroscopy results for the non-classical HLA molecules. My initial samples failed mid-run on the machine and the repeated experiments were unable to be analysed to the pandemic lab shutdown.

There were several aims of the mass spectroscopy work which I was unable to complete. I wished to confirm the presence of HLA-E and -F within the liver samples to support my immunoprecipitation findings. I would also have been able to identify any potential binding partners for these proteins if they are expressed intracellularly. Finally, I intended to identify the band seen during western blotting with the non-conformational antibodies to identify what it was cross-reacting with.

An interesting finding was the expression of HLA-G RNA in the hepatitis B liver samples. Further work was planned as discussed in chapter 3 but ultimately a lack of further samples meant that the further work could not be undertaken during my thesis. Unfortunately, this leaves small numbers and limited data to support possible conclusions which could be drawn. Follow up work is planned into this area which could be important.

7.4 Further Options

There is ongoing work within the department on the expression of TAPBPR in liver tissue and specifically its role in cancer. It would be important to explore whether the findings from this study do support a role for TAPBPR in upregulating and altering the peptide presentation pathway in cirrhosis leading to the accumulation of senescent hepatocytes.

The results for the presence of TAP, and to a lesser extent tapasin, were inconclusive in this work. I would like to further optimise these immunoprecipitation experiments and undertake the planned immunohistochemistry to investigate the true role they may play in liver disease.

One of the interesting findings was the expression of HLA-G RNA in hepatitis B liver tissue. If a source of hepatitis B tissue could be found, then further investigation in this area would be beneficial. It would help to prove or refute the potential hypothesis discussed above.

7.5 Final Conclusion

On review of the whole project, there are several novel and firm conclusions that act as a base for future studies.

- HLA class I is present in liver tissue and is upregulated in cirrhosis.
- HLA-E and HLA-F are expressed in liver tissue and are also upregulated in cirrhosis. The expression appears to be intracellular and could be representative of localisation within the golgi, while some surface expression is also seen but to a lesser extent.
- The expression of HLA-G is less conclusive. While my immunohistochemistry data are congruent with the published data showing expression in cirrhosis, all other biochemical techniques showed no expression of HLA-G.
- HLA-G RNA was only identified in the hepatitis B infected liver tissue and suggests a viral cause not cirrhosis.
- NK cell receptors KIR2DL2/2DS2 were significantly upregulated in cirrhosis although the numbers studied were low. Further work needs to be undertaken in this area but does suggest that NK cell activation is altered in cirrhosis and therefore could explain the accumulation of senescent hepatocytes.
- TAPBPR and tapasin are expressed in liver tissue and show a slight upregulation in liver disease. These are both peptide editors in the antigen presentation pathway and suggest that aberrant expression via this pathway may be part of the liver pathology.

In all, the changes seen in altered expression of HLA molecules in cirrhosis, specifically HLA-E and HLA-F, alongside the altered expression of inhibitory molecules on circulating NK cells, remain consistent with reduced clearance of damaged hepatocytes in cirrhosis. This altered expression may have a role in the pathogenesis of cirrhosis and could be a target for future therapies.

References

ABEL, A., YANG, C., THAKAR, M. & MALARKANNAN, S. 2018. Natural Killer Cells: Development, Maturation, and Clinical Utilization *Frontiers in Immunology,* 9**,** 1869.

AKBAR, A., BEVERLEY, P. & SALMON, M. 2004. Will Telomere Erosion Lead to a Loss of T-Cell Memory? *Nature Reviews Immunology,* 4**,** 737–743.

AKBAR, A., SOARES, M., PLUNKETT, F. & SALMON, M. 2000. Differential Regulation of $CD8^+$ T Cell Senescence in Mice and Men. *Mechanisms of Ageing and Development,* 121**,** 69-76.

ALAM, S., RANGASWAMY, D., PRAKASH, S., SHARMA, R., KHAN, M., SONAWANE, A. & AGRAWAL, S. 2015. Impact of Killer Immunoglobulin-like Receptor-Human Leukocyte Antigens Ligand Incompatibility Among Renal Transplantation. *Indian Journal of Nephrology,* 25**,** 27-33.

ALBERTS, B., JOHNSON, A., LEWIS, J., RAFF, M., ROBERTS, K. & WALTER, P. 2002. *Molecular Biology of the Cell,* New York Garland.

ALEGRE, E., RIZZO, R., BORTOLOTTI, D., FERNANDEZ-LANDAZURI, S., FAINARDI, E. & GONZALEZ, A. 2014. Some Basic Aspects of HLA-G Biology. *Journal of Immunology Research,* 2014**,** 657625.

APPS, R., GARDNER, L., HIBY, S., SHARKEY, A. & MOFFETT, A. 2008a. Conformation of Human Leucocyte Antigen-C Molecules at the Surface of Human Trophoblast Cells. *Immunology,* 124**,** 322-328.

APPS, R., GARDNER, L. & MOFFETT, A. 2008b. A Critical Look at HLA-G. *Trends in Immunology,* 29**,** 313-321.

APPS, R., GARDNER, L., TRAHERNE, J., MALE, V. & MOFFETT, A. 2008c. Natural-Killer Cell Ligands at the Maternal-Fetal Interface: UL-16 Binding Proteins, MHC Class-I Chain Related Molecules, HLA-F and CD48. *Human Reproduction,* 23**,** 2535-2548.

APPS, R., MURPHY, S., FERNANDO, R., GARDNER, L., AHAD, T. & MOFFETT, A. 2009. Human Leucocyte Antigen (HLA) Expression of Primary Trophoblast Cells and Placental Cell Lines, Determined using Single Antigen Beads to Characterize Allotype Specificities of Anti-HLA Antibodies. *Immunology,* 127**,** 26-39.

ARAUJO, R., DIAS, F., BERTOL, B., SILVA, D., ALMEIDA, P., TEIXEIRA, A., SOUZA, F., VILLANOVA, M., RAMALHO, L., DONADI, E. & MARTINELLI, A. 2018. Liver HLA-E Expression is Associated with Severity of Liver Disease in Chronic Hepatitis C. *Journal of Immunology Research,* 2018**,** 2563563.

ARAVINTHAN, A., PIETROSI, G., HOARE, M., JUPP, J., MARSHALL, A., VERRILL, C., DAVIES, S., BATEMAN, A., SHERON, N., ALLISON, M. & ALEXANDER, G. 2013a. Hepatocyte Expression of the Senescence Marker p21 is Linked to Fibrosis and an Adverse Liver-Related Outcome in Alcohol-Related Liver Disease. *PLOS one* 8**,** e72904.

ARAVINTHAN, A., SCARPINI, C., TACHTATZIS, P., VERMA, S., PENRHYN-LOWE, S., HARVEY, R., DAVIES, S., ALLISON, M., COLEMAN, N. & ALEXANDER, G. 2013b. Hepatocyte Senescence Predicts Progression in Non-Alcohol Related Fatty Liver Disease. *Journal of Hepatology,* 58**,** 549-556.

ARAVINTHAN, A., SHANNON, N., HEANEY, J., HOARE, M., MARSHALL, A. & ALEXANDER, G. 2014. The Senescent Hepatocyte Gene Signature and Chronic Liver Disease. *Experimental Gerontology,* 60**,** 37-45.

ARAVINTHAN, A., VERMA, S., COLEMAN, N., DAVIES, S., ALLISON, M. & ALEXANDER, G. 2012. Vacuolation in Hepatocyte Nuclei is a Marker of Senescence. *Journal of Clinical Pathology* 65**,** 557-560.

BAHRAM, S., BRESNAHAN, M., GERAGHTY, D. & SPIES, T. 1994. A Second Lineage of Mammalian Major Histocompatibility Complex Class I Genes. *Proceedings of the National Academy of Sciences,* 91**,** 6259-6263.

BAKER, D., WIJSHAKE, T., TCHKONIA, T., LEBRASSEUR, N., CHILDS, B., VAN-DE-SLUIS, B., KIRKLAND, J. & VAN-DEURSEN, J. 2011. Clearance of p16Ink4a-Positive Senescent Cells Delays Ageing-Associated Disorders. *Nature,* 479**,** 232-236.

BARBATIS, C., WOODS, J., MORTON, J., FLEMING, K., MCMICHAEL, A. & MCGEE, J. 1981. Immunohistochemical Analysis of HLA (A, B, C) Antigens in Liver Disease using a Monoclonal Antibody. *Gut,* 22**,** 985-991.

BEN-PORATH, I. & WEINBERG, R. 2005. The Signals and Pathways Activating Cellular Senescence. *International Journal of Biochemistry and Cell Biology,* 37**,** 961-976.

BENEVOLO, M., MOTTOLESE, M., PIPERNO, G., SPERDUTI, I., CIONE, A., SIBILIO, L., MARTAYAN, A., DONNORSO, R., COSIMELLI, M. & GIACOMINI, P. 2007. HLA-A, -B, -C Expression in Colon Carcinoma Mimics that of the Normal Colonic Mucosa and is Prognostically Relevant. *American Journal of Surgical Pathology,* 31**,** 76-84.

BENHAM, A., GROMME, M. & NEEFJES, J. 1998. Allelic Differences in the Relationship Between Proteasome Activity and MHC Class I Peptide Loading. *Journal of Immunology,* 161**,** 83-89.

BERETTA, A., GRASSI, F., PELAGI, M., CLIVIO, A., PARRAVICINI, C., GIOVINAZZO, G., ANDRONICO, F., LOPALCO, L., VERANI, P., BUTTÒ, S., TITTI, F., ROSSI, G., VIALE, G., GINELLI, E. & SICCARDI, A. 1987. HIV Env Glycoprotein Shares a Cross-Reacting Epitope with a Surface Protein Present on Activated Human Monocytes and Involved in Antigen Presentation. *European Journal of Immunology,* 17**,** 1793-1798.

BILLERBECK, E., MOMMERSTEEG, M., SHLOMAI, A., XIAO, J., ANDRUS, L., BHATTA, A., VERCAUTEREN, K., MICHAILIDIS, E., DORNER, M., KRISHNAN, A., CHARLTON, M., CHIRIBOGA, L., RICE, C. & JONG, Y. D. 2016. Humanized Mice Efficiently Engrafted with Fetal Hepatoblasts and Syngeneic Immune Cells Develop Human Monocytes and NK Cells. *Journal of Hepatology,* 65**,** 334-343.

BILZER, M., ROGGEL, F. & GERBES, A. 2006. Role of Kupffer Cells in Host Defense and Liver Disease. *Liver International,* 26**,** 1175-1186.

BJORKMAN, P., SAPER, M., SAMRAOUI, B., BENNETT, W., STROMINGER, J. & WILEY, D. 1987. Structure of the Human Class I Histocompatibility Antigen, HLA-A2. *Nature,* 329**,** 506-512.

BLOOM, S., WEBSTER, G. & MARKS, D. 2012. *Oxford Handbook of Gastroenterology and Hepatology*, Oxford University Press.

BOEGEL, S., LOWER, M., BUKUR, T., SORN, P., CASTLE, J. & SAHIN, U. 2018. HLA and Proteasome Expression Body Map. *BMC Medical Genomics,* 11**,** 36.

BONILLA, F. & OETTGEN, H. 2010. Adaptive Immunity. *Journal of Allergy and Clinical Immunology,* 125**,** S33-S40.

BORGES, L., HSU, M., FANGER, N., KUBIN, M. & COSMAN, D. 1997. A Family of Human Lymphoid and Myeloid Ig-like Receptors, some of which Bind to MHC Class I Molecules. *Journal of Immunology,* 159**,** 5192-5196.

BORST, L., VAN-DER-BURG, S. & VAN-HALL, T. 2020. The NKG2A-HLA-E Axis as a Novel Checkpoint in the Tumor Microenvironment. *Clinical Cancer Research,* 26**,** 1-8.

BOTTIROLI, G. & CROCE, A. 2004. Autofluorescence Spectroscopy of Cells and Tissues as a Tool for Biomedical Diagnosis. *Photochemical and Photobiological Sciences,* 3**,** 189-210.

BOYLE, L., GILLINGHAM, A., MUNRO, S. & TROWSDALE, J. 2006. Selective Export of HLA-F by its Cytoplasmic Tail. *Journal of Immunology,* 176**,** 6464-6472.

BOYLE, L., HERMANN, C., BONAME, J., PORTER, K., PATEL, P., BURR, M., DUNCAN, L., HARBOUR, M., RHODES, D., SKJODT, K., LEHNER, P. & TROWSDALE, J. 2013. Tapasin-Related Protein TAPBPR is an Additional Component of the MHC Class I Presentation Pathway. *Proceedings of the National Academy of Sciences* 110**,** 3465-3470.

BRADBURY, L., KANSAS, G., LEVY, S., EVANS, R. & TEDDER, T. 1992. The CD19/CD21 Signal Transducing Complex of Human B Lymphocytes Includes the Target of Antiproliferative Antibody-1 and Leu-13 Molecules. *Journal of Immunology,* 149**,** 2841-2850.

BRAUD, V., ALLAN, D., O'CALLAGHAN, C., SODERSTROM, K., D'ANDREA, A., OGG, G., LAZETIC, S., YOUNG, N., BELL, J., PHILLIPS, J., LANIER, L. & MCMICHAEL, A. 1998a. HLA-E Binds to Natural Killer Cell Receptors CD94/NKG2A, B and C. *Nature,* 391**,** 795-799.

BRAUD, V., ALLAN, D., WILSON, D. & MCMICHAEL, A. 1998b. TAP- and Tapasin-Dependent HLA-E Surface Expression Correlates with the Binding of an MHC Class I Leader Peptide. *Current Biology,* 8**,** 1-10.

BRAUD, V., JONES, E. & MCMICHAEL, A. 1997. The Human Major Histocompatibility Complex Class Ib Molecule HLA-E Binds to Signal Sequence-Derived Peptides with Primary Anchor Residues at Positions 2 and 9. *European Journal of Immunology* 27**,** 1164-1169.

BRISSOT, P., PIETRANGELO, A., ADAMS, P., DE-GRAAFF, B., MCLAREN, C. & LOREAL, O. 2018. Haemochromatosis. *Nature Reviews. Disease Primers,* 4**,** 18016.

BRITISHLIVERTRUST. 2020. *Liver Disease: Statistics* [Online]. https://britishlivertrust.org.uk/about-us/media-centre/statistics/#stats: BritishLiverTrust. [Accessed March 2021].

BURT, D., JOHNSTON, D., RINKE-DE-WIT, T., VAN-DEN-ELSEN, P. & STERN, P. 1991. Cellular Immune Recognition of HLA-G-Expressing Choriocarcinoma Cell Line JEG-3. *International Journal of Cancer,* 47**,** 117-122.

CAI, L., ZHANG, Z., ZHOU, L., WANG, H., FU, J., ZHANG, S., SHI, M., ZHANG, H., YANG, Y., WU, H., TIEN, P. & WANG, F. 2008. Functional Impairment in Circulating and Intrahepatic NK Cells and Relative Mechanism in Hepatocellular Carcinoma Patients. *Clinical Immunology,* 129**,** 428-437.

CAI, M., XU, Y., QIU, S., JU, M., GAO, Q., LI, Y., ZHANG, B., ZHOU, J. & FAN, J. 2009. Human Leukocyte Antigen-G Protein Expression is an Unfavorable Prognostic Predictor of Hepatocellular Carcinoma Following Curative Resection. *Clinical Cancer Research,* 15**,** 4686-4693.

CAMILLI, G., CASSOTTA, A., BATTELLA, S., PALMIERI, G., SANTONI, A., PALADINI, F., FIORILLO, M. & SORRENTINO, R. 2016. Regulation and Trafficking of the HLA-E Molecules during Monocyte-Macrophage Differentiation. *Journal of Leukocyte Biology,* 99**,** 121-130.

CAMPISI, J. 2001. Cellular Senescence as a Tumor-Suppressor Mechanism. *Trends in Cell Biology,* 11**,** S27-S31.

CAMPISI, J. 2005. Senescent Cells, Tumor Suppression, and Organismal Aging: Good Citizens, Bad Neighbors. *Cell,* 120**,** 513-522.

CAMPISI, J. & FAGAGNA, F. 2007. Cellular Senescence: When Bad Things Happen to Good Cells. *Nature Reviews Molecular Cell Biology,* 8**,** 729-740.

CARBOTTI, G., NIKPOOR, A., VACCA, P., GANGEMI, R., GIORDANO, C., CAMPELLI, F., FERRINI, S. & FABBI, M. 2017. IL-27 Mediates HLA Class I Up-Regulation, which can be Inhibited by the IL-6 Pathway, in HLA-Deficient Small Cell Lung Cancer Cells. *Journal of Experimental and Clinical Cancer Research,* 36**,** 140.

CAROSELLA, E., MOREAU, P., ARACTINGI, S. & ROUAS-FREISS, N. 2001. HLA-G: A Shield Against Inflammatory Aggression. *Trends in Immunology,* 22**,** 553-555.

CARRILLO-BUSTAMANTE, P., KESMIR, C. & BOER, R. D. 2016. The Evolution of Natural Killer Cell Receptors. *Immunogenetics,* 68**,** 3-18.

CATAMO, E., ZUPIN, L., CROVELLA, S., CELSI, F. & SEGAT, L. 2014. Non-Classical MHC-I Human Leukocyte Antigen (HLA-G) in Hepatotropic Viral Infections and in Hepatocellular Carcinoma. *Human Immunology,* 75**,** 1225-1231.

CAWTHON, R., SMITH, K., O'BRIEN, E., SIVATCHENKO, A. & KERBER, R. 2003. Association Between Telomere Length in Blood and Mortality in People Aged 60 Years or Older. *Lancet,* 361**,** 393-395.

CHEN, M., TABACZEWSKI, P., TRUSCOTT, S., VAN-KAER, L. & STROYNOWSKI, I. 2005. Hepatocytes Express Abundant Surface Class I MHC and Efficiently use Transporter Associated with Antigen Processing, Tapasin, and Low Molecular Weight Polypeptide Proteasome Subunit Components of Antigen Processing and Presentation Pathway. *Journal of Immunology,* 175**,** 1047-1055.

CHEN, Y., CHENG, M. & TIAN, Z. 2006. Hepatitis B Virus Down-Regulates Expressions of MHC Class I Molecules on Hepatoplastoma Cell Line. *Cellular and Molecular Immunology,* 3**,** 373-378.

CHILDS, B., BAKER, D., KIRKLAND, J., CAMPISI, J. & VAN-DEURSEN, J. 2014. Senescence and Apoptosis: Dueling or Complementary Cell Fates? *EMBO Reports,* 15**,** 1139-1153.

COLLADO, M., BLASCO, M. & SERRANO, M. 2007. Cellular Senescence in Cancer and Aging. *Cell,* 130**,** 223-233.

COLONNA, M. & SAMARIDIS, J. 1995. Cloning of Immunoglobulin-Superfamily Members Associated with HLA-C and HLA-B Recognition by Human Natural Killer Cells. *Science,* 268**,** 405-408.

COOPER, M. 2015. The Early History of B Cells. *Nature Reviews Immunology,* 15**,** 191-197.

COPPÉ, J., DESPREZ, P., KRTOLICA, A. & CAMPISI, J. 2010. The Senescence-Associated Secretory Phenotype: The Dark Side of Tumor Suppression. *Annual Review of Pathology,* 5**,** 99-118.

COPPÉ, J., KAUSER, K., CAMPISI, J. & BEAUSÉJOUR, C. 2006. Secretion of Vascular Endothelial Growth Factor by Primary Human Fibroblasts at Senescence. *The Journal of Biological Chemistry,* 281**,** 29568-29574.

CROCKER, P., JEFFERIES, W., CLARK, S., CHUNG, L. & GORDON, S. 1987. Species Heterogeneity in Macrophage Expression of the CD4 Antigen. *Journal of Experimental Medicine,* 166**,** 613-618.

D'SOUZA, M., ADAMS, E., ALTMAN, J., BIRNBAUM, M., BOGGIANO, C., CASORATI, G., CHIEN, Y., CONLEY, A., ECKLE, S., FRÜH, K., GONDRÉ-LEWIS, T., HASSAN, N., HUANG, H., JAYASHANKAR, L., KASMAR, A., KUNWAR, N., LAVELLE, J., LEWINSOHN, D., MOODY, B., PICKER, L., RAMACHANDRA, L., SHASTRI, N., PARHAM, P., MCMICHAEL, A. & YEWDELL, J. 2019. Casting a Wider Net: Immunosurveillance by Nonclassical MHC Molecules. *PLOS pathology,* 15**,** e1007567.

DAUSSET, J. 1981. The Major Histocompatibility Complex in Man. *Science,* 213**,** 1469-1474.

DAVID, G., DJAOUD, Z., WILLEM, C., LEGRAND, N., RETTMAN, P., GAGNE, K., CESBRON, A. & RETIERE, C. 2013. Large Spectrum of HLA-C Recognition by Killer Ig-like Receptor (KIR)2DL2 and KIR2DL3 and Restricted C1 SPECIFICITY of KIR2DS2: Dominant Impact of KIR2DL2/KIR2DS2 on KIR2D NK Cell Repertoire Formation. *Journal of Immunology,* 191**,** 4778-4788.

DAVIS, A., RICHTER, A., BECKER, S., MOYER, J., SANDOUK, A., SKINNER, J. & TAUBENBERGER, J. 2014. Characterizing and Diminishing Autofluorescence in Formalin-Fixed Paraffin-Embedded Human Respiratory Tissue. *Journal of Histochemistry and Cytochemistry,* 62**,** 405-423.

DERRÉ, L., CORVAISIER, M., CHARREAU, B., MOREAU, A., GODEFROY, E., MOREAU-AUBRY, A., JOTEREAU, F. & GERVOIS, N. 2006. Expression and Release of HLA-E by Melanoma Cells and Melanocytes: Potential Impact on the Response of Cytotoxic Effector Cells. *Journal of Immunology,* 177**,** 3100-3107.

DESAI, D., SAP, J., SILVENNOINEN, O., SCHLESSINGER, J. & WEISS, A. 1994. The Catalytic Activity of the CD45 Membrane-Proximal Phosphatase Domain is Required for TCR Signaling and Regulation. *EMBO Journal,* 13**,** 4002-4010.

DICK, T., BANGIA, N., PEAPER, D. & CRESSWELL, P. 2002. Disulfide Bond Isomerization and the Assembly of MHC Class I-Peptide Complexes. *Immunity,* 16**,** 87-98.

DIXON, L., BARNES, M., TANG, H., PRITCHARD, M. & NAGY, L. 2013. Kupffer Cells in the Liver. *Comprehensive Physiology,* 3**,** 785-797.

DJURISIC, S. & HVIID, T. 2014. HLA Class Ib Molecules and Immune Cells in Pregnancy and Preeclampsia. *Frontiers in Immunology,* 5**,** 652.

DOMOGALA, A., MADRIGAL, J. & SAUDEMONT, A. 2016. Cryopreservation has No Effect on Function of Natural Killer Cells Differentiated in Vitro from Umbilical Cord Blood CD34+ Cells. *Cytotherapy,* 18**,** 754-759.

DULBERGER, C., MCMURTREY, C., HÖLZEMER, A., NEU, K., LIU, V., STEINBACH, A., GARCIA-BELTRAN, W., SULAK, M., JABRI, B., LYNCH, V., ALTFELD, M., HILDEBRAND, W. & ADAMS, E. 2017. Human Leukocyte Antigen F Presents Peptides and Regulates Immunity through Interactions with NK Cell Receptors. *Immunity,* 46**,** 1018-1029.

EBRAHIMKHANI, M., MOHAR, I. & CRISPE, I. 2011. Cross-Presentation of Antigen by Diverse Subsets of Murine Liver Cells. *Hepatology,* 54**,** 1379-1387.

EISSMANN, P. 2020. *Natural Killer Cells* [Online]. https://www.immunology.org/public-information/bitesized-immunology/cells/natural-killer-cells: British Society for Immunology. [Accessed March 2021].

ELHELU, M. 1983. The Role of Macropahges in Immunology. *Journal of the National Medical Association,* 75**,** 314-317.

ELLIS, E. & MANN, D. 2012. Clinical Evidence for the Regression of Liver Fibrosis. *Journal of Hepatology,* 56**,** 1171-1180.

EUROPEANASSOCIATIONFORTHESTUDYOFTHELIVER 2012. EASL-EORTC Clinical Practice Guidelines: Management of Hepatocellular Carcinoma. *Journal of Hepatology,* 56**,** 908-943.

FAN, X. & RUDENSKY, A. 2016. Hallmarks of Tissue-Resident Lymphocytes. *Cell,* 164**,** 1198-1211.

FENG, Z., HU, W., TERESKY, A., HERNANDO, E., CORDON-CARDO, C. & LEVINE, A. 2007. Declining p53 Function in the Aging Process: A Possible Mechanism for the Increased Tumor Incidence in Older Populations. *Proceedings of the National Academy of Sciences,* 104**,** 16633-16638.

FERREIRA, L., MEISSNER, T., TILBURGS, T. & STROMINGER, J. 2017. HLA-G: At the Interface of Maternal-Fetal Tolerance. *Trends in Immunology,* 38**,** 272-286.

FISETTE, O., WINGBERMUHLE, S., TAMPE, R. & SCHAFER, L. 2016. Molecular Mechanism of Peptide Editing in Tapasin-MHC I Complex. *Scientific Reports* 6**,** 19085.

FREVERT, U., ENGELMANN, S., ZOUGBEDE, S., STANGE, J., NG, B., MATUSCHEWSKI, K., LIEBES, L. & YEE, H. 2005. Intravital Observation of *Plasmodium Berghei* Sporozoite Infection of the Liver. *PLOS Biology,* 3**,** e192.

FRICKEL, E., RIEK, R., JELESAROV, I., HELENIUS, A., WUTHRICH, K. & ELLGAARD, L. 2002. TROSY-NMR Reveals Interaction Between ERp57 and the Tip of the Calreticulin P-Domain. *Proceedings of the National Academy of Sciences,* 99**,** 1954-1959.

FUKUSATO, T., GERBER, M., THUNG, S., FERRONE, S. & SCHAFFNER, F. 1986. Expression of HLA Class I Antigens on Hepatocytes in Liver Disease. *American Journal of Pathology,* 123**,** 264-270.

GACZYNSKA, M., ROCK, K., SPIES, T. & GOLDBERG, A. 1994. Peptidase Activities of Proteasomes are Differentially Regulated by the Major Histocompatibility Complex-Encoded Genes for LMP2 and LMP7. *Proceedings of the National Academy of Sciences,* 91**,** 9213-9217.

GARBI, N., TAN, P., DIEHL, A., CHAMBERS, B., LJUNGGREN, H., MOMBURG, F. & HAMMERLING, G. 2000. Impaired Immune Responses and Altered Peptide Repertoire in Tapasin-Deficient Mice. *Nature Immunology,* 1**,** 234-238.

GARCIA-BELTRAN, W., HÖLZEMER, A., MARTRUS, G., CHUNG, A., PACHECO, Y., SIMONEAU, C., RUCEVIC, M., LAMOTHE-MOLINA, P., PERTEL, T., KIM, T., DUGAN, H., ALTER, G., DECHANET-MERVILLE, J., JOST, S., CARRINGTON, M. & ALTFELD, M. 2016. Open Conformers of HLA-F are High-Affinity Ligands of the Activating NK-Cell Receptor KIR3DS1. *Nature Immunology,* 17**,** 1067-1074.

GARRETT, T., SAPER, M., BJORKMAN, P., STROMINGER, J. & WILEY, D. 1989. Specificity Pockets for the Side Chains of Peptide Antigens in HLA-Aw68. *Nature,* 342**,** 692-696.

GASTEIGER, G., D'OSUALDO, A., SCHUBERT, D., WEBER, A., BRUSCIA, E. & HARTL, D. 2017. Cellular Innate Immunity: An Old Game with New Players. *Journal of Innate Immunity,* 9**,** 111-125.

GERAGHTY, D., WEI, X., ORR, H. & KOLLER, B. 1990. Human Leukocyte Antigen F (HLA-F). An Expressed HLA Gene Composed of a Class I Coding Sequence Linked to a Novel Transcribed Repetitive Element. *Journal of Experimental Medicine,* 171**,** 1-18.

GINES, P., QUINTERO, E., ARROYO, V., TERES, J., BRUGUERA, M., RIMOLA, A., CABALLERIA, J., RODES, J. & ROZMAN, C. 1987. Compensated Cirrhosis: Natural History and Prognostic Factors. *Hepatology,* 7**,** 122-128.

GLASSNER, A., EISENHARDT, M., KRAMER, B., KORNER, C., COENEN, M., SAUERBRUCH, T., SPENGLER, U. & NATTERMANN, J. 2012. NK Cells from HCV-Infected Patients Effectively Induce Apoptosis of Activated Primary Human Hepatic Stellate Cells in a TRAIL-, FasL- and NKG2D-Dependent Manner. *Laboratory Investigation* 92**,** 967-977.

GONZALEZ-REIMERS, E., BRAJIN-RODRIGUEZ, M., BATISTA-LOPEZ, N., SANTOLARIA-FERNANDEZ, F., MARTINEZ-RIERA, A. & ESSARDAS-DARYANANI, H. 1988. Hepatocyte and Nuclear Areas and Fatty Infiltration of the Liver in Chronic Alcoholic Liver Disease. *Drug and Alcohol Dependence,* 22**,** 195-203.

GOODRIDGE, J., LEE, N., BURIAN, A., PYO, C., TYKODI, S., WARREN, E., YEE, C., RIDDELL, S. & GERAGHTY, D. 2013. HLA-F and MHC Class I Open Conformers Cooperate in a MHC Class I Antigen Cross-Presentation Pathway. *Journal of Immunology,* 191**,** 1567-1577.

GORER, P. 1936. The Detection of Antigenic Differences in Mouse Erythrocytes by the Employment of Immune Sera. *The British Journal of Experimental Pathology,* 17**,** 42-50.

GREGORY, S., SAGNIMENI, A. & WING, E. 1996. Bacteria in the Bloodstream are Trapped in the Liver and Killed by Immigrating Neutrophils. *Journal of Immunology,* 157**,** 2514-2520.

GRIFFITH, J., SOKOL, C. & LUSTER, A. 2014. Chemokines and Chemokine Receptors: Positioning Cells for Host Defense and Immunity. *Annual Review of Immunology,* 32**,** 659-702.

GRUEN, J. & WEISSMAN, S. 2001. Human MHC Class III and IV Genes and Disease Associations. *Frontiers in Bioscience,* 6**,** D960-D972.

HAMID, M., WANG, R., YAO, X., FAN, P., LI, X., CHANG, X., FENG, Y., JONES, S., MALDONADO-PEREZ, D., WAUGH, C., VERRILL, C., SIMMONS, A., CERUNDOLO, V., MCMICHAEL, A., CONLON, C., WANG, X., PENG, Y. & DONG, T. 2019. Enriched HLA-E and CD94/NKG2A Interaction Limits Antitumor $CD8^+$ Tumor-Infiltrating T Lymphocyte Responses. *Cancer Immunology Research,* 7**,** 1293-1306.

HANAHAN, D. & WEINBERG, R. 2000. The Hallmarks of Cancer. *Cell,* 100**,** 57-70.

HANVESAKUL, R., SPENCER, N., COOK, M., GUNSON, B., HATHAWAY, M., BROWN, R., NIGHTINGALE, P., COCKWELL, P., HUBSCHER, S., ADAMS, D., MOSS, P. & BRIGGS, D. 2008. Donor HLA-C Genotype has a Profound Impact on the Clinical Outcome Following Liver Transplantation. *American Journal of Transplantation,* 8**,** 1931-1941.

HARLEY, C., FUTCHER, A. & GREIDER, C. 1990. Telomeres Shorten during Ageing of Human Fibroblasts. *Nature,* 345**,** 458-460.

HARRIS, H., COSTELLA, A., HARRIS, R. & MANDAL, S. 2020. *Hepatitis C in the UK 2020. Working to Eliminate Hepatitis C as a Major Public Health Threat* [Online]. https://assets.publishing.service.gov.uk/government/uploads/system/uploads/attachment_data/file/943154/HCV_in_the_UK_2020.pdf: Public Health England. [Accessed April 2021].

HATA, K., VAN-THIEL, D., HERBERMAN, R. & WHITESIDE, T. 1991. Natural Killer Activity of Human Liver-Derived Lymphocytes in Various Liver Diseases. *Hepatology,* 14**,** 495-503.

HAYFLICK, L. & MOORHEAD, P. 1961. The Serial Cultivation of Human Diploid Cell Strains. *Experimental Cell Research,* 25**,** 585-621.

HERMANN, C., STRITTMATTER, L., DEANE, J. & BOYLE, L. 2013. The Binding of TAPBPR and Tapasin to MHC Class I is Mutually Exclusive. *The Journal of Immunology,* 191**,** 5743-5750.

HERMANN, C., VAN-HATEREN, A., TRAUTWEIN, N., NEERINCX, A., DURIEZ, P., STEVANOVIC, S., TROWSDALE, J., DEANE, J., ELLIOTT, T. & BOYLE, L. 2015. TAPBPR Alters MHC Class I Peptide Presentation by Functioning as a Peptide Exchange Catalyst. *Elife,* 4**,** e09617.

HEWITT, E. 2003. The MHC Class I Antigen Presentation Pathway: Strategies for Viral Immune Evasion. *Immunology,* 110**,** 163-169.

HOARE, M., DAS, T. & ALEXANDER, G. 2010a. Ageing, Telomeres, Senescence and Liver Injury. *Journal of Hepatology,* 53**,** 950–961.

HOARE, M., GELSON, W., DAS, A., FLETCHER, J., DAVIES, S., CURRAN, M., VOWLER, S., MAINI, M., AKBAR, A. & ALEXANDER, G. 2010b. CD4+ T-Lymphocyte Telomere Length is Related to Fibrosis Stage, Clinical Outcome and Treatment Response in Chronic Hepatitis C Virus Infection. *Journal of Hepatology,* 53**,** 252-260.

HURKS, H., VALTER, M., WILSON, L., HILGERT, I., VAN-DEN-ELSEN, P. & JAGER, M. 2001. Uveal Melanoma: No Expression of HLA-G. *Investigative Opthalmology and Visual Science,* 42**,** 3081-3084.

IANNELLO, A., DEBBECHE, O., SAMARANI, S. & AHMAD, A. 2008. Antiviral NK Cell Responses in HIV Infection: I. NK Cell Receptor Genes as Determinants of HIV Resistance and Progression to AIDS. *Journal of Leukocyte Biology,* 84**,** 1-26.

IBRAHIM, E., ARACTINGI, S., ALLORY, Y., BORRINI, F., DUPUY, A., DUVILLARD, P., CAROSELLA, E., AVRIL, M. & PAUL, P. 2004. Analysis of HLA Antigen Expression in Benign and Malignant Melanocytic Lesions Reveals that Upregulation of HLA-G Expression Correlates with Malignant Transformation, High Inflammatory Infiltration and HLA-A1 Genotype. *International Journal of Cancer,* 108**,** 243-250.

ILCA, F., DREXHAGE, L., BREWIN, G., PEACOCK, S. & BOYLE, L. 2019. Distinct Polymorphisms in HLA Class I Molecules Govern Their Susceptibility to Peptide Editing by TAPBPR. *Cell Reports,* 29**,** 1621-1632.

ISHITANI, A., SAGESHIMA, N. & HATAKE, K. 2006. The Involvement of HLA-E and -F in Pregnancy. *Journal of Reproductive Immunology,* 69**,** 101-113.

ISHITANI, A., SAGESHIMA, N., LEE, N., DOROFEEVA, N., HATAKE, K., MARQUARDT, H. & GERAGHTY, D. 2003. Protein Expression and Peptide Binding Suggest Unique and Interacting Functional Roles for HLA E, F and G in Maternal-Placental Immune Recognition. *Journal of Immunology,* 171**,** 1376-1384.

JEONG, W. & GAO, B. 2008. Innate Immunity and Alcoholic Liver Fibrosis. *Journal of Gastroenterology and Hepatology,* 23**,** S112-S118.

JOHNHOPKINSMEDICINE. 2020. *Liver: Anatomy and Functions* [Online]. https://www.hopkinsmedicine.org/health/conditions-and-diseases/liver-anatomy-and-functions. [Accessed March 2021].

JOHNSON, D. & MOOK-KANAMORI, B. 2000. Dependence of Elevated Human Leukocyte Antigen Class I Molecule Expression on Increased Heavy Chain, Light Chain (Beta 2-Microglobulin), Transporter Associated with Antigen Processing, Tapasin, and Peptide. *Journal of Biological Chemistry,* 275**,** 16643-16649.

JONES, E., FUGGER, L., STROMINGER, J. & SIEBOLD, C. 2006. MHC Class II Proteins and Disease: A Structural Perspective. *Nature Reviews Immunology,* 6**,** 271-282.

JOOSTEN, S., SULLIVAN, L. & OTTENHOFF, T. 2016. Characteristics of HLA-E Restricted T-Cell Responses and Their Role in Infectious Diseases. *Journal of Immunology Research,* 2016**,** 2695396.

KANG, T., YEVSA, T., WOLLER, N., HOENICKE, L., WUESTEFELD, T., DAUCH, D., HOHMEYER, A., GEREKE, M., RUDALSKA, R., POTAPOVA, A., IKEN, M., VUCUR, M., WEISS, S., HEIKENWALDER, M., KHAN, S., GIL, J., BRUDER, D., MANNS, M., SCHIRMACHER, P., TACKE, F., OTT, M., LUEDDE, T., LONGERICH, T., KUBICKA, S. & ZENDER, L. 2011. Senescence Surveillance of Pre-Malignant Hepatocytes Limits Liver Cancer Development. *Nature,* 479**,** 547-551.

KARRE, K., LJUNGGREN, H., PIONTEK, G. & KIESSLING, R. 1986. Selective Rejection of H-2-Deficient Lymphoma Variants Suggests Alternative Immune Defence Strategy. *Nature,* 319**,** 675-678.

KATZ, H. 2006. Inhibition of Inflammatory Responses by Leukocyte Ig-Like Receptors. *Advances in Immunology,* 91**,** 251-272.

KESKINEN, P., RONNI, T., MATIKAINEN, S., LEHTONEN, A. & JULKUNEN, I. 1997. Regulation of HLA Class I and II Expression by Interferons and Influenza A Virus in Human Peripheral Blood Mononuclear Cells. *Immunology,* 91**,** 421-429.

KIKUCHI-MAKI, A., YUSA, S., CATINA, T. & CAMPBELL, K. 2003. KIR2DL4 is an IL-2-Regulated NK Cell Receptor that Exhibits Limited Expression in Humans but Triggers Strong IFN-Gamma Production. *Journal of Immunology,* 171**,** 3415-3425.

KIRKWOOD, T. & AUSTAD, S. 2000. Why Do We Age? *Nature,* 408**,** 233-238.

KLEIN, J. & SATO, A. 2000. The HLA System. A Review Article. 1st Part. *The New England Journal of Medicine,* 343**,** 702-709.

KNOLLE, P. 2016. Staying Local - Antigen Presentation in the Liver. *Current Opinion in Immunology,* 40**,** 36-42.

KOOPMAN, L., KOPCOW, H., RYBALOV, B., BOYSON, J., ORANGE, J., SCHATZ, F., MASCH, R., LOCKWOOD, C., SCHACHTER, A., PARK, P. & STROMINGER, J. 2003. Human Decidual Natural Killer Cells are a Unique NK Cell Subset with Immunomodulatory Potential. *Journal of Experimental Medicine,* 198**,** 1201-1212.

KOVATS, S., MAIN, E., LIBRACH, C., STUBBLEBINE, M., FISHER, S. & DEMARS, R. 1990. A Class I Antigen, HLA-G, Expressed in Human Trophoblasts. *Science,* 248**,** 220-223.

KRIZHANOVSKY, V., YON, M., DICKINS, R., HEARN, S., SIMON, J., MIETHING, C., YEE, H., ZENDER, L. & LOWE, S. 2008. Senescence of Activated Stellate Cells Limits Liver Fibrosis. *Cell,* 134**,** 657-667.

KUILMAN, T., MICHALOGLOU, C., VREDEVELD, L., DOUMA, S., VAN-DOORN, R., DESMET, C., AARDEN, L., MOOI, W. & PEEPER, D. 2008. Oncogene-Induced Senescence Relayed by an Interleukin-Dependent Inflammatory Network. *Cell,* 133**,** 1019-1031.

KUILMAN, T. & PEEPER, D. 2009. Senescence-Messaging Secretome: SMS-ing Cellular Stress. *Nature Reviews Cancer,* 9**,** 81-94.

LANGHANS, B., ALWAN, A., KRAMER, B., GLASSNER, A., LUTZ, P., STRASSBURG, C., NATTERMANN, J. & SPENGLER, U. 2015. Regulatory CD4+ T-Cells Modulate the Interaction Between NK Cells and Hepatic Stellate Cells by Acting on Either Cell Type. *Journal of Hepatology,* 62**,** 398-404.

LANIER, L. 1997. Natural Killer Cells: From No Receptors to Too Many. *Immunity,* 6**,** 371-378.

LAPTEVA, N., DURETT, A., SUN, J., ROLLINS, L., HUYE, L., FANG, J., DANDEKAR, V., MEI, Z., JACKSON, K., VERA, J., ANDO, J., NGO, M., COUSTAN-SMITH, E., CAMPANA, D., SZMANIA, S., GARG, T., MORENO-BOST, A., VANRHEE, F., GEE, A. & ROONEY, C. 2012. Large-Scale Ex *Vivo* Expansion and Characterization of Natural Killer Cells for Clinical Applications. *Cytotherapy,* 14**,** 1131-1143.

LASH, G., ROBSON, S. & BULMER, J. 2010. Review: Functional Role of Uterine Natural Killer (uNK) Cells in Human Early Pregnancy Decidua. *Placenta,* 31(s)**,** S87-S92.

LEE, A., FENSTER, B., ITO, H., TAKEDA, K., BAE, N., HIRAI, T., YU, Z., FERRANS, V., HOWARD, B. & FINKEL, T. 1999. Ras Proteins Induce Senescence by Altering the Intracellular Levels of Reactive Oxygen Species. *Journal of Biological Chemistry,* 274**,** 7936-7940.

LEE, N. & GERAGHTY, D. 2003. HLA-F Surface Expression on B Cell and Monocyte Cell Lines is Partially Independent from Tapasin and Completely Independent from TAP. *Journal of Immunology,* 171**,** 5264-5271.

LEE, N., GOODLETT, D., ISHITANI, A., MARQUARDT, H. & GERAGHTY, D. 1998. HLA-E Surface Expression Depends on Binding of TAP-Dependent Peptides Derived from Certain HLA Class I Signal Sequences. *Journal of Immunology,* 160**,** 4951-4960.

LEHNER, P., SURMAN, M. & CRESSWELL, P. 1998. Soluble Tapasin Restores MHC Class I Expression and Function in the Tapasin-Negative Cell Line .220. *Immunity,* 8**,** 221-231.

LEPIN, E., BASTIN, J., ALLAN, D., RONCADOR, G., BRAUD, V., MASON, D., VAN-DER-MERWE, P., MCMICHAEL, A., BELL, J., POWIS, S. & O'CALLAGHAN, C. 2000. Functional Characterization of HLA-F and Binding of HLA-F Tetramers to ILT2 and ILT4 Receptors. *European Journal of Immunology,* 30**,** 3552-3561.

LIN, A. & YAN, W. 2018. Heterogeneity of HLA-G Expression in Cancers: Facing the Challenges. *Frontiers in Immunology,* 9**,** 2164.

LIN, Z., KUROKI, K., KUSE, N., SUN, X., AKAHOSHI, T., QI, Y., CHIKATA, T., NARUTO, T., KOYANAGI, M., MURAKOSHI, H., GATANAGA, H., OKA, S., CARRINGTON, M., MAENAKA, K. & TAKIGUCHI, M. 2016. HIV-1 Control by NK Cells via Reduced Interaction Between KIR2DL2 and HLA-C*12:02/C*14:03. *Cell Reports,* 17**,** 2210-2220.

LITTERA, R., CHESSA, L., ONALI, S., FIGORILLI, F., LAI, S., SECCI, L., NASA, G. L., CAOCCI, G., ARRAS, M., MELIS, M., CAPPELLINI, S., BALESTRIERI, C., SERRA, G., CONTI, M., ZOLFINO, T., CASALE, M., CASU, S., PASETTO, M., BARCA, L., SALUSTRO, C., MATTA, L., SCIOSCIA, R., ZAMBONI, F., FAA, G., ORRU, S. & CARCASSI, C. 2016. Exploring the Role of Killer Cell Immunoglobulin-Like Receptors and Their HLA Class I Ligands in Autoimmune Hepatitis. *PLoS One,* 11**,** e0146086.

LIU, P., CHEN, L. & ZHANG, H. 2018. Natural Killer Cells in Liver Disease and Hepatocellular Carcinoma and the NK Cell-Based Immunotherapy. *Journal of Immunology Research,* 2018**,** 1206737.

LOKE, Y., KING, A., BURROWS, T., GARDNER, L., BOWEN, M., HIBY, S., HOWLETT, S., HOLMES, N. & JACOBS, D. 1997. Evaluation of Trophoblast HLA-G Antigen with a Specific Monoclonal Antibody. *Tissue Antigens,* 50**,** 135-146.

LOPEZ-BOTET, M., VILCHES, C., REDONDO-PACHON, D., MUNTASELL, A., PUPULEKU, A., YELAMOS, J., PASCUAL, J. & CRESPO, M. 2017. Dual Role of Natural Killer Cells on Graft Rejection and Control of Cytomegalovirus Infection in Renal Transplantation. *Frontiers in Immunology,* 8**,** 166.

LOPEZ-VERGES, S., MILUSH, J., PANDEY, S., YORK, V., ARAKAWA-HOYT, J., PIRCHER, H., NORRIS, P., NIXON, D. & LANIER, L. 2010. CD57 Defines a Functionally Distinct Population of Mature NK Cells in the Human $CD56^{dim}CD16^{+}$ NK-Cell Subset. *Blood,* 116**,** 3865-3874.

LOTZE, M. & TRACEY, K. 2005. High-Mobility Group Box 1 Protein (HMGB1): Nuclear Weapon in the Immune Arsenal. *Nature Reviews Immunology,* 5**,** 331-342.

LOZANO, J., GONZALEZ, R., KINDELAN, J., ROUAS-FREISS, N., CABALLOS, R., DAUSSET, J., CAROSELLA, E. & PENA, J. 2002. Monocytes and T Lymphocytes in HIV-1-Positive Patients Express HLA-G Molecule. *AIDS,* 16**,** 347-351.

LUCKHEERAM, R., ZHOU, R., VERMA, A. & XIA, B. 2012. $CD4^{+}$ T cells: Differentiation and Functions. *Clinical and Developmental Immunology,* 2012**,** 925135.

MALATO, Y., NAQVI, S., SCHURMANN, N., NG, R., WANG, B., ZAPE, J., KAY, M., GRIMM, D. & WILLENBRING, H. 2011. Fate Tracing of Mature Hepatocytes in Mouse Liver Homeostasis and Regeneration. *Journal of Clinical Investigation,* 121**,** 4850-4860.

MANGALAM, A., TENEJA, V. & DAVID, C. 2013. HLA Class II Molecules Influence Susceptibility vs Protection in Inflammatory Diseases by Determining the Cytokine Profile. *The Journal of Immunology,* 190**,** 513-519.

MANNA, S., MCCARTHY, C. & MCCARTHY, F. 2019. Placental Ageing in Adverse Pregnancy Outcomes: Telomere Shortening, Cell Senescence, and Mitochondrial Dysfunction. *Oxidative Medicine and Cell Longevity,* 2019**,** 3095383.

MARCOTTE, R., LACELLE, C. & WANG, E. 2004. Senescent Fibroblasts Resist Apoptosis by Downregulating Caspase-3. *Mechanisms of Ageing and Development,* 125**,** 777-783.

MARQUARDT, N., BEZIAT, V., NYSTROM, S., HENGST, J., IVARSSON, M., KEKALAINEN, E., JOHANSSON, H., MJOSBERG, J., WESTGREN, M., LANKISCH, T., WEDEMEYER, H., ELLIS, E., LJUNGGREN, H., MICHAELSSON, J. & BJORKSTROM, N. 2015. Cutting Edge: Identification and Characterisation of Human Intrahepatic CD49a+ NK Cells. *Journal of Immunology,* 194**,** 2467-2471.

MARSHALL, A., RUSHBROOK, S., DAVIES, S., MORRIS, L., SCOTT, I., VOWLER, S., COLEMAN, N. & ALEXANDER, G. 2005. Relation Between Hepatocyte G1 Arrest, Impaired Hepatic Regeneration and Fibrosis in Chronic Hepatitis C Virus Infection. *Gastroenterology,* 128**,** 33-42.

MATTEONI, C., YOUNOSSI, Z., GRAMLICH, T., BOPARAI, N., LIU, Y. & MCCULLOUGH, A. 1999. Nonalcoholic Fatty Liver Disease: A Spectrum of Clinical and Pathological Severity. *Gastroenterology,* 116**,** 1413-1419.

MCMASTER, M., ZHOU, Y., SHORTER, S., KAPASI, K., GERAGHTY, D., LIM, K. & FISHER, S. 1998. HLA-G Isoforms Produced by Placental Cytotrophoblasts and Found in Amniotic Fluid are Due to Unusual Glycosylation. *Journal of Immunology,* 160**,** 5922-5928.

MEIJNIKMAN, A., HERREMA, H., SCHEITHAUER, T., KROON, J., NIEUWDORP, M. & GROEN, A. 2021. Evidence Causality of Cellular Senescence in Non-Alcoholic Fatty Liver Disease. *Journal of Hepatology Reports,* 3**,** 100301.

MELA, M., SMEETON, W., DAVIES, S., MIRANDA, E., SCARPINI, C., COLEMAN, N. & ALEXANDER, G. 2020. The Alpha-1 Antitripsin Polymer Load Correlates With Hepatocyte Senescence, Fibrosis Stage and Liver-Related Mortality. *Chronic Obstructive Pulmonary Diseases,* 7**,** 151-162.

MENIER, C., SAEZ, B., HOREJSI, V., MARTINOZZI, S., KRAWICE-RADANNE, I., BRUEL, S., LE-DANFF, C., REBOUL, M., HILGERT, I., RABREAU, M., LARRAD, M., PLA, M., CAROSELLA, E. & ROUAS-FREISS, N. 2003. Characterization of Monoclonal Antibodies Recognizing HLA-G or HLA-E: New Tools to Analyze the Expression of Non-Classical HLA Class I Molecules. *Human Immunology,* 64**,** 315-326.

MEYER, T., VAN-ENDERT, P., UEBEL, S., EHRING, B. & TAMPE, R. 1994. Functional Expression and Purification of the ABC Transporter Complex Associated with Antigen Processing (TAP) in Insect Cells. *FEBS Letters,* 351**,** 443-447.

MICHAELSSON, J., TEIXEIRA-DE-MATOS, C., ACHOUR, A., LANIER, L., KARRE, K. & SODERSTROM, K. 2002. A Signal Peptide Derived from Hsp60 Binds HLA-E and Interferes with CD94/NKG2A Recognition. *Journal of Experimental Medicine,* 196**,** 1403-1414.

MICHALOGLOU, C., VREDEVELD, L., SOENGAS, M., DENOYELLE, C., KUILMAN, T., VAN-DER-HORST, C., MAJOOR, D., SHAY, J., MOOI, W. & PEEPER, D. 2005. $BRAF^{E600}$-Associated Senescence-like Cell Cycle Arrest of Human Naevi. *Nature,* 436**,** 720-724.

MIKULAK, J., BRUNI, E., ORIOLO, F., DI-VITO, C. & MAVILIO, D. 2019. Hepatic Natural Killer Cells: Organ-Specific Sentinels of Liver Immune Homeostasis and Physiopathology. *Frontiers in Immunology,* 10**,** 946.

MIN, B., CHOI, H., HER, J., JUNG, M., KIM, H., JUNG, M., LEE, E., CHO, S., HWANG, Y. & SHIN, E. 2018. Optimization of Large-Scale Expansion and Cryopreservation of Human Natural Killer Cells for Anti-Tumor Therapy *Immune Network,* 18**,** e31.

MINDANTHOLOGY. 2012. *Cell Cycle Regulators Related to the Glucocorticoid Receptor* [Online]. https://mindanthology.com/2012/01/21/cell-cycle-regulators-related-to-the-glucocorticoid-receptor/. [Accessed April 2021].

MOFFETT-KING, A. 2002. Natural Killer Cells and Pregnancy. *Nature Reviews Immunology,* 2**,** 656-663.

MORALES, P., PACE, J., PLATT, J., LANGAT, D. & HUNT, J. 2007. Synthesis of β_2-Microglobulin-Free, Disulphide-Linked HLA-G5 Homodimers in Human Placental Villous Cytotrophoblast Cells. *Immunology,* 122**,** 179-188.

MORANDI, F., AIROLDI, I. & PISTOIA, V. 2014. IL-27 Driven Upregulation of Surface HLA-E Expression on Monocytes Inhibits IFN-γ Release by Autologous NK Cells. *Journal of Immunology Research,* 2014**,** 938561.

MOROSO, V., VAN-CRANENBROEK, B., MANCHAM, S., SIDERAS, K., BOOR, P., BIERMANN, K., DE-VOGEL, L., DE-KNEGT, R., VAN-DER-EIJK, A., VAN-DER-LAAN, L., DE-JONGE, J., METSELAAR, H., JOOSTEN, I. & KWEKKEBOOM, J. 2015. Prominent HLA-G Expression in Liver Disease But Not After Liver Transplantation. *Transplantation,* 99**,** 2514-2522.

MOROZOV, G., ZHAO, H., MAGE, M., BOYD, L., JIANG, J., DOLAN, M., VENNA, R., NORCROSS, M., MCMURTREY, C., HILDEBRAND, W., SCHUCK, P., NATARAJAN, K. & MARGULIES, D. 2016. Interaction of TAPBPR, a Tapasin Homolog, with MHC-I Molecules Promotes Peptide Editing. *Proceedings of the National Academy of Sciences,* 113**,** e1006-e1015.

MOYA-QUILES, M., MURO, M., TORIO, A., SANCHEZ-BUENO, F., MIRAS, M., MARIN, L., GARCIA-ALONSO, A., PARRILLA, P., DAUSSET, J. & ALVAREZ-LOPEZ, M. 2003. Human Leukocyte Antigen-C in Short- and Long-Term Liver Graft Acceptance. *Liver Transplantation,* 9**,** 218-227.

NAKAYA, R., KOHGO, Y., MOGI, Y., NAKAJIMA, M., KATO, J. & NIITSU, Y. 1994. Regulation of Asialoglycoprotein Receptor Synthesis by Inflammation-Related Cytokines in HepG2 Cells. *Journal of Gastroenterology,* 29**,** 24-30.

NARITA, M., NÜNEZ, S., HEARD, E., NARITA, M., LIN, A., HEARN, S., SPECTOR, D., HANNON, G. & LOWE, S. 2003. Rb-Mediated Heterochromatin Formation and Silencing of E_2F Target Genes during Cellular Senescence. *Cell* 113**,** 703-716.

NATTERMANN, J., NISCHALKE, H., HOFMEISTER, V., AHLENSTIEL, G., ZIMMERMANN, H., LEIFELD, L., WEISS, E., SAUERBRUCH, T. & SPENGLER, U. 2005. The HLA-A2 Restricted T-Cell Epitope HCV

Core 35-44 Stabilizes HLA-E Expression and Inhibits Cytolysis Mediated by Natural Killer Cells. *American Journal of Pathology,* 166**,** 443-453.

NEERINCX, A., HERMANN, C., ANTROBUS, R., VAN-HATEREN, A., CAO, H., TRAUTWEIN, N., STEVANOVIC, S., ELLIOTT, T., DEANE, J. & BOYLE, L. 2017. TAPBPR Bridges UDP-Glucose: Glycoprotein Glucosyltransferase 1 onto MHC Class I to Provide Quality Control in the Antigen Presentation Pathway. *eLife,* 6**,** e23049.

NELSON, G., WORDSWORTH, J., WANG, C., JURK, D., LAWLESS, C., MARTIN-RUIZ, C. & VON-ZGLINICKI, T. 2012. A Senescent Cell Bystander Effect: Senescence-Induced Senescence. *Aging Cell,* 11**,** 345-349.

NESMIYANOV, P. 2020. *Antigen Processing and Presentation* [Online]. https://www.immunology.org/public-information/bitesized-immunology/systems-and-processes/antigen-processing-and-presentation: British Society for Immunology. [Accessed March 2021].

NEUROENDOCRINETUMORRESEARCHFOUNDATION. 2020. *Interventional Radiology as a Treatment for Neuroendocrine Tumors* [Online]. https://netrf.org/for-patients/nets-info/net-treatment/interventional-radiology/: NeuroendocrineTumorResearchFoundation. [Accessed March 2021].

NHS24. 2020. *Liver Disease* [Online]. https://www.nhsinform.scot/illnesses-and-conditions/stomach-liver-and-gastrointestinal-tract/liver-disease: NHS. [Accessed March 2021].

NORRIS, S., COLLINS, C., DOHERTY, D., SMITH, F., MCENTEE, G., TRAYNOR, O., NOLAN, N., HEGARTY, J. & O'FARRELLY, C. 1998. Resident Human Hepatic Lymphocytes are Phenotypically Different from Circulating Lymphocytes. *Journal of Hepatology,* 28**,** 84-90.

OBARA, H., NAGASAKI, K., HSIEH, C., OGURA, Y., ESQUIVEL, C., MARTINEZ, O. & KRAMS, S. 2005. IFN-Gamma, Produced by NK Cells that Infiltrate Liver Allografts Early After Transplantation, Links the Innate and Adaptive Immune Responses. *American Journal of Transplantation,* 5**,** 2094-2103.

ONG, S., TENG, K., NEWELL, E., CHEN, H., CHEN, J., LOY, T., YEO, T., FINK, K. & WONG, S. 2019. A Novel, Five-Marker Alternative to CD16-CD14 Gating to Identify the Three Human Monocyte Subsets. *Frontiers in Immunology,* 10**,** 1761.

ONNO, M., PANGAULT, C., FRIEC, G. L., GUILLOUX, V., ANDRE, P. & FAUCHET, R. 2000. Modulation of HLA-G Antigens Expression by Human Cytomegalovirus: Specific Induction in Activated Macrophages Harboring Human Cytomegalovirus Infection. *Journal of Immunology,* 164**,** 6426-6434.

ORTMANN, B., COPEMAN, J., LEHNER, P., SADASIVAN, B., HERBERG, J., GRANDEA, A., RIDDELL, S., TAMPÉ, R., SPIES, T., TROWSDALE, J. & CRESSWELL, P. 1997. A Critical Role for Tapasin in the Assembly and Function of Multimeric MHC Class I-TAP Complexes. *Science,* 277**,** 1306-1309.

PALMISANO, G., CONTARDI, E., MORABITO, A., GARGAGLIONE, V., FERRARA, G. & PISTILLO, M. 2005. HLA-E Surface Expression is Independent of the Availability of HLA Class I Signal Sequence-Derived Peptides in Human Tumor Cell Lines. *Human Immunology,* 66**,** 1-12.

PARHAM, P., BARNSTABLE, C. & BODMER, W. 1979. Use of a Monoclonal Antibody (W6/32) in Structural Studies of HLA-A, B, C Antigens. *Journal of Immunology,* 123**,** 342-349.

PATERSON, A., SCIOT, R., KEW, M., CALLEA, F., DUSHEIKO, G. & DESMET, V. 1988. HLA Expression in Human Hepatocellular Carcinoma. *British Journal of Cancer,* 57**,** 369-373.

PAUL, P., CABESTRE, F., LE-GAL, F., KHALIL-DAHER, I., LE-DANFF, C., SCHMID, M., MERCIER, S., AVRIL, M., DAUSSET, J., GUILLET, J. & CAROSELLA, E. 1999. Heterogeneity of HLA-G Gene Transcription in Malignant Melanoma Biopsies. *Cancer Research,* 59**,** 1954-1960.

PELLICORO, A., RAMACHANDRAN, P., IREDALE, J. & FALLOWFIELD, J. 2014. Liver Fibrosis and Repair: Immune Regulation of Wound Healing in a Solid Organ. *Nature Reviews Immunology,* 14**,** 181-194.

PENG, H. & SUN, R. 2017. Liver-Resident NK Cells and their Potential Functions. *Cellular and Molecular Immunology,* 14**,** 890-894.

PEPPA, D., GILL, U., REYNOLDS, G., EASOM, N., PALLETT, L., SCHURICH, A., MICCO, L., NEBBIA, G., SINGH, H., ADAMS, D., KENNEDY, P. & MAINI, M. 2013. Up-Regulation of a Death Receptor Renders Antiviral T Cells Susceptible to NK Cell-Mediated Deletion. *The Journal of Experimental Medicine,* 210**,** 99-114.

PEPPA, D., MICCO, L., JAVAID, A., KENNEDY, P., SCHURICH, A., DUNN, C., PALLANT, C., ELLIS, G., KHANNA, P., DUSHEIKO, G., GILSON, R. & MAINI, M. 2010. Blockade of Immunosuppressive Cytokines Restores NK Cell Antiviral Function in Chronic Hepatitis B Virus Infection. *PLOS Pathology,* 6**,** e1001227.

PEREIRA, B., DEVINE, O., VUKMANOVIC-STEJIC, M., CHAMBERS, E., SUBRAMANIAN, P., PATEL, N., VIRASAMI, A., SEBIRE, N., KINSLER, V., VALDOVINOS, A., LESAUX, C., PASSOS, J., ANTONIOU, A., RUSTIN, M., CAMPISI, J. & AKBAR, A. 2019. Senescent Cells Evade Immune Clearance via HLA-E-Mediated NK and CD8+ T Cell Inhibition. *Nature Communications* 10**,** 2387.

PERSSON, G., JORGENSEN, N., NILSSON, L., HEIDAM, L., ANDERSEN, J. & HVIID, T. 2020. A Role for both HLA-F and HLA-G in Reproduction and during Pregnancy? *Human Immunology,* 81**,** 127-133.

POISSON, J., LEMOINNE, S., BOULANGER, C., DURAND, F., MOREAU, R., VALLA, D. & RAUTOU, P. 2017. Liver Sinusoidal Endothelial Cells: Physiology and Role in Liver Diseases. *Journal of Hepatology,* 66**,** 212-227.

PROTZER, U., MAINI, M. & KNOLLE, P. 2012. Living in the Liver: Hepatic Infections. *Nature Reviews Immunology,* 12**,** 201-213.

PROTZER, U. & SCHALLER, H. 2000. Immune Escape by Hepatitis B Viruses. *Virus Genes,* 21**,** 27-37.

PUCHE, J., SAIMAN, Y. & FRIEDMAN, S. 2013. Hepatic Stellate Cells and Liver Fibrosis. *Comprehensive Physiology* 3**,** 1473-1492.

RACANELLI, V. & REHERMANN, B. 2006. The Liver as an Immunological Organ. *Hepatology,* 43**,** S54-S62.

RAHBARI, R., SHEAHAN, T., MODES, V., COLLIER, P., MACFARLANE, C. & BADGE, R. 2009. A Novel L1 Retrotransposon Marker for HeLa Cell Line Identification. *Biotechniques,* 46**,** 277-284.

RAHMAN, A. & ALOMAN, C. 2013. Dendritic Cells and Liver Fibrosis. *Biochimica et Biophysica Acta,* 1832**,** 998-1004.

RAJAGOPALAN, S. 2014. HLA-G-Mediated NK Cell Senescence Promotes Vascular Remodeling: Implications for Reproduction. *Cellular and Molecular Immunology* 11**,** 460-466.

RAJAGOPALAN, S. & LONG, E. 2005. Understanding how Combinations of HLA and KIR Genes Influence Disease. *Journal of Experimental Medicine,* 201**,** 1025-1029.

RAJAGOPALAN, S. & LONG, E. 2012. Cellular Senescence Induced by CD158d Reprograms Natural Killer Cells to Promote Vascular Remodeling. *Proceedings of the National Academy of Sciences,* 109**,** 20596-20601.

REIMERS, M., ENGELS, C., PUTTER, H., MORREAU, H., LIEFERS, G., VAN-DE-VELDE, C. & KUPPEN, P. 2014. Prognostic Value of HLA Class I, HLA-E, HLA-G and Tregs in Rectal Cancer: A Retrospective Cohort Study. *BMC Cancer,* 14**,** 486.

RITEAU, B., MOREAU, P., MENIER, C., KHALIL-DAHER, L., KHOSROTEHRANI, K., BRAS-GONCALVES, R., PAUL, P., DAUSSET, J., ROUAS-FREISS, N. & CAROSELLA, E. 2001a. Characterization of HLA-G1, -G2, -G3, and -G4 Isoforms Transfected in a Human Melanoma Cell Line. *Transplant Proceedings,* 33**,** 2360-2364.

RITEAU, B., ROUAS-FREISS, N., MENIER, C., PAUL, P., DAUSSET, J. & CAROSELLA, E. 2001b. HLA-G2, -G3, and -G4 Isoforms Expressed as Nonmature Cell Surface Glycoproteins Inhibit NK and Antigen-Specific CTL Cytolysis. *Journal of Immunology,* 166**,** 5018-5026.

ROBINSON, M., HARMON, C. & O'FARRELLY, C. 2016. Liver Immunology and its Role in Inflammation and Homeostasis. *Cellular and Molecular Immunology,* 13**,** 267-276.

ROCK, K. & GOLDBERG, A. 1999. Degradation of Cell Proteins and the Generation of MHC Class I-Presented Peptides. *Annual Review of Immunology,* 17**,** 739-779.

ROSALES, C. 2018. Neutrophil: A Cell with Many Roles in Inflammation or Several Cell Types? *Frontiers in Physiology,* 9**,** 113.

ROSENBERG, E., HERBERMAN, R., LEVINE, P., HALTERMAN, R., MCCOY, J. & WUNDERLICH, J. 1972. Lymphocyte Cytotoxicity Reactions to Leukaemia-Associated Antigens in Identical Twins. *International Journal of Cancer,* 9**,** 648-658.

SADASIVAN, B., LEHNER, P., ORTMANN, B., SPIES, T. & CRESSWELL, P. 1996. Roles for Calreticulin and a Novel Glycoprotein, Tapasin, in the Interaction of MHC Class I Molecules with TAP. *Immunity* 5**,** 103-114.

SCHMUCKER, D. & WANG, R. 1980. Effects of Animal Age and Phenobarbital on Rat Liver Glucose-6-Phosphatase Activity. *Experimental Gerontology,* 15**,** 7-13.

SCHNELL, S., STAINES, W. & WESSENDORF, M. 1999. Reduction of Lipofuscin-like Autofluorescence in Fluorescently Labeled Tissue. *Journal of Histochemistry and Cytochemistry,* 47**,** 719-730.

SCHUPPAN, D. & AFDHAL, N. 2008. Liver Cirrhosis *Lancet,* 371**,** 838-851.

SCHWEIZER, J., BOWDEN, P., COULOMBE, P., LANGBEIN, L., LANE, E., MAGIN, T., MALTAIS, L., OMARY, M., PARRY, D., ROGERS, M. & WRIGHT, M. 2006. New Consensus Nomenclature for Mammalian Keratins *Journal of Cell Biology,* 174**,** 169-174.

SEICH-AL-BASATENA, N., MACNAMARA, A., VINE, A., THIO, C., ASTEMBORSKI, J., USUKU, K., OSAME, M., KIRK, G., DONFIELD, S., GOEDERT, J., BANGHAM, C., CARRINGTON, M., KHAKOO, S. & ASQUITH, B. 2011. KIR2DL2 Enhances Protective and Detrimental HLA Class I-Mediated Immunity in Chronic Viral Infection. *PLOS Pathology,* 7**,** e1002270.

SEITZ, C., UCHANSKA-ZIEGLER, B., ZANK, A. & ZIEGLER, A. 1998. The Monoclonal Antibody HCA2 Recognises a Broadly Shared Epitope on Selected Classical as well as Several Non-Classical HLA Class I Molecules. *Molecular Immunology,* 35**,** 819-827.

SERWOLD, T., GONZALEZ, F., KIM, J., JACOB, R. & SHASTRI, N. 2002. ERAAP Customizes Peptides for MHC Class I Molecules in the Endoplasmic Reticulum. *Nature,* 419**,** 480-483.

SETINI, A., BERETTA, A., DE-SANTIS, C., MENEVERI, R., MARTAYAN, A., MAZZILLI, M., APPELLA, E., SICCARDI, A., NATALI, P. & GIACOMINI, P. 1996. Distinctive Features of the Alpha 1-Domain Alpha Helix of HLA-C Heavy Chains Free of Beta 2-Microglobulin. *Human Immunology,* 46**,** 69-81.

SHAY, J. & WRIGHT, W. 2007. Hallmarks of Telomeres in Ageing Research. *The Journal of Pathology,* 211**,** 114-123.

SHELTON, D., CHANG, E., WHITTIER, P., CHOI, D. & FUNK, W. 1999. Microarray Analysis of Replicative Senescence. *Current Biology,* 9**,** 939-945.

SHIMIZU, Y., GERAGHTY, D., KOLLER, B., ORR, H. & DEMARS, R. 1988. Transfer and Expression of Three Cloned Human Non-HLA-A, -B, -C Class I Major Histocompatibility Complex Genes in Mutant Lymphoblastoid Cells. *Proceedings of the National Academy of Sciences,* 85**,** 277-231.

SINHA, S., BOYDEN, A., ITANI, F., CRAWFORD, M. & KARANDIKAR, N. 2015. CD8+ T-Cells as Immune Regulators of Multiple Sclerosis. *Frontiers in Immunology,* 6**,** 619.

SOUTO, F., CRISPIM, J., FERREIRA, S., DA-SILVA, A., BASSI, C., SOARES, C., ZUCOLOTO, S., ROUAS-FREISS, N., MOREAU, P., MARTINELLI, A. & DONADI, E. 2011. Liver HLA-G Expression is Associated with Multiple Clinical and Histopathological Forms of Chronic Hepatitis B Virus Infection. *Journal of Viral Hepatitis,* 18**,** 102-105.

SPIES, T., BRESNAHAN, M., BAHRAM, S., ARNOLD, D., BLANCK, G., MELLINS, E., PIOUS, D. & DEMARS, R. 1990. A Gene in the Human Major Histocompatibility Complex Class II Region Controlling the Class I Antigen Presentation Pathway. *Nature,* 348**,** 744-747.

SPIESS, M. 1990. The Asialoglycoprotein Receptor: A Model for Endocytic Transport Receptors. *Biochemistry,* 29**,** 10009-10018.

STAM, N., SPITS, H. & PLOEGH, H. 1986. Monoclonal Antibodies Raised Against Denatured HLA-B Locus Heavy Chains Permit Biochemical Characterization of Certain HLA-C Locus Products. *Journal of Immunology,* 137**,** 2299-2306.

STEIN, G., DRULLINGER, L., ROBETORYE, R., PEREIRA-SMITH, O. & SMITH, J. 1991. Senescent Cells Fail to Express cdc2, cycA, and cycB in Response to Mitogen Stimulation. *Proceedings of the National Academy of Sciences,* 88**,** 11012-11016.

STEIN, G., DRULLINGER, L., SOULARD, A. & DULIC, V. 1999. Differential Roles for Cyclin-Dependent Kinase Inhibitors p21 and p16 in the Mecanisms of Senescence and Differentiation in Human Fibroblasts. *Molecular Cell Biology,* 19**,** 2109-2017.

SULTANA, Z., MAITI, L., AITKEN, J., MORRIS, J., DEDMAN, L. & SMITH, R. 2017. Oxidative Stress, Placental Ageing-Related Pathologies and Adverse Pregnancy Outcomes. *American Journal of Reproductive Immunology,* 77**,** e12653.

TACHTATZIS, P., MARSHALL, A., ARVINTHAN, A., VERMA, S., PENRHYN-LOWE, S., MELA, M., SCARPINI, C., DAVIES, S., COLEMAN, N. & ALEXANDER, G. 2015. Chronic Hepatitis B Virus Infection: The Relation Between Hepatitis B Antigen Expression, Telomere Length, Senescence, Inflammation and Fibrosis. *PLoS One,* 10**,** e0127511.

TAN, P., KROPSHOFER, H., MANDELBOIM, O., BULBUC, N., HÄMMERLING, G. & MOMBURG, F. 2002. Recruitment of MHC Class I Molecules by Tapasin into the Transporter Associated with Antigen Processing-Associated Complex is Essential for Optimal Peptide Loading. *Journal of Immunology,* 168**,** 1950 - 1960.

TANAKA, K. & KASAHARA, M. 1998. The MHC Class I Ligand-Generating System: Roles of Immunoproteosomes and the Interferon-Gamma-Inducible Proteasome Activator PA28. *Immunology Review,* 163**,** 161-176.

TANG, L., PENG, H., ZHOU, J., CHEN, Y., WEI, H., SUN, R., YOKOYAMA, W. & TIAN, Z. 2016. Differential Phenotypic and Functional Properties of Liver-Resident NK Cells and Mucosal ILC1s. *Journal of Autoimmunity,* 67**,** 29-35.

TENG, M., STEPHENS, R., DU-PASQUIER, L., FREEMAN, T., LINDQUIST, J. & TROWSDALE, J. 2002. A Human TAPBP (TAPASIN)-Related Gene, TAPBP-R. *European Journal of Immunology,* 32**,** 1059-1068.

THOMSON, A. & KNOLLE, P. 2010. Antigen-Presenting Cell Function in the Tolerogenic Liver Environment. *Nature Review Immunology,* 10**,** 753-766.

TRAK-SMAYRA, V., CONTRERAS, J., DONDERO, F., DURAND, F., DUBOIS, S., SOMMACALE, D., MARCELLIN, P., BELGHITI, J., DEGOTT, C. & PARADIS, V. 2004. Role of Replicative Senescence in the Progression of Fibrosis in Hepatitis C Virus (HCV) Recurrence after Liver Transplantation. *Transplantation,* 77**,** 1755-1760.

TRIPATHI, P., NAIK, S. & AGRAWAL, S. 2007. Role of HLA-G, HLA-E and KIR2DL4 in Pregnancy. *International Journal of Human Genetics,* 7**,** 219-233.

TROWSDALE, J. & MOFFETT, A. 2008. NK Receptor Interactions with MHC Class I Molecules in Pregnancy. *Seminars in Immunology,* 20**,** 317-320.

TSUCHIDA, T. & FRIEDMAN, S. 2017. Mechanisms of Hepatic Stellate Cell Activation *Nature Reviews Gastroenterology and Hepatology,* 14**,** 397-411.

TSUKAHARA, T., KAWAGUCHI, S., TORIGOE, T., ASANUMA, H., NAKAZAWA, E., SHIMOZAWA, K., NABETA, Y., KIMURA, S., KAYA, M., NAGOYA, S., WADA, T., YAMASHITA, T. & SATO, N. 2006. Prognostic Significance of HLA Class I Expression in Osteosarcoma Defined by Anti-Pan HLA Class I Monoclonal Antibody, EMR8-5. *Cancer Science,* 97**,** 1374-1380.

TZENG, C., ADAMS, E., GUMPERZ, J., PERCIVAL, L., WELLS, R., PARHAM, P. & BARBER, L. 1996. Peptides Bound Endogenously by HLA-Cw*0304 Expressed in LCL 721.221 Cells Include a Peptide Derived From HLA-E. *Tissue Antigens,* 48**,** 325-328.

VALDES, A., ANDREW, T., GARDNER, J., KIMURA, M., OELSNER, E., CHERKAS, L., AVIV, A. & SPECTOR, T. 2005. Obesity, Cigarette Smoking, and Telomere Length in Women. *Lancet,* 366**,** 662-664.

VAN-DEURSEN, J. 2014. The Role of Senescent Cells in Ageing. *Nature,* 509**,** 439-446.

VAN-HATEREN, A., JAMES, E., BAILEY, A., PHILLIPS, A., DALCHAU, N. & ELLIOTT, T. 2010. The Cell Biology of Major Histocompatibility Complex Class I Assembly: Towards a Molecular Understanding. *Tissue Antigens,* 76**,** 259-275.

VASSILAKOS, A., COHEN-DOYLE, M., PETERSON, P., JACKSON, M. & WILLIAMS, D. 1996. The Molecular Chaperone Calnexin Facilitates Folding and Assembly of Class I Histocompatibility Molecules. *The EMBO Journal,* 15**,** 1495-1506.

VIEGAS, M., MARTINS, T., SECO, F. & DO-CARMO, A. 2007. An Improved and Cost-Effective Methodology for the Reduction of Autofluorescence in Direct Immunofluorescence Studies on Formalin-Fixed Paraffin-Embedded Tissues. *European Journal of Histochemistry,* 51**,** 59-66.

VIETZEN, H., ZOUFALY, A., TRAUGOTT, M., ABERLE, J., ABERLE, S. & PUCHHAMMER-STÖCKL, E. 2021. Deletion of the NKG2C Receptor Encoding KLRC2 Gene and HLA-E Variants are Risk Factors for Severe COVID-19. *Genetics in Medicine,* 23**,** 963-967.

VON-ZGLINICKI, T., SARETZKI, G., DÖCKE, W. & LOTZE, C. 1995. Mild Hyperoxia Shortens Telomeres and Inhibits Proliferation of Fibroblasts: A Model for Senescence? *Experimental Cell Research,* 220**,** 186-193.

WANG, H. & YIN, S. 2015. Natural Killer T Cells in Liver Injury, Inflammation and Cancer. *Expert Review in Gastroenterology and Hepatology,* 9**,** 1077-1085.

WANG, Y. & ZHANG, C. 2019. The Roles of Liver-Resident Lymphocytes in Liver Diseases. *Frontiers in Immunology,* 10**,** 1582.

WICK, M., LEITHAUSER, F. & REIMANN, J. 2002. The Hepatic Immune System. *Critical Review Immunology,* 22**,** 47-103.

WILLIAMS, A., PEH, C. & ELLIOTT, T. 2002. The Cell Biology of MHC Class I Antigen Presentation. *Tissue Antigens,* 59**,** 3-17.

WILLIAMS, R., ASPINALL, R., BELLIS, M., CAMPS-WALSH, G., CRAMP, M., DHAWAN, A., FERGUSON, J., FORTON, D., FOSTER, G., GILMORE, I., HICKMAN, M., HUDSON, M., KELLY, D., LANGFORD, A., LOMBARD, M., LONGWORTH, L., MARTIN, N., MORIARTY, K., NEWSOME, P., O'GRADY, J., PRYKE, R., RUTTER, H., RYDER, S., SHERON, N. & SMITH, T. 2014. Addressing Liver Disease in the UK: A Blueprint for Attaining Excellence in Health Care and Reducing Premature Mortality from Lifestyle Issues of Excess Consumption of Alcohol, Obesity, and Viral Hepatitis. *Lancet,* 384**,** 1953-1997.

WINCHESTER, R. 2008. 5-The Major Histocompatibility Complex. *In:* RICH, R., SHEARER, W., FREW, A., FLEISHER, T., SCHROEDER, H. & WEYAND, C. (eds.) *Clinical Immunology Principles and Practice.* Mosby.

WUERFEL, F., HUEBNER, H., HÄBERLE, L., GASS, P., HEIN, A., JUD, S., HACK, C., WUNDERLE, M., SCHULZ-WENDTLAND, R., ERBER, R., HARTMANN, A., EKICI, A., BECKMANN, M., FASCHING, P. & RUEBNER, M. 2020. HLA-G and HLA-F Protein Isoform Expression in Breast Cancer Patients Receiving Neoadjuvant Treatment. *Scientific Reports,* 10**,** 15750.

YANG, H., REI, M., BRACKENRIDGE, S., BRENNA, E., SUN, H., ABDULHAQQ, S., LIU, M., MA, W., KURUPATI, P., XU, X., CERUNDOLO, V., JENKINS, E., DAVIS, S., SACHA, J., FRÜH, K., PICKER, L., BORROW, P., GILLESPIE, G. & MCMICHAEL, A. 2021. HLA-E–Restricted, Gag-Specific $CD8^+$ T Cells can Suppress HIV-1 Infection, Offering Vaccine Opportunities. *Science Immunology,* 6**,** eabg1703.

YAWATA, M., YAWATA, N., ABI-RACHED, L. & PARHAM, P. 2002. Variation within the Human Killer Cell Immunoglobulin-like (KIR) Gene Family. *Critical Reviews in Immunology,* 22**,** 463-482.

ZHANG, J., MAI, S., CHEN, H., KANG, K., LI, X., CHEN, S. & PAN, P. 2017. Leukocyte Immunoglobulin-like Receptors in Human Diseases: An Overview of Their Distribution, Function, and Potential Application for Immunotherapies. *Journal of Leukocyte Biology,* 102**,** 351-360.

ZHANG, W., WEARSCH, P., ZHU, Y., LEONHARDT, R. & CRESSWELL, P. 2011. A Role for UDP-Glucose Glycoprotein Glucosyltransferase in Expression and Quality Control of MHC Class I Molecules. *Proceedings of the National Academy of Sciences,* 108**,** 4956-4961.

ZHANG, Y., BAIG, E. & WILLIAMS, D. 2006. Functions of ERp57 in the Folding and Assembly of Major Histocompatibility Complex Class I Molecules. *Journal of Biological Chemistry,* 281**,** 14622-14631.

ZHAO, J., LI, Y., JIN, L., ZHANG, S., FAN, R., SUN, Y., ZHOU, C., SHANG, Q., LI, W., ZHANG, Z. & WANG, F. 2012a. Natural Killer Cells are Characterized by the Concomitantly Increased Interferon-Gamma and Cytotoxicity in Acute Resolved Hepatitis B Patients. *PLoS One,* 7**,** e49135.

ZHAO, L., TEKLEMARIAM, T. & HANTASH, B. 2012b. Reassessment of HLA-G Isoform Specificity of MEM-G/9 and 4H84 Monoclonal Antibodies. *Tissue Antigens,* 80**,** 231-238.

ZHOU, Z., XU, M. & GAO, B. 2016. Hepatocytes: A Key Cell Type for Innate Immunity. *Cellular and Molecular Immunology,* 13**,** 301-315.

ZIDI, L., LAARIBI, A., BORTOLOTTI, D., BELHADJ, M., MEHRI, A., YAHIA, H., BABAY, W., CHAOUCH, H., ZIDI, N., LETAIEF, A., YACOUB, S., BOUKADIDA, J., LUCA, D. D., HANNACHI, N. & RIZZO, R. 2016. HLA-E Polymorphism and Soluble HLA-E Plasma Levels in Chronic Hepatitis B Patients. *HLA,* 87**,** 153-159.

Appendices

Appendix 1 MD Information

I) The work was undertaken at the University of Cambridge, Department of Pathology, Tennis Court Road, Cambridge. CB2 1QP.

II) All the work was performed by myself once I had been taught each technique by colleagues unless otherwise stated. Three experiments cited in chapter 6 were undertaken by a medical student under my supervision (Miss Jessica Clifton).

III) Support and training were provided by the following people in teaching me the initial biochemical techniques.
- Western blotting and Immunoprecipitation – Dr Louise Boyle and Dr Andreas Neerincx
- Flow Cytometry – Dr Martin Ivarsson and Dr Oisin Huhn
- Immunohistochemistry – Dr Cinzia Scarpini and Mrs Dawn Ward

IV) No work has yet been published. A paper is being prepared for submission to the Journal of Hepatology.

V) See Appendices 2 and 3 for the Ethical approval information and consent documents.

Appendix 2 Ethical Approval

NRES Committee South Central - Oxford B
Whitefriars
Level 3, Block B
Lewin's Mead
Bristol
BS1 2NT

Telephone: 0117 342 1333

06 March 2015 – Amended Protocol Date 20.03.2015

Dr Graeme J. M. Alexander
Consultant Hepatologist
Addenbrooke's Hospital
Box 210
Hills Road
Cambridge
CB2 0QQ

Dear Dr Alexander

Study title:	**Senescent Hepatocytes and the Innate immune System**
REC reference:	**15/SC/0127**
IRAS project ID:	**166865**

Thank you for your letter of 05/03/2015, responding to the Proportionate Review Sub-Committee's request for changes to the documentation for the above study.

The revised documentation has been reviewed and approved by the sub-committee.

We plan to publish your research summary wording for the above study on the HRA website, together with your contact details. Publication will be no earlier than three months from the date of this favourable opinion letter. The expectation is that this information will be published for all studies that receive an ethical opinion but should you wish to provide a substitute contact point, wish to make a request to defer, or require further information, please contact the REC Manager Mrs Siobhan Bawn, nrescommittee.southcentral-oxfordb@nhs.net . Under very limited circumstances (e.g. for student research which has received an unfavourable opinion), it may be possible to grant an exemption to the publication of the study.

Confirmation of ethical opinion

On behalf of the Committee, I am pleased to confirm a favourable ethical opinion for the above research on the basis described in the application form, protocol and supporting documentation as revised.

Conditions of the favourable opinion

The favourable opinion is subject to the following conditions being met prior to the start of the study.

Management permission or approval must be obtained from each host organisation prior to the start of the study at the site concerned.

Management permission ("R&D approval") should be sought from all NHS organisations involved in the study in accordance with NHS research governance arrangements.

Guidance on applying for NHS permission for research is available in the Integrated Research Application System or at http://www.rdforum.nhs.uk.

Where a NHS organisation's role in the study is limited to identifying and referring potential participants to research sites ("participant identification centre"), guidance should be sought from the R&D office on the information it requires to give permission for this activity.

For non-NHS sites, site management permission should be obtained in accordance with the procedures of the relevant host organisation.

Sponsors are not required to notify the Committee of approvals from host organisations.

Registration of Clinical Trials

All clinical trials (defined as the first four categories on the IRAS filter page) must be registered on a publically accessible database. This should be before the first participant is recruited but no later than 6 weeks after recruitment of the first participant.

There is no requirement to separately notify the REC but you should do so at the earliest opportunity e.g. when submitting an amendment. We will audit the registration details as part of the annual progress reporting process.

To ensure transparency in research, we strongly recommend that all research is registered but for non-clinical trials this is not currently mandatory.

If a sponsor wishes to request a deferral for study registration within the required timeframe, they should contact hra.studyregistration@nhs.net. The expectation is that all clinical trials will be registered, however, in exceptional circumstances non registration may be permissible with prior agreement from NRES. Guidance on where to register is provided on the HRA website.

It is the responsibility of the sponsor to ensure that all the conditions are complied with before the start of the study or its initiation at a particular site (as applicable).

Ethical review of research sites

The favourable opinion applies to all NHS sites taking part in the study, subject to management permission being obtained from the NHS/HSC R&D office prior to the start of the study (see "Conditions of the favourable opinion" above).

Approved documents

The documents reviewed and approved by the Committee are:

Document	*Version*	*Date*
Covering letter on headed paper [Ethics reply letter]	1.1	04 March 2015
IRAS Checklist XML [Checklist_05032015]		05 March 2015
Letters of invitation to participant [Patient Cover Letter]	1,1	04 March 2015
Participant consent form [Consent form]	2.1	03 March 2015
Participant information sheet (PIS) [Information Sheet]	2.1	03 March 2015
REC Application Form [REC_Form_05032015]		05 March 2015
Research protocol or project proposal [Protocol]	1.2	12 January 2015
Summary CV for Chief Investigator (CI) [CV]	1	03 November 2014
Summary CV for student		

Statement of compliance

The Committee is constituted in accordance with the Governance Arrangements for Research Ethics Committees and complies fully with the Standard Operating Procedures for Research Ethics Committees in the UK.

After ethical review

Reporting requirements

The attached document "After ethical review – guidance for researchers" gives detailed guidance on reporting requirements for studies with a favourable opinion, including:

- Notifying substantial amendments
- Adding new sites and investigators
- Notification of serious breaches of the protocol
- Progress and safety reports
- Notifying the end of the study

The HRA website also provides guidance on these topics, which is updated in the light of changes in reporting requirements or procedures.

Feedback

You are invited to give your view of the service that you have received from the National Research Ethics Service and the application procedure. If you wish to make your views known please use the feedback form available on the HRA website:
http://www.hra.nhs.uk/about-the-hra/governance/quality-assurance

We are pleased to welcome researchers and R & D staff at our NRES committee members' training days – see details at http://www.hra.nhs.uk/hra-training/

With the Committee's best wishes for the success of this project.

Yours sincerely

Dr Kim Cheetham
Vice Chair

Email: nrescommittee.southcentral-oxfordb@nhs.net

Enclosures: *"After ethical review – guidance for researchers"*

Copy to: Dr Anne EM Robins

Mr Stephen Kelleher

Appendix 3 Information Sheet and Consent Form

Cambridge University Hospitals NHS
NHS Foundation Trust

Research Study: The role of the immune system in chronic liver disease.

You are being invited to take part in a research study at Addenbrooke's Hospital. Before you decide whether you wish to participate it is important for you to understand why the research is being undertaken and what it would involve for you. Please take time to read the following information carefully and discuss it with others if you wish. One of the team will meet with you at your next clinic appointment to discuss this further, so please ask us if there is anything that is not clear or if you would like more information. Take your time to decide whether you wish to participate.

What is the purpose of the Study?
The underlying process that leads to chronic liver disease is not fully understood. Our group has shown that in livers which are damaged (known as fibrosis or cirrhosis) there is a higher number cells with 'senescence' than in healthy liver. These abnormal cells do not function correctly, leading to many of the complications of liver disease. Healthy people and people with liver disease that get better are able to get rid of these cells from the liver. We want to work out why your liver has been slow to do this. Our plan is to find out whether the immune system in your liver is also abnormal so cannot remove these cells.

Who is organising and funding this Study?
The study is organised and funded by the Department of Hepatology at Addenbrooke's Hospital. The study team is not receiving any payment for you to be in the study.

Why have I been chosen?
For this study we need to use liver samples from patients with chronic liver disease and compare those with liver samples from people with a normal (undamaged) liver. We will use surplus tissue samples and will not perform extra tests or take extra tissue.

We would like to study your liver because

1) You have liver disease and are on the waiting list for a liver transplant. We will collect a small piece of your removed liver at the end of the operation which is usually discarded.

2) You have liver disease and are due to undergo a routine liver biopsy and if there is spare liver which is usually discarded, we would like to use that for research

3) You are having an operation on your liver but the liver itself is healthy. We would like to study any healthy liver tissue that needs to be removed and is usually discarded as part of your operation.

Do I have to take part?
Taking part is entirely voluntary, but if you do decide to take part you will be given this information sheet to keep and will be asked to sign a consent form. You are still free to withdraw your consent at any time

and you do not have to specify a reason. Any decision to leave or not participate in the study will not effect your medical treatment.

What happens if I say yes?
To participate in this study we simply need to collect a sample of your liver tissue which is usually discarded.

At the end of the liver transplant.
After your liver biopsy.
At the end of your liver operation.

No additional tests need to be performed or any extra tissue samples taken. Any samples will be stored for use during the study period and up to five years.

What are the advantages of taking part?
There will be no benefit to your care in the clinic or on the ward, but if there is progress made from this research, this may benefit other patients in the future.

What are the disadvantages of taking part?
There are no disadvantages or risks associated with study itself. No procedure is being undertaken that was not planned for medical reasons. The risks of your *transplant, liver biopsy or liver operation* remain the same.

Will my taking part in this study be kept confidential?
All information that is collected about you during the study will be kept completely confidential. No personal information will be available to anyone other than the doctors involved in your care. Any information that leaves the hospital will have your name and address removed.

Who has reviewed the study?
This study has been looked at and approved by the Cambridge research ethics committee.

Further Information
You can contact Dr Anne Robins and Dr Nicola Owen at Addenbrooke's Hospital via switchboard or on 01223 336008. You can contact Dr Graeme Alexander on 01223 586614. If you wish to complain formally, you can do this through the NHS Complaints Procedure. The PALS (Patient Advice and Liaison Service) can be contacted on 01223 216756.

Thank you for taking the time to read about the study. We realise that participation is voluntary and are grateful to those who consider entering the study.

Cambridge University Hospitals NHS
NHS Foundation Trust

Centre Number:
Study Number:
Patient Identification Number for this trial:

CONSENT FORM

Title of Project: The role of the immune system in Chronic Liver disease

Name of Researcher: Dr Anne Robins, Dr Nicola Owen, Dr William Gelson, Dr Graeme Alexander

Please initial box

1 I confirm that I have read and understand the information sheet dated 03/03/2015 (version 2.1) for the above study. I have had the opportunity to consider the information, ask questions and have had these answered satisfactorily. ☐

2 I understand that my participation is voluntary and that I am free to withdraw at any time, without giving any reason, without my medical care or legal rights being affected. ☐

3 I understand that relevant sections of any of my medical notes and data collected during the study may be looked at by responsible individuals from regulatory authorities or from the NHS Trust, where it is relevant to my taking part in this research. I give permission for these individuals to have access to my records. ☐

4 I agree to take part in the above study. I agree to donate a sample of surplus liver tissue for research and this sample may be stored for use in future research subject to the necessary approvals. ☐

_____	_____	_____
Name of Patient	Date	Signature
_____	_____	_____
Name of Person taking consent (If different from researcher)	Date	Signature
_____	_____	_____
Researcher	Date	Signature

Appendix 4 Localisation of HLA Class I in Liver by Immunohistochemistry

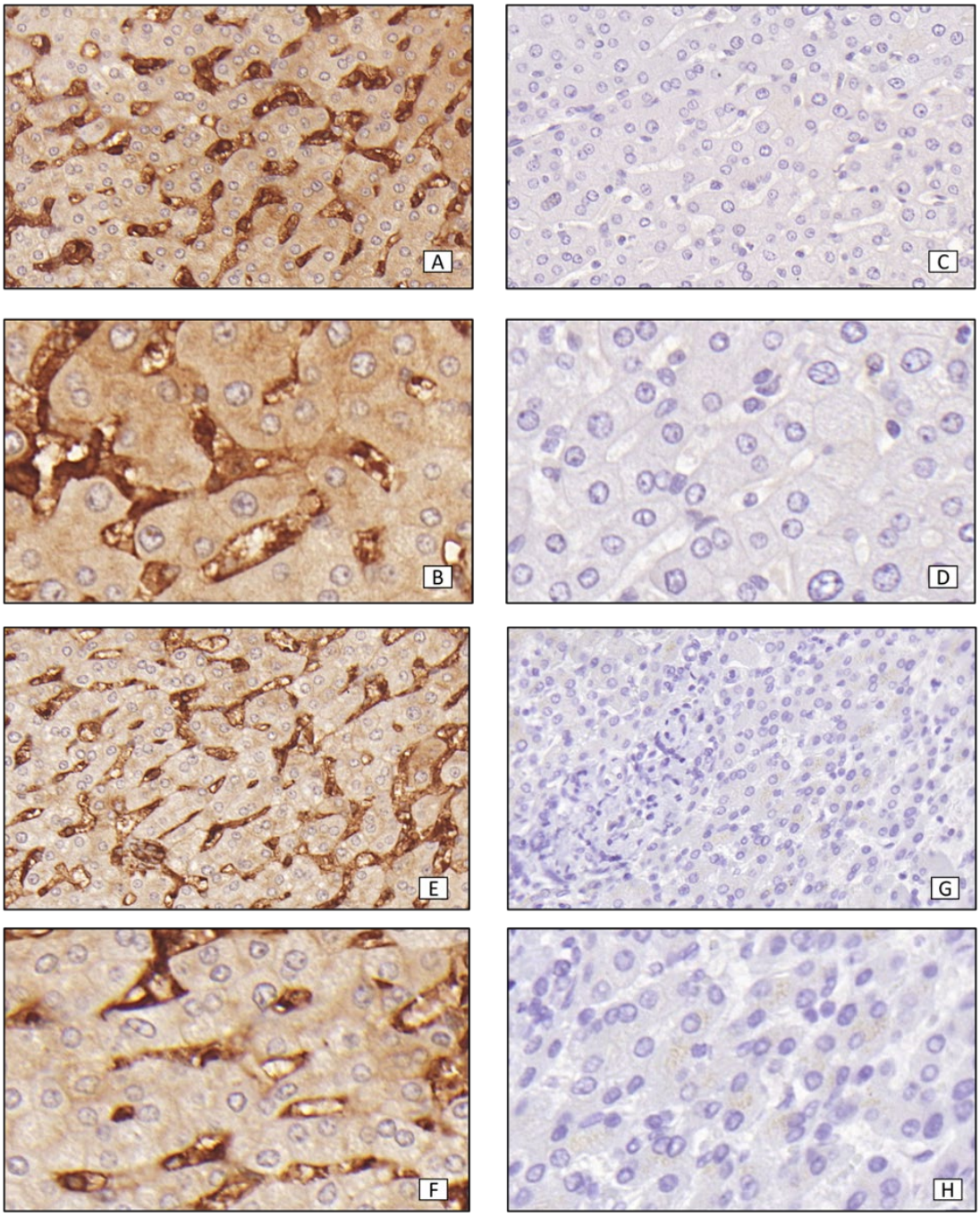

Appendix Figure 4.1 – Immunohistochemistry of HLA class I with HC10 antibody. *Antigen retrieval with EDTA buffer. Positive staining is seen as brown as the secondary antibody was tagged with DAB. Images A (20x) and B (40x) showing cirrhotic tissue with HLA class I. Images C (20x) and D (40x) showing cirrhotic tissue with an IgG2a control. Images E (20x) and F (40x) showing HLA class I staining in healthy control liver tissue and images G (20x) and H (40x) showing healthy control tissue with an IgG2a control antibody.*

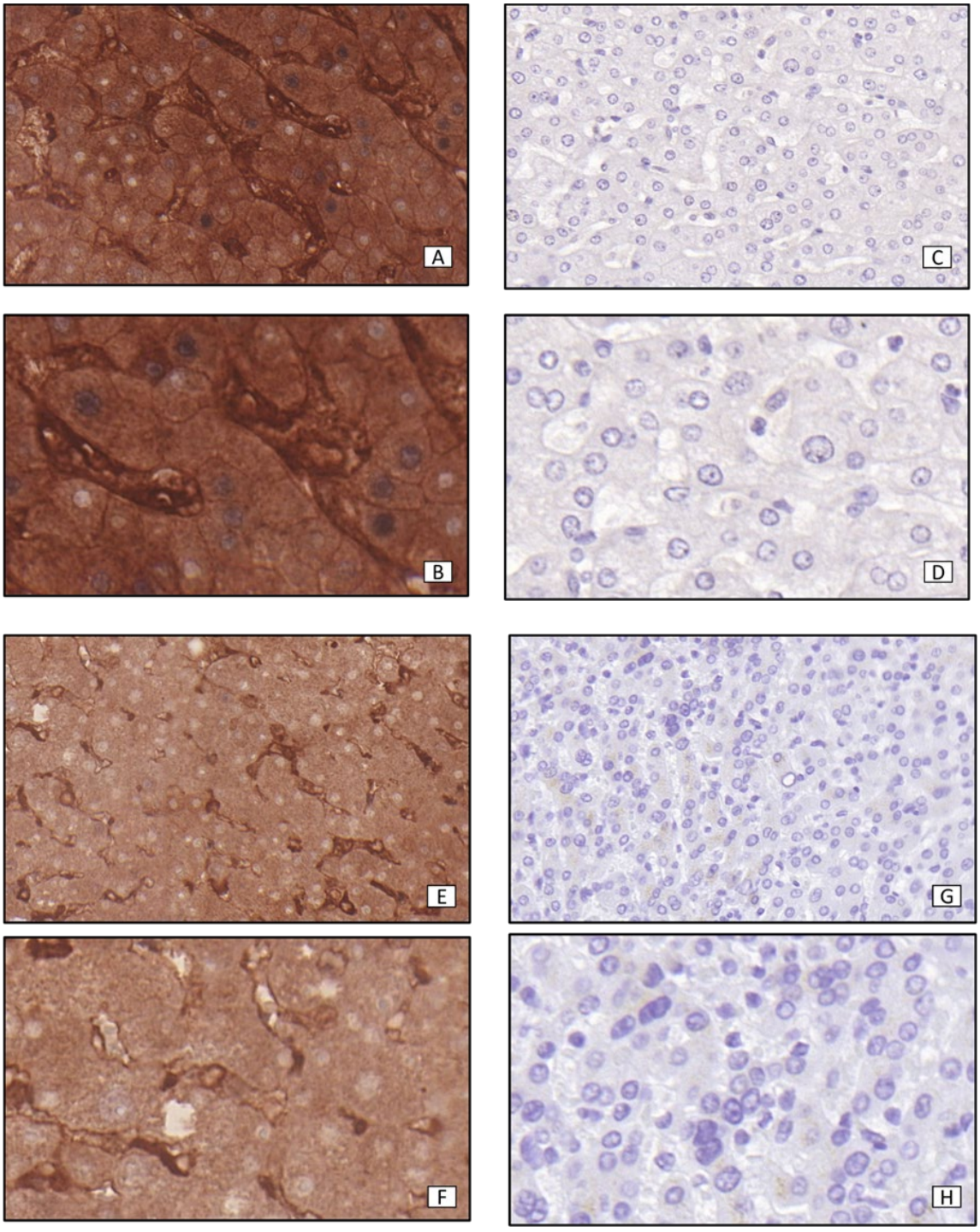

Appendix Figure 4.2 – Immunohistochemistry of HLA-C with L31 antibody. *Antigen retrieval with EDTA buffer. Positive staining was brown as the secondary antibody was tagged with DAB. Images A (20x) and B (40x) showing staining in cirrhotic tissue and images C (20x) and D (40x) staining in cirrhosis with an IgG2a control. Images E (20x) and F (40x) showing staining in healthy control liver tissue; G (20x) and H (40x) showing healthy control tissue with an IgG2a control antibody.*

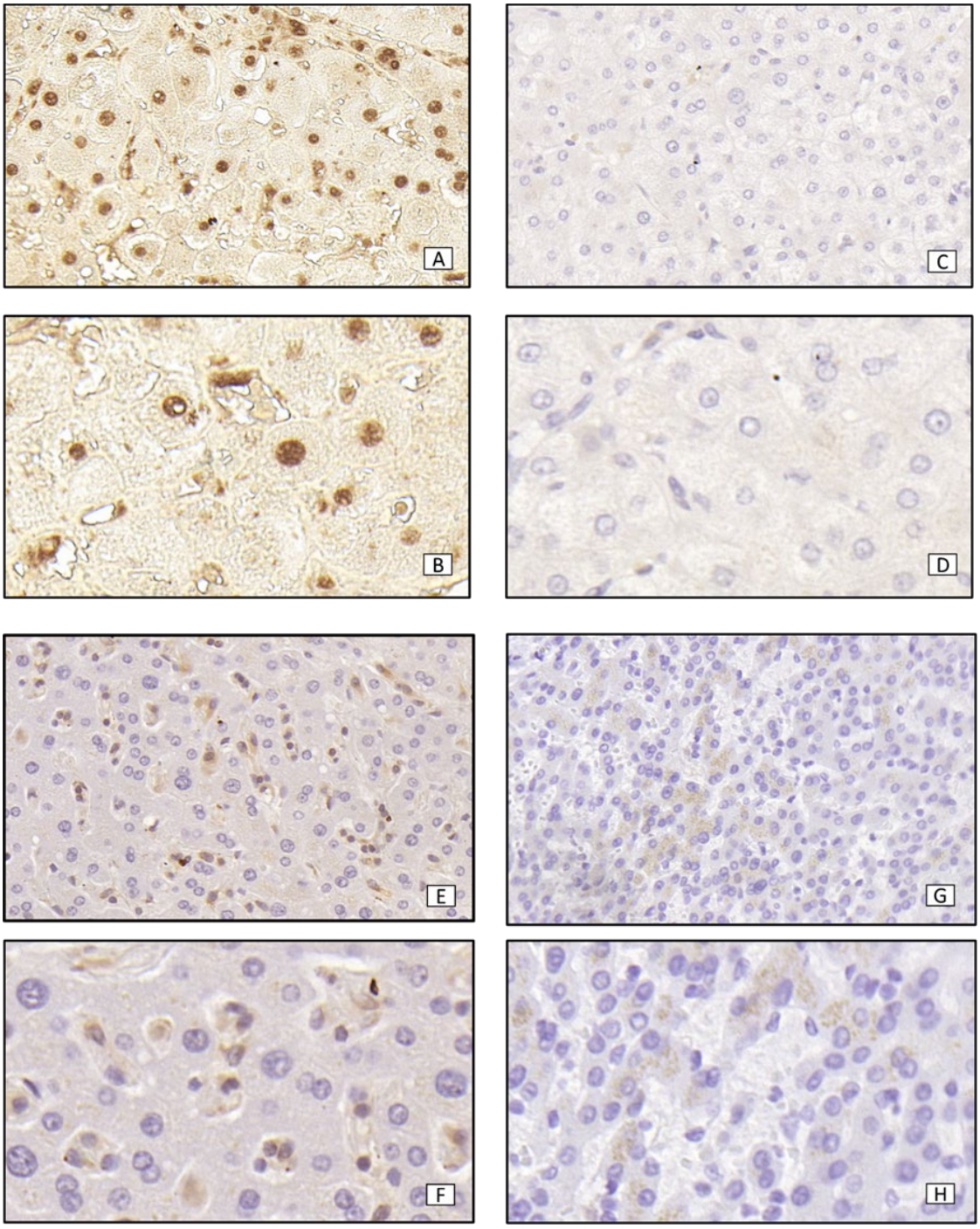

Appendix Figure 4.3 - Immunohistochemistry of HLA-E with MEME02 antibody. *Antigen retrieval with EDTA buffer. Positive staining is seen as brown as the secondary antibody was tagged with DAB. Images A (20x) and B (40x) showing staining of hepatocytes in cirrhotic tissue, while C (20x) and D (40x) show staining in cirrhosis with an IgG2a control. Images E (20x) and F (40x) show hepatocyte staining in healthy control liver tissue, while G (20x) and H (40x) show staining in healthy control tissue with an IgG2a control antibody.*

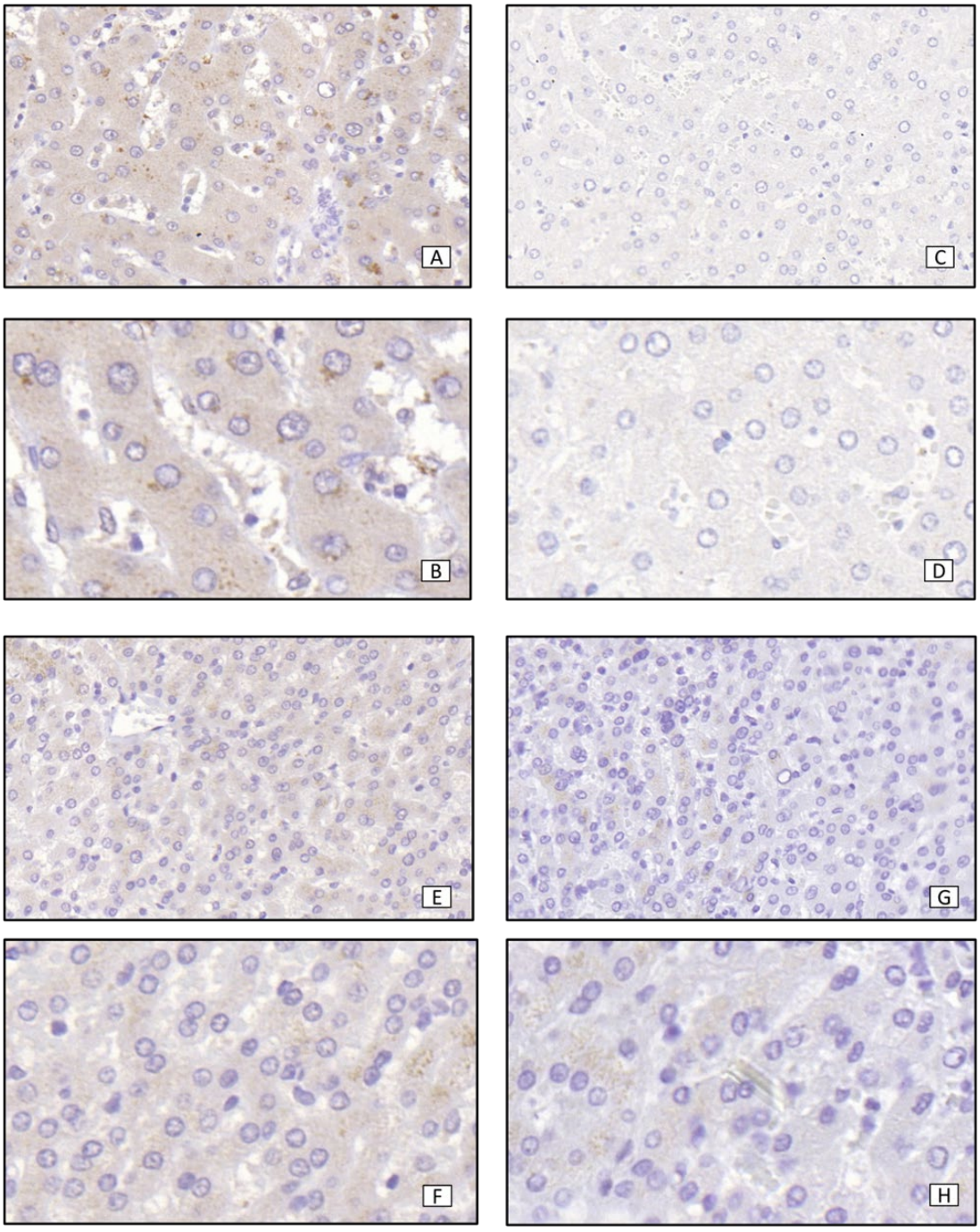

Appendix Figure 4.4 – Immunohistochemistry of HLA-F with FG1 antibody. *Antigen retrieval with EDTA buffer. Positive staining is seen as brown since the secondary antibody was tagged with DAB. Images A (20x) and B (40x) showing hepatocyte staining in cirrhotic tissue; C (20x) and D (40x) showing staining in cirrhosis with an IgG2a control. Images E (20x) and F (40x) showing staining in healthy control liver tissue and G (20x) and H (40x) showing no staining with an IgG2a control antibody.*

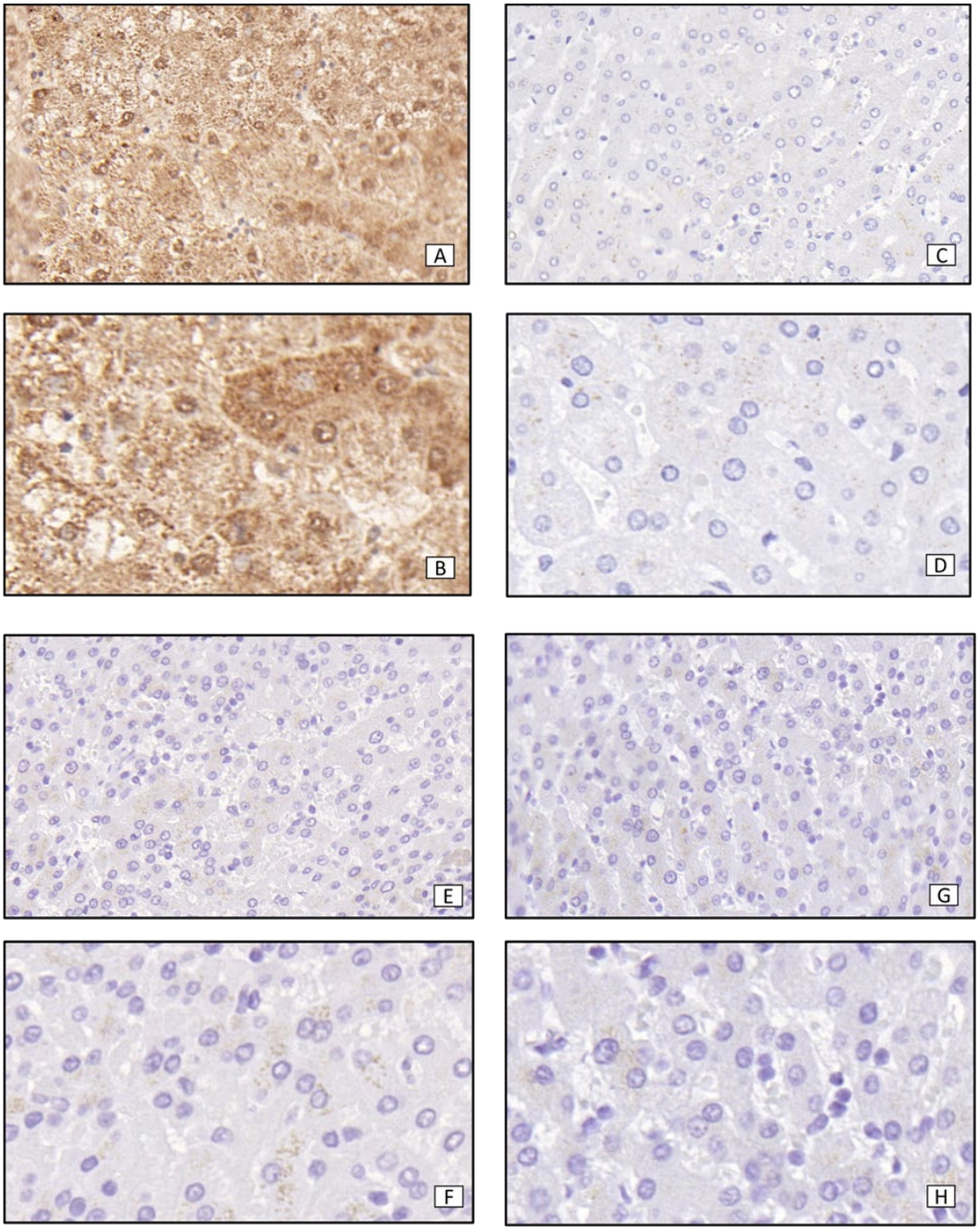
A
C
B
D
E
G
F
H

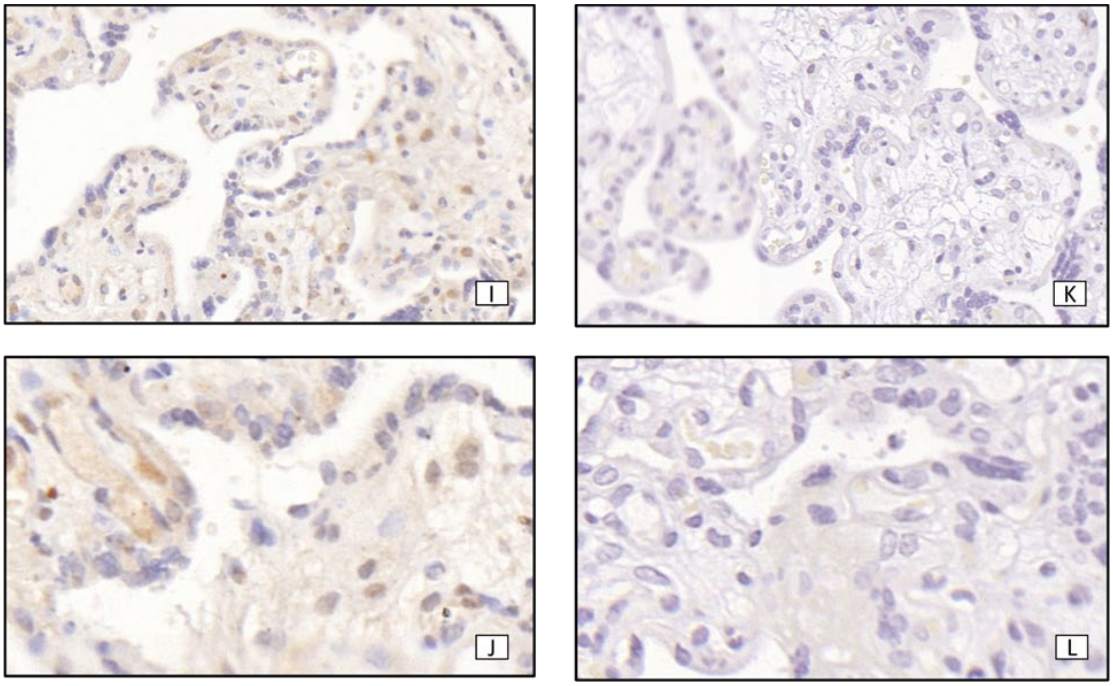

Appendix Figure 4.5 – Immunohistochemistry of HLA-G with MEMG01 antibody. *Antigen retrieval with EDTA buffer. Positive staining seen as brown since the secondary antibody was tagged with DAB. Images A (20x) and B (40x) showing staining in cirrhotic tissue; C (20x) and D (40x) showing staining in cirrhosis with an IgG2a control. Images E (20x) and F (40x) showing staining in healthy control liver tissue; G (20x) and H (40x) showing no staining of healthy control liver tissue with an IgG2a control antibody. Images I (20x) and J (40x) show staining of placenta tissue for HLA-G, while K (20x) and L (40x) again show the IgG2a control in the same tissue samples.*

Appendix 5 Localisation of HLA Class I in Liver Tissue by Immunofluorescence

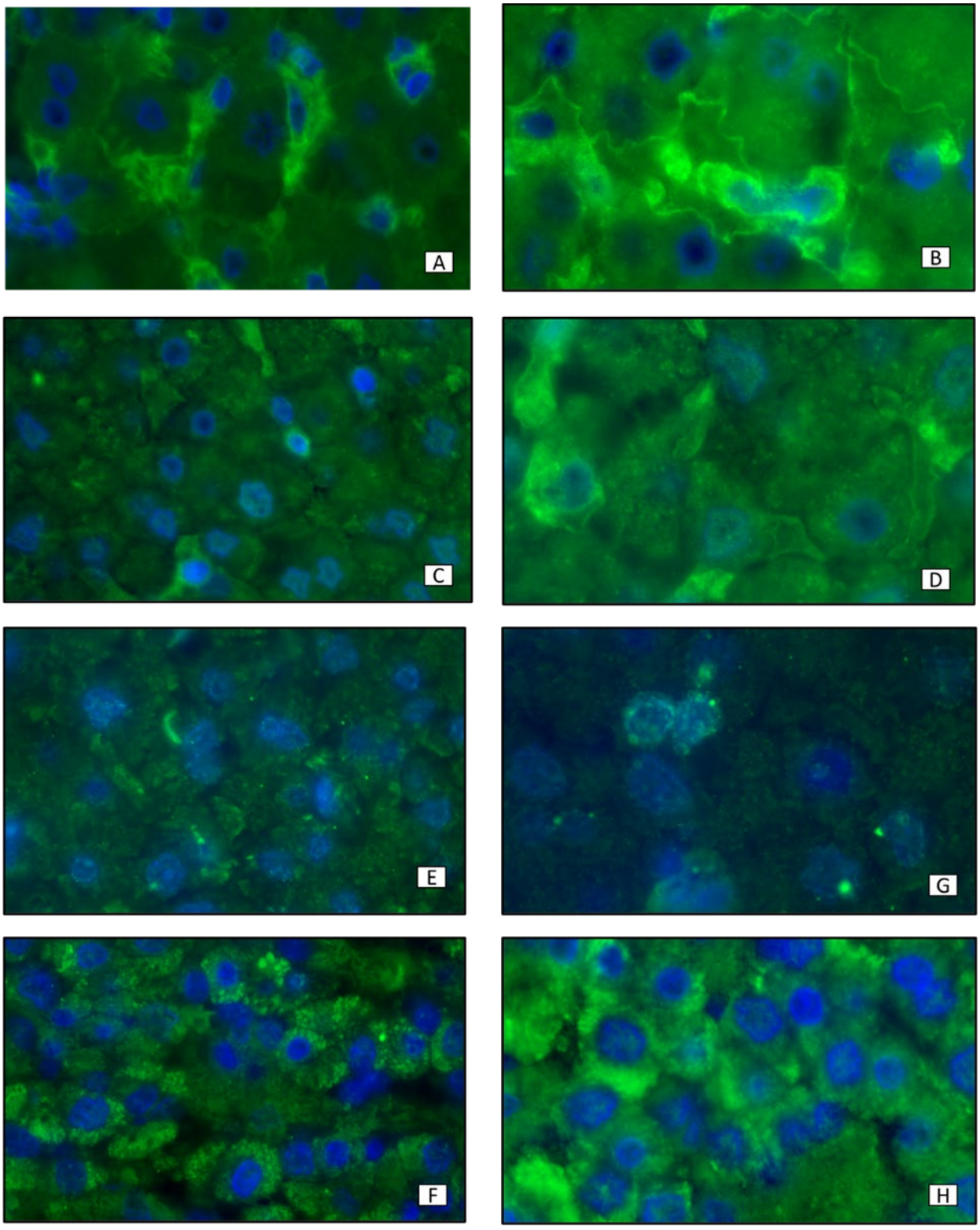

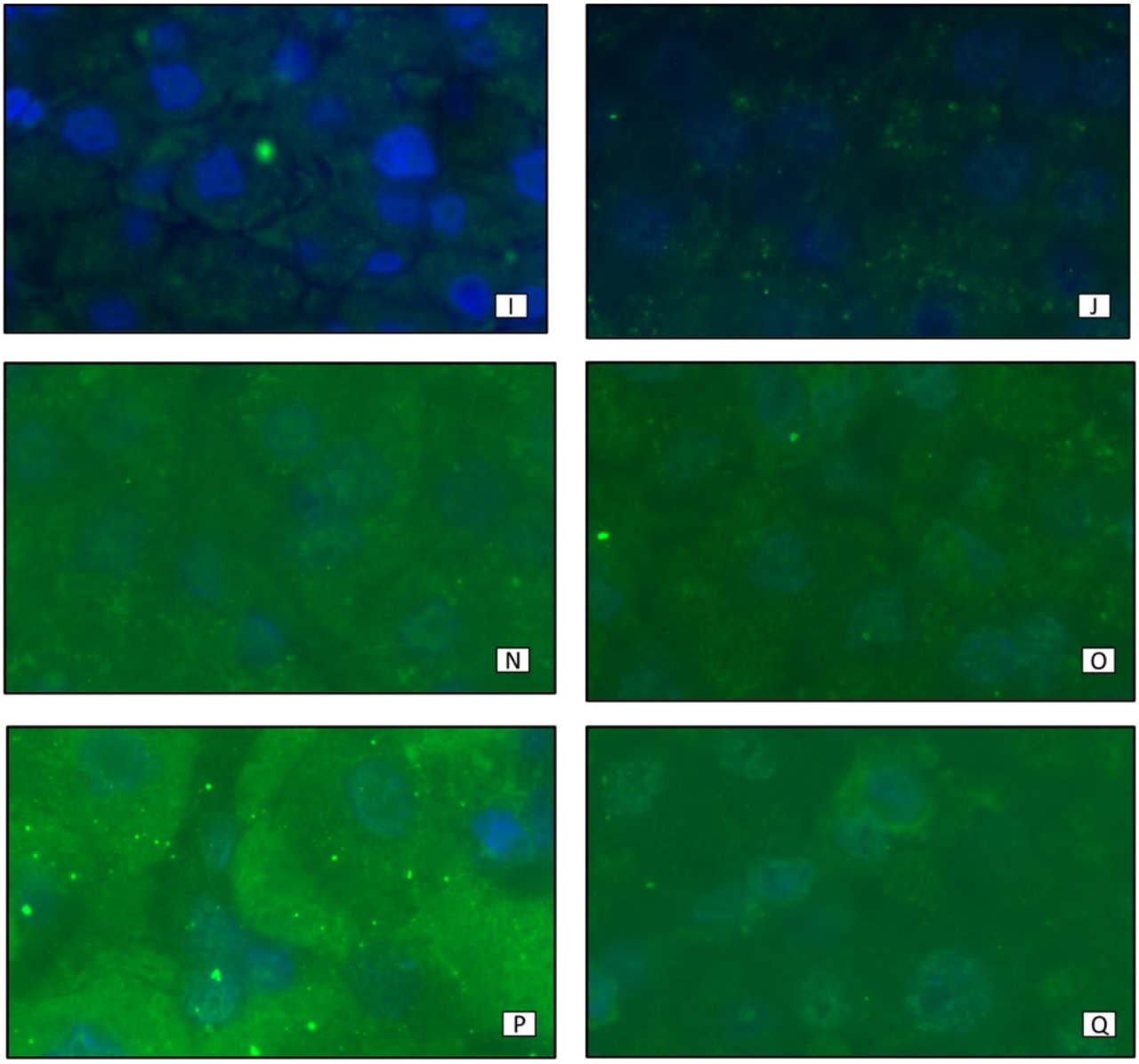

Appendix Figure 5.1 – Immunofluorescent staining of HLA class I and specially HLA-E, -F and -G using a green laser*. Nuclei are stained blue with Dapi. Images A (20x) and B (63x) show staining in cirrhotic tissue for HLA class I with HC10 antibody. Images C (20x) and D (63x) show staining of HLA-E with MEME02 antibody in cirrhosis. Images E (20x) and G (63x) show staining of HLA-F with FG1 antibody in cirrhosis. Images F (20x) and H (63x) show staining of HLA G with MEMG01 antibody in cirrhotic tissue. Images I (20x) and J (63x) show staining with the IgG2a, antibody used as a negative control in cirrhosis revealing prominent background auto-fluorescent staining of liver tissue. Image N (63x) shows prominent staining with the same negative control antibody in healthy control liver. Images O, P and Q (63x) show staining of HLA-E (MEM02), -F (FG1) and -G (MEMG01) respectively in healthy control liver.*

Appendix 6 Investigation of Cell Surface Expression of MHC Class I using Endo H Digest

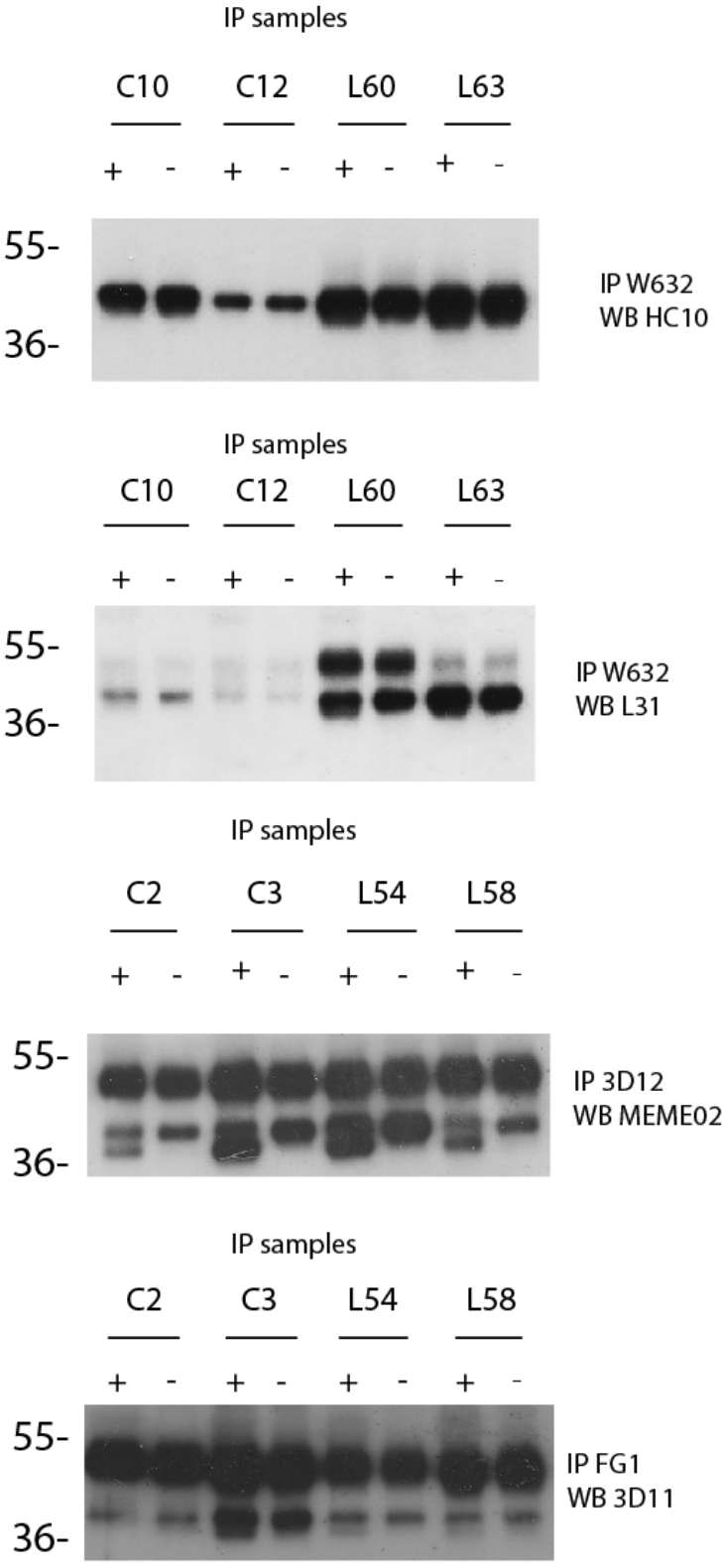

Appendix Figure 6.1 – Endo H digest investigating expression of HLA Class I, HLA-C, -E and -F. *Immunoprecipitation samples using W6/32, W6/32, 3D12 and FG1 for HLA Class I, HLA-C, -E and -F respectively treated with Endo H digest. Western blots were performed with HC10, L31, MEME02 and 3D11 antibodies respectively in both control (C) and cirrhotic (L) lysates. The band seen at 50kDa is a cross-reactive band as discussed previously.*

Appendix 7 Full Data for the Analysis of p21 and HLA Class I Expression by Immunohistochemistry

	HLA Class I Expression	p21 Expression
Cirrhotic 1	4	3
Cirrhotic 2	5	2
Cirrhotic 3	3	2
Cirrhotic 4	4	4
Cirrhotic 5	5	3
Cirrhotic 6	3	3
Cirrhotic 7	3	2
Cirrhotic 8	3	4
Cirrhotic 9	2	4
Cirrhotic 10 (Negative)	1	1
Mean	**3.3**	**2.8**
Median	**3**	**3**
Control 1	2	2
Control 2	5	2
Control 3	3	3
Control 4	2	2
Control 5	3	2
Control 6 (Negative)	1	1
Mean	**3**	**2**
Median	**2.5**	**2**

Appendix Table 7.1 – The expression of p21 and HLA class I in the cirrhotic and control liver samples by immunohistochemistry. *Samples are from cirrhotic and control liver. Each sample scored on the Likert scale (1-5) before both a median and mean were calculated.*

	HLA Class I Expression	p21 Expression
Post-Transplant 1 (Negative)	1	1
Post-Transplant 2	5	3
Post-Transplant 3	5	2
Post-Transplant 4	4	5
Post-Transplant 5	3	5
Post-Transplant 6	4	3
Post-Transplant 7	5	5
Post-Transplant 8	4	5
Post-Transplant 9	5	4
Post-Transplant 10	3	3
Post-Transplant 11	5	4
Post-Transplant 12	4	4
Post-Transplant 13	5	3
Post-Transplant 14	3	5
Post-Transplant 15	4	5
Post-Transplant 16	2	3
Post-Transplant 17	3	2
Post-Transplant 18	4	3
Post-Transplant 19	3	2
Post-Transplant 20	4	3
Post-Transplant 21	4	4
Post-Transplant 22	2	3
Post-Transplant 23	4	4
Post-Transplant 24	3	3
Post-Transplant 25	2	5
Post-Transplant 26	5	2
Post-Transplant 27	4	5
Post-Transplant 28	5	4
Post-Transplant 29	5	2
Mean	**3.76**	**3.52**
Median	**4**	**3.5**

Appendix Table 7.2 – The expression of p21 and HLA class I in the post-transplant liver samples by immunohistochemistry. *Samples are from post-transplant biopsies representative of acute rejection. Each sample scored on the Likert scale (1-5) before both a median and mean were calculated.*

	HLA-E Expression	p21 Expression
Cirrhotic 1	3	4
Cirrhotic 2	4	3
Cirrhotic 3	2	2
Cirrhotic 4	5	5
Cirrhotic 5 (Negative)	1	1
Cirrhotic 6	4	3
Cirrhotic 7	3	2
Cirrhotic 8	4	4
Cirrhotic 9	4	4
Cirrhotic 10	3	2
Mean	**3.5**	**3.2**
Median	**4**	**3**
Control 1	3	2
Control 2	3	2
Control 3	3	2
Control 4	4	3
Control 5	3	3
Control 6 (Negative)	1	1
Mean	**3.2**	**2.4**
Median	**3**	**2**

Appendix Table 7.3 – The expression of p21 and HLA-E in the cirrhotic and control liver samples by immunohistochemistry. *Samples are from cirrhotic and control liver. Each sample scored on the Likert scale (1-5) before both a median and mean were calculated.*

	HLA-E Expression	P21 Expression
Post-Transplant 1 (Negative)	1	1
Post-Transplant 2	5	3
Post-Transplant 3	5	2
Post-Transplant 4	4	3
Post-Transplant 5	5	3
Post-Transplant 6	4	2
Post-Transplant 7	5	3
Post-Transplant 8	3	4
Post-Transplant 9	2	4
Post-Transplant 10	4	3
Post-Transplant 11	4	4
Post-Transplant 12	5	3
Post-Transplant 13	5	2
Post-Transplant 14	5	4
Post-Transplant 15	5	2
Post-Transplant 16	3	2
Post-Transplant 17	5	2
Post-Transplant 18	4	5
Post-Transplant 19	3	2
Post-Transplant 20	4	5
Post-Transplant 21	3	2
Post-Transplant 22	5	2
Post-Transplant 23	4	4
Post-Transplant 24	2	2
Post-Transplant 25	5	4
Post-Transplant 26	4	2
Post-Transplant 27	4	4
Post-Transplant 28	4	3
Post-Transplant 29	3	2
Mean	**4.1**	**2.9**
Median	**4**	**3**

Appendix Table 7.4 – The expression of p21 and HLA-E in the post-transplant liver samples by immunohistochemistry. *Samples are from post-transplant biopsies representative of acute rejection. Each sample scored on the Likert scale (1-5) before both a median and mean were calculated.*

	HLA-F Expression	P21 Expression
Cirrhotic 1	2	4
Cirrhotic 2	3	3
Cirrhotic 3	4	2
Cirrhotic 4	4	4
Cirrhotic 5	5	2
Cirrhotic 6	3	2
Cirrhotic 7	4	2
Cirrhotic 8	4	3
Cirrhotic 9	4	4
Cirrhotic 10 (Negative)	1	1
Mean	**3.4**	**2.7**
Median	**4**	**2.5**
Control 1	3	2
Control 2	4	2
Control 3	4	3
Control 4	3	2
Control 5	2	2
Control 6 (Negative)	1	1
Mean	**2.8**	**2**
Median	**3**	**2**

Appendix Table 7.5 – The expression of p21 and HLA-F in the cirrhotic and control liver samples by immunohistochemistry. *Samples are from cirrhotic and control liver. Each sample scored on the Likert scale (1-5) before both a median and mean were calculated.*

	HLA-F Expression	P21 Expression
Post-Transplant 1 (Negative)	1	1
Post-Transplant 2	5	2
Post-Transplant 3	5	3
Post-Transplant 4	5	5
Post-Transplant 5	4	5
Post-Transplant 6	3	3
Post-Transplant 7	3	3
Post-Transplant 8	2	5
Post-Transplant 9	3	3
Post-Transplant 10	5	5
Post-Transplant 11	5	5
Post-Transplant 12	2	4
Post-Transplant 13	4	2
Post-Transplant 14	4	5
Post-Transplant 15	2	5
Post-Transplant 16	3	2
Post-Transplant 17	3	2
Post-Transplant 18	4	3
Post-Transplant 19	4	2
Post-Transplant 20	3	4
Post-Transplant 21	5	5
Post-Transplant 22	5	3
Post-Transplant 23	2	5
Post-Transplant 24	5	3
Post-Transplant 25	2	4
Post-Transplant 26	3	3
Post-Transplant 27	5	3
Post-Transplant 28	2	5
Post-Transplant 29	4	2
Mean	**3.6**	**3.5**
Median	**4**	**3**

Appendix Table 7.6 – The expression of p21 and HLA-F in the post-transplant liver samples by immunohistochemistry. *Samples are from post-transplant biopsies representative of acute rejection. Each sample scored on the Likert scale (1-5) before both a median and mean were calculated.*

	HLA-G Expression	P21 Expression
Cirrhotic 1	4	3
Cirrhotic 2	4	2
Cirrhotic 3	4	2
Cirrhotic 4	2	4
Cirrhotic 5	4	2
Cirrhotic 6	3	2
Cirrhotic 7	3	2
Cirrhotic 8	5	3
Cirrhotic 9	3	3
Cirrhotic 10 (Negative)	1	1
Mean	**3.3**	**2.4**
Median	**3.5**	**2**
Control 1	5	2
Control 2	4	2
Control 3	3	2
Control 4	3	2
Control 5	3	2
Control 6 (Negative)	1	1
Mean	**3.2**	**1.8**
Median	**3**	**2**

Appendix Table 7.7 – The expression of p21 and HLA-G in the cirrhotic and control liver samples by immunohistochemistry. *Samples are from cirrhotic and control liver. Each sample scored on the Likert scale (1-5) before both a median and mean were calculated.*

	HLA-G Expression	P21 Expression
Post-Transplant 1 (Negative)	1	1
Post-Transplant 2	3	2
Post-Transplant 3	4	2
Post-Transplant 4	2	2
Post-Transplant 5	3	4
Post-Transplant 6	2	2
Post-Transplant 7	4	4
Post-Transplant 8	4	3
Post-Transplant 9	4	5
Post-Transplant 10	3	2
Post-Transplant 11	5	4
Post-Transplant 12	3	3
Post-Transplant 13	4	2
Post-Transplant 14	2	4
Post-Transplant 15	2	2
Post-Transplant 16	2	2
Post-Transplant 17	3	2
Post-Transplant 18	4	2
Post-Transplant 19	2	2
Post-Transplant 20	2	2
Post-Transplant 21	4	4
Post-Transplant 22	3	2
Post-Transplant 23	2	2
Post-Transplant 24	4	3
Post-Transplant 25	4	3
Post-Transplant 26	2	4
Post-Transplant 27	4	2
Post-Transplant 28	3	2
Post-Transplant 29	4	2
Mean	**3.1**	**2.6**
Median	**3**	**2**

Appendix Table 7.8 – The expression of p21 and HLA-G in the post-transplant liver samples by immunohistochemistry. *Samples are from post-transplant biopsies representative of acute rejection. Each sample scored on the Likert scale (1-5) before both a median and mean were calculated.*

Appendix 8 **Raw Data Showing Percentage Population and MFI of the NK Cell Receptors in the Control, Cirrhotic and Acute Rejection Samples**

	NK cells	CD56 Bright	CD56 Dim	NKG2A Positive	NKG2C Positive	KIR2DL4 Positive	LILRB1 Positive	LILRB2 Positive
Control 1	18	6.47	92	46.1	32.6	0.33	0.14	0.35
Control 2	25	8.88	91.1	52.7	3.43	1.77	1.22	2.0
Control 3	29.1	4.58	95.2	39.1	11.5	0.89	6.51	2.95
Control 4	12.8	11.3	88.2	58.2	26.0	7.04	9.30	3.82
Control 5	18.6	2.71	95.9	95.6	7.50	0.72	0.42	2.72
Mean	20.7	6.788	92.48	58.34	16.206	2.15	3.518	2.368
Median	18.6	6.47	92	52.7	11.5	0.89	1.22	2.72
Interquartile Range	7	4.3	4.1	12.1	18.5	1.05	6.09	0.95

Appendix Table 8.1 – Percentage population of the NK cell receptors expressed on NK cells in the control samples. *Values taken from parent population the NK cells and include mean, median and interquartile range.*

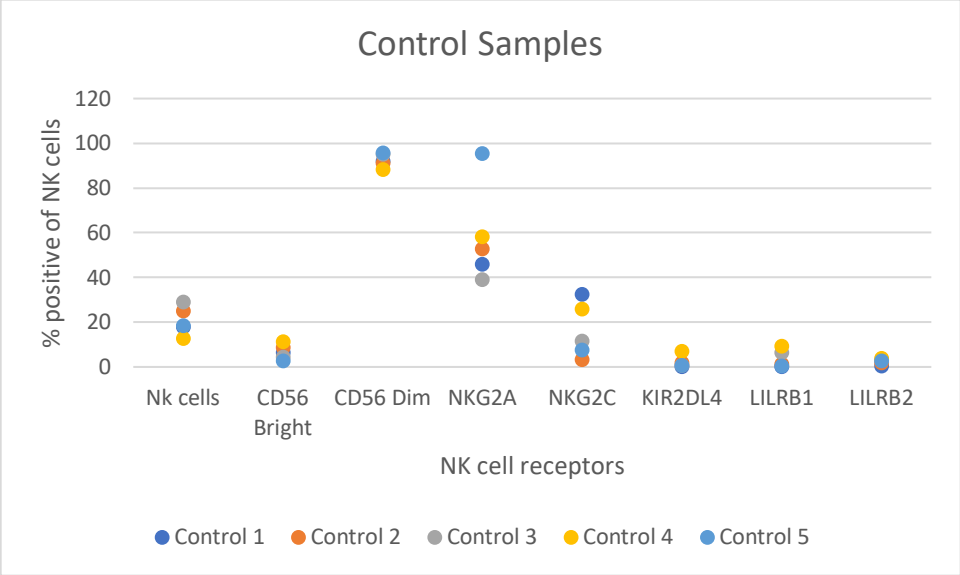

Appendix Figure 8.1 – Percentage population of the NK cell receptors expressed on NK cells in the control samples. *Values taken from parent population the NK cells and include mean, median and interquartile range.*

	2DL1 Positive	2DL2/S2 Positive	2DL3 Positive	2DS1 Positive	3DL1 Positive	3DS1 Positive
Control 1	12.2	16.1	23.8	8.11	19.3	2.49
Control 2	12.5	0.055	22.1	6.16	2.19	0.024
Control 3	16.7	0	27.1	15.4	16.0	0.03
Control 4	10.9	0	46.1	10.4	15.3	0.05
Control 5	22.6	0.26	26.8	8.43	38.0	14.4
Mean	14.98	3.283	29.18	9.7	18.158	3.3988
Median	12.5	0.055	26.8	8.43	16	0.05
Interquartile Range	4.5	0.26	3.3	2.29	4	2.46

Appendix Table 8.2 – Percentage population of the KIR receptors expressed on NK cells in the control samples. *Values taken from parent population the NK cells and include mean, median and interquartile range.*

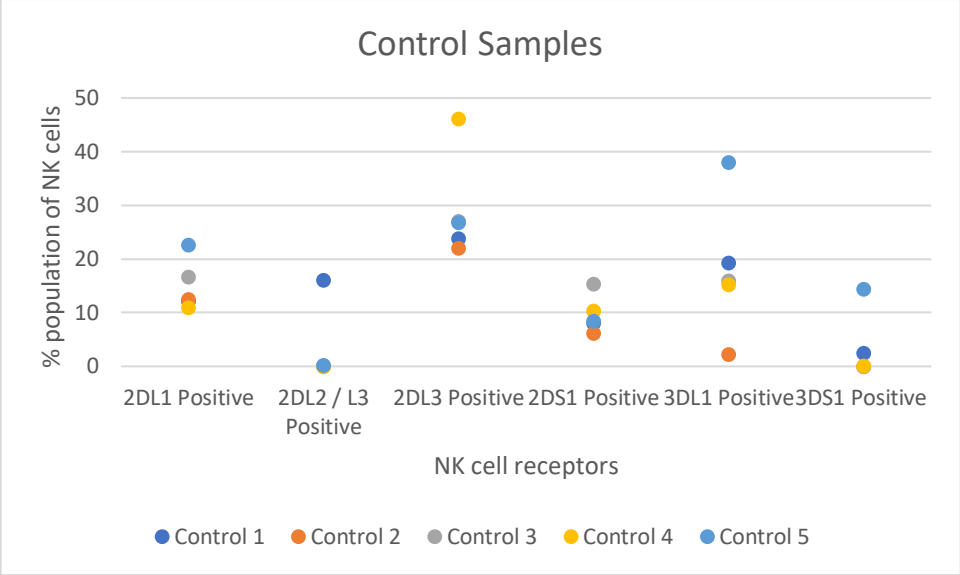

Appendix Figure 8.2 – Percentage population of the KIR receptors expressed on NK cells in the control samples. *Values taken from parent population the NK cells and include mean, median and interquartile range.*

	NK cells	CD56 Bright	CD56 Dim	NKG2A Positive	NKG2C Positive	KIR2DL4 Positive	LILRB1 Positive	LILRB2 Positive
Control 1	876	3789	489	224	746	340	739	651
Control 2	967	3599	573	242	551	334	393	362
Control 3	755	4398	610	1715	287	2325	209	128
Control 4	821	4448	526	4267	407	2228	195	134
Control 5	563	2525	533	4426	347	251	591	330
Mean	796.4	3751.8	546.2	2174.8	467.6	1095.6	425.4	321
Median	821	3789	533	1715	407	340	393	330
Interquartile Range	121	799	47	4025	204	1894	382	228

Appendix Table 8.3 – MFI of the NK cell receptors expressed on NK cells in the control samples. *Values taken from parent population the NK cells and include mean, median and interquartile range.*

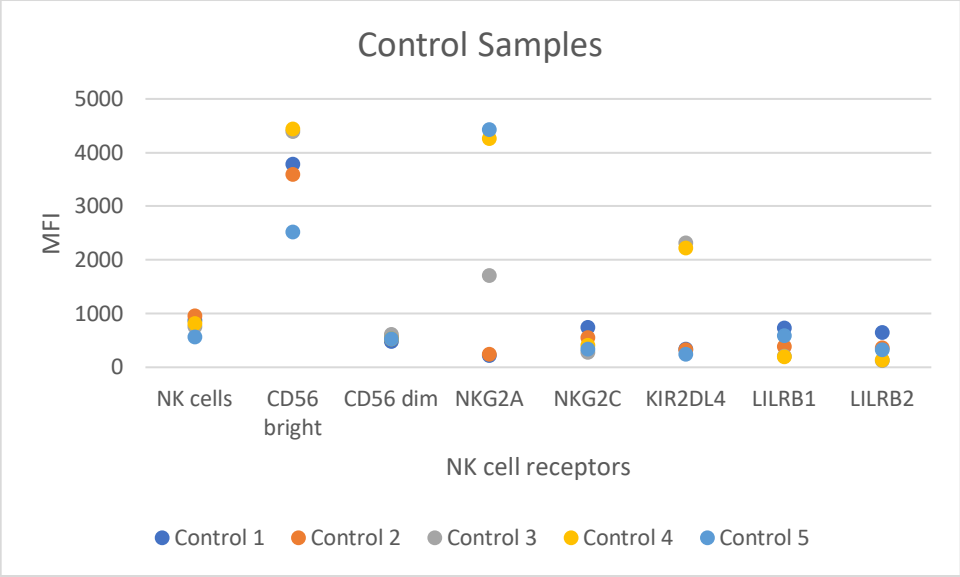

Appendix Figure 8.3 – MFI of the NK cell receptors expressed on NK cells in the control samples. *Values taken from parent population the NK cells and include mean, median and interquartile range.*

	2DL1 Positive	2DL2/S2 Positive	2DL3 Positive	2DS1 Positive	3DL1 Positive	3DS1 Positive
Control 1	519	2060	1187	1084	2204	4972
Control 2	459	1103	1241	793	1642	8871
Control 3	849	0	789	862	367	6258
Control 4	717	0	945	879	348	5998
Control 5	362	475	778	528	1683	1048
Mean	581.2	727.6	988	829.2	1248.8	5429.4
Median	519	475	945	862	1642	5998
Interquartile Range	258	1103	398	86	1316	1286

Appendix Table 8.4 – MFI of the KIR receptors expressed on NK cells in the control samples. *Values taken from parent population the NK cells and include mean, median and interquartile range.*

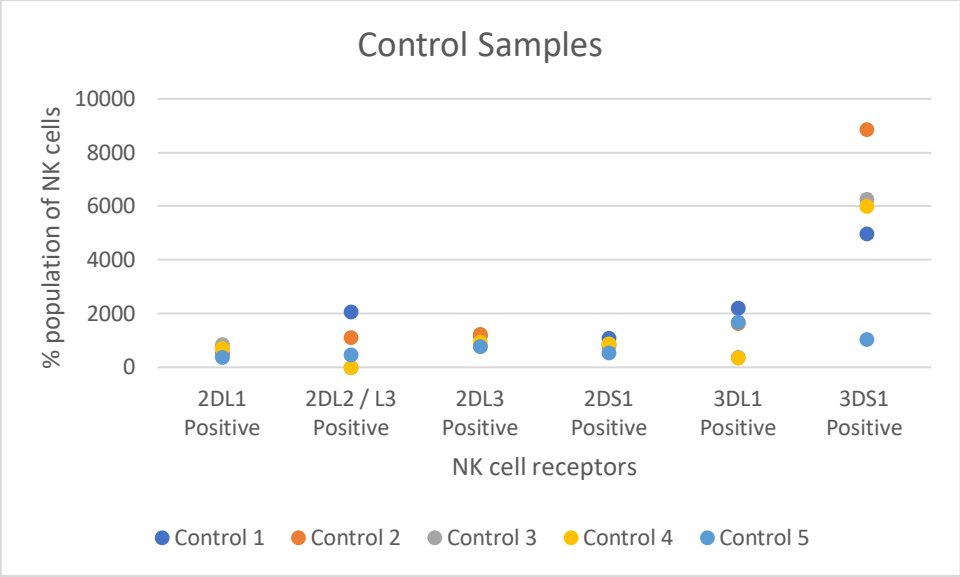

Appendix Figure 8.4 – MFI of the KIR receptors expressed on NK cells in the control samples. *Values taken from parent population the NK cells and include mean, median and interquartile range.*

	NK cells	CD56 Bright	CD56 Dim	NKG2A Positive	NKG2C Positive	KIR2DL4 Positive	LILRB1 Positive	LILRB2 Positive
Cirrhotic 1	6.26	13.0	86	48.4	4.35	4.33	1.41	0.28
Cirrhotic 2	7.96	10.2	89.2	79.3	6.88	0.75	1.43	0.19
Cirrhotic 3	18.9	14.3	85.9	58.0	15.5	0.51	18.1	3.78
Cirrhotic 4	32.3	34.1	64.9	63.7	10.4	2.11	8.75	3.18
Cirrhotic 5	8.25	4.89	92.6	79.1	11.5	0.42	3.23	9.17
Cirrhotic 6	68.9	5.03	94.6	87.5	5.68	8.06	0.29	61.6
Cirrhotic 7	26.0	16.5	82.5	53.4	1.83	19.1	0.15	0.37
Cirrhotic 8	35.8	8.18	91.1	35.7	1.23	11.0	0.21	0.11
Cirrhotic 9	25.2	14.4	85.3	52.9	4.93	18.9	0.53	0
Mean	25.51	13.4	85.79	62	6.92	7.24	3.79	8.74
Median	25.2	13	86	58	5.68	4.33	1.41	0.37
Interquartile Range	24.05	6.22	5.8	26.2	6.05	10.25	2.94	3.59

Appendix Table 8.5 – Percentage population of the NK cell receptors expressed on NK cells in the cirrhotic samples. *Values taken from parent population the NK cells and include mean, median and interquartile range.*

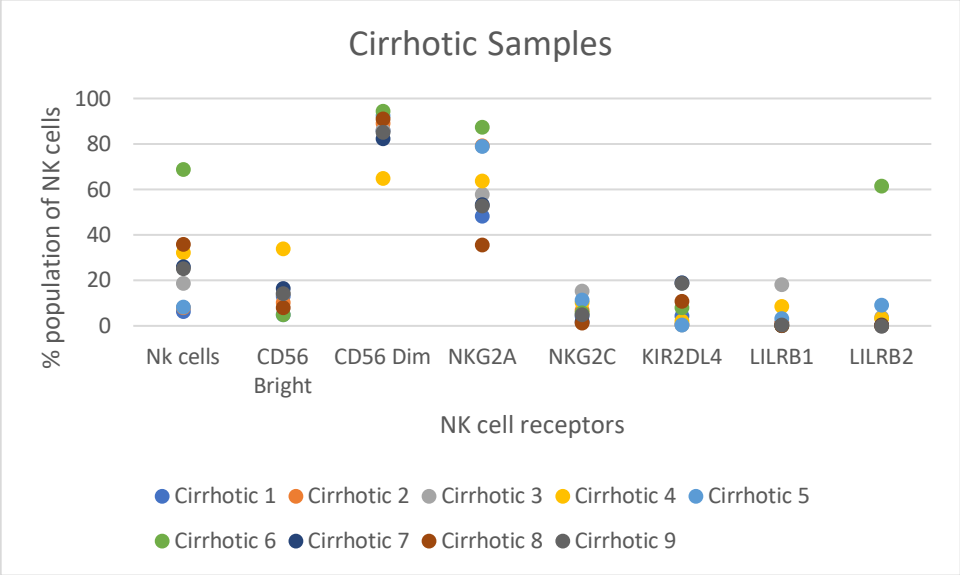

Appendix Figure 8.5 – Percentage population of the NK cell receptors expressed on NK cells in the cirrhotic samples. *Values taken from parent population the NK cells and include mean, median and interquartile range.*

	2DL1 Positive	2DL2/S2 Positive	2DL3 Positive	2DS1 Positive	3DL1 Positive	3DS1 Positive
Cirrhotic 1	10.1	10.8	4.84	4.04	9.59	0
Cirrhotic 2	10.4	18.9	19.6	10.6	8.24	0.047
Cirrhotic 3	10.8	25.9	25.9	10.7	12.5	0.079
Cirrhotic 4	29.1	44.6	44.6	15.4	19.5	0
Cirrhotic 5	6.15	15.7	11.7	6.77	6.77	0.088
Cirrhotic 6	23.8	0.26	34.3	25.3	14.2	1.75
Cirrhotic 7	14.6	14.4	14.3	11.1	29.6	5.86
Cirrhotic 8	20.6	2.04	34.1	18.9	27.3	2.55
Cirrhotic 9	13.1	7.19	22.0	10.1	19.3	3.31
Mean	15.41	15.53	23.48	12.54	16.33	1.52
Median	13.1	14.4	22	10.7	14.2	0.088
Interquartile Range	10.2	11.71	19.8	5.3	9.91	2.503

Appendix Table 8.6 – Percentage population of the KIR receptors expressed on NK cells in the cirrhotic samples.

Values taken from parent population the NK cells and include mean, median and interquartile range.

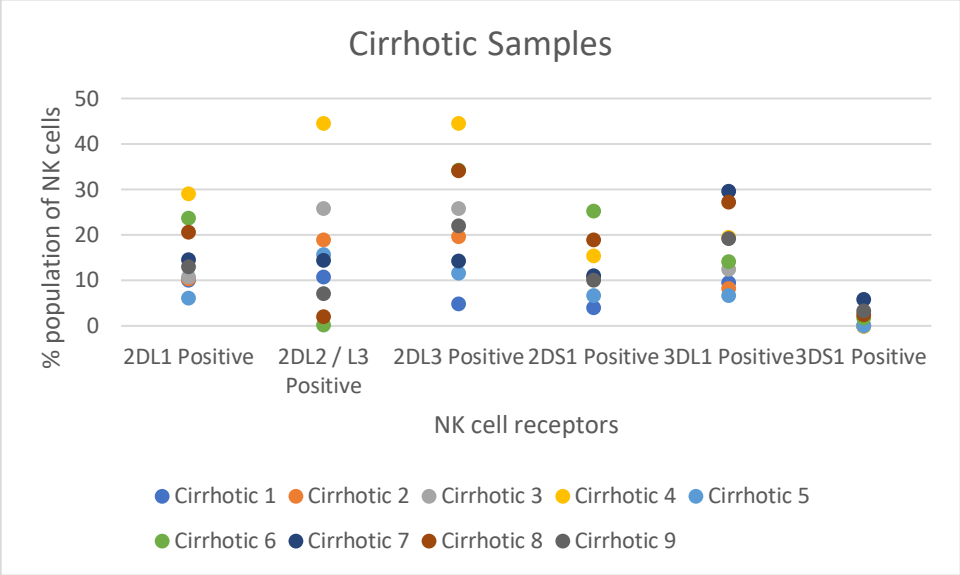

Appendix Figure 8.6 – Percentage population of the KIR receptors expressed on NK cells in the cirrhotic samples.

Values taken from parent population the NK cells and include mean, median and interquartile range.

	NK cells	CD56 Bright	CD56 Dim	NKG2A Positive	NKG2C Positive	KIR2DL4 Positive	LILRB1 Positive	LILRB2 Positive
Cirrhotic 1	660	1937	385	206	506	340	506	336
Cirrhotic 2	747	2728	556	321	554	321	335	1050
Cirrhotic 3	802	3726	632	3524	323	2187	205	129
Cirrhotic 4	1180	3927	650	4919	322	2094	195	129
Cirrhotic 5	387	1881	347	5536	354	198	591	355
Cirrhotic 6	508	2426	468	5944	297	217	502	405
Cirrhotic 7	916	3570	691	3403	676	995	1395	2673
Cirrhotic 8	670	3646	567	2270	621	998	1663	9322
Cirrhotic 9	830	3629	645	3063	700	997	1319	0
Mean	744.44	3052.2	549	3242.9	483.67	927.44	745.67	1599.9
Median	747	3570	567	3403	506	995	506	355
Interquartile Range	170	1220	177	2649	298	677	984	921

Appendix Table 8.7 – MFI of the NK cell receptors expressed on NK cells in the cirrhotic samples. *Values taken from parent population the NK cells and include mean, median and interquartile range.*

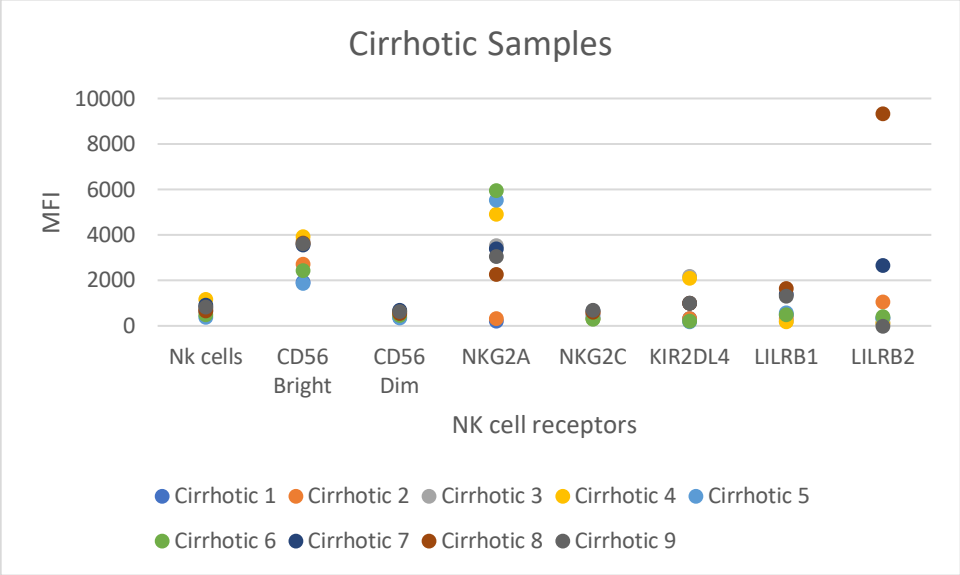

Appendix Figure 8.7 – MFI of the NK cell receptors expressed on NK cells in the cirrhotic samples. *Values taken from parent population the NK cells and include mean, median and interquartile range.*

	2DL1 Positive	2DL2/S2 Positive	2DL3 Positive	2DS1 Positive	3DL1 Positive	3DS1 Positive
Cirrhotic 1	735	1808	809	792	1446	0
Cirrhotic 2	662	1977	1045	937	1276	6964
Cirrhotic 3	895	0	719	724	340	5061
Cirrhotic 4	754	0	863	853	431	6057
Cirrhotic 5	275	1479	978	635	573	1095
Cirrhotic 6	669	459	789	718	912	1144
Cirrhotic 7	1187	1599	979	1251	2580	3882
Cirrhotic 8	1007	600	715	1031	2559	4182
Cirrhotic 9	1114	1376	842	1037	2716	3773
Mean	810.89	1033.1	859.89	886.44	1425.9	3573.1
Median	754	1376	842	853	1276	3882
Interquartile Range	338	1140	189	307	1986	3917

Appendix Table 8.8 – MFI of the KIR receptors expressed on NK cells in the cirrhotic samples. *Values taken from parent population the NK cells and include mean, median and interquartile range.*

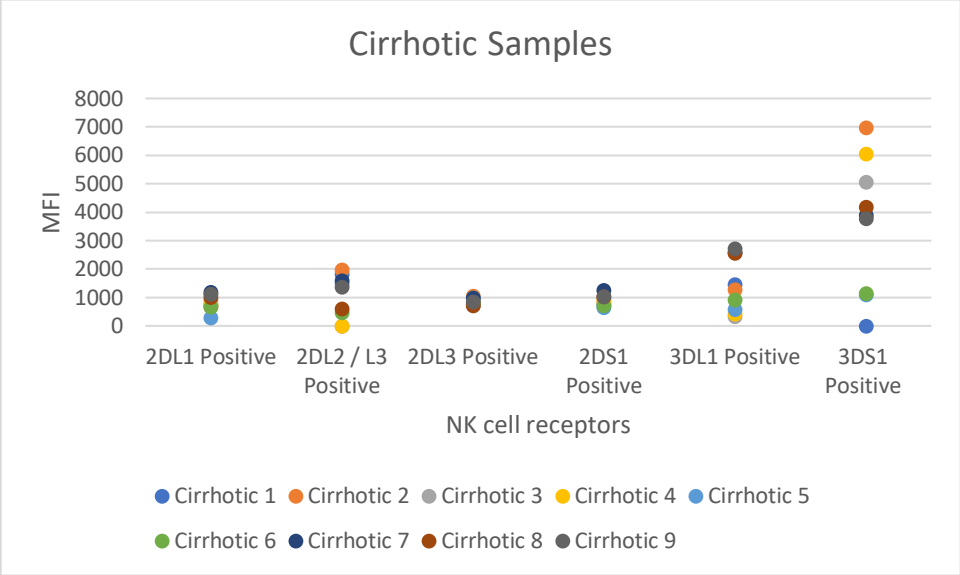

Appendix Figure 8.8 – MFI of the KIR receptors expressed on NK cells in the cirrhotic samples. *Values taken from parent population the NK cells and include mean, median and interquartile range.*

	NK cells	CD56 Bright	CD56 Dim	NKG2A Positive	NKG2C Positive	KIR2DL4 Positive	LILRB1 Positive	LILRB2 Positive
Acute Rejection 1	7.33	11.2	87.5	25.8	21.1	5.69	0.50	0.50
Acute Rejection 2	2.89	12.9	86.7	90.6	11.7	2.05	2.94	0.84
Acute Rejection 3	12.0	47.8	48.7	83.7	14.0	0	5.26	2.63
Acute Rejection 4	7.30	11.8	87.3	62.9	17.1	0	7.89	6.58
Acute Rejection 5	7.36	17.1	77.6	80.3	9.40	5.08	5.97	23.8
Acute Rejection 6	7.23	9.62	91.7	46.5	0	3.33	0	0
Mean	7.35	18.4	79.91	64.97	12.22	2.7	3.76	5.73
Median	7.315	12.35	87	71.6	12.85	2.69	4.1	1.735
Interquartile Range	0.105	4.7	7.575	32.25	6.35	4.13	4.6825	5.0075

Appendix Table 8.9 – Percentage population of the NK cell receptors expressed on NK cells in the acute rejection samples. *Values taken from parent population the NK cells and include mean, median and interquartile range.*

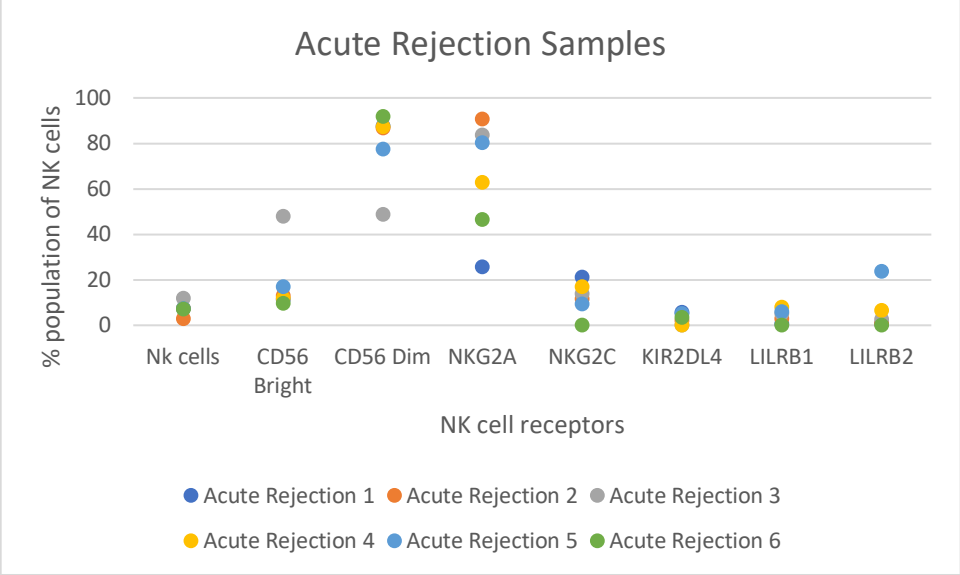

Appendix Figure 8.9 – Percentage population of the NK cell receptors expressed on NK cells in the acute rejection samples. *Values taken from parent population the NK cells and include mean, median and interquartile range.*

	2DL1 Positive	2DL2/S2 Positive	2DL3 Positive	2DS1 Positive	3DL1 Positive	3DS1 Positive
Acute Rejection 1	7.68	0	50.1	0.58	14.2	0
Acute Rejection 2	5.30	0	10.0	2.58	0	0
Acute Rejection 3	5.45	0	5.45	1.82	1.82	0
Acute Rejection 4	19.6	0	6.23	20.1	10.1	0
Acute Rejection 5	7.68	3.07	8.94	5.03	4.61	2.09
Acute Rejection 6	19.1	22.6	11.5	16.1	2.46	0
Mean	10.8	4.28	15.37	7.71	5.53	0.35
Median	7.68	0	9.47	3.805	3.535	0
Interquartile Range	10.24	2.3	4.22	11.32	6.75	0

Appendix Table 8.10 – Percentage population of the KIR receptors expressed on NK cells in the acute rejection samples. *Values taken from parent population the NK cells and include mean, median and interquartile range.*

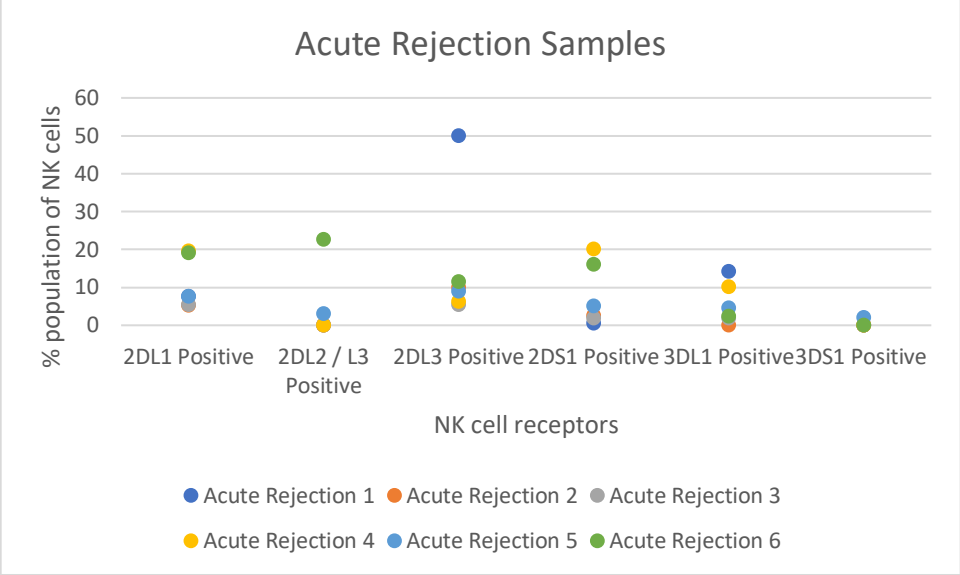

Appendix Figure 8.10 – Percentage population of the KIR receptors expressed on NK cells in the acute rejection samples. *Values taken from parent population the NK cells and include mean, median and interquartile range.*

	NK cells	CD56 Bright	CD56 Dim	NKG2A Positive	NKG2C Positive	KIR2DL4 Positive	LILRB1 Positive	LILRB2 Positive
Acute Rejection 1	704	2517	544	25.8	21.1	351	669	2502
Acute Rejection 2	533	2557	430	90.6	11.7	329	411	1893
Acute Rejection 3	1394	3352	614	4243	345	0	162	110
Acute Rejection 4	589	2289	487	2801	225	0	206	172
Acute Rejection 5	459	1252	361	9670	311	202	629	420
Acute Rejection 6	476	2169	407	2690	0	1000	0	0
Mean	692.5	2356	473.83	3253.4	152.3	313.67	346.17	849.5
Median	561	2403	458.5	2745.5	123.05	265.5	308.5	296
Interquartile Range	185	348	117	3142.05	275.45	295	401.5	1399.25

Appendix Table 8.11 – MFI of the NK cell receptors expressed on NK cells in the acute rejection samples. *Values taken from parent population the NK cells and include mean, median and interquartile range.*

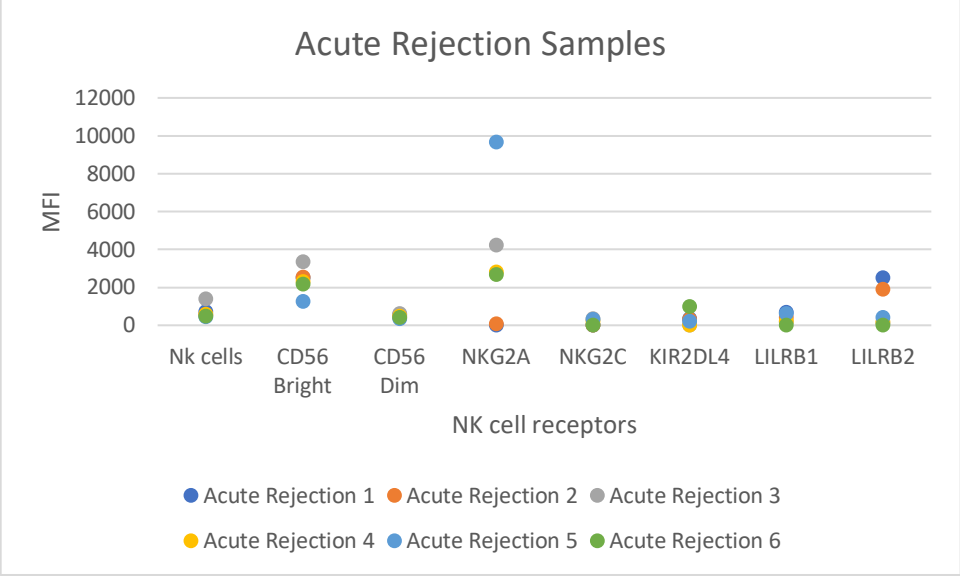

Appendix Figure 8.11 – MFI of the NK cell receptors expressed on NK cells in the acute rejection samples. *Values taken from parent population the NK cells and include mean, median and interquartile range.*

	2DL1 Positive	2DL2/S2 Positive	2DL3 Positive	2DS1 Positive	3DL1 Positive	3DS1 Positive
Acute Rejection 1	631	0	852	1119	1408	0
Acute Rejection 2	707	0	1010	826	0	0
Acute Rejection 3	823	0	757	997	922	0
Acute Rejection 4	802	0	863	950	388	0
Acute Rejection 5	433	1027	749	662	595	1189
Acute Rejection 6	993	1670	703	1240	951	0
Mean	731.5	449.5	822.3333	965.6667	710.6667	198.1667
Median	754.5	0	804.5	973.5	758.5	0
Interquartile Range	167.75	770.25	109.25	231.5	504	0

Appendix Table 8.12 – MFI of the KIR receptors expressed on NK cells in the acute rejection samples. *Values taken from parent population the NK cells and include mean, median and interquartile range.*

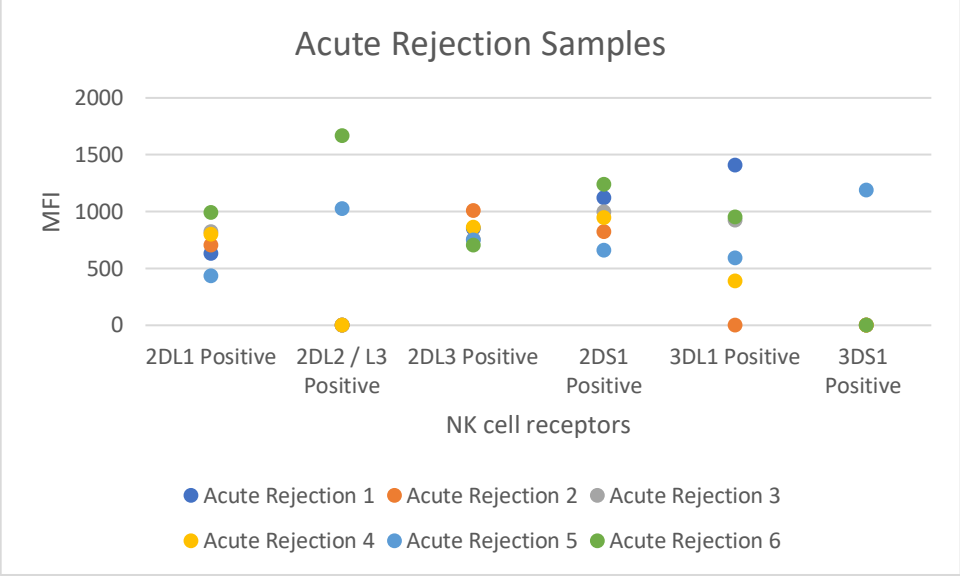

Appendix Figure 8.12 – MFI of the KIR receptors expressed on NK cells in the acute rejection samples. *Values taken from parent population the NK cells and include mean, median and interquartile range.*

Appendix 9 **Raw Data Showing Percentage Population and MFI of the NK Cell Maturity Markers in the C Control, Cirrhotic and Acute Rejection Samples**

	CD57 Positive	CD69 Positive	NKG2A Positive
Control 1	60.5	11.5	36.8
Control 2	52.4	10.6	25.5
Control 3	64.9	14.7	46.4
Control 4	50.8	20.7	51.9
Control 5	51.9	21.7	86.1
Mean	56.1	15.84	49.34
Median	52.4	14.7	46.4
Interquartile Range	8.6	9.2	15.1

Appendix Table 9.1 – Percentage population of the NK cell maturity markers expressed on NK cells in the control samples. *Values taken from parent population the NK cells and include mean, median and interquartile range.*

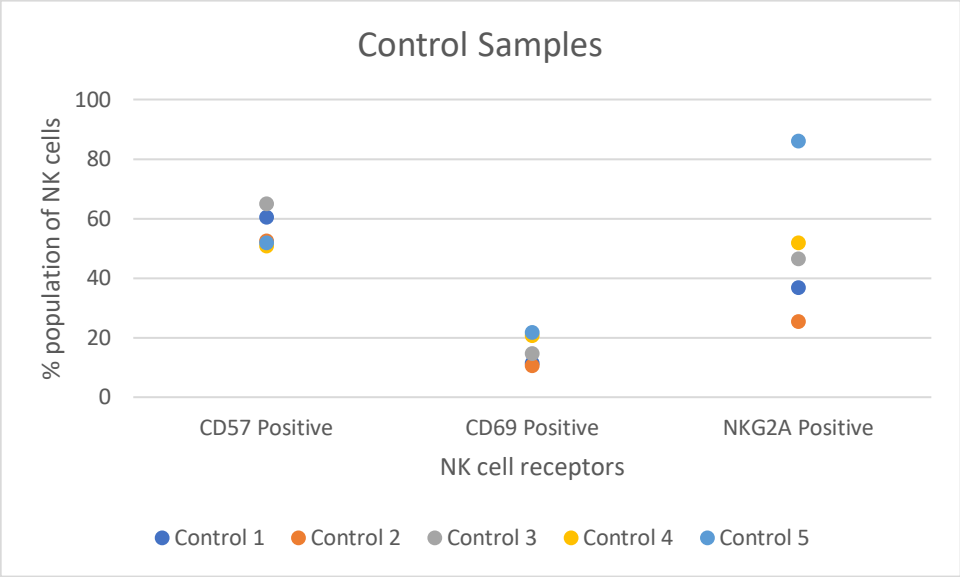

Appendix Figure 9.1 – Percentage population of the NK cell maturity markers expressed on NK cells in the control samples. *Values taken from parent population the NK cells and include mean, median and interquartile range.*

	CD57 Positive	CD69 Positive	NKG2A Positive
Control 1	2662	996	225
Control 2	1949	668	193
Control 3	6505	386	1695
Control 4	4331	438	1686
Control 5	2167	790	378
Mean	3522.8	655.6	835.4
Median	2662	668	378
Interquartile Range	2164	352	1461

Appendix Table 9.2 – MFI of the NK cell maturity markers expressed on NK cells in the control samples. *Values taken from parent population the NK cells and include mean, median and interquartile range.*

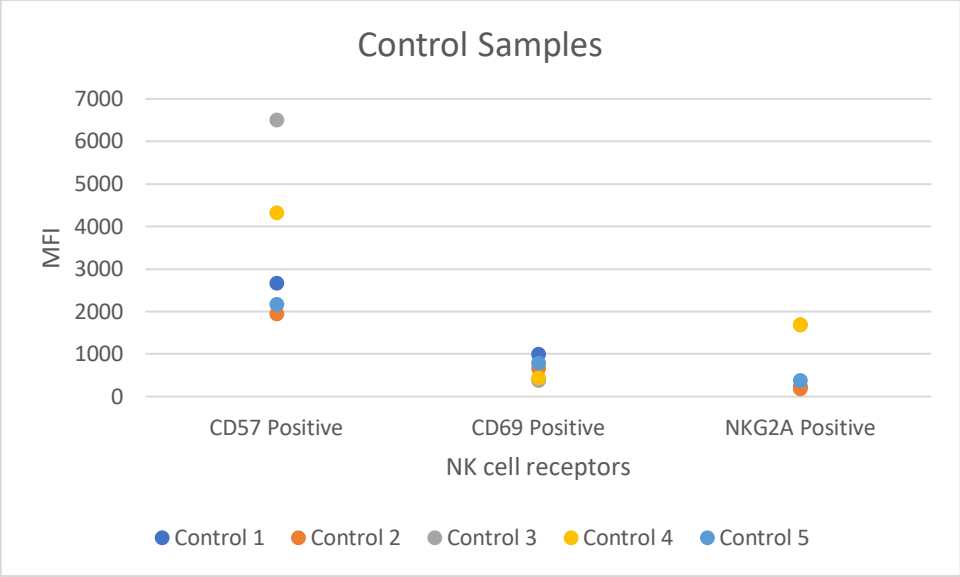

Appendix Figure 9.2 – MFI of the NK cell maturity markers expressed on NK cells in the control samples. *Values taken from parent population the NK cells and include mean, median and interquartile range.*

	CD57 Positive	CD69 Positive	NKG2A Positive
Cirrhotic 1	44.1	8.16	32.2
Cirrhotic 2	44.4	21.5	50.1
Cirrhotic 3	58.4	19.8	44.4
Cirrhotic 4	73.9	13.9	50.0
Cirrhotic 5	66.3	2.34	89.0
Cirrhotic 6	44.9	1.5	91.1
Cirrhotic 7	50.5	19.8	78.5
Cirrhotic 8	34.8	18.5	74.4
Cirrhotic 9	53.2	21.3	79.7
Mean	52.28	14.09	65.49
Median	50.5	18.5	74.4
Interquartile Range	14	11.64	29.7

Appendix Table 9.3 – Percentage population of the NK cell maturity markers expressed on NK cells in the cirrhotic samples. *Values taken from parent population the NK cells and include mean, median and interquartile range.*

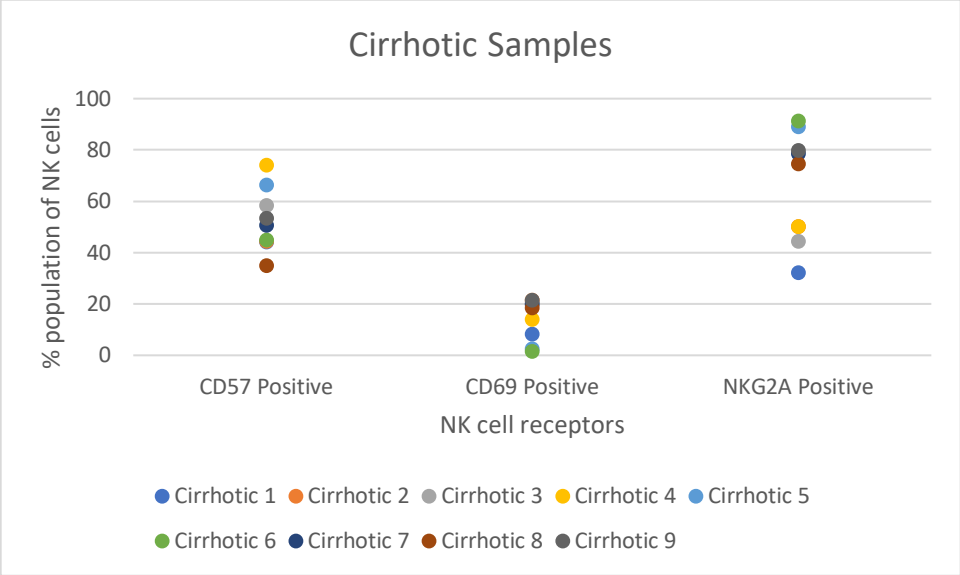

Appendix Figure 9.3 – Percentage population of the NK cell maturity markers expressed on NK cells in the cirrhotic samples. *Values taken from parent population the NK cells and include mean, median and interquartile range.*

	CD57 Positive	CD69 Positive	NKG2A Positive
Cirrhotic 1	2654	765	162
Cirrhotic 2	2599	792	171
Cirrhotic 3	4390	408	1483
Cirrhotic 4	7174	396	1893
Cirrhotic 5	4989	1429	1740
Cirrhotic 6	2069	1155	1795
Cirrhotic 7	5239	1615	4789
Cirrhotic 8	3774	1894	4670
Cirrhotic 9	6115	1723	3937
Mean	4333.7	1130.8	2293.3
Median	4390	1155	1795
Interquartile Range	2585	850	2454

Appendix Table 9.4 – MFI of the NK cell maturity markers expressed on NK cells in the cirrhotic samples. *Values taken from parent population the NK cells and include mean, median and interquartile range.*

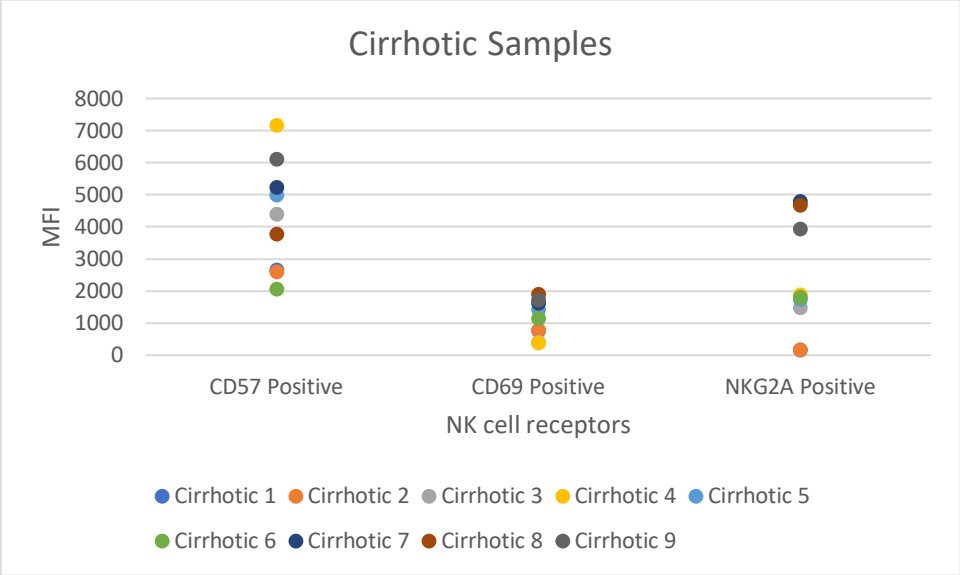

Appendix Figure 9.4 – MFI of the NK cell maturity markers expressed on NK cells in the cirrhotic samples. *Values taken from parent population the NK cells and include mean, median and interquartile range.*

	CD57 Positive	CD69 Positive	NKG2A Positive
Acute Rejection 1	45.1	13.1	19.6
Acute Rejection 2	11.8	26.1	60.5
Acute Rejection 3	39.5	34.2	59.3
Acute Rejection 4	17.5	21.1	59.3
Acute Rejection 5	22.2	2.33	73.1
Acute Rejection 6	15.8	15.6	66.0
Mean	25.32	18.74	56.3
Median	19.85	18.35	59.9
Interquartile Range	18.95	11.125	5.325

Appendix Table 9.5 – Percentage population of the NK cell maturity markers expressed on NK cells in the acute rejection samples. *Values taken from parent population the NK cells and include mean, median and interquartile range.*

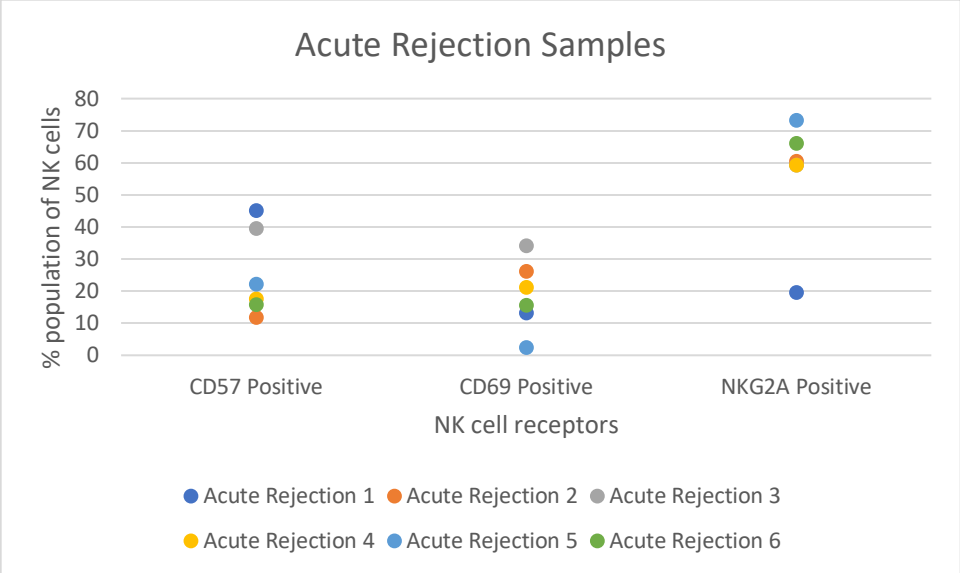

Appendix Figure 9.5 – Percentage population of the NK cell maturity markers expressed on NK cells in the acute rejection samples. *Values taken from parent population the NK cells and include mean, median and interquartile range.*

	CD57 Positive	CD69 Positive	NKG2A Positive
Acute Rejection 1	2657	810	198
Acute Rejection 2	2901	1073	193
Acute Rejection 3	2185	544	1515
Acute Rejection 4	1401	475	1843
Acute Rejection 5	1167	1198	847
Acute Rejection 6	2002	1065	4426
Mean	2052.2	860.83	1503.7
Median	2093.5	937.5	1181
Interquartile Range	987.75	460.5	1400.75

Appendix Table 9.6 – MFI of the NK cell maturity markers expressed on NK cells in the acute rejection samples.

Values taken from parent population the NK cells and include mean, median and interquartile range.

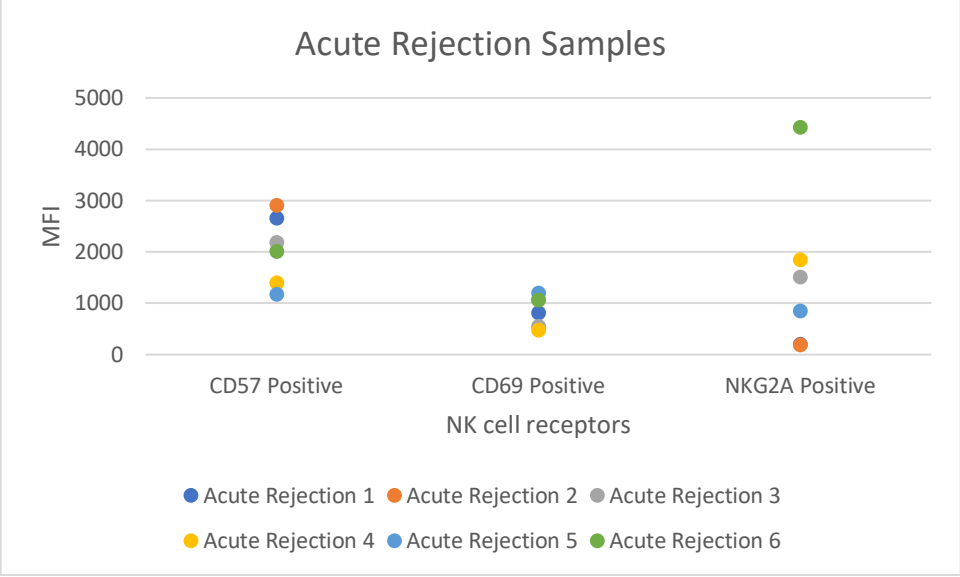

Appendix Figure 9.6 – MFI of the NK cell maturity markers expressed on NK cells in the acute rejection samples.

Values taken from parent population the NK cells and include mean, median and interquartile range.

.

Appendix 10 Localisation of TAPBPR

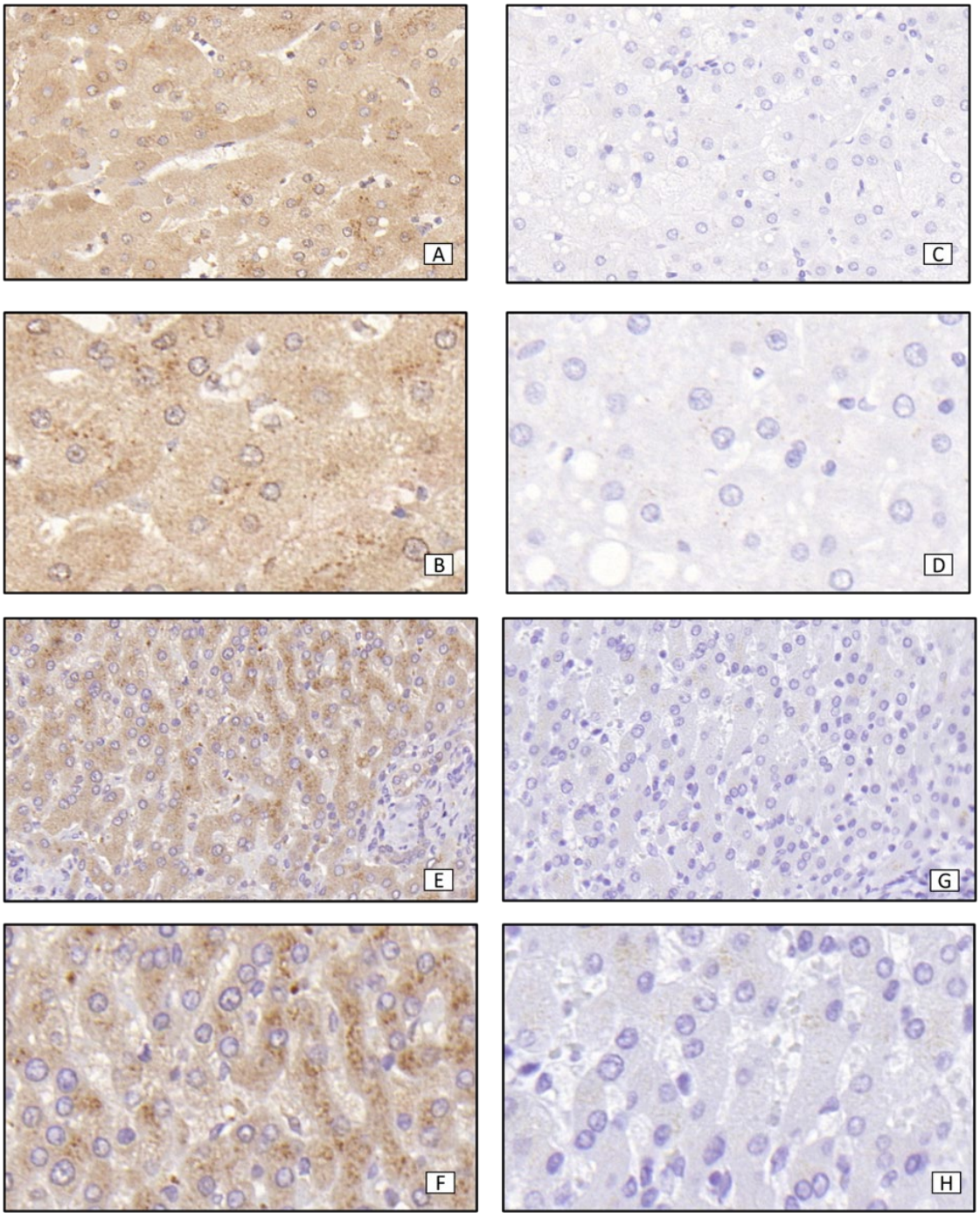

Appendix Figure 10.1 – Immunohistochemistry of TAPBPR with PeTe4 antibody in liver tissue. *Antigen retrieval with EDTA buffer. Positive staining is seen as brown as the secondary antibody was tagged with DAB. Images A (20x) and B (40x) showing hepatocyte staining in cirrhotic tissue. Images C (20x) and D (40x) were negative for staining in cirrhosis with an IgG2a control. Images E (20x) and F (40x) showed hepatocyte staining in healthy control liver tissue. Images G (20x) and H (40x) showed no staining in healthy control tissue with an IgG2a control antibody.*